Soil Erosion in a Highly Dynamic, Terraced Environment

The Effect of the Three Gorges Dam in China

Dissertation

der Mathematisch-Naturwissenschaftlichen Fakultät

der Eberhard Karls Universität Tübingen

zur Erlangung des Grades eines

Doktors der Naturwissenschaften

(Dr. rer. nat.)

vorgelegt von

Diplom Geographin Sarah Schönbrodt-Stitt

aus Eberswalde

Tübingen

2013

Tag der mündlichen Prüfung:	29. April 2014
Dekan:	Prof. Dr. Wolfgang Rosenstiel
Erster Gutachter:	Prof. Dr. Thomas Scholten
Zweiter Gutachter:	Prof. Dr. Gerhard Gerold

Global land lost to soil erosion in the first half of the year 2013

(January 1st to July 1st, 2013)

2,912,287 HECTARES

from FAO - dimensions of need: restoring the land, http://www.worldometers.info/ (06/01/2013)

LIST OF CONTENT

LIST OF FIGURES

LIST OF TABLES

ABBREVIATIONS

BMBF	German Federal Ministry of Education and Research	MEP	Ministry of Environmental Protection of the People's Republic of China
BMP	Best Management Practice	MLR	Ministry of Land and Resources of the People's Republic of China
CSTC	Chinese Soil Taxonomic Classification	NMIC	National Meteorological Information Centre of China
CUG	China University of Geosciences	NDVI	Normalized Differenced Vegetation Index
CYJV	Canadian Yangtze Joint Venture	P_d	Precipitation per day
DEM	Digital Elevation Model	R_a	Mean annual *R* factor
EUROSEM	European Soil Erosion Model	RD	Relieving and De-farming mode
FAO	Food and Agriculture Organization of the United Nations	RS	Remote sensing
FONA	BMBF Framework Programme 'Research for Sustainable Development'	RTD	Rebuilding Terrace and De-farming mode
F_{mod}	Modified Fournier Index	RUSLE	Revised Universal Soil Loss Equation
FVC	Fractional Vegetation Cover	SEPA	State Environmental Protection Administration
GFG	Grain for Green Programme	SNSS	Second National Soil Survey in China
GIS	Geographic Information System	SP	Subproject
ICOLD	International Commission on Large Dams	SRTM	Shuttle Radar Topographic Mission
IECA	International Erosion Control Association	*TerraCE*	Terrace-Condition-Erosion model
ISWM	Integrated Small Watershed Management	TGR	Three Gorges Reservoir
IUCN	International Union for Conservation of Nature	TGA	Three Gorges Area
LUCC	Land use and land cover change	TGD	Three Gorges Dam
MAP	Mean annual precipitation	USDA	U.S. Department for Agriculture
USLE	Universal Soil Loss Equation		

UYR	Upper Yangtze River
UYRB	Upper Yangtze River Basin
YRB	Yangtze River Basin
WCD	World Commission on Dams
WEPP	Water Erosion Prediction Project
WMO	World Meteorological Organization
WSC	Water and soil conservation
WSCL	Water and Soil Conservation Law
WRB	World Reference Base

PREFACE

The dissertation entitled *"Soil Erosion in a Highly Dynamic, Terraced Environment - Effect of the Three Gorges Dam in China"* was developed by the author as a cumulative thesis at the Chair of Physical Geography and Soil Science, Department of Geosciences at the University of Tübingen. It is submitted for the degree of Doctor of Natural Sciences.

The thesis is part of an interdisciplinary joint research project aiming at the ecological consequences of the changing environmental conditions in the newly created reservoir of the Three Gorges Area at the Yangtze River in Central China. The results presented herein required comprehensive field surveys, data analysis and modeling using Geographical Information Systems and data mining approaches, and laboratory analyses. Based on those, one book chapter and three peer-reviewed articles dealing with the impact of the Three Gorges Dam on the risk potential of soil erosion by water and the modification of the bench terraces, i.e., terraced degradation, as the most important soil conservation measure in the study area, were published. As a mismatch between existing data and data required as input for soil erosion modeling constrained the study, the research herein is largely based on remote sensing data serving as a fast and available supplier for the derivation of area-wide and spatially explicit data on the landscape level.

The purpose of this dissertation is to introduce and demonstrate an approach to soil erosion modeling and assessment of those processes triggering soil erosion by water in a highly dynamic, terraced environment that currently belongs to the most dynamic large-scale anthropogenic influenced and disturbed regions in the world - The Three Gorges Area. The current situation in this area highly elicits a call for action in order to control soil erosion and its slow and devastating effects. It implies the reduction of agricultural depletion and environmental risks linked to water erosion, and the contribution to ecological protection and sustainability of one of the most populated regions in China. Minimizing soil erosion through best management practices, such as well-adapted farming terraces, is an indispensable prerequisite for good soil management and includes the urgent need for understanding the processes triggering soil erosion and their spatial and temporal variability.

Therefore, this thesis combines physio-geographic and anthropo-geographic aspects to assess the relevant processes and driving forces of the soil erosion risk potential in a region undergoing high land use dynamics. The unique contribution of this thesis is the model framework *TerraCE* (Terrace Condition Erosion) developed for the identification and spatial analysis of different terrace conditions and their causes. It considers the sparse data availability and limited access to terrain and thus, improves the knowledge on terrace degradation by conducting the first inventory of bench terraces in the Three Gorges Area and throughout China.

Thus, this thesis might be of interest to those studying the impact of land use change in a terraced landscape in the context of soil erosion research and environmental planning as *TerraCE* is readily transferable to other regions when the requirements on the data are fulfilled. The thesis might also be of interest to those studying the soil erosion potential on the catchment scale of mountainous regions characterized by data scarcity.

Chapter 1 "Introduction and State-of-the-Art" spins the common thread from soil erosion in the global context to soil erosion in China and in the Three Gorges Area where the mountainous study area is located. Thus, *Chapter 1* creates the basics for the derivation and for the answer of the research objectives that are presented in *Chapter 2 'Staring Point of the Research and Objectives'*.

Chapter 3 'Materials and Methods' introduces into the study framework and the study area and presents the geo-basis data as well as soil erosion modeling approach used.

Chapter 4 '*Overview on the manuscripts*' explores the most relevant and intrinsic results and discussions of each study. Thereby, the overview on the manuscripts follows the chronological order regarding the date of publication of the peer-reviewed articles. Except *Manuscript 1*, all manuscripts were originally published in English language. They are attached in the end of this thesis as they were originally published in international peer-reviewed journals. *Manuscript 1* is attached in the German language.

Chapter 5 'Conclusions and Outlook' concludes the central findings of the thesis with respect to the research objectives and issues an outlook of application possibilities of those findings and further need of research. The summary of the research is given in *Chapter 6*.

In *Chapter 7* all references cited in the thesis are listed. Attached to this thesis, the Annex intends to provide supplementary information on the history and combat of soil erosion in China, on the Yangtze River and its Basin, as well as on the effect of large dam projects on soil erosion and technical information about the Three Gorges Dam in China. This thesis then finishes with words of thanks and appreciation addressing all persons who directly and indirectly made their part in the author's scientific work and process and contributed to the success of the study.

The dissertation completes with the author's *Curriculum Vitae*, the compilation of the *'Scientific Publications, Books and Conference Contributions'* that were almost exclusively conducted within the thesis framework, and the *'Declaration by the Candidate*'.

This research was supported by the German Federal Ministry of Education and Research (BMBF, grant no. 03 G 0669).

1 INTRODUCTION AND STATE OF THE ART

„Should we be shocked that we are skinning our planet? Perhaps, but the evidence is everywhere. We see it in brown streams bleeding off construction sites and in sediment-choked rivers downstream from clear-cut forests. We see it where farmers' tractors detour around gullies, where mountain bikes jump deep ruts carved into dirt roads, and where new suburbs and strip malls pave fertile valleys. This problem is no secret. Soil is our most underappreciated, least valued, and yet essential natural resource."

David R. Montgomery,
Dirt - The erosion of civilization, 2007a, p. 3

1.1 SOIL EROSION IN THE GLOBAL CONTEXT

1.1.1 THE NATURAL GEOMORPHIC PROCESS OF SOIL EROSION

Soil erosion is a natural geomorphic, interactive process involving the four stages of detachment of individual soil particles from the soil mass, their breakdown, their transport and redistribution by water and wind, and deposition with declining transport energy (LAL, 2003; MORGAN, 2005). Both, water and wind erosion are major land surface processes (BRESHEARS ET AL., 2002; ZHANG ET AL., 2011). Due to both processes generally being studied as separate and the difficulties in determining the contributing area of sediment transported by wind, the magnitude of wind erosion relative to water erosion is not fully quantified across ecosystems (ZHANG ET AL., 2011). MIDDLETON and THOMAS (1997), LAL (2001), and MORGAN (2005), however, revealed a globally higher potential and significance of water erosion. According to LAL (2001), water erosion is the biggest driver of soil degradation. At the end of the 20th century, almost 67% of the worldwide approximately 16.4 million km² of degraded soil was linked to water erosion. Wind erosion amounted to approximately 33% (LAL, 2001).

Particularly, the detachment of soil particles by raindrop impact - splash detachment - (e.g., MORGAN and NEARING, 2011; GEIßLER ET AL., 2012) and their transport downslope by overland flow are recognized as the two main driving processes of water erosion (CHORLEY, 1978; GHAHRAMANI ET AL., 2011). This soil erosion by water is referred to as 'sheet erosion' or overland flow and removes and transports detached soil in form of rainsplash, surface runoff, and shallow flows (MORGAN, 2005). Initiated by a critical distance downslope, overland flow becomes channeled as small ephemeral concentrated flow (rill erosion) or breaks up into small channels (microrill erosion). Rill erosion accounts for the most powerful erosive agent on hillsides as it is also non-selective in the particle sizes

to be transported (MOSS ET AL., 1982; MORGAN, 2005). Amongst permanent gully erosion, developing from intense soil piping typically on deeply weathered regolith or soft bedrock (HOWARD, 1999; POESEN, 2011), and interrill erosion, referring to water erosion between rills by the combined action of raindrop impact and overland flow (MORGAN, 2005), sheet and rill erosion constitute the principal mechanism of water erosion (NEARING, 1997). Factors triggering the natural process of water erosion to a varying extent dependent from their interaction are: the erosivity of the eroding agent (i.e., rainfall amount and intensity, wind speed), the erodibility referring to the soil's resistance to particle detachment and transport, the land's slope steepness and slope length, and the vegetation cover acting as protective layer against the erosive impact (MORGAN, 2005).

Ranging from very low soil losses up to 2 t ha^{-1} a^{-1} on relatively flat grasslands and forests to 1 to 5 t ha^{-1} a^{-1} in mountainous regions completely covered with vegetation (PATRIC, 2002 quoted in PIMENTEL, 2006), water erosion is of earth-historical relevance. In most ecosystems it normally almost equals the average rate of natural soil formation ranging from 0.5 to 1 t ha^{-1} a^{-1} (PIMENTEL and KOUNANG, 1998; WACHS and THIBAULT, 2009). The redistribution of soil and associated plant essential nutrients from weathering to depressional sites made the natural water erosion over geologic time one of the most powerful natural forces in landscape evolution (FIGUEIREDO ET AL., 1999).

Nevertheless, soil erosion in general, and water erosion in particular, is on top of the world's agenda as one of the most pressing environmental problems of present times (HURNI ET AL., 2006). In the scientific discourse, it is even recognized as 'silent global crisis' (MONTGOMERY, 2007a) concurrent with climate change. Here, the concern is not about the natural complex system of soil erosion and its 'long-term geological' process (MONTGOMERY, 2007b), but rather about the accelerated soil erosion due to multiple human interferences into ecosystems and, subsequently, soil systems.

1.1.2 THE ANTHROPOGENIC-INDUCED ACCELERATION OF SOIL EROSION

Anthropogenic-induced changes in the land cover and land uses (e.g., shifts and expansion in agriculture, intensification of cultivation, deforestation and logging, urban sprawl, infrastructure construction and mega construction sites) extraordinarily alter the somewhat balanced natural system of soil loss and soil formation. On the one hand, land use is the only factor of soil erosion that can actively be modified to reduce soil loss (GILLEY, 2004). On the other hand, land use leads to accelerated soil losses that can strongly exceed the sustainable replacement rate by natural soil formation. According to BRANTLEY (2008), the human activities have globally increased the long-term soil erosion rate by a factor of approximately 30. For instance, as stated by the *International Erosion Control Association* (IECA, 1991) construction activities such as road and housing

construction can cause extreme short-term soil erosion ranging from 20 to 500 t ha^{-1} a^{-1} and can further enhance runoff that contributes to increased soil erosion in the long-term.

The largest and most continuous destroyer of natural soil systems and main contributor to water erosion is the agricultural production which accounts for about 75% of the worldwide soil erosion (PIMENTEL, 2006). Cropland is among those agricultural land uses that is most vulnerable (PIMENTEL, 2006). Inappropriate cropland management, such as conventional farming (e.g., row cropping, clean weeding, intensive tillage, and reduced fallow), especially enhances the effect of agriculture (MORGAN, 2005).

According to PIMENTEL (2006) and MONTGOMERY (2007a), small-scale subsistence farms in developing countries with hilly and mountainous terrain are particularly vulnerable to water erosion since they are often located on marginal land with poor soil quality and frequently steep topography. According to SOUTHGATE and WHITAKER (1992), STONE and MOORE (1997), and PIMENTEL (2006), subsistence farming is often attributed by inappropriate land management and thus, is susceptible to soil erosion. Here, the erosive effect of rainfall and terrain as well as inappropriate land management can be most effectively alleviated by establishing adequate soil conservation measures, such as sufficient crop cover, contour-aligned cultivation and planting of hedgerows, intercropping, mulching, and farming terraces (HUDSON, 1981; MORGAN, 2005). They all act as a quasi fifth factor on soil erosion in the human-induced water erosion on cropland. By reducing the terrain-induced runoff potential, especially, bench terraces are the major recommended type of soil conservation measure on sloping land (HUDSON, 1981).

1.1.3 FARMING TERRACES AS KEY SOIL CONSERVATION TECHNOLOGY

Bench terraces (synonym for slope or stone terraces) are the major recommended type of terrace for steep sloping areas (HUDSON, 1981; SHI ET AL., 2012). In order to stabilize the vertical terrace riser, dry-stone walling along the contour lines is largely applied (HUDSON, 1981; BELLIN ET AL., 2009; SHI ET AL., 2012). Since the ancient world and early modern age, terracing serves as key technology for soil and water conservation and for a suitable land management in mountainous regions throughout the world (e.g., TOY ET AL., 2002; SHRESTRA ET AL., 2004; CAO ET AL., 2007).

Due to the terracing, steep slopes are converted into an artificial sequence of relatively flat surfaces (MONTGOMERY, 2007a). The erosive slope length and angle and thus, the runoff potential distinctly decrease resulting in a reduction of terrain-induced soil erosion and sediment yield (ARNAEZ ET AL., 2010; EL ATTA and AREF, 2010; SHI ET AL., 2012).

Under optimum conditions, these engineering structures form a ‘hydraulic equilibrium’ state between the geomorphic settings and anthropogenic use (BRANCUCCI and PALIAGA, 2006; CHEMIN

and VAROTTO, 2008). From the Mediterranean, for instance, HAMMAD ET AL. (2004) report a decrease of average soil loss on bench terraces compared to non-terraced plots by factors up to 20. In the highly vulnerable Chinese Loess region, decreases of soil loss of average 49% were observed (LI and NGUYEN, 2008). Applying the WATEM/SEDEM erosion and sediment transportation model for a small watershed sloping in average with 23° in Central China, SHI ET AL. (2012) report a reduction of soil loss and sediment yield by approximately 17% and 32% for bench terraces combined with furrow-ridge tillage. Terraces are further likely to favor the interception of overland flow and to enhance the infiltration in the long-term (e.g., BELLIN ET AL., 2009; EL ATTA and AREF, 2010; SHI ET AL., 2012), to reduce the erosion-induced nutrient loss (DAMENE ET AL., 2012), to promote agricultural productivity (POSTHUMUS and STROOSNIJDER, 2010), and to expand available land for cultivation (ZHANG, 2008).

In contrast to the above benefits, numerous studies such as from Saudi Arabia (EL ATTA and AREF, 2010), the Andes in Peru (INBAR and LLERENA, 2000), from the Chinese Loess region (e.g., LI and LINDSTROM, 2001), from Italy (e.g., BAZZOFFI and GARDIN, 2011), from Greece (e.g., KOULOURI and GIOURGA, 2007), from Spain (e.g., BELLIN ET AL., 2009), Indonesia (VAN DIJK, 2002), and Thailand (SANG-ARUN ET AL., 2006) have proven that bench terraces react sensitively to changes in land use. Subsequently, despite terracing, soil erosion can be a serious problem.

Particularly, inadequate terrace design and mismanagement strongly affect the stability of bench terraces and favor soil erosion (e.g., SANG-ARUN ET AL., 2006; KOULOURI and GIOURGA, 2007; LESSCHEN ET AL., 2008; BELLIN ET AL., 2009). Causes for this phenomenon are seen in a lack of local knowledge of adequate terracing (e.g., ESTEVE ET AL., 2004), in a lack of individual farmers' motivation and uncertainty regarding tenure (WILLIAMS, 1990; DEININGER and JIN, 2006), in a shortage of labor and investments (INBAR and LLERENA, 2000), a shift of production (BELLIN ET AL., 2009; BEVAN ET AL., 2012), and land shortage and fragmentation (CORBEELS ET AL., 2000). Mostly, these causes interact with each other and are discussed to result from an agricultural abandonment (e.g., KOULOURI and GIOURGA, 2007; LESSCHEN ET AL., 2008; EL ATTA and AREF, 2010) due to social, economic and/or political upheavals, such as rural-urban migration (e.g., AW-HASSAN ET AL., 2000; INBAR and LLERENA, 2000; KOULOURI and GIOURGA, 2007).

According to INBAR and LLERENA (2000) who studied erosional processes on bench terraces in Peru, the supporting terrace wall mainly determines the terrace stability. Typically, walls of bench terraces left to degrade exhibit bulges and upsetting by erosive action followed by more intense wall disorders such as breaches that further lead to complete collapses (INBAR and LLERENA, 2000; LASANTA ET AL., 2001; BRANCUCCI and PALIAGA, 2006; LESSCHEN ET AL., 2008; BELLIN ET AL., 2009). The natural geomorphic system will progressively annul the former balanced terraced system (BRANCUCCI and PALIAGA, 2006; BAZZOFFI and GARDIN, 2011). This will increase the slope length

and slope gradient, followed by an acceleration of runoff (e.g., EL ATTA and AREF, 2010; KOULOURI and GIOURGA, 2007). Consequently, the capability of a terrace to protect the soil against surface erosion by water is reduced, defined as terrace degradation by BAZZOFFI and GARDIN (2011).

By evaluating the potential of the terrace design to reduce soil erosion and applying flow traces, BELLIN ET AL. (2009) proved that terraces that were not longer maintained do not longer retain water and promote an increased contribution of runoff from cropland to the drainage network. Within 50 years, the portion of runoff was observed to increase from 9% to 31%. According to SIDLE ET AL. (2006) and BAZZOFFI and GARDIN (2011) poorly designed and maintained terraces represent significant sediment sources.

1.1.4 FIGURES AND EFFECTS OF SOIL EROSION

Estimated 75 billion tons of fertile soils are eroded from agricultural land each year around the world (e.g., ESWARAN ET AL., 2001; LAL, 2003; PIMENTEL, 2006; WACHS and THIBAULT, 2009). Globally, the estimated average water erosion rate on cropland is 30 t ha^{-1} a^{-1} and ranges from 0.5 to 400 t ha^{-1} a^{-1} (PIMENTEL ET AL., 1995, PIMENTEL, 2006; WACHS and THIBAULT, 2009). Thereby, highest water erosion on cropland is reported for Asia, Africa, and South America with average soil loss rates ranging from 30 to 40 t ha^{-1} (TADDESE 2001 quoted in PIMENTEL, 2006). In the 1990s, 105 million hectares in Europe amounting to 16 per cent of the continent's total area (without Russia) were affected by water erosion (JONES ET AL., 2012). New calculations by the Joint Research Centre of the European Union estimate the current area affected to be distinctly higher, with 1.3 million km^2 for the EU-27 (before EU accession of Croatia in July 2013). Approximately 20% of this area exhibits soil losses of more than 10 t ha^{-1} a^{-1} (JONES ET AL., 2012). According to PIMENTEL (2006) this severe soil erosion is directly linked to cropland and equals the average water erosion rate on cropland across the United States.

Soil erosion leads to manifold on-site and off-site disruptions that can interact with each other and can reinforce soil losses by erosive action. It affects the soil's water storage capacity and water availability due to decreased water infiltration (e.g., PIMENTEL ET AL., 1995; JONES ET AL., 2012). The loss of soil organic matter and the subsequent loss of stable soil aggregates lead to a decline in soil porosity, again influencing slaking, infiltration, and runoff potential (PIMENTEL, 2006; BARTHÈS and ROOSE, 2002; SIX ET AL., 2002). The reduction of soil depth and disruptions in the essential plant nutrients cycle distinctly reduce the (top)soil fertility and land productivity (JONES ET AL., 2012), and considerably influence the soil biodiversity and plant diversity (e.g., PIMENTEL ET AL., 1992; HEYWOOD, 1995; JONES ET AL., 2012). This is especially true for shallow soils where water erosion may lead to an irreversible loss of the entire soil body within short erosive events (JONES ET AL., 2012) triggered by abundant rainfalls. Worldwide, the productivity loss due to soil erosion by water is

estimated to make up to 50% (ESWARAN ET AL., 2001). Particularly, African and South Asian countries are affected. Here, the average annual yield reduction by water erosion is estimated to be approximately 8%, respectively to equal to 36 million tons of cereals (ESWARAN ET AL., 2001).

Water erosion is also widely discussed to largely contribute to global warming due to releases of oxidized biomass carbon (CO_2) from the soil into the atmosphere. Based on experimental analyses and national scale modeling for England and Wales, QUINTON ET AL. (2006), for instance, report the carbon that was mobilized as particulate organic matter by water erosion from cropland to range from annually 0.2 to 0.76 Mt. The losses of carbon associated to water erosion accounted for a wide range of 2 to 50% of soil carbon change (QUINTON ET AL., 2006). However, due to the complexity of soil erosion in general, its effects on C emissions and the global terrestrial carbon budget still remain not fully understood and quantifications are vague (e.g., LAL, 2003, 2004; QINTON ET AL., 2006; VAN OOST ET AL., 2007; LAL and PIMENTEL, 2008; JONES ET AL., 2012). *Vice versa*, future water erosion is expected to react very sensitive on climate change that will drive a 'vigorous hydrological cycle' inducing erosive torrential rainfall with higher rainfall amounts and intensities, and triggering changes in plant biomass (e.g., YANG ET AL., 2003; DUFKOVA and TOMAN, 2004¸ NEARING ET AL., 2004). For instance, based on simulation studies across the United States, NEARING ET AL. (2004) predict an increase in water erosion of 1.7% for each 1% change in annual rainfall amount.

Off-site water erosion damages mainly result in and from discharge of sediments and associated contamination of waterbodies due to diffuse matter transport and particle-bounded agrochemicals from cropland (e.g., BENNETT and RHOTON, 2007). They deteriorate the quality of aquatic systems and threaten biodiversity and human health (e.g., PIMENTEL, 2006; MAINSTONE ET AL., 2008). Enormous potential of economic damages is also attributed to extreme overland flow and floods resulting from improper upstream management and from wind-driven dust storms originating from degraded land with porous vegetation (PIMENTEL ET AL., 1995; WACHS and THIBAULT, 2009).

Against the background of an increasing world population to estimated 9 billion people by the year 2050 (UNITED NATIONS, 2011), an increasing demand for food of 60 to 70% by the same year (ALEXANDRATOS and BRUINSMA, 2012), and 99.7 % of the food already coming from the land (FAO 1998 quoted in PIMENTEL, 2006), water erosion has a global significance. It constitutes a global threat to food security and drinking water quality in many parts of the world. Both, available soil resources and clean water are expected to present a future source of conflict. Thus, combating soil erosion will be a major challenge of the world community (BRADY and WEIL, 2007).

1.2 SOIL EROSION IN CHINA

Globally, China belongs to one of those countries most affected by soil erosion (HUANG, 1987; ALDHOUS, 1993; VAN LYNDEN and OLDEMANN, 1997; KOLB, 2003; HAO ET AL., 2004; WANG, 2004; CAI ET AL., 2005) and is strongly challenged with its combat. The mere fact that steeplands and shallow mountain soils, accounting for 52%, respectively 29% of China's totals (BOT ET AL., 2000), are largely linked to subtropical monsoon climate (ZHAO, 1986) already indicates a high to very high physical vulnerability to water erosion, especially, in the great river basins in north, east and central China (Figure 1). Additionally, China exhibits large regions of low to very low protective vegetation cover. This is mainly a result from former phases of development-driven deforestation and agriculturally expansion in China's great river basins where vegetation could not completely recover through the centuries (ZHANG, 2000; c.f., Annex I).

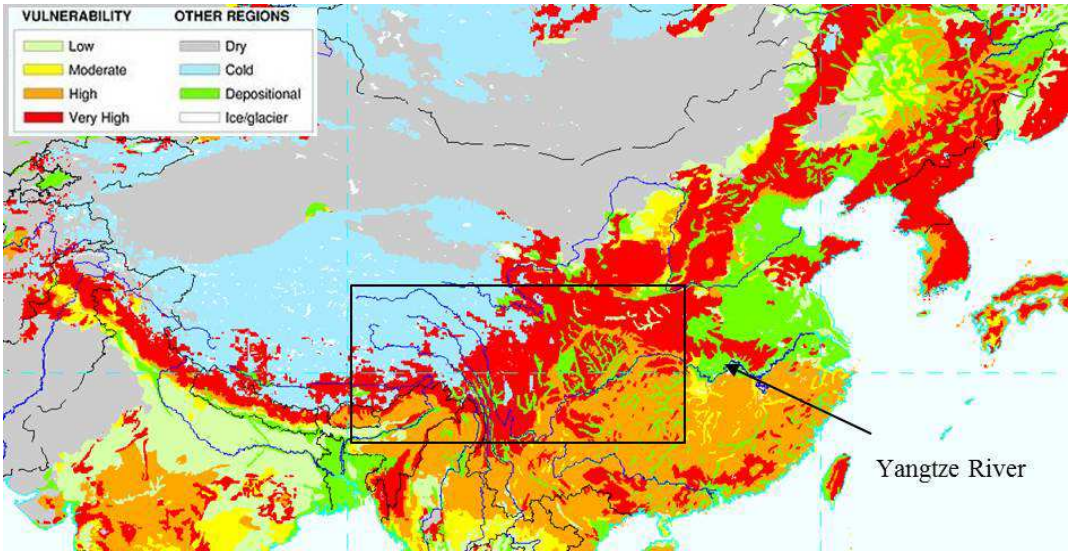

Figure 1 *Water erosion vulnerability in China, in the Yangtze River Basin, and in the Upper Yangtze River Basin (framed). (after U.S. Department of Agriculture, Natural Resources Conservation Service, Soil Survey Division, World Soil Resources, 1998; modified).*

At the same time China has the largest population in the world with a relatively high proportion of rural inhabitants (49%) and employment in agriculture of (37%; both in 2011) of nationals totals (WORLD BANK, 2013). Thus, it seems not surprising that physical vulnerability combined with population pressure on land and soil resources tremendously trigger water erosion and contribute to nationwide environmental degradation (e.g., ROZELLE ET AL., 1997; WANG, 2004; XU ET AL., 2005; TAN and GUO, 2007).

However, figures on the actual soil loss by water erosion and the area affected in China are controversial. They range from recently estimated annual 4.5 billion tons (Xinhua, 2008) to already estimated average 5.5 billion tons per year in the 1990s (e.g., LAL and STEWART, 1990; WEN, 1997;

PIMENTEL, 2006). Based on the report on land resource potential and constraints by BOT ET AL. (2000), 16% of China's territory show soil erosion risk. Based on remote-sensing based studies from the latest Chinese three-year *Soil Conservation Scientific Survey*, 37% to 40% of China's territory - accounting for about 3.6 million km² - are recently classified as suffering from soil loss by water erosion (SUN ET AL., 2002; HAO ET AL., 2004; XINHUA, 2008). According to the 2013's report by the *UN Desertification Convention* (UNCCD), more than 400 million people in China are directly affected by the on-site and off-site effects; such as serious losses in agricultural productivity of more than annually 20% since the 1990s (ESWARAN ET AL., 2001) and annual economic losses of estimated US$10 billion (UNCCD, 2013).

China's severe soil erosion problem, and the anthropogenic effects triggering soil erosion and eco-environmental deterioration led to comprehensive countermeasures by the government during the second half of the 20th century (c.f., Annex II). With the nationwide implementation of the *Water and Soil Conservation Law* (WSCL) in 1991 and its revised version in 2011, especially the prevention and rehabilitation of land prone to water erosion were aimed. Thereby, sloping farmland or sloping land to be reclaimed for cultivation with inclinations greater than 25° is in the focus of the WSCL and prescribed as 'reclamation-forbidden' (LIU, 2012). The enhanced installation of conducive water erosion control measures such as farming terraces (XU ET AL., 2005) and the governmental-driven 'Sloped Land Conversion Program' based on the above slope steepness criterion (e.g., XU ET AL., 2006; WANG ET AL., 2007; c.f., Annex II) aimed at the distinct reduction of runoff and water erosion potential by controlling the terrain effect and converting cropland to forestland. By identifying key prevention and rehabilitation areas and implementing the *Integrated Small Watershed Management* (ISWM) since the 1990ies, in particular, the water-eroded, largely mountainous Yangtze River Basin became part of the governmental action plan to control soil erosion (XU ET AL., 20005; LIU, 2012; ZHU ET AL., 2013).

Notwithstanding these efforts, the Yangtze River Basin - presenting a 'critical global ecoregion' rich in biodiversity and one of the 35 worldwide ecological priority areas - recently shows the highest rates of soil erosion by water out of the whole of China (YIN ET AL., 2006; ZHOU, 2008; WWF China, 2013).

1.2.1 SOIL EROSION IN THE UPPER YANGTZE RIVER BASIN

Thirty-three percent (560,000 km²) of the area of the *Yangtze River Basin* (YRB) – the largest watershed in China – is severely affected by water erosion, mainly alongside the upper reaches of the Yangtze River (ZHOU, 2008).

Accounting for approximately 56% of the entire basin area, the mountainous *Upper Yangtze River Basin* (UYRB) distinctly dominates the YRB. It extends from the Qinghai Tibetan Plateau

through mountainous terrain mainly ranging between 500 and 4,000 m a.s.l. towards the plains in Central China (c.f., Annex III). Accelerated water erosion resulting from deforestation, agricultural expansion, and intensification in cropland due to industrialization and increasing population pressure, seriously affected the UYBR since the last decades (YANG ET AL., 2005; ZHANG, 2008). Within approximately 50 years, the area exhibiting water erosion dramatically increased by more than 100% from 350,000 to 711,000 km², amounting to approximately 40% of the total area of the YRB (ZHANG, 2008. Thereby, the proportion of affected area in the UYRB alone constituted more than 60 to 66% of the YRB' total (ZHANG, 2008).

According to YANG ET AL. (2005), the area affected by water erosion positively correlated to the sediment yield during the observed period. While at the begin of the 1950s sediment deposition in reservoirs and lakes was recorded as nearly zero, the rate of deposition increased to approximately 740×10^6 t annually already taking into account the effect of areas under water erosion control (~35% in the YBR, ~23% in the UYBR; YANG ET AL., 2005). With an average annual sediment load of approximately 500 million tons, the UYBR accounts for the principal area of sediment production in the entire basin (DAI and TAN, 1996; YANG ET AL., 2006; ZHANG, 2008). The effect of the high soil erosion, due to inappropriate land uses and causing high deposition of sediments, and siltation of lakes and floodplains, resulted in frequent flooding and was particularly evident in 1998 and 2010 when severe flood disasters hit Hubei province (YIN and LI, 2001; LONG ET AL., 2006; PITTOCK and XU, 2011).

YANG ET AL. (2004) reported intensive and inappropriate land uses on steep slopes to be typical for the UYRB. Their effect on water erosion and sediment yield is even enhanced by abundant precipitation, erodible soil textures, and population pressure (e.g., LU and HIGGITT, 1999; ZHANG ET AL., 2002). Soil erosion by water in the UYRB affects about 35.2 million hectares accounting for approximately 63% of the entire UYRB (LONG ET AL., 2006). The total annual soil loss by water erosion in the UYRB is estimated to be 1,410 million tones with an average annual rate of water erosion of 40 t ha^{-1} (SHI, 1998). Thereby, sheet and rill erosion, and occasionally gully erosion constitute the major water erosion processes (LONG ET AL., 2006)

Despite the efforts on controlling soil erosion in the UYBR via key environmental programs, such as ISWM (c.f., Section 1.2), the further industrial development of the basin seems to be at odds with the general protection idea and soil conservation need.

Due to the significant elevation drop of the deeply incised Yangtze River in the UYRB (c.f., Annex III), the river has huge hydropower potential. Its usage as relevant transportation path connecting the east with the west already gave the Yangtze River an integral role in the historical development and exploitation of China (PONSETI and LÓPEZ-PUJOL, 2006). This is even more the case nowadays, since the Yangtze River plays a crucial role in the development strategic plans of the

Chinese central government (WU ET AL., 2010). These include, *inter alia*, the provision of electricity, goods and measures, and water to eradicate the water scarcity in North China (PONSETI and LÓPEZ-PUJOL, 2006; CHENG ET AL., 2012).

In the surrounding of major projects being economically important for the industrial development, a boost of soil erosion can be expected. Large dam projects and hydropower engineering schemes are such major projects and attract worldwide scientific and media interest due to their serious upstream and downstream environmental impacts and associated intensive land use changes (e.g., NILSSON ET AL., 2005; STONE and JIA, 2006). For instance, NORTON ET AL. (2001), COCHRANE ET AL. (2002), ALIXANDRINI (2010), ARVELA ET AL. (2012) and FERREIRA and PANAGOPOULUS (2012) could reveal a distinct raise of the soil erosion risk in the affected watersheds of the Alqueva (Portugal) and Itaipú (Brazil and Paraguay) dams due to post-construction shifts in land use and human activities (c.f., Annex IV). Both projects met unfavorable prerequisites in terms of physical vulnerability (e.g., erosion-prone soils, high rainfall erosivity, and steep terrain) and poor environment-related planning (SERAFIM ET AL., 2006; ALIXANDRINI, 2010; FERREIRA and PANAGOPOULUS, 2012). As a consequence of the increased soil erosion risk, Alqueva and Itaipú lakes are facing an accelerated sediment production and reservoir siltation leading to serious environmental and economic off-site damage (COCHRANE ET AL., 2002; FERREIRA and PANAGOPOULUS, 2012). An extreme example on the causality of 'increased soil erosion - increased sediment production - reservoir siltation' and consequently decreased lifespan of dam projects is reported from the Yellow River in China where trapped sediment behind the SanMenXia dam led to a loss of initial storage capacity within the first four years after construction (ZHU ET AL., 2013).

In the case of the UYBR, a strongly ranging number of more than 42,000 to more than 50,000 dams were already constructed from 1950 to 2003 at the Yangtze River and its tributaries (XU and MILLIMAN, 2009; YANG ET AL., 2005; YANG and LU, 2012). At present, a total of 4,688 km of streams are already regulated by dams that strongly control the discharge in the UYRB (LEHNER et al., 2011; YANG and LU, 2012), but also indicate high relevance and significance of anthropogenic-induced soil erosion in the UYRB.

Probably, the currently most prominent example on large dam projects in China and worldwide is the multipurpose Three Gorges Dam (TGD) at the Yangtze River (c.f., Annex V). It is less the dimension of the dam construction itself, but rather the short period of construction and the huge dimensions of the reservoir with a length of 660 km and a surface area of 1,084 km² (PONSETI and LÓPEZ-PUJOL, 2006) that attract worldwide scientific, societal and political interests.

1.2.2 SOIL EROSION IN THE THREE GORGES AREA

The impoundment of the Yangtze River in the zone of the 'Three Gorges' and further beyond towards Chongqing (c.f., Annex V) make the Three Gorges Area (TGA) the currently most dynamic large-scale anthropogenic influenced region in the world (e.g., YANG ET AL., 2002). Though the TGD project is accepted to significantly reduce China's greenhouse gases and emissions by hydropower generation (GUO, 2010), the dam is largely assumed to have negative impacts, too. Thus, the dam-induced impoundment and newly created reservoir are expected to have unprecedented long-term environmental consequences and to threaten the ecology in an unforeseeable dimension (STONE, 2008). Subsequently, expected increases in water erosion will constitute enormous environmental planning challenges in the large drainage area of the TGA of about 1 million km² (REYNOLDS, 2011; ZHU ET AL., 2013).

1.2.2.1 LAND USE CHANGES IN THE THREE GORGES AREA

Due to an enormous transformation process attributed to the construction of the TGD and ongoing associated hydraulic engineering projects after river impoundment, such as small barrages in the tributary valleys and bank reinforcement, the TGA is largely characterized by rapid land use changes. In total, an area of 635 km² has been flooded alongside the Yangtze River and its tributaries (Figure 2). Twelve counties and municipalities, and 116 cities with their whole infrastructure are affected (PONSETI and LÓPEZ-PUJOL, 2006; WU and LUO, 2006; GLEICK, 2009). Estimated 29,500 to 40,000 ha of this flooded land, accounting for about 41 to 63% of the total submerged area, was classified as agricultural land on fertile valley soils (JACKSON and SLEIGH, 2000; DAI ET AL., 2006; PONSETI and LÓPEZ-PUJOL, 2006; GLEICK, 2009).

Figure 2 *Impoundment of the Yangtze River by the Three Gorges Dam, here in the surrounding of the dam before the flooding in 1993 (left) and after the flooding in 2009 (right). From GUO (2010).*

The massive loss of settlements and farmland area had to be rapidly compensated. Rural and urban resettlements of more than 1.25 million people by the end of the year 2008 (MEP, 2009) and new land reclamation for the purposes of infrastructure connection and settlements as well as subsistence farming and cash crop production has taken place (MCDONALD ET AL., 2008; SUBKLEW ET AL., 2010, CUI ET AL., 2011). Consequently, this land reclamation in pre- and post-construction times of the TGD affected the steep sloping up-hill sites adjacent to the new river line after impoundment (Figure 3).

According to the *State Environmental Protection Agency* (SEPA), respectively, *Ministry of Environmental Protection* (MEP), from 2005 to 2008 alone, more than 778 km of rural roads were constructed (SEPA, 2006; MEP, 2008, 2009). Based on the IECA (1991), the road construction alone implies extreme short-term water erosion potential (c.f., Section 1.1.2). Alone during the two years from 2007 to 2008, more than 1.6 million m² and 1.15 million m² of new rural and urban houses had to be constructed for 114,229 resettled people (44% rural relocates, 56% urban relocates) within the same period (MEP, 2008, 2009). In 2009, the area of arable land in the TGA was 209,647 ha which is about 7% higher than in 2008 (195,588 ha) and almost 9% higher than in 2007 (192,672 ha; MEP, 2009; 2010). With the river impoundment, the implementation of orange orchards became highly recommended in the TGA, too, as it is supposed to reduce soil and nutrient losses and to favor a suitable use on critical uphill-sites exceeding slopes of 25° (MENG ET AL., 2001). Moreover, the installation of orange orchards as a cash crop is intended to boost the farmer's income after the TGD-associated resettlement (SHI ET AL., 2012). For instance, investigations by SHI ET AL. (2012) in the hilly Wangjiaqiao watershed in Zigui county close to the TGD revealed an increase of orange orchards by the 2.8-fold. For the whole TGA, the proportion of orange orchards on the total arable land was approximately 35% in 2009 (73,142 ha). Compared to the previous year, the increase in orange orchards alone is about 18% (61,760 ha in 2008; MEP, 2010).

However, similar to the examples on the dams Alqueva and Itaipú (c.f., Annex IV), the TGD project and associated rapid land use changes are regarded to meet unfavorable prerequisites in a vulnerable region exhibiting an already low environmental carrying capacity (e.g., HEGGELUND, 2006) and the highest soil erosion rates in the UYRB and throughout whole China (ZHOU, 2008).

The limited environmental capacity is mainly due to the steep to extremely steep, mountainous topography accounting for 90% of the total TGA and the impact of the Southeast Asian monsoon with abundant precipitation (mean annual precipitation of 1055 mm) and high rainfall erosivities (SUTTON, 2004; TAN ET AL., 2005; HE ET AL., 2008; MEP, 2010). Additionally, the shallow and fragile, and partially uncovered soils on the steep sloping uphill-sites are characterized as predominantly poor in soil organic matter with low stability of soil aggregates and as highly erodible (SHI ET AL., 2004). They typically show poor fertility and low agricultural productivity compared to the now inundated

valley soils below the impoundment level (SHI ET AL., 2004; CUI ET AL., 2011). This difference in soil's productivity increases the need of sloping agricultural land to produce the same amount of the former harvest. According to HIGGITT and LU (2001) this proportion is 1:5.

Though a total of approximately 19,895 ha of slopes were already transformed into terraced farmland and more than 20,400 ha of cropland was restored to forest or grassland from 2008 to 2009 (MEP, 2009, 2010) according to the slope steepness criterion (c.f., Annex II), soil erosion is a serious threat in the TGA. It dramatically increased in the post-construction time of the TGD. Also, the implementation of hedgerows by the local governments, *per se*, cannot be considered as effective at reducing runoff and soil loss (NG ET AL., 2008).

1.2.2.2 CURRENT STATUS OF SOIL EROSION IN THE THREE GORGES AREA

Before dam construction and resettlements started, the total annual soil loss in the TGA was estimated to be 157 million tons (~11% of annual soil loss by water erosion in the entire UYRB) producing an annual sediment delivery of about 41 million into the Yangtze River (SHI ET AL., 1992). For post-construction times, estimations on soil loss based on empirical soil erosion modeling, remote sensing, and radionuclides inventory revealed an increase of total annual eroded soil of about 20% accounting for 189 million tons. HU ET AL. (2009) estimate the sediment trapped behind the TGD to amount to annually 162 million tons from 2003 to 2007. The recent, average soil loss by water erosion is reported to range from 32.8 to 45 t ha^{-1} (LU and HIGGITT, 2000; ZHANG, 2008; WU ET AL., 2011b) for the whole TGA. This is distinctly more (~9 to 12.5%) than the average reported for Asian countries (c.f., Section 1.1). For extreme storm events during summer monsoon, ZHU ET AL. (2013) reported very high soil loss rates of 23 t km^{-2} on loamy to sandy loamy soils and a precipitation amount of 106 mm.

According to the *Soil Erosion Rate Standard* (c.f., XU ET AL., 2009), almost 77% of the total soil loss in the TGA occurs in areas of high to extreme erosion grades (WU ET AL., 2011b). The total area affected is estimated to be 33,000 km^2 (NG ET AL., 2008).

The water erosion is strongly linked to cultivated slopes (LU and HIGGITT, 2000; LONG ET AL., 2006; CUI ET AL., 2011). Sloping farmland greater than 10° accounts for approximately 78% of the total arable farmland in the TGA. Approximately 16% of the farmland occurs on slopes above the critical threshold of 25° over which cultivation is actually prohibited according to the WSCL (ZHANG, 2008; MEP, 2010; CUI ET AL., 2011). According to CUI ET AL. (2011), the regional average annual soil loss rates on sloping farmland ranges from almost 45 to 67 t ha^{-1} and are likely to exceed 10×10^3 t km^2 a^{-1} in places. For the small-scale catchments HeMinGuan and LiZiKou (< 20 km^2) in the watershed of the Yangtze tributary Jia Ling Jiang River, ZHU ET AL. (2013) proved the soil loss to be highly linked to the land use, also. Whereas from cropland areas the eroded soil amounted to 20 up to

hundreds of tons per km², soil loss in woodland was very low (< 10 t km^{-2}). The reported soil loss rates increased with higher slope gradients (ZHU ET AL., 2013). Thus, cultivation on slopes, especially conventional slope farming, is the largest contributor to soil erosion and sediment delivery in the TGA (c.f., LU and HIGGITT, 2000; NG ET AL., 2008; ZHANG, 2008; CUI ET AL., 2011; WU ET AL., 2011a).

1.2.2.3 ECOLOGICAL IMPLICATIONS OF SOIL EROSION IN THE THREE GORGES AREA

Along with the soil erosion, manifold environmental and socio-economic threats also occur. Soil erosion in the TGA is widely recognized as the reason for the reduction of soil fertility and agricultural productivity (NG ET AL., 2008), the impoverishment of the local people (XU ET AL., 2005; LIU and WU, 2010), and the reservoir siltation with threat to the long-term safe operation of the TGD (SHI ET AL., 2004; DAI ET AL., 2008; ZHANG, 2008; HU ET AL., 2009).

For instance, the farmland supply of suspended material is estimated to be 90% (CUI ET AL., 2011). Considering the application of pesticides to improve the farming performances in terms of crop yield and soil conservation (NG ET AL., 2008), the discharge of sediment linked to soil erosion might particularly increase the risk of eutrophication (DAI ET AL., 2010). From 2005 to 2009, the use of chemical fertilizers and pesticides increased by approximately 81% and 29% from 88,400 to 160,000 tons of fertilizers, respectively from about 541 to 699 tons of pesticides (SEPA, 2006; MEP, 2010). Most of these are nitrogen fertilizers (63-66%) and organic phosphorous fertilizers (48-49%) that are assumed to distinctly change the trophic status of the Yangtze River, especially in combination with the standing water of the reservoir (BIEGER, 2013). These figures might be even higher as they are based on the monitoring of only 156 towns and villages in 19 counties in the TGA (MEP, 2010). Due to diffuse matter transport by soil erosion and non-point source pollution, those particle-bounded agrochemicals enter the waterbodies and deteriorate the aquatic systems (e.g., LIU ET AL., 2003; PONSETI and LÓPEZ-PUJOL, 2006; DAI ET AL., 2010; CUI ET AL., 2011) with further effects on the drinking water quality, and aquatic biodiversity (LÓPEZ-PUJOL and REN, 2009; BERGMANN ET AL., 2012).

1.2.2.4 NEED FOR ENHANCED UNDERSTANDING OF SOIL EROSION IN THE THREE GORGES AREA

The destabilization of slopes during artificial drawdown processes at the dam (c.f., Annex V), high cutting slopes formed during the infrastructure construction, and the increasing number of landslides (e.g., WU and LUO, 2006; CUI ET AL., 2011; CHU ET AL., 2012) still might accelerate the potential of hillslope erosion. As reported by PIMENTEL (2006) landslides can trigger water erosion by dislodging soil and moving it downhill, consequently followed by an enhanced use of alternative land.

Furthermore, the economic-driven decisions by local farmers are expected to indirectly increase the soil erosion potential in the TGA. Whereas farmers participating in the *'Grain for Green Program'* (GFG; c.f., Annex II) were paid for converting their farmland into grassland or forests, no considerable improvement of their livelihood was observed (LONG ET AL., 2006). According to JIM and YANG (2006) and LONG ET AL. (2006), those farmers are even expected to reinstall their former farmland due to an end of the payments in order to improve their financial situation through agricultural products. Moreover, GFG that has been proved to effectively reduce the potential of runoff and soil erosion on converted land, decreased the available land for agriculture. This in turn is regarded to further increase the economic pressure on the remaining cropland (JIM and YANG 2006).

ZHANG (2008) concerns an already serious soil erosion problem causing a latent crisis of the agricultural environment which can likely been aggravated by the conflict potential between relocation from the resettlements and agricultural land. The fact that the, probably underestimated, 1.3 million people to be resettled (e.g., MCDONALD ET AL., 2008) had to be upwardly corrected to another 4 million that are expected to move by the year 2020 (OSTER, 2007), and that the infrastructure construction and land reclamation will still continue on a high and long lasting level, e.g., due to slope failure (LONG ET AL., 2008), distinctly reduce the carrying capacity of the TGA. The rapid population growth (i.e., growth of 2.5% from ~20.2 to ~20.7 million people from 2005 to 2008) combined with the intended increases in tourism throughout the entire TGA (china.org.cn[2]; c.f., Annex V) even accelerates the high conflict potential between available and suitable land (ZHOU ET AL., 2006; ZHANG ET AL., 2009; SEPA 2006, MEP, 2009).

Figure 3 *Challenging location of housing and farmland on frequently steep to very steep slopes in the TGA as observed in a large mountainous catchment of a first class tributary to the Yangtze River. Picture by S. Schönbrodt-Stitt.*

Also considering the projected future climate change, the water erosion is expected to increase across China, and thus in the soil-erosion prone TGA, too. Based on historical data and UKMO Hadley 3 climate scenarios, and the application of hydrological and soil erosivity models for the short-term (2001 to 2030), middle-term (2031-2060), and long-term (2061-2099) projections, SUN ET AL. (2002) predict a significant middle to long-term increase in rainfall erosivity, following a dry period in the short-term. From 2061 to 2099, the change of annual precipitation in the UYRB and TGA accounts for an increase of 10 to 30%. The predicted change of rainfall erosivity in this region amounts up to average 50% (SUN ET AL., 2002). Taking into account that the current land cover and land management throughout China would not change, the predicted water erosion rates will increase by 37 to 93% across China, subsequently referring to a distinct increase also for the TGA (SUN ET AL., 2002).

Against the background of the current physio-geographic and anthropogenic situation in the TGA and expected future changes for both, the control of soil erosion highly gains relevance and elicits a call for action. The control of soil erosion is an urgent and indispensable prerequisite for good soil management (BOT ET AL., 2000). It further implies the reduction of agricultural depletion and environmental risks linked to water erosion, and the contribution to ecological protection and to the functionality of the TGD. Minimizing soil erosion, e.g., through best managements practices (BMPs), such as well-adapted farming terraces, includes the urgent need for understanding the processes triggering soil erosion and their spatial and temporal variability. Additionally, sound knowledge and information on the quality and quantity, and the spatial distribution of hotspots of soil loss by water erosion are urgently needed. For large areas, predictive tools, such as erosion models, are commonly applied. Such models can provide a scientific base for decision making by assessing current erosion processes and predicting future trends of soil erosion (MORGAN, 2011). Though, ISWM (c.f., Section 1.2) has been integrated in more than 5,000 small watersheds typically less in size than 20 km² (SHI ET AL., 2012; ZHU ET AL., 2013), comprehensive analyses on water erosion in the TGA are largely constraint by a mismatch between existing data and data required for modeling and predicting the soil loss potential (ZHU ET AL., 2013). In addition to the data scarcity, by now little, respectively, hardly anything is known about the status and dynamic of soil erosion and its processes on the scale of complete catchments of major tributaries to the Yangtze River covering by far more than the above mentioned 20 km². According to ZHU ET AL. (2013), the large majority of those studies conducted on soil erosion and its countermeasures in the TGA refer to experimental designs and do not take into account the typical field settings. As the large drainage area of the TGA (c.f., Section 1.2.2) is subject to a variety of land use changes and physio-geographic settings, especially those ‘typical field settings’ on the catchment-scale are expected to reflect the current situation and to hold a great significance for the knowledge on the quality and quantity on soil erosion and its improvement. Moreover, such highly dynamic ecosystems under high socio-economic pressure from large dam building projects are of

particular interest for geo-risk (e.g., soil erosion) research since they are an integral part of the economic development in less-developed countries (e.g., ADAMS, 1993; BROWN ET AL., 2008). In addition, they often represent highly diverse and pristine geo-ecosystems, which offer valuable and particularly sensitive ecosystem functions and services (GUO and GAN, 2002; TIAN ET AL., 2007).

Moreover, the partly dramatic environmental TGD-induced impacts are assumed to gradually expand towards the currently largely wooded headwater zones in the TGA (SCHÖNBRODT-STITT ET AL., 2012). Considering this fact, the urgent need of proper management and conservation decisions, in order to reduce the extent and intensity of soil erosion in such a mountainous region with a low carrying capacity, even increases. Also looking at further more than 20 large dam projects that have been projected in the 'Yangtze cascade' (PONSETI and LÓPEZ-PUJOL, 2006) and large-scale hydropower projects on the global scale, it seems logical to perceive soil erosion in the surrounding of large dams and their reservoirs as a serious environmental threat and to contribute to a better understanding of human-induced land use changes and its effects on soil erosion.

2 STARTING POINTS OF THE RESEARCH AND OBJECTIVES

The overall aim of the present thesis is to investigate the risk potential of soil erosion by water and to identify the processes triggering soil erosion by water in a large hydrological and mountainous catchment that was considered to adequately reflect the typical physio-geographic settings and anthropogenic interferences in the TGA.

As the interaction of factors and processes enhancing or reducing water erosion in the TGA are highly complex, a sound knowledge on the inherent physical vulnerability to water erosion, respectively, natural soil erosion risk potential is considered to present a suitable starting point for the assessment of the natural soil erosion potential and - based on that - the evaluation of the effect of the TGD on the water erosion. In the newly created and highly dynamic reservoir of the TGA, the associated land use changes are assumed to result in a distinct change in the spatial distribution and quantitative dimension of the water erosion potential. Considering the vegetation cover to constitute a key factor in the erosive process and to be highly influenced by land use changes, precise information on its spatial and temporal variability are essential for soil erosion analysis. Due to the water erosion being strongly influenced by rainfall erosivity and in order to account for the superimposed role of the climate and terrain on the rainfall characteristics, knowledge on the rainfall erosivity at a certain place is also essential. Since bench terraces exhibit a key technology for the control of soil erosion with a long tradition in the TGA, the rapid ongoing and extensive land use changes are also expected to likewise impact the cultivated farming bench terraces and to lead to their degradation. Assuming those bench terraces to have a crucial role in the sustainable land management in mountain areas, they are additionally considered as essential precondition in the soil erosion risk evaluation.

Based on the considerations and restrictions imposed by the data scarcity, the central research objectives of the present thesis are:

(i) Spatial analysis and assessment of the soil erosion risk potential under natural conditions and the effect of the TGD on the soil erosion risk potential,

(ii) Spatial and temporal analysis of the vegetation cover and its effects on the soil erosion potential,

(iii) Determination and spatial regionalization of the rainfall erosivity that can be run with limited data and addresses the mountainous topography and

(iv) Analysis of the current status of cultivated bench terraces and spatial analysis of the strength and direction of the effect of TGD project on the terraced landscape.

After a brief introduction into the study framework providing an overall context of this thesis and the description of the study area, available data are listed and the modeling framework is presented

(*Chapter 3*). The description of the study area is essentially based, unless quoted otherwise, on results from the field campaigns and GIS-based analyses conducted within the study framework.

Chapter 4 addresses the research objectives (i) to (iv), and explores and summarizes the most relevant and intrinsic results and discussions. Each of the subchapters in *Chapter 4* refers to published contributions in a book (*Chapter 4.1*) and peer-reviewed journals (*Chapters 4.2*, *4.3*, *4.4*).

Chapter 4.1 aims at the modeling of the natural soil erosion risk potential and the soil erosion risk under former and current land uses in order to assess the erosion-relevant effect of the TGD and to identify hotspots of soil erosion in the mountainous study area. *Chapter 4.2* aims at the spatially more detailed and multi-temporal analysis of the vegetation cover represented by a crop and management factor. Due to remote sensing (RS) as only available data source, environmental covariates on the vegetation were derived from space-borne data and a regression function was applied. Serving as reference to the computed results, data on the land uses were taken from literature. The effect of both on the soil erosion risk potential was then modeled using the same approach as in *Chapter 4.1*. The central aim of *Chapter 4.3* is to present a methodology on the best approximation of the rainfall erosivity for a subtropical and mountainous catchment based on worldwide applied regressions functions. Finally, *Chapter 4.3* focuses on the spatial regionalization of the rainfall erosivity performing best onto the catchment scale. Both aspects covered in *Chapter 4.3* account for the data scarcity in terms of spatial and temporal resolution. *Chapter 4.4* introduces into *TerraCE* (Terrace Condition Erosion), a framework that was specifically developed for modeling and analyzing terrace conditions in order to invest their current status and the terrace degradation. By embedding environmental and anthropogenic indicators derived from RS data as well as classes on the terrace conditions from field mapping surveys into a spatial data mining approach, *Chapter 4.4* aims at a better understanding of the terrace degradation and the strength and direction of its driving factors.

As this thesis is part of an interdisciplinary project aiming on the ecological and environmental risks of the TGD project, the results provide information on areas at risk linked to soil erosion and contribute to further ecological and eco-hydrological modeling, and an enhanced understanding of the complexity of human-environmental interactions in the TGA.

3 MATERIALS AND METHODS

3.1 STUDY FRAMEWORK

The environmental changes in the TGA resulting from the huge dimensions of the dam project form the scientific focus of the German-Chinese joint YANGTZE Project 'Sustainable Management of the Newly Created Ecosystem at the Three Gorges Dam'. This joint research collaboration was initiated by the Research Centre Jülich (Germany) in 2002. It consists of two thematic blocks aiming at the ecological consequences resulting from the (i) land use changes, soil erosion, mass movements, and diffuse matter inputs (YANGTZE GEO) and from the (ii) interactions of water, sediment and contaminants in the reservoir of the TGA (YANGTZE HYDRO; BERGMANN ET AL., 2012).

YANGTZE GEO aims at the assessment and analysis of soil erosion, landslides, and diffuse matter inputs as well as particle-bounded contaminants such as phosphorus into the reservoir. The main goal is to gain a better and profound understanding of the causes and mechanisms of the ecological consequences of the TGD and their spatial and temporal dimensions and dynamics by analyzing, modeling, predicting, and evaluating their risk potential.

For this purpose, five subprojects (SPs) located at the German universities of Tübingen (SP 'Soil Erosion'), Erlangen-Nuremberg (SP 'Mass Movements'), Giessen (SP 'Land Use Change'), Kiel (SP 'Diffuse Matter Inputs'), and Potsdam (SP 'Remote Sensing'), and their Chinese partner from the China University of Geosciences in Wuhan (P.R. China) used a multidisciplinary approach on the catchment scale combining research from the fields of soil science, geology and geo-engineering, hydrology, and RS. Close thematic and methodological linkages of the five subprojects enabled for a rapid transfer of data but also for a synthesis of the results and detailed consideration of the interactions of the dynamic land use changes and the above geo-risks.

Within YANGTZE GEO, the environmental studies were conducted in the mountainous catchment of the Xiangxi River. The Xiangxi catchment was considered to adequately represent the reservoir of the TGA in terms of physical settings and human interventions attributing to the TGD.

3.2 STUDY AREA

3.2.1 GEOGRAPHICAL POSITION AND STUDY SCALES

The hydrological catchment of the Xiangxi River (香溪) is located in western Hubei province in Central China and covers an area of 3,208.8 km². It is largely covered by the preponderantly rural counties Zigui, Xingshan, and Shennongjia. The largest towns in the Xiangxi catchment are Xiakou, Gaoyang, and Gufu (Figure 4).

The Xiangxi River originates in the Shennongjia Forest Nature Reserve. After a passage of approximately 100 km, the Xiangxi River joins the Yangtze River as a first class tributary almost 40

km westward of the TGD. The largest distances in west-east direction and from north to south are approximately 72 km and 73 km, respectively.

Due to the Yangtze River impoundment by the TGD, the Xiangxi River is also affected. The newly created reservoir (Xiangxi Bay) in the 'Backwater area' stretches from the outlet approximately 35 km towards Gaoyang in the central Xiangxi catchment (Figure 4). This Backwater area (558.9 km²) and two further hydrological sub-catchments were selected for further detailed, multi-scale environmental research within YANGTZE GEO as here dam-induced consequences are obvious and were observed to be directly linked to the TGD project (SEEBER ET AL., 2010). The two sub-catchments are Xiangjiaba (2.8 km²) on the eastern riverside and Quyuan (87.3 km²) on the western riverside (Figure 4).

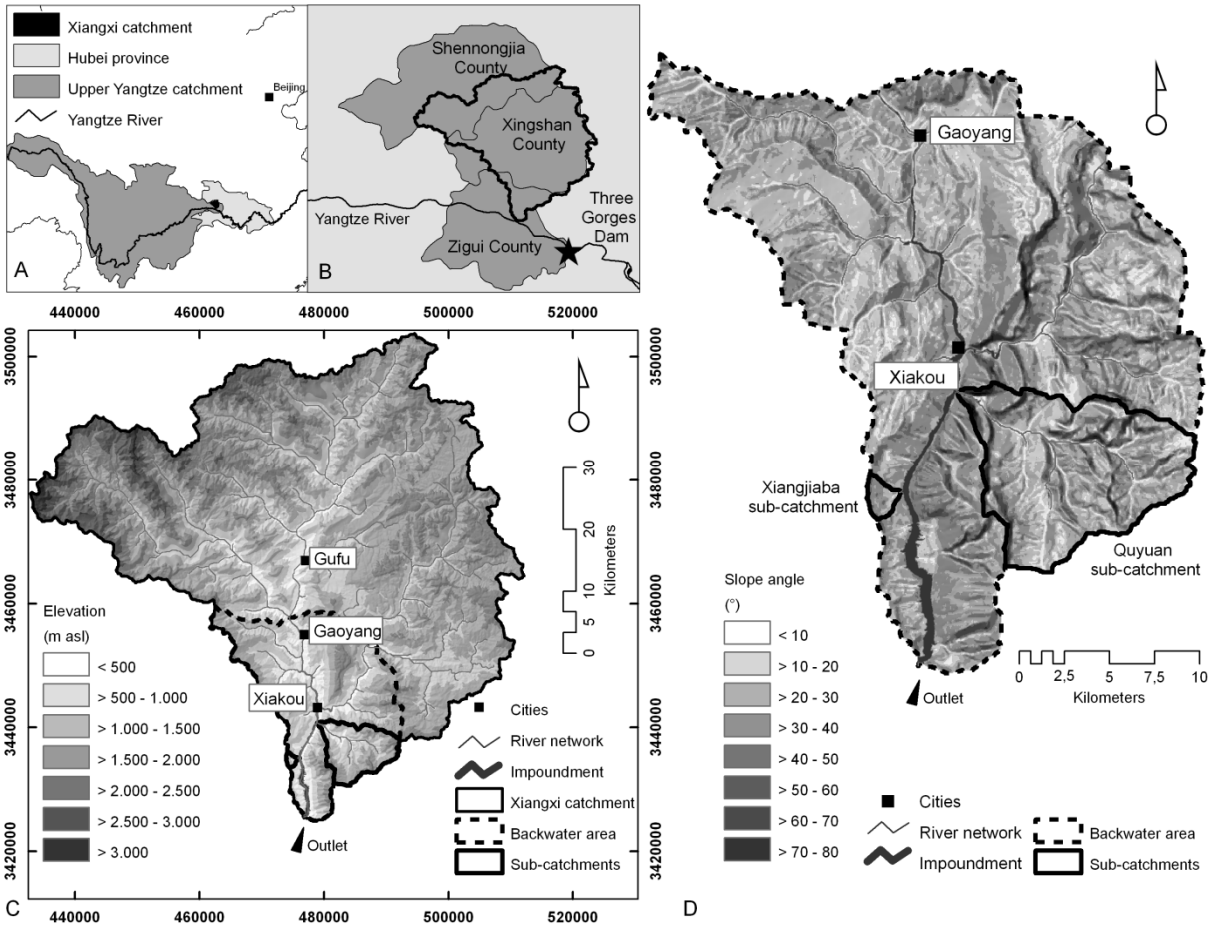

Figure 4 *Location of the Xiangxi catchment in the Upper Yangtze River Basin in China and in the western Hubei province (A) with the counties Shennongjia, Xingshan, and Zigui (B). Geographical position (UTM WGS 1984, Zone 49 N) of the Xiangxi catchment and its range of elevation (m a.s.l.) based on the SRTM-DEM in a spatial resolution of 45 m × 45 m (C). Slope angels in the Backwater area with the sub-catchments Xiangjiaba and Quyuan (D). The slope angle is based on the steepest slope algorithm introduced by* TARBOTON *(1997). GIS and Layout by S. Schönbrodt-Stitt.*

3.2.2 CLIMATE IN THE XIANGXI CATCHMENT

Located in the humid subtropics of China, the climate of the Xiangxi catchment is mainly characterized by prevailing winds from the north, and the impact of the southwest monsoon (HE ET AL., 2003). It is further strongly influenced by the Qinling mountain range in the north. This mountain range serves as climatic border between North and Central China and hinders cold air masses from the north advancing to the south (HE ET AL., 2003). Consequently, the Xiangxi catchment typically exhibits an unimodal rainfall regime with humid and hot summers and moderate dry winters (Figure 5). Mean annual precipitation (MAP) at Xingshan climate station close to Gaoyang is 1,000 mm for the WMO climate normal period from 1961 to 1990. Approximately 77% of the MAP during this period falls in rainy season from May to October. From 1971 to 2000, MAP is slightly lower (991 mm), however, about 78% of rainfall occurs during rainy season. Mean annual temperature is 16.9 °C for both periods. According to HE ET AL. (2003) and WU ET AL. (2006), the precipitation in the Xiangxi catchment is typically convective referring to an orographic precipitation pattern based on the range of elevation. The range of elevation causes a distinct vertical climate spectrum with thermal zones referring to specific elevation bands and strongly correlating with the increases in MAP (WU ET AL., 2006). These are from the outlet of the Xiangxi River at 62 m a.s.l. to the highest elevation (Mount Shennongjia in the northern catchment) at 3,078 m a.s.l.: the Mid subtropics (1,000 mm MAP at < 500 m a.s.l.), the Northern subtropics (1,200 mm MAP up to 500 m a.s.l.), the Southern temperate (1,600 mm MAP up to 800 m a.s.l.), the Mid temperate (2,000 mm MAP up to 1,200 m a.s.l.), and the Northern temperate (2,400 mm MAP above 1,200 m a.s.l.).

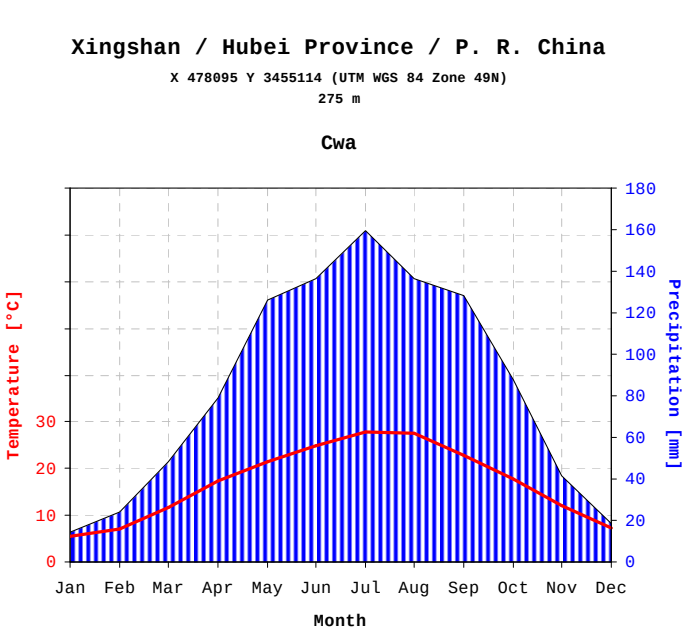

Data from 1961 to 1990

Data by: National Meteorological Information Center, China

Layout by: S. Schönbrodt, 2009

Month	Temp. [°C]	Prec. [mm]
Jan	5.4	14
Feb	7.0	24
Mar	11.6	48
Apr	17.2	79
May	21.3	126
Jun	24.9	137
Jul	27.8	159
Aug	27.6	136
Sep	22.8	128
Oct	17.7	88
Nov	12.1	42
Dec	7.2	19

Mean temperature
16.9 °C

Precipitation
1000 mm

Figure 5 *Climate diagram for Xingshan station in the central Xiangxi catchment with long-term average monthly temperature (°C) and precipitation (mm) from 1961 to 1990.*

3.2.3 TERRAIN AND GEOLOGY IN THE XIANGXI CATCHMENT

The mountainous Xiangxi catchment, ranging in average with 1,230 m a.s.l., is characterized by steep to extremely steep slopes (Figure 4). Seventy-three percent of the catchment area exhibits inclinations above 20°. In average, the slopes incline with 39° (standard deviation is approximately 23°). Occasionally, slopes in the southern Xiangxi catchment exhibit maximum inclinations of 78°. Typical for the steepest slopes, mainly belonging to the Triassic formation at the eastern riverside in the Backwater area, are extreme slope lengths (Figure 6). In exceptional cases, they can reach lengths of maximum 760 m.

***Figure** 6 The Xiangxi River, and the alternation of the Triassic limestone exhibiting extreme slope lengths and the less steep sloping and morphological softer Jurassic sandstone, siltstone, and claystone in the Backwater area of the Xiangxi catchment. The viewing direction is northeast. Picture by S. Schönbrodt-Stitt.*

The terrain of the Xiangxi catchment reflects the geological structure of the TGA. The crystalline basement composed of pre-Sinian magmatic and metamorphic rocks belongs to the Yangtze Block (EHRET ET AL., 2010). The Sinian to Middle Triassic sequence consists of predominantly marine carbonate-clastic sediments. Upper Triassic to tertiary formations are dominated by continental shallow-water clastic and, partly, organic sediments. Crystalline rocks are prevailing in the eastern part of the Xiangxi catchment and sedimentary rocks in the southern, western, and northern

catchment area (EHRET ET AL., 2010). Central feature of the southern Xiangxi catchment is the alternation of Triassic limestone resistant to weathering in higher altitudes and morphological softer Jurassic sandstone, siltstone, and claystone in the lower regions (EHRET ET AL., 2010; Figure 6).

3.2.4 SOILS AND SOIL ERODIBILITY IN THE XIANGXI CATCHMENT

Linked to the high terrain energy and to the lithology, the Xiangxi catchments shows a high diversity of soils (THORP, 1936; KOVDA, 1959). According to data of the Second National Soil Survey (SNSS) in China that was conducted from 1979 to 1994 (SHI ET AL., 2010), eight major soil groups can be located in the Xiangxi catchment (Figure 7). Following the *Chinese Soil Taxonomic Classification* (CSTC) and their area percentage, the soils are classified as Chao soils (< 1%), Paddy soils (2%; ~64 km²), Yellow soils (4%; ~128 km²), Dark brown soils (4%; ~128 km²), Purple soils (5%; ~160 km²), Brown soils (7%; ~225 km²), Limestone soils (38%; ~1219 km²), and Yellow browns soils (40%; ~1284 km²).

Brown soils develop in higher altitudes, typically under coniferous forest conditions on carbonate-free bedrock (HONG and CHEN, 1990). They are located in the eastern Xiangxi catchment and stretch belt-like above the humous Dark brown soils. Dark brown soils develop under humid temperate monsoon climate. They are characterized by a high solum thickness, high base saturation, and neutral to alkaline pH. In China, Dark brown soils constitute typical soils of mountain regions and form optimal locations for large forest areas (HONG and CHEN, 1990). In the Xiangxi catchment, they are exclusively distributed in altitudes from 2,200 to 3,000 m a.s.l. in Shennongjia county (Figure 4). The fersialitic subtropic Yellow brown soils are typical for the low mountains and hilly regions alongside the Yangtze River. Dependent from their bedrock, the solum thickness of those soils strongly varies (HONG and CHEN, 1990). In the Xiangxi catchment, the Yellow brown soils belong to the dominating soil types. Their main distributional range is located in the eastern and northeastern as well as in the central study area. The clayey, fersialitic and acidic Yellow soils are mainly distributed alongside the lower reaches of the Xiangxi River, and in the central and eastern catchment area. In China, Yellow soils typically occur in tropic and subtropic mountain areas (HONG and CHEN, 1990). Shallow carbonate Limestone soils are very characteristic for the Xiangxi catchment. They are largely linked to the Sinian to Middle Triassic sequence and the Upper Triassic to tertiary formation. In the Backwater area of the Xiangxi catchment, the Limestone soils exclusively occur on the eastern riverside that is characterized by the extreme steep sloping Triassic limestone. Paddy soils are typical agricultural soils throughout subtropical China. Due to artificial land leveling and terracing in combination with seasonal, artificial flooding, they exhibit typical processes of oxidation and reduction (HONG and CHEN, 1990). Paddy soils are rather atypical for the Xiangxi catchment and are only located on scattered plots in the eastern Backwater area. The silty Purple soils typically

predominate as Regosols in the Xiangxi catchment and have been primarily developed in lower altitudes on hematite-rich Jurassic purple sandy shale and purple sandstone, and Jurassic siltstone. Compared to the Purple soils on uphill-slope positions those on downhill-slope position show higher solum thicknesses. Together with the Paddy soils, Purple soils account for the most fertile soils in the Yangtze River region (HONG and CHEN, 1990). In the study area they are exclusively distributed on the Jurassic formation at the western side of the Xiangxi River. Due to the CSTC being strongly focused on the agricultural relevance of the soils, the soils in the Xiangxi catchment can only roughly be transferred into the standard of the international classification system of the *World Reference Base for Soil Resources* of the FAO (SHI ET AL., 2010). In terms of their geomorphologic positions and their bedrock, the soils in the Xiangxi catchment mainly refer to Cambisols, Luvisols, Alisols, Regosols, Leptosols, Fluvisols, and Gleysols (IUSS Working Group WRB, 2007).

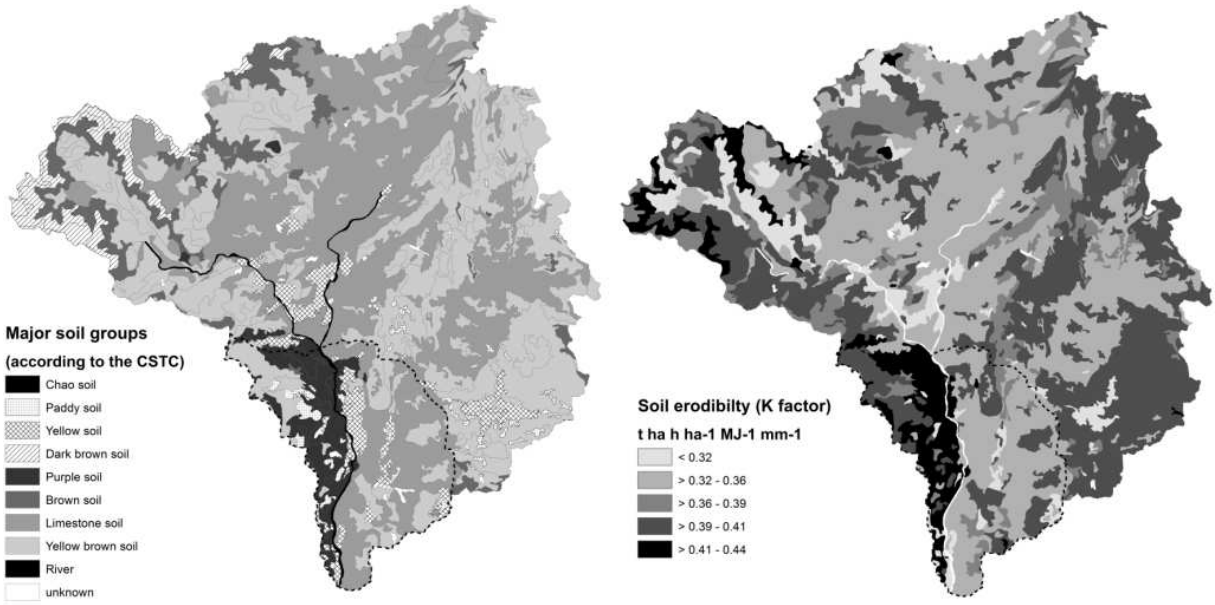

Figure 7 *Spatial distribution of the major soil groups in the Xiangxi catchment based on the Chinese Second National Soil Survey (below). The classification of soils refers to the Chinese Soil Taxonomic Classification (CSTC). Spatial distribution of the soil erodibility (t ha h ha^{-1} MJ^{-1} mm^{-1}) based on the major soil groups in the Xiangxi catchment (above). GIS and layout by S. Schönbrodt-Stitt.*

The erodibility of the topsoils (0 - 20 cm depth) in the Xiangxi catchment strongly refers to the soils' mostly silty-loamy soil texture. Based on the analysis of the available 126 topsoil samples in the Xiangxi catchment taken from the SNSS and the calculation of the erodibility according to SHIRAZI and BOERSMA (1984), the topsoils show a moderate to high erodibility to water erosion ranging from 0.30 to 0.44 t ha h ha^{-1} MJ^{-1} mm^{-1}. With 0.39 t ha h ha^{-1} MJ^{-1} mm^{-1}, the average soil erodibility, represented by the RUSLE *K* factor (WISCHMEIER and SMITH, 1978), in the Xiangxi catchment is high. The standard deviation is 0.05 t ha h ha^{-1} MJ^{-1} mm^{-1}. Based on 245 topsoil samples taken during

the field campaigns, the average soil erodibility in the Xiangxi catchment is slightly lower (0.36 t ha h ha^{-1} MJ^{-1} mm^{-1}). The standard deviation is 0.13 t ha h ha^{-1} MJ^{-1} mm^{-1}. The total range of soil erodibility based on field data varies from 0.09 to 0.64 t ha h ha^{-1} MJ^{-1} mm^{-1}, indicating much higher but also very low topsoil's resistance to particle detachment and transport by water. Highest soil erodibilities (> 0.39 to 0.44 t ha h ha^{-1} MJ^{-1} mm^{-1}, respectively, 0.64 t ha h ha^{-1} MJ^{-1} mm^{-1}) are located on the western bank of the Xiangxi River in the Backwater area, respectively, in the Xiangjiaba sub-catchment (Figure 7). Here, the high soil erodibility refers to the Purple soils on Jurassic strata, however, they are also linked to Yellow brown soils, Dark brown soils, and Paddy soils (Figure 7). Lowest soil erodibilities (< 0.32 t ha h ha^{-1} MJ^{-1} mm^{-1}) are linked to Yellow soils and Brown soils, mainly distributed in the central and northern Xiangxi catchment (Figure 7). Moderate soil erodibilities ranging from more than 0.32 to 0.39 t ha h ha^{-1} MJ^{-1} mm^{-1} are typical for the Limestone soils that largely cover the catchment area, and partially for Yellow brown soils (Figure 7).

In the Xiangxi catchment, sheet and rill erosion constitute the major processes of water erosion. Sheet erosion in form of rainsplash and shallow flows, but also microrills (< 2cm depth) can be found on nearly every place throughout the whole Xiangxi catchment, on agricultural and non-agricultural land (Figure 8). They typically exhibit an initial stage of frequently distributed linear rill erosion (> 10 cm depth). Rill erosion typically occurs on cultivated non-terraced, but also terraced farmland where they can be manually obliterated. Rill erosion also occurs alongside narrow paths (Figure 8). Although gullies (> 40 cm depth) can be observed at a few places without any soil conservation on steep land with porous vegetation (Figure 8), they do not constitute typical types of water erosion in the Xiangxi catchment. Soil trapped behind trunks of trees, and silted up stairways, runoff disposals and dry-stone walling of terraces as well as larger amounts of accumulated soil alongside the high cutting roads further indicate high soil erosion dynamics in the Xiangxi catchment.

3.2.5 LAND USE AND LAND USE CHANGE

The land use in the Backwater area is strongly linked to the terrain, with the Xiangxi River acting as a kind of dividing line between mainly agricultural cultivation on the western riverside and mainly forests and shrubs with scattered plots of cultivation on the eastern riverside (Figure 6). Management cash crop farming mixed with lower productive subsistence farming located on higher altitudes strongly characterizes the cultivation on the western bank. Steep garden plots are characterized by the small-scale cultivation of legumes, vegetables, fruits, and chili (SEEBER ET AL., 2010). The rainfed cultivation of oranges classified as garden land according to SEEBER ET AL., (2010), and paddy rice, dry land and steep garden plots, referring to the land use class arable land, are typical for the southern Xiangxi catchment. Typical dry land crops are rape, wheat, sesame, soybeans, potatoes, and maize.

Figure 8 *Soil erosion in the Xiangxi catchment.*

Plate A. Micro-rills on a field cropped with vegetables.

Plate B. A special type of soil erosion - little earth pillars.

Plate C. Rill erosion on a non-terraced plot cropped with vegetables.

Plate D. Extreme rill erosion on a non-terraced plot cropped with oranges.

Plate E. Extreme rill erosion observed along a path.

Plate F. Extreme rill erosion on a terraced plot cropped with maize and vegetables.

Plate G. Gully erosion on a silty-clayey loam on a non-terraced plot cropped with oranges.

Plate H. A deep-carved erosion rill stretches for approximately 20 meters along a terrace cropped with a few soybeans. Partially, this rill is deeper than 40 cm and initially forms a gully.

Plate I. Extreme rill erosion on a silty-clayey loam makes this plot permanently unusable.

Plate J. Extreme rill erosion on a very steep sloping hillside exposes the residential house and farmland to risk.

Pictures by S. Schönbrodt-Stitt (2008-2012).

Farming typically occurs on contour-aligned bench terraced with dry-stone walling (Figure 9). Those bench terraces are spatially distributed all-over the hillslopes on almost the whole range of altitudes, particularly adjacent to the impounded Xiangxi River. In the Backwater area, they typically show a high small-scale diversity of terrace conditions in terms of terrace design (e.g., terrace slope, height of terrace wall, and width of terrace riser) and state of maintenance with a varying number of

wall disorders, such as wall collapses (Figure 9F). According to a survey on bench terraces conducted in the Backwater area, the terraces are predominantly (> 75 %) outward sloping (Figure 9G). Only in very rare cases, the bench terraces show level or inward sloping terrace risers (Figures 9C and 9D). This diversity of terrace conditions due to inadequate terrace design and lack of constant maintenance is assumed to indicate the process of terrace degradation with the effect of a varying effectiveness of protecting the soil against surface erosion by runoff.

The headwater zone of the Xiangxi catchment is strongly characterized by large dense woodland with deciduous trees and conifers (GUO ET AL., 2000). Evergreen forests, sparse shrubland, and grassland occur on the highest elevations in Shennongjia county (SEEBER ET AL., 2010). Large areas of cultivation are atypical for the mountainous and steep sloping headwater zone. Scattered plots of arable land with dry land crop cultivation and rarely paddy rice exclusively occur alongside the river network with less steep sloping topography and on the plateau of HuangLiangPing northeast of Gaoyang (Figure 10). Occasionally, the cultivation of tobacco can be observed, too (SEEBER ET AL., 2012). Tea plantations are typical for the Northern temperate zone above 1,200 m a.s.l, however do not appear in the land use classification due to difficulties in differentiating their spectral signature from woodland (BIEGER, 2013).

According to SEEBER ET AL. (2010), the land use in 2007 in the Xiangxi catchment was characterized as the following: woodland 87%, arable land 9.5%, and garden land with orange orchards (2.2%). Only marginal areas in the Xiangxi catchment were covered with bare rock and grassland (both 0.4%), reservoir, respectively inland water (0.3%), and built-up land (0.2%) as shown in Figure 10.

In their study on land use change in the Xiangxi catchment using satellite imagery, SEEBER ET AL. (2010) estimated the area lost to the river impoundment by the TGD to be approximately 9.4 km² from 1987 to 2007. This land previously used for agriculture and settlement had to be compensated causing land use changes on approximately 26% of the Backwater area in close distance to the new Xiangxi reservoir (Figure 10). With 66%, the broadest change is observed in the Xiangjiaba sub-catchment close to the flooded Xiangxi River. In the Quyuan sub-catchment, the land use changes account to 17%, thus, almost four times lower compared to the Xiangjiaba sub-catchment. Within the entire Xiangxi catchment, the portion of area affected by land use changes equates to 12% from 1987 to 2007 (SEEBER ET AL., 2010).

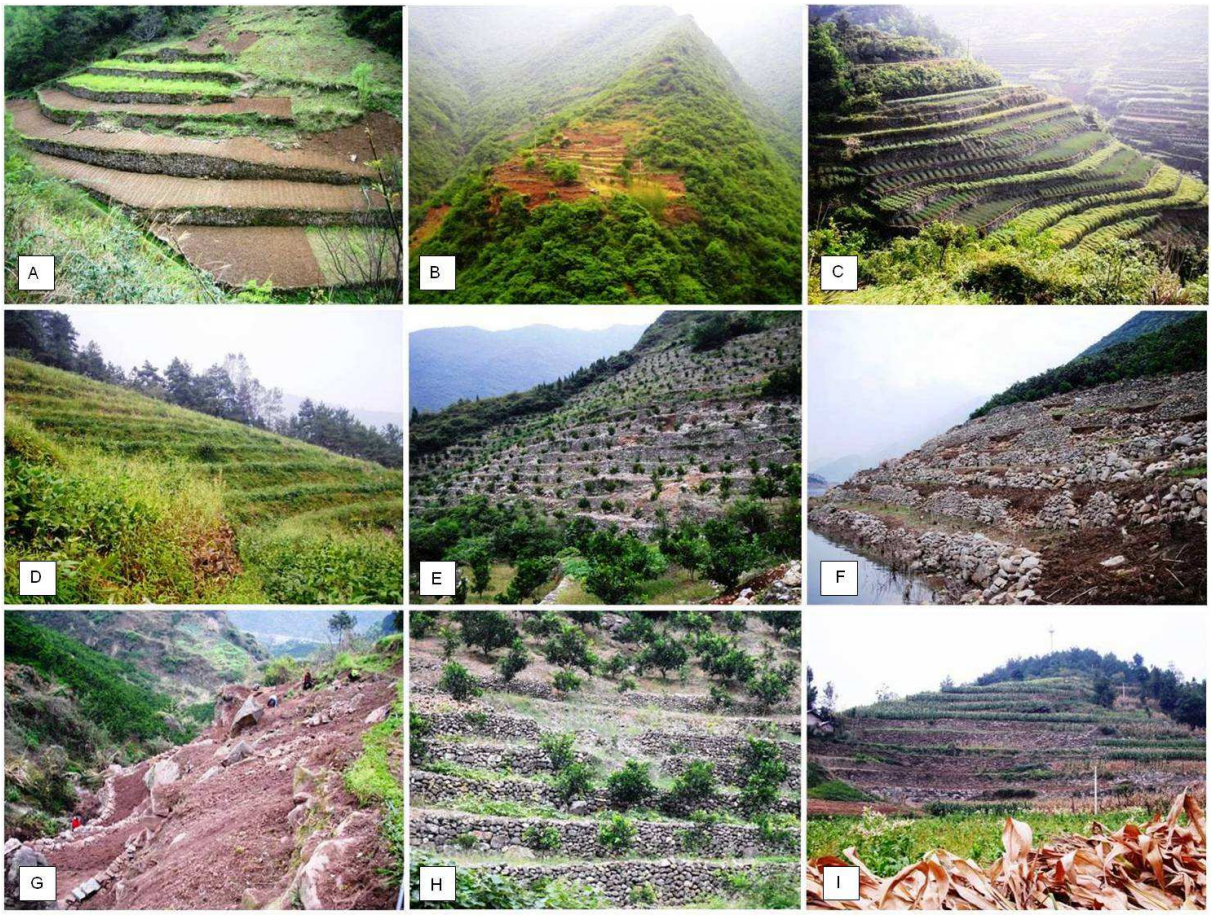

Figure 9 *Diversity of farming bench terraces in the Xiangxi catchment on hillsides sloping with more than 5°. Plates A and B. Steep garden terraces for subsistence farming; Quyuan sub-catchment. Plate C. Paddy terrace that is also used for the cultivation of rape; Quyuan sub-catchment. Plate D. Slightly inward sloping bench terrace completely covered with dense vegetation; headwater zone of the Xiangxi catchment. Plate E. Terrace cropped with oranges on a steep slope adjacent to the seasonally impounded Gaolan River, a first class tributary to the Xiangxi River. Plate F. Terrace cropped with oranges that is on the half of its area seasonally flooded due to the artificial water level fluctuations at the dam (c.f., Annex V); Backwater area. Plate G. Small-scale subsistence farming terrace under construction (April 2009) on steep slopes adjacent to a depth contour; Xiangjiaba sub-catchment. Plate H. A terrace that is no longer used for subsistence farming but cropped with oranges; Quyuan sub-catchment. Plate I. Terrace cropped with maize near HuangLiangPing on a plateau; western Xiangxi catchment. Pictures by S. Schönbrodt-Stitt (2008-2010).*

The remote areas in the north-eastern and north-western part of the Xiangxi catchment only show slight land use changes (Figure 10) in form of a decrease of arable land from approximately 13% to 10% from 1987 to 2007 and an increase of woodland from approximately 84% to 87% for the same period. According to SEEBER ET AL. (2010) this greening is likely to be induced by governmental programs such as GFG (c.f., Annex II). Contrary to a general greening in the Xiangxi catchment, the immediate vicinity of the reservoir, particularly the Xiangjiaba sub-catchment, shows a decrease of woodland from about 49% to 45% (SEEBER ET AL., 2010). The portion of arable land in the Backwater area decreases from about 21% to 12%, and more notably from approximately 36% to 14% in the

Xiangjiaba sub-catchment SEEBER ET AL. (2010) state that arable land in the Backwater area has largely been replaced by orange land, again especially pronounced in the Xiangjiaba catchment and immediate vicinity of the reservoir. Here, the area with orange orchards increased from 15% to about 42%. The change of rate of orange orchards in the entire Xiangxi catchment from 1987 to 2007 amounts to approximately 29%. In the Backwater area and further beyond towards Gufu, orange orchards distinctly predominate on terraces close to large settlements and main transportation routes such as trafficable main roads and navigable rivers (SEEBER ET AL., 2010). Climatologically, this area also refers to the mid-tropic zone below an elevation of 500 m a.s.l. that is suitable for citrus growth (WU ET AL., 2009) and allows for optimal cash crop production (c.f., Section 1.2.2.1).

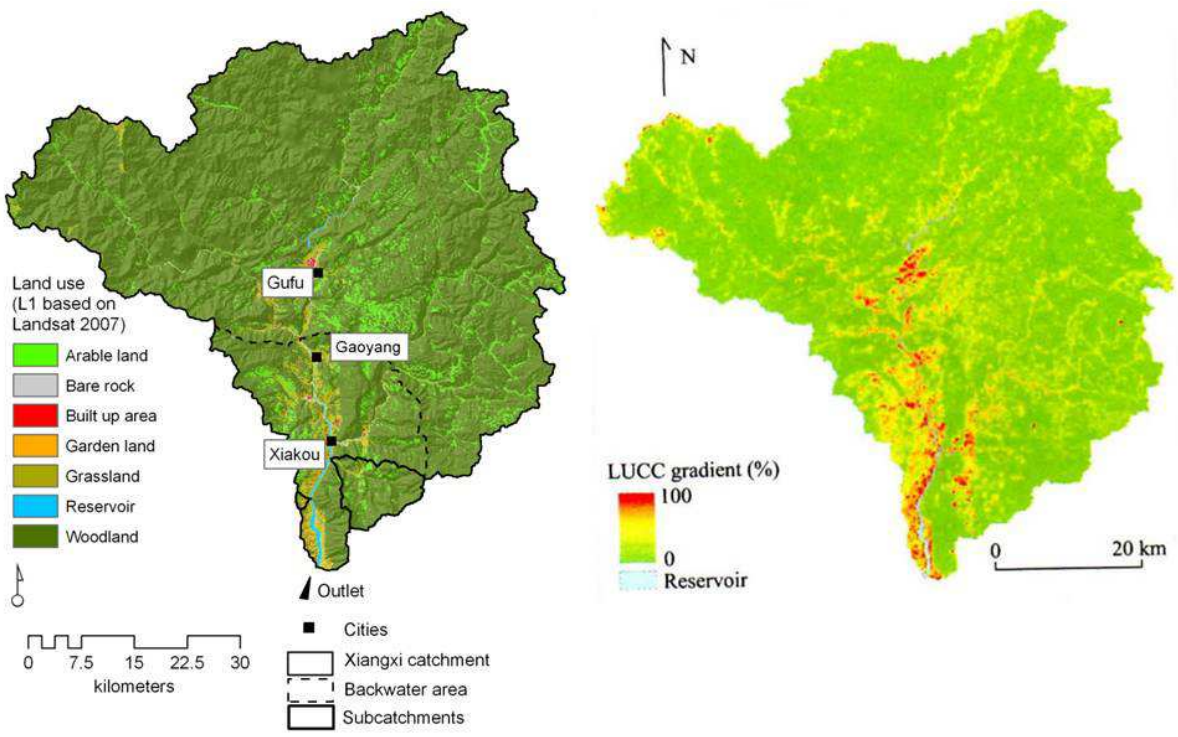

Figure 10 *Land use classification in the Xiangxi catchment based on Landsat-TM 2007 (left) and gradient on the land use and land cover change (LUCC) on the catchment scale (right) from 1987 to 2007. LUCC gradient was derived from post-classification change analysis, expressing the change intensity in a spatial resolution of 150 m × 150 m from 0 (no change within raster cell) to 100% (complete change within raster cell). For the left figure: data by SEEBER ET AL. (2010), GIS and layout by S. Schönbrodt-Stitt. Right figure after SEEBER ET AL. (2010).*

Though, the change of rate of built-up land from 1987 to 2007 was revealed as negligible in the Xiangxi River and Backwater area (SEEBER ET AL., 2010), road and building constructions strongly determine the landscape in the southern catchment (Figure 11). Such stresses imposed by human activities happen in steep sloping challenging topography. For instance, in the entire Xiangxi catchment, sloping farmland greater than 5° accounts for almost 94% of the total cultivated area in the year 2007 (calculations based on the land use classification from 2007). In the Backwater area, this

proportion is even higher by 4%. Approximately one third of these slopes (Xiangxi catchment: ~35%, Backwater area: ~36%) are classified as 'reclamation-forbidden' according to the WSCL as they exhibit inclinations greater than 25° (c.f., Annex II).

Figure 11 *Land use dynamic in the Xiangxi catchment associated with the impoundment of the Yangtze River by the Three Gorges Dam.*

Plate A. Though the Chinese government has implemented the WSCL prohibiting illegal logging (Chapter II, Article 13; c.f. Annex II), people - even if rarely - cut trees for the reasons of firewood and land reclamation.

Plate B. Construction sites for rural houses and agriculture compete with each other on steep slopes (Xiangxi catchment).

Plates C and D. During the process of resettlement, new residential houses have to be built in a challenging topography (Xiangxi catchment and Badong).

Plate E. New roads carve their way into the mountainous and wooded landscape (near Badong).

Plates F and G. For the crossing of difficult terrain and rivers, new bridges and roads were built in an exhilarating tempo. Therefore, tunnels had to be blasted into the bedrock of limestone, siltstone, and claystone as observed in the Xiangxi catchment, here at Gaolan river.

Pictures by S. Schönbrodt-Stitt (2008-2012).

3.3 GEODATABASE

In the Xiangxi catchment legacy data is rarely available and access to terrain is limited or restricted due to missing roads and other logistic reasons. Available data vary in spatial coverage, spatial resolution, and temporal consistency (Tables 1 and 2). Thus, the most suitable database to assess relevant variables covering large areas is provided by space-borne RS data.

In particular, information from Digital Elevation Models (DEM) from the Shuttle Radar Topographic Mission (SRTM) are widely applied in soil erosion studies (e.g., HANCOCK ET AL., 2006; VRIELING, 2007; VRŠČAJ ET AL., 2007) since they provide presentations of landforms and allow for derivation of topographic information for grid-based analysis.

For poorly mapped regions, such as the Xiangxi catchment, SRTM-DEM data can offer large benefits for catchment studies. Contrary to SRTM-DEMs in a resolution of 1-arc-second (30 m cell size), those in a coarser resolution of 3-arc-second (90 m cell size) are freely available for most regions of the world (ZANDBERGEN, 2008). However, topographic features representing the geomorphology and hydrology relevant for soil erosion modeling (e.g., slope, aspect, flow accumulation flow path length, contributing area) cannot always be adequately captured at the coarse scale of 90 m and thus, produce artifacts (e.g., LYNN USERY ET AL., 2004). Since the SRTM-DEM in 3-arc-second were generated from the 1-arc-second data by sub-sampling using the center values of each 3×3 cells (KEERATIKASIKORN and TRISIRISATAYAWONG, 2008) for regions outside the United States, refinement of the DEM data to a finer resolution than 90 m using different interpolation techniques, such as bicubic polynomical interpolation, kriging, spline, IDW, and natural neighbor, proved as successful without a loss of significance and, thus, as beneficial in terms of adequate landscape representation (GROHMANN, 2006, VALERIANO ET AL., 2006; HER and HEATWOLE, 2008; KEERATIKASIKORN and TRISIRISATAYAWONG, 2008). Because of this, the spatial resolution of the available SRTM-DEM covering the Xiangxi catchment was improved using bilinear re-sampling as no impact of the re-sampling on the analysis but benefit from the higher spatial resolution was expected. The 'target' resolution was set to 45 m × 45 m as this cell size adequately captures the environmental indicators by avoiding artifacts resulting from a few pixels along a slope compared to the original resolution of 90 m. Moreover, this cell size allows for reasonable computation time.

Since terracing as a key soil conservation technology in the Xiangxi catchment (c.f., Section 3.2.5) is also linked to specific terrain conditions, digital terrain analysis can further provide indicators, which show effects on terrace conditions. Rather than providing indicators describing the local terrace design which is limited by the spatial resolution of the DEM, terrain analysis aim at providing information on the natural landscape surface characteristics without terraces. This allows determining effects relevant for differentiating terrace conditions, since the general flow paths and velocities of runoff still follows the natural terrain above the terrace plot scale. For instance, if the

contributing area increases, the water pressure by infiltration and interflow on the terrace plot is assumed to increase, too. Additionally, terrain can be used as a proxy for other environmental covariates such as climate or parent material (BEHRENS ET AL., 2010a, b). A typical example is the elevation as a spatially explicit covariate on the rainfall (c.f., Section 3.2.2). Thus, the DEM (Table 1) served as most powerful data source and has been mostly used throughout the studies for digital terrain analyses such as the derivation of erosion-relevant properties of the terrain (e.g., erosive slope length and slope angle).

Table 1 *Available data sources for soil erosion modeling in the Xiangxi catchment and their spatial resolution and applicability as well as references of use in the studies conducted within the framework of the present thesis.*

Type	Data*	Purpose/Applicability	Resolution**/ Recording	Reference
Remote sensing data	DEM based on SRTM data version 4 (JARVIS ET AL., 2008)	Digital terrain analyses	90 m × 90 m / 45 m × 45 m	*Manuscripts 1,2,3, and 4*
	Landsat-5-TM (Thematic Mapper), path 125, row 38, 2005 (2005-09-09), 2006 (2006-09-12), and 2007 (2007-09-15	Land cover analyses, derivation of environmental covariates on the crop and management factors	30 m × 30 m / 45 m × 45 m	*Manuscripts 2 and 4*
	Land use classification from 1987 and 2007 (SEEBER ET AL., 2010)	Model parameterization, random agricultural plot selection for the terrace survey	30 m × 30 m / 45 m × 45 m	*Manuscripts 1, 2, and 4*
	SPOT5 image from 2007 (2007-09-21) and Google Earth data (varying dates)	Reference base, basis for field mapping and for deriving data on the road network, settlements, and the shoreline of the Xiangxi River after the impoundment	5 m × 5 m	*Manuscript 4*
Maps	Soil types based on the Second National Soil Survey in China (SHI ET AL., 2010)	Soil classification, calculation of the soil erodibility	1:180,000 and 1:160,000, 126 soil profiles	*Manuscript 1, 2*
Point data	Soil profiles and topsoil samples (0 - 20 cm) roperties)	Analysis of erosion-relevant soil physical and chemical properties, plausibility check	245 soil profiles and topsoil samples	*Manuscript 1, 2*
Poyline data	Road network	Plausibility check for the road networks digitized from SPOT5	More than 386 kilo-meters of road	*Manuscript 4*
Point data	Rainfall data from the National Meteorological Information Centre of China	Determination of rainfall characteristics and calculation of rainfall erosivity	6 stations, daily recording	*Manuscript 2*

** all data were projected to UTM WGS 1984, Zone 49N, ** original/re-sampled*

Data on the land cover, and vegetation cover, respectively, is based on Landsat-5 (Thematic Mapper) images. In total, three Landsat-TM scenes showing the lowest cloud and haze cover

throughout the observations years were used for gridded analyses (Table 1). They served as data source for the derivation of environmental covariates on the crop and management cover on the catchment scale and as available input for the analyses of a possible influence of the land cover on the terrace degradation over time. Internal and external errors of these RS images, primarily due to atmospheric and topographic effects of rugged and steep sloping areas (JENSEN, 2000; RICHARDS and JIA, 2006), were reduced by means of image preprocessing (atmospheric, radiometric, and geometric corrections) using ATCOR for ERDAS IMAGINE® according to NEUBERT and MEINEL (2005) and RICHTER (2010).

Additionally, two land use classifications based on Landsat-TM images from 1987 and 2007 (Table 1), conducted for the Xiangxi catchment by SEEBER ET AL. (2010), were applied for parameterization of the soil erosion model and for random plot selection of agricultural land for the field mapping of terrace conditions. According to SEEBER ET AL. (2010), the land use classification from 1987 presents the time before the political enforcement of the TGD, its first feasibility study, and the environmental impact assessment (c.f., Annex V). In contrast to the pre-construction land use classification, the one from 2007 presents the post-construction phase referring to the time after the establishment of resettlement schemes as well as completion of dam construction (c.f., Annex V).

An ortho-rectified, panchromatic, and geo-referenced SPOT image (Table 1) was used as master scene for geo-referencing multi-spectral datasets and for data conducted within field surveys such as GPS-tracks of roads (Table 1). In combination with available, adequate Google Earth data covering the study area, both datasets further served as basis for field mapping and for deriving anthropogenic indicators by digitizing (Table 1). For instance, since neither precise information nor spatial data on the human activities in the TGA were available, both datasets were used to derive proxy indicators. According to INBAR and LLERENA (2000), the distance from a village is an important component in the erosion-relevant process of terrace degradation. Hence, spatial Euclidian distance transforms (e.g., of the digitized settlement areas) served as one indicator on the human influence. The same influence was assumed for the distance to roads and to the river network. Due to the river impoundment, the Xiangxi River and its major tributaries in the Backwater area became navigable. Consequently, comparable to the road network, Euclidian distance transforms to different orders of the river network system served as proxies on the accessibility of terraces and thus human activity.

Besides RS data, available legacy data on the soil erosion factors 'rainfall' and 'soil' were checked for their applicability and accordingly pre-processed.

For the derivation of the rainfall erosivity from precipitation data, climate data from the National Meteorological Information Centre of China (NMIC) were used. As daily precipitation data were only available for one station (Xingshan station) in the central Xiangxi catchment, precipitation data from five other available climate stations lying closest to the study area were included. According

to the NMIC, these stations are Badong, Shennongjia, Yichang, Yichangxian, and Zigui (Table 2). Despite for Yichangxian station, rainfall erosivity was calculated for each station as the requirement on long-term recording is fulfilled allowing for a comparison of long-term average observation and climate trends according to the recommendation by the World Meteorological Organization (WMO).

Table 2 *Geographical position (UTM WGS 1984, Zone 49 N; X = Northing, Y = Easting), elevation, and length of daily rainfall records of the climate stations in the Xiangxi catchment and its surrounding area.*

Station	X	Y	Altitude (m a.s.l.)	Start date of record (day-month-year)	End date of record (day-month-year)	Length of daily record (year/month/day)
Badong	442491	3437891	295	01-07-1952	31-12-2007	45/06/00
Shennongjia	469423	3512773	950	01-01-1975	31-12-2007	32/11/29
Xingshan	477772	3455484	275	01-01-1958	31-12-2007	50/00/00
Yichang	528850	3396689	134	01-08-1951	31-12-2007	56/07/00
Yichangxian	530978	3396689	116	01-01-2003	31-12-2007	05/00/00
Zigui	469765	3429644	151	01-04-1959	31-12-2007	48/09/00

Soil data originates from soil maps and descriptions based on the SNSS (c.f., Section 3.2.4). In the Xiangxi catchment, the soils were surveyed at a scale of 1:160,000 to 1:180,000. The available data were pre-processed in terms of geo-referencing and digitizing. An additional *in situ* soil survey was conducted at a scale of 1:5,000 to 1:10,000. The focus of this soil survey was to determine soil types according to the WRB and to get erosion-relevant soil physical and chemical properties (i.e., grain sizes, bulk density, carbonate, soil organic matter). In total, 245 soil profiles, respectively, topsoil samples (0 - 20 cm) from forest and farmland plots were analyzed and used for a plausibility check of the soil map from the SNSS after personal communication with Prof. Dr. X. Shi from the Institute of Soil Science in Nanjing, Chinese Academy of Sciences. Based on this, the gridded soil map covering the whole Xiangxi catchment and linked soil profile descriptions from the SNSS were used as input in the soil erosion modeling.

Considering the DEM as most relevant base for digital terrain, all further available, conducted, and computed data were converted to exact the same spatial resolution of 45 m × 45 m and same grid origin. This provides exact support of field data and computed data for modeling to avoid negative, random influences from finer scales.

3.4 SOIL EROSION MODELING

In order to minimize soil erosion, e.g., through well-adapted land management and conservation practices, information on the soil erosion risk potential and its spatial and temporal variability is needed. For large areas, such as the Xiangxi catchment, predictive tools (e.g., soil erosion models) are commonly applied.

3.4.1 THE REVISED UNIVERSAL SOIL LOSS EQUATION

The soil erosion risk potential in the Xiangxi catchment was estimated using the Revised Universal Soil Loss Equation (RUSLE; RENARD ET AL., 1997). It is a soil erosion prediction technology and presents an advanced version of the empirical Universal Soil Loss Equation (USLE).

Based on long-term series of measurements and studies by ZINGG (1940) and MUSGRAVE (1947), the USLE was originally developed by WISCHMEIER and SMITH (1965) to predict the average annual rate of soil erosion at the field scale on gently undulating land. The USLE was designed for conditions in the Middle West of the U.S., based on investigations of standardized unit plots on clean-tilled continuous bare fallow and slopes inclining with 9% and a slope length of 22.13 m (WISCHMEIER and SMITH, 1965). By integrating statistical analyses and relationships from more than 11,000 plot-years of research data from 47 locations in 24 states (GILLEY and FLANAGAN, 2007), the grey-box model structure of the USLE expresses the long-term annual average conditions under different cropping and management systems in the U.S. for a given set of rainfall, soil, and topographic settings (MORGAN, 2011). Though, this standardized, empirical model has been widely applied in soil science and environmental planning, critiques on the restriction of the parameter calibration and on its applicability to the conditions for which it was developed (e.g., EL-SWAIFY ET AL., 1982; MCCOOL ET AL., 1987; RENARD ET AL., 1991) led to subsequent revisions by the U.S. Department of Agriculture (USDA; RENARD ET AL., 1997).

Major regionally and locally specific improvements of the basic model structure aimed at the strength of the prediction of soil loss on a wider range of field conditions above the field scale or standardized 'Wischmeier plot' (TOY and RENARD, 1998). A runoff factor was added to the driving force of flow detachment processes that has been primarily described with the modification of the rainfall energy by the slope length and slope angle (JETTEN and MANETA, 2011). RENARD ET AL. (1997) further define the criteria for the identification of an erosive single storm event, e.g., a threshold value of >12.7 mm to separate erosive from nonerosive rainfall as suggested by WISCHMEIER and SMITH (1978) and BROWN and FOSTER (1987). Further improvements, for instance, included the modification of the calculation of the soil erodibility and the crop and management factors to account for their inter-annual variability and dynamic by implementing more field- and time-specific sub-factors, such as the surface cover and roughness sub-factors, and the soil moisture sub-factor (RENARD ET AL., 1997; TOY and RENARD, 1998; MORGAN, 2011). The calculations of the slope steepness and slope angle were also reconstituted to improve their accuracy and to extend the model applicability to steeper hillslope gradients in complex areas that was primarily considered as one of the most stressed arguments on the inability of the USLE (e.g., MCCOOL ET AL., 1987; EL-SWAIFY, 1997; RENARD ET AL., 1997; KONZ ET AL., 2009

Following these improvements, the RUSLE represents a much more 'fit-to-purpose' model (GOVERS, 2011). It can be applied as land use independent to a much higher variety of field settings including disturbed and undisturbed lands (e.g., agricultural sites, forests, mining and constructions sites), and newly or established reclaimed land (TOY and RENARD, 1998). Thus, it is a widely used tool on the assessment and inventory of soil erosion to assist public development and to improve soil conservation and environmental planning by governments and private consultants (RENARD ET AL., 1997; USDA-ARS, 2010).

As its predecessor, the RUSLE involves six major factors that affect upland soil erosion in terms of sheet erosion by raindrop impact and overland flow, and rill erosion (TOY and RENARD, 1998). These factors are: rainfall erosivity, soil erodibility, slope length, slope steepness, cropping management techniques, and supporting conservation practices (WISCHMEIER and SMITH, 1978; RENARD et al., 1997). Using a set of mathematical equations in a multiplicatory approach, the RUSLE for agricultural land is written as (Eq. 1):

$$A = LS \times R \times K \times C \times P \qquad \text{(Eq. 1)}$$

where A is the potential long-term, average annual soil loss (t ha^{-1} a^{-1}), R is the rainfall erosivity (MJ mm ha^{-1} h^{-1} a^{-1}), LS is the combined factor from the terrain-based slope length factor L (dimensionless; -) and the terrain-based slope steepness factor S (dimensionless; -), K is the soil erodibility (t ha h ha^{-1} MJ^{-1} mm^{-1}), C is the crop and management factor (dimensionless; -), and P is the support practice factor (dimensionless; -).

The RUSLE can be run by using computer interfaces such as RUSLE2 (USDA-ARS, 2010), but can also be implemented into GIS-based modeling by integrating and manipulating spatial gridded data on the above factors, for instance based on available RS, DEM, and maps. According to MORGAN (2011), the success and wider range of application of the RUSLE, especially, lies in the fact that DEMs can be converted into *LS* maps based on direct calculations or on the integration of the drainage network (e.g., flow accumulation, contributing area), and thus soil losses can be predicted on the catchment scale for each grid-cell.

Compared to more detailed process-based models like WEPP (Water Erosion Prediction Project; FLANAGAN and NEARING, 1995), EROSION3D (SCHMIDT ET AL., 1999), and EUROSEM (European Soil Erosion Model; MORGAN ET AL., 1998), the empirical RUSLE is however regarded to have limitations in terms of describing more complex physically-based water erosion processes (e.g., sediment delivery and deposition). Nevertheless, the easy to parameterize model structure, the lower requirements of input data, and less model run time give the RUSLE an advantage in comparison to the more complex models. Thus, it belongs to one of the worldwide most applied soil erosion prediction technologies (TOY and RENARD, 1998), which was already often applied in China and in

the TGA focusing on the evaluation of soil conservation measures, on the soil erosion risk potential, and on soil erosion dynamics (e.g., SHI ET AL., 2004; LIU and LUO, 2005; ZHOU AND WU, 2008; XU ET AL., 2009; LI ET AL., 2010; HUANG ET AL., 2012; PANG ET AL., 2013). Considering all these facts and against the background of sheet and rill erosion being the dominating water erosion processes (c.f., Section 3.2.4), the complex steep sloping mountainous areas (c.f., Section 3.2.3), and the data scarcity in terms of spatial and temporal resolution (c.f., Section 3.3), the RUSLE was thus considered to fit to the conditions in the Xiangxi catchment.

3.4.2 MODEL PARAMETERIZATION

Model parameterization of the RUSLE was done for two first model runs on the soil erosion risk potential under natural conditions, and under former and current land use conditions. This enabled to analyze to what extent the Xiangxi catchment is prone to soil erosion without any human influence, and to analyze the effect of the land use change associated to the TGD on the soil erosion risk potential.

The soil erosion risk potential under natural conditions - or natural disposition to soil erosion - was estimated following (Eq. 1), however, without consideration of any soil conservation measure as the Xiangxi catchment was assumed to be undisturbed by human activities. Contrary to the approach used by DA SILVA ET AL. (2011) to predict the natural erosion potential for the Brazilian territory without taking into account potential natural vegetation, the Xiangxi catchment was assumed to be completely covered with woodland. Large woodland areas without any human impact resulting from agriculture or settlement can recently be observed for Shennongjia region in the northwestern headwater zone of the Xiangxi catchment (Figure 10). Moreover, based on experimental plot studies in a Chinese subtropical forest ecosystem, GEIßLER ET AL. (2010, 2013) proved the erosive power of throughfall drops and a distinct impact of forest vegetation on soil erosion. Thus, the *C* factor was set to 0.005 as proposed by LIU and LUO (2005) for woodland in the TGA.

The natural soil erosion risk potential in the Xiangxi catchment was calculated using (Eq. 2):

$$A_{nat} = R \times K \times LS \times C_{wood} \quad \text{(Eq. 2)}$$

where A_{nat} is the average annual natural soil erosion risk potential (t ha^{-1} a^{-1}) and C_{wood} refers to the crop and management factor (dimensionless; -), however, is here dealt as vegetation cover.

The combined topographic, DEM-based factor *LS* was derived from pre-processed separate grids on *S* and *L* using the RUSLE approach according to RENARD ET AL. (1997) that was also applied by KONZ ET AL. (2009) for complex steep sloping areas using (Eq. 3) and (Eq. 4).

$$L\,factor = (\lambda / 22.13)^m \quad \text{(Eq. 3)}$$

with

$$m = \beta / (1 + \beta), \quad \beta = (sin(\theta)) / 0.0896) / (3 * [sin(\theta)]^{0.8} + 0.56)$$

and

$$S\,factor = 0.063 + 10.461 * \sin(\theta) \quad \text{for slopes} < 5.14° \quad \text{(Eq. 4a)}$$

$$S\,factor = 16.8 * \sin(\theta) - 0.5 \quad \text{for slopes} \geq 5.14° \quad \text{(Eq. 4b)}$$

where θ is the slope gradient (°), λ is the real slope length referring to the flow length (m), m is the slope length exponent (-), and β is the susceptibility to rill erosion (-). Therefore, the *S* factor was derived from a slope grid based on the steepest slope algorithms introduced by TARBOTON (1997). Before computation of the *L* factor, the upstream flow length (m) was derived using Monte-Carlo-aggregation to simulate flow divergence reflecting a more natural spatial flow pattern in complex landscapes (BEHRENS ET AL., 2008).

Due to the facts that at the time of the first model runs precipitation data on a daily basis were only available for one climate station (Xingshan station near Gaoyang; Figure 4) and that the precise calculation of the *R* factor necessitates consistent long-term data with a high temporal resolution to assess single storm events (WISCHMEIER and SMITH, 1978; RENARD ET AL., 1997), a single *R* value was taken from literature. The used value on rainfall erosivity is *R* = 2,880 MJ mm ha^{-1} h^{-1} a^{-1} (SHI ET AL., 2004). It was derived for the mountainous Wangjiaqiao watershed in Zigui County 50 km northwest of the TGD. The value is based on the method by WISCHMEIER and SMITH (1978) and is assumed to correspond to the climate regime of the Xiangxi catchment.

As the classification of the soil texture throughout the SNSS (Table 1) refers to the Russian classification system according to KACHINSKY (1965) based on the ratio of particle sizes smaller than 0.01 mm, the *K* factor was calculated according to SHIRAZI and BOERSMA (1984) using (Eq. 5):

$$K = 7.594 \left\{0.0017 + 0.0494 exp\left[-\frac{1}{2}\left(\frac{log(Dg) + 1.675}{0.6987}\right)^2\right]\right\} \quad \text{(Eq. 5)}$$

where D_g is the geometric average particle size. The equation is based on the symmetric Gaussian distribution of geometrically average particle sizes and was recommended by SONG ET AL. (2005) for Chinese soil textures and for short enough data. The *K* factor was calculated for the topsoil data of each of the 126 available soil profiles from the SNSS (Table 1) using the original soil particles data.

Aiming at the TGD-induced impact of the land use changes on the soil erosion, the soil erosion risk potential in the Xiangxi catchment was estimated using (Eq. 1) for agricultural land (c.f., Section 3.4.1). Therefore, the two land use classifications from 1987 and 2007 (Table 1, c.f., Section

3.3) were used for model parameterization. Both classifications incorporate the same land use classes (Table 3; SEEBER ET AL., 2010).

For the first model set up, values on the *C* factor were taken from literature, as no previous adequate data were available and monitoring on specific vegetation and crop parameters in the study area was considered not practical and unfeasible. Those *C* factor values refer to the land use classes depicted for the Xiangxi catchment by SEEBER ET AL. (2010) as shown in Table 3 and have been assigned to the according land use pixel on the catchment scale. They represent common seasonal crop rotations within one year for subtropical agriculture in the Wangjiaqiao and Taipingxi watersheds in the TGA (SHI ET AL., 2004; LIU and LUO, 2005) close to the Xiangxi catchment. Thus, they are supposed to adequately represent the conditions in the study area. Contrary to the original purpose of the USLE to predict soil erosion solely on agricultural land (WISCHMEIER and SMITH, 1978), the potential soil loss in the Xiangxi catchment was modeled including all land use classes representing soil vegetative cover (i.e., woodland and grassland; Table 3) in order to assess the complete land cover-induced range of soil erosion. The classes 'bare ground' and 'reservoir' (Figure 10) were not considered. Assuming the settlements in the Xiangxi catchment (rural and urban) to be associated with small-scale home gardening - as often observed during the field campaigns from 2008 to 2010 - the class 'built-up' was also parameterized (Table 3). Generally, the higher the *C* factor values, the less the crop and vegetation cover and thus, protection against soil erosion.

Table 3 *C factor values for model parameterization of the RUSLE for the land use in the Xiangxi catchment. The land uses refer to the classification by SEEBER ET AL. (2010).*

Land use class	*C* factor value	Reference
Arable land	0.46	LIU and LUO (2005)
Orange orchard*	0.13	SHI ET AL. (2004)
Paddy field**	0.18	LIU and LUO (2005)
Steep garden plots**	0.1	LIU and LUO (2005)
Woodland	0.005	LIU and LUO (2005)
Grassland	0.2	ERENCIN (2000)
Built-up land	0.08	LIU and LUO (2005)

** The land use class 'orange orchard' refers to 'garden land' in the land use classification by SEEBER ET AL., (2010; c.f., Section 3.2.5). ** Only parameterized in the prediction of the soil erosion risk potential in Manuscript 2.*

For both calculations, the further RUSLE factors *K* and *R* were kept constant. The *LS* factor was calculated with (Eq. 3) and (Eq. 4) using a slope grid based on the steepest slope algorithm introduced by TARBOTON (1997) as done in estimating A_{nat}. The *L* factor also refers to the upstream flow length (m) that was derived using Monte-Carlo-aggregation. However here, the flow lengths were calculated grid-based from the DEM individually for each agricultural class considered in the model parameterization according to the separate land use classification from 1987 and 2007. Doing so allows for simulating flow divergence reflecting the spatial agricultural pattern.

Since dry-stone walling bench terraces are common features in the Xiangxi catchment (c.f., Section 3.2.5), terraces were considered in the estimation of the soil erosion risk potential under former (1987) and current (2007) land use with the *P* factor assigned to the land use classes 'arable land' and 'orange orchard' (Table 3). As for the first model runs no data on the spatial distribution and design of bench terraces were available, data on the supporting conservation practices refer to rough estimates. Thus, *P* was set to 0.55 as suggested by SHI ET AL. (2004) and LIU and LUO (2005) for dry-stone walling level bed terraces on land sloping between 20° and 25°.

The grid-based estimates on the A_{nat}, and A_{1987} and A_{2007} were then classified according to the Chinese Soil Erosion Rate Standard (Technological Standard of Soil and Water Conservation SD238-87). Thus, five numerical classes issued by the Ministry of Water Resources (LU and HIGGITT, 2000; XU ET AL., 2008; XU ET AL., 2009) give information about the soil erosion risk potential based on the calculated average annual soil loss.

The spatial resolution of all soil loss estimations in the Xiangxi catchment, the Backwater area, the sub-catchments Xiangjiaba and Quyuan is 45 m × 45 m as this is the spatial resolution of the database (c.f., Section 3.3).

4 OVERVIEW ON THE MANUSCRIPTS

4.1 SOIL EROSION IN THE MOUNTAINOUS CATCHMENT OF THE XIANGXI RIVER

(Manuscript 1, published as book chapter in TÜBINGER GEOGRAPHISCHE STUDIEN 151, pp. 27-83, ISBN 978-3-88121-089-8)

Based on the model assumptions and parameterization using the RUSLE, ***Manuscript 1***, *inter alia*, deals with the average annual soil erosion risk potential under former land use conditions in 1987 and under current land use conditions in 2007 to assess the impact of the TGD on the soil erosion by water in the Xiangxi catchment (c.f., Sections 3.3 and 3.4.2). To oppose the soil erosion risk potential under the influence of land use and thus, human impact, to quasi natural conditions, *Manuscript 1* further aims at the average annual natural soil erosion risk potential (natural disposition to soil erosion).

The average annual soil erosion risk potential considering the Xiangxi catchment as completely forested (c.f., Section 3.4.2) ranges from about 6 to 11 t ha^{-1} a^{-1} (Table 4). The average annual soil losses under the impact of land uses, such as arable land and orange orchards, are distinctly higher and range from average 264 t ha^{-1} a^{-1} in 1987 to average 188 t ha^{-1} a^{-1} in 2007. This is basically due to the effect of the *C* factor ranging from completely forested with high vegetative protection cover to agricultural uses with less protection by the crop cover (c.f., Section 3.4.2). Even the soil conservative effect of the terracing, considered with the *P* factor, cannot completely mitigate the effect of the crop cover. Interestingly, the land use in 2007 has a mitigating effect on the soil erosion risk potential compared to the land use in 1987. The differences are particularly obvious when looking at the maxima soil losses (Table 4). In the sub-catchments, the maxima annual soil losses reduce by approximately 300 to 400 t ha^{-1} a^{-1} from 1987 to 2007 (Table 4). This reduction is mainly due to the conversion of arable land to orange orchards and small scattered forested plots as well as abandonment of farmland driven by governmental programs, such as GFG (c.f., Annex II; c.f., Section 3.2.5). Independent of the period considered the potential average annual soil losses in the Quyuan sub-catchment, ranging from about 11 to 345 t ha^{-1} a^{-1}, are always highest throughout the sub-units (Table 4). This is mainly due to extreme high slope lengths and angles of the mainly Triassic formation reflecting the steeper topography in the Quyuan sub-catchment compared to the Xiangjiaba sub-catchment that generally shows lower relief energy (c.f., Section 3.2.3).

The spatial distribution of soil losses underpins the very high soil erosion risk potential in the Backwater area. Whereas under natural conditions only 6.3 % (~35 km^2) of the Backwater area exhibit moderate to extreme (> 25 - > 80 t ha^{-1} a^{-1}) potential annual soil losses, a trend of reciprocal conditions can be observed under the influence of land use. With 25.3 % (~141 km^2) in 1987 and 26.7 % (~149 km^2) in 2007, the percentage of areas exhibiting moderate annual soil losses is distinctly higher (Figures 12B-C). This trend develops in favor of a greater extent of areas under high (1987: 2 % or

~11 km²; 2007: 2.5 % or ~14 km²) and extreme (1987: 17.9 % or ~100 km²; 2007: 11.4 % or ~64 km²) soil erosion risk potential. The areas of moderate to high natural soil erosion risk potential occur as scattered plots mainly alongside the steep to extremely steep sloping Triassic formation on the eastern side of the Xiangxi River (Figure 12A). Under the consideration of land use as well as terraces, a different spatial pattern of average annual soil losses emerge with distinct hotspots of the soil erosion risk potential. These predominantly stretch alongside the lower reaches of the Xiangxi River and on the western side of the Xiangxi River, such as in the Xiangjiaba sub-catchment (Figures 12B-C).

Table 4 *Average annual soil erosion risk potential (t ha^{-1} a^{-1}) under natural conditions (natural soil erosion risk potential) and under the impact of land use in 1987 and 2007 in the Xiangxi catchment and the sub-units considered.*

	Natural soil erosion risk potential	Soil erosion risk potential under land use in 1987	Soil erosion risk potential under land use in 2007
Xiangxi catchment			
Maximum	146.4	5,264.6	5,057.9
Minimum	0.0	0.0	0.0
Average	10.3	263.8	188.3
SD	8.9	332.2	260.6
Backwater area			
Maximum	104.2	3,898.0	3,812.3
Minimum	0.0	0.0	0.0
Average	9.6	256.5	169.3
SD	9.0	306.9	227.2
Quyuan sub-catchm.			
Maximum	69.4	2,673.2	2,256.9
Minimum	0.0	0.0	0.0
Average	10.7	344.9	229.3
SD	9.0	376.2	283.2
Xiangjiaba sub-catchm.			
Maximum	24.7	1,232.9	945.1
Minimum	0.0	0.0	0.0
Average	5.9	245.5	128.2
SD	4.8	230.0	142.1

SD = standard deviation, sub-catchm. = sub-catchment, SD = standard deviation

Based on the Caesium-137 (^{137}Cs) technique, QUINE ET AL. (1999) reported rates of actual soil loss by water erosion under comparable subtropical conditions for Yanting in Sichuan province (UYRB) of 51.5 t ha^{-1} a^{-1} for farming land sloping with 6.2°, which is comparable to the Xiangxi catchment where average annual soil losses on farmland sloping with 5° to 8° amount to 54.4 t ha^{-1} a^{-1} in 1987 to 50.7 t ha^{-1} a^{-1} in 2007.

Although the modeling results have a limited spatial resolution of 45 m × 45 m, *Manuscript 1* demonstrates that the application of the RUSLE adequately reflects the general situation and the spatial distribution of areas highly prone to soil erosion in the Xiangxi catchment. It gives reliable estimations of soil erosion that are comparable to results revealed by other studies in the TGA (e.g., YAO, 1993; QUINE ET AL., 1999; LU and HIGGITT, 2000; GUO ET AL., 2001; SHI ET AL., 2004).

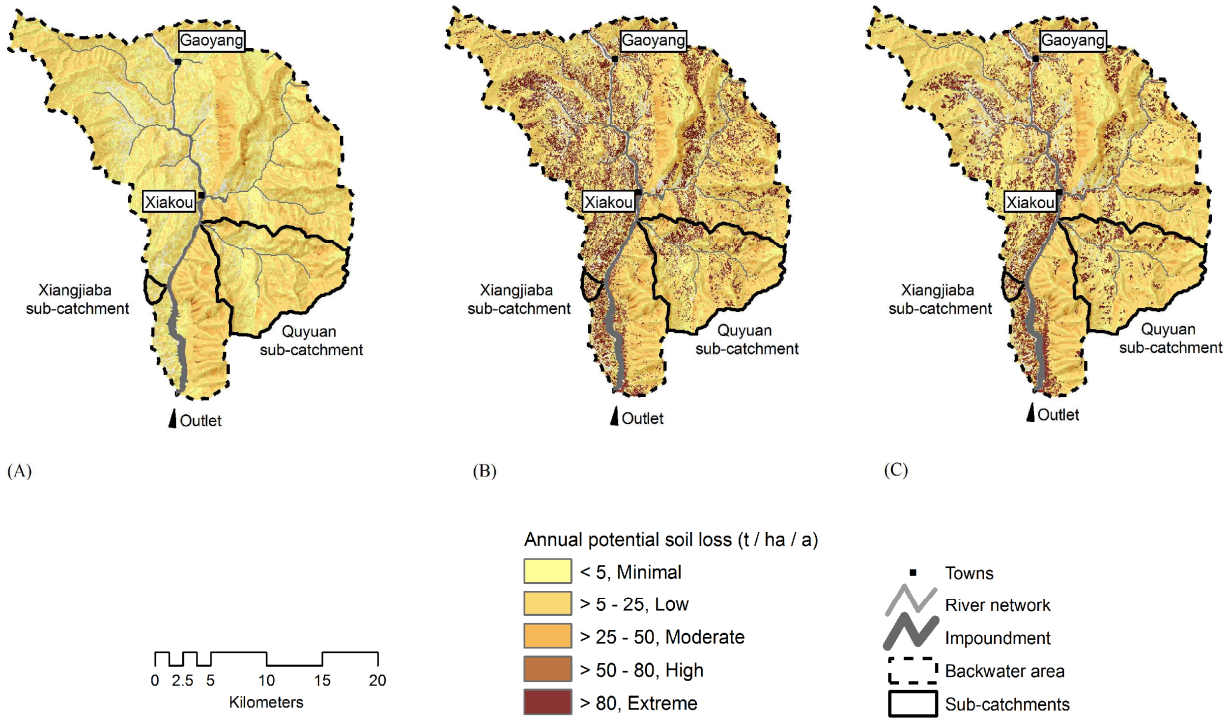

Figure 12 *Potential annual average soil loss (t ha^{-1} a^{-1}) under natural conditions (A), under former land use in 1987 (B), and under recent land use in 2007 (C) in the Backwater area with the sub-catchments Quyuan and Xiangjiaba.*

The limited spatial resolution is due to the coarse spatial resolution of the database (Table 1). The spatial validity of the modeled soil loss, for instance, is limited by the fact that only one *R* factor was taken for the whole catchment. In such mountainous subtropical areas spatially explicit information on the rainfall erosivity is needed to determine area-specific patterns of soil erosion risk potential. Another modeling constraint originates from the assumption of equal conservation practices for the entire catchment. Considering a *P* factor of 0.55 (c.f., Section 3.4) and thus, assuming the farmland on slopes between 20° to 25° being completely terraced with level bed terraces, the same terrace design, and no variations in the terrace conditions, is likely to either over- or underestimate the soil erosion locally. This is particularly important in areas with high relief energy (CAO ET AL., 2007; LESSCHEN ET AL., 2008). However, taking into account a *P* factor of 0.55 is likely to estimate soil erosion in an adequate range. This is true for 31% and 23% of the cultivated slopes in the Xiangxi catchment and Backwater area, and for 61% and 37% of the cultivated slopes in the sub-catchments Xiangjiaba and Quyuan with inclinations ranging from 20° to 25°.

Manuscripts 2 to 4 deal with the above mentioned model constraints and attempt to adequately consider the situation in the Xiangxi catchment by deriving *C* factor values (*Manuscript 2*) for grid based analyses, by spatially regionalizing the rainfall erosivity (*Manuscript 3*), and by analyzing the current situation of bench terraces as most important soil conservation practices and thus, crucial soil erosion factor in the study area (*Manuscript 4*).

4.2 ASSESSING THE USLE CROP AND MANAGEMENT FACTOR C FOR SOIL EROSION MODELLING IN A LARGE MOUNTAINOUS WATERSHED IN CENTRAL CHINA

(Manuscript 2, published in JOURNAL OF EARTH SCIENCE 21 (6), pp. 817-823, December 2010)

One of the key factors in soil erosion control is the vegetation cover and crop type that is expressed as *C* factor in the (R)USLE (c.f., Section 3.4.1). According to the resulting soil loss ratio, a series of sub-factors need to be considered (RENARD ET AL., 1997). However, their precise assessment is very time-consuming especially in mountain areas, such as the Xiangxi catchment. Large effort has been made on precise calculating and mapping *C* factors by means of GIS, RS data, and spectral indices (SURIYAPRASIT and SHRESTHA, 2008; ZHOU ET AL., 2008; DE ASIS and OMASA, 2007; WANG ET AL., 2002; DE JONG, 1994) to avoid time and cost intensive field investigations and to offer the possibility of a multi-temporal observation. The Normalized Differenced Vegetation Index (NDVI) derived from multispectral images is one of the most common environmental covariates to monitor and analyze vegetation properties, and their spatial and temporal changes (BOETTINGER ET AL., 2008; SUN ET AL., 2008; LILLESAND ET AL., 2007). As a function of the NDVI, the Fractional Vegetation Cover (FVC) provides information on the percentage of the vegetation cover (BOETTINGER ET AL., 2008). Thus, FVC can be used to predict the *C* factor using regression functions considering the soil loss ratio resulting from the specific conditions of the sub-factors (ZHOU ET AL., 2008).

Manuscript 2 focuses on the capability of the FVC based on Landsat-TM data in order to derive *C* factor values for soil erosion modeling on the large scale of the mountainous Xiangxi catchment.

Three pre-processed Landsat-TM scenes (c.f., Section 3.3) were used for the study introduced by *Manuscript 2*. The NDVI was computed for each of those images based on the red and near infrared bands according to ROUSE ET AL. (1974). The NDVI values were renormalized, providing an estimated value of vegetation cover (e.g., BOETTINGER ET AL., 2008) and used as input to calculate the percentage of the FVC taking into account the range of uncovered, bare ground to ground completely covered with, respectively, from lowest to highest NDVI values. *C* factor values were then calculated taking the logarithm of the percentage of FVC ranging from 0 to 78.3% using a regression function by YANG and SHI (1994). This function was established for a subtropical watershed in the TGA using more than 200 soil loss ratios measured from 30 runoff erosion plots. Serving as a reference to the *C* factor values derived from the FVC (C_{FVC}), *C* factor values were taken from literature (C_{LIT}) as described in Section 3.3. As the USLE was originally considered for agricultural used land (c.f., Section 3.4.1), *C* factor values in *Manuscript 2* were assigned accordingly for classes only referring to agriculture as given in Table 3. The effect of C_{FVC} and C_{LIT} on the soil erosion risk potential was then

modeled for the Xiangxi catchment, the Backwater area, and the two sub-catchments as in *Manuscript 1* (c.f., Section 3.4.2).

In the entire Xiangxi catchment, the FVC ranges from 0% to 100% and reflects the spatial distribution of the NDVI ranging from -1 to 0.99 throughout the three observation years. The results presented in *Manuscript 2* demonstrate that from 2005 to 2007, the Xiangxi catchment is characterized by a comparably similar spatial pattern of the FVC that only slightly changes from approximately 93% to 94%. Changes in FVC in the same period are most pronounced in the Xiangjiaba sub-catchment with average FVCs ranging from 75-85%, showing highest variation throughout the years and subunits considered (Table 5). Decreases of FVCs by nearly 20% from the scale of the Xiangxi catchment to the Backwater area are assumed to mainly results from the TGD-induced land use changes (c.f., Section 3.2.5) as infrastructure, settlements, and farmland are reflected lower in NDVI values. As the FVC was calculated based on the NDVI, the FVC is accordingly lower.

Manuscript 2 shows that, analogous to the FVC, C_{FVC} values were predominantly derived for areas adjacent to the river network in the headwater zone, for the larger settlement areas and their close surroundings, almost for the complete western Backwater area with the Xiangjiaba sub-catchment, alongside the Xiangxi Bay, and in the western Quyuan sub-catchment. For large areas in the northern, western, and eastern headwater zone, and scattered plots in the backwater area, no C_{FVC} values were derived as these areas correspond to a FVC of 80% and more. In *Manuscript 2* this is discussed to result from the threshold of 78.3% from the regression function that equals to a *C* factor of 0. It limits the calculation of *C* factor values to only agricultural land assuming the areas with FVC of more than 78.3% to represent forest land. Taking only farmland into account and comparing C_{FVC} to C_{LIT}, a similar spatial pattern can be observed.

Generally, high FVC values result in low *C* factor values (close to 0) and low FVC values result in high *C* factor (close to 1). Average C_{FVC} values range from 0.02 to 0.05 for all subunits and years, hardly showing any spatial and temporal change. Compared to the average C_{FVC} values in 2007, the C_{LIT} values in 2007 are distinctly higher ranging from highest 0.32 to lowest 0.21 (Table 5). The C_{FVC} values are assumed to be distinctly underestimated compared to the values of C_{LIT}. Whereas the C_{LIT} values represent common seasonal crop rotations within one year in the TGA and are considered to reflect the situation in the Xiangxi catchment, C_{FVC} corresponds to the given crop cover of the date of survey. Thus, the C_{FVC} values exclusively refer to the month September as this is the date of the scan flights of the Landsat images (Table 1). Whereas the range of C_{LIT} starts with lowest 0.08 for built-up land, the broad majority (86-89%) of C_{FVC} values in the Xiangxi catchment is below this value. Slight agreements between C_{FVC} and C_{LIT} are observed only for the larger settlement areas of Gufu and Gaoyang with *C* factor values of 0.08. This is explained with the fact that settlement areas are expected to show hardly any inter-annual and annual variations of FVC.

Table 5 *Multi-temporal analysis of the fractional vegetation cover (FVC) in percent and of C factors (dimensionless) derived from FVC (C_{FVC}) from 2005 to 2007 compared to C factors (dimensionless) taken from literature (C_{LIT}) based on the land use classification from 2007.*

	2005 FVC (%)	2005 C_{FVC} (-)	2006 FVC (%)	2006 C_{FVC} (-)	2007 FVC (%)	2007 C_{FVC} (-)	2007 C_{LIT} (-)
Xiangxi catchment							
Minimum	0.0	0.001	0.0	0.001	0.0	0.01	0.08
Maximum	100.0	0.87	100.0	0.93	100.0	0.98	0.46
Mean	93.9	0.04	92. 9	0.04	93.9	0.05	0.32
SD	12.7	0.07	13.6	0.06	12.4	0.07	0.17
N	——	113,929	——	146,564	——	103,287	250
Backwater Area							
Minimum	0.0	0.001	0.0	0.001	0.0	0.01	0.08
Maximum	100.0	0.87	100.0	0.93	100.0	0.98	0.46
Mean	86.5	0.03	85.2	0.04	88.6	0.05	0.27
SD	17.7	0.06	19.8	0.06	18.4	0.07	0.17
N	——	48,996	——	59,124	——	37,245	79,510
Quyuan sub-catchm.							
Minimum	0.0	0.001	0.0	0.001	0.0	0.01	0.10
Maximum	100.0	0.59	100.0	0.66	100.0	0.98	0.46
Mean	91.1	0.03	89.9	0.03	93.2	0.04	0.29
SD	11.9	0.04	11.5	0.04	10.5	0.04	0.17
N	——	5,494	——	5,794	——	3,515	9,198
Xiangjiaba sub-catchm.							
Minimum	0.0	0.001	0.0	0.001	0.0	0.01	0.10
Maximum	100.0	0.13	100.0	0.58	100.0	0.20	0.46
Mean	79.5	0.02	75.1	0.03	83.3	0.03	0.21
SD	11.6	0.02	13.3	0.03	12.6	0.02	0.14
N	——	582	——	764	——	370	921

N = count of pixels of estimated and assigned C factor values referring to a pixel size of 45m × 45 m, SD = standard deviation, sub-catchm. = sub-catchment

The higher the *C* factor values, the less their effect from crop and management practices and the higher their contribution to a high soil loss potential (Tables 5 and 6). Average annual soil losses based on C_{FVC} in the Xiangxi catchment range from 9.3 to 11.5 t ha^{-1} a^{-1} from 2005 to 2007. The sub-catchment Xiangjiaba shows the highest average annual potential soil losses throughout the catchment ranging from 11.7 to 16.3 t ha^{-1} a^{-1} (Table 6). Compared to the potential average annual soil losses estimated based on C_{FVC}, the average soil losses and ranges estimated with C_{LIT}, are considerable higher for all scales (Table 6). While average annual soil loss based on C_{LIT} in the Xiangxi catchment in 2007 is approximately 2,662 t ha^{-1} a^{-1}, the average potential soil loss based on C_{FVC} in 2007 is lower by a factor of 1.6. This difference in average annual soil losses still increases by a factor of 2.7 for the Backwater area, and by the factors of 5.9 and 8.7 for the sub-catchments Quyuan and Xiangjiaba (Table 6). Based on the comparison of the *C* factors derived from multispectral images and from literature for comparable subtropical study areas, those based on literature are considered to offer optimal results in the study presented in *Manuscript 2*. They represent the annual crop cycle in the TGA and are concluded to contribute to reliable results of the potential average annual soil loss in the Xiangxi catchment of approximately 121 t ha^{-1} a^{-1}.

Table 6 *Annual average soil loss potential (t ha^{-1} a^{-1}) in the Xiangxi catchment and in the subunits for the years 2005, 2006, and 2007 (all for September).*

	Soil loss in 2005 based on C_{FVC} in 2005	Soil loss in 2006 based on C_{FVC} in 2006	Soil loss in 2007 based on C_{FVC} in 2007	Soil loss in 2007 based on C_{LIT} for land use classific. 2007
Xiangxi catchment				
Minimum	0.00	0.0	0.0	0.0
Maximum	1,133.4	1,498.2	1,646.9	2,662.1
Average	9.3	11.0	11.5	120.6
SD	21.9	26.0	28.8	170.4
Backwater area				
Minimum	0.0	0.0	0.0	0.0
Maximum	607.1	708.6	873.6	2,397.9
Average	11.0	13.6	14.2	125.8
SD	23.5	24.5	28.3	174.6
Quyuan sub-catchm.				
Minimum	0.0	0.0	0.0	0.0
Maximum	385.7	180.3	285.6	1,689.9
Average	10.4	9.1	11.1	157.8
SD	18.6	14.8	18.9	228.9
Xiangjiaba sub-				
Minimum	0.0	0.0	0.0	0.0
Maximum	66.7	99.3	109.6	957.1
Average	11.7	16.3	14.6	129.9
SD	13.1	19.5	16.6	150.6

SD = standard deviation, sub-catchm. = sub-catchment, classific. = classification

4.3 APPROXIMATION AND SPATIAL REGIONALIZATION OF RAINFALL EROSIVITY BASED ON SPARSE DATA IN A MOUNTAINOUS CATCHMENT OF THE YANGTZE RIVER IN CENTRAL CHINA

(Manuscript 3, published in ENVIRONMENTAL SCIENCE AND POLLUTION RESEARCH, January 2013, DOI: 10.1007/S11356-012-1441-8)

Since FOURNIER's (1960) monograph 'Climat et erosion', dealing with the relations between precipitation, topography, and soil erosion processes, numerous attempts have been made to assess the main intrinsic factors of the rainfall erosivity and its spatial and temporal variability (e.g., BROWN and FOSTER, 1987; ELSENBEER ET AL., 1993; DE LIMA ET AL., 2009; ALIPOUR ET AL., 2012). Those studies have a common element which accounts for the regionally highly variable intensity and kinetic energy of rainfall as both determine its erosivity and crucially influence soil erosion (e.g., TOY and RENARD, 1998). They also account for the superimposed role of the climate regime and terrain on the rainfall erosivity (e.g., BOLINNE ET AL., 1980; MIKHAILOVA ET AL., 1997; GOOVAERTS, 1999; WANG ET AL., 2002). Most soil erosion models, such as the RUSLE, use rainfall intensity and duration, and/or kinetic energy alone to describe the role of precipitation (e.g., MORGAN and NEARING, 2011). The RUSLE uses the average annual rainfall erosivity factor *R* taking into account the number of record years and of erosive storm events in a given year, as well as the rainfall erosivity index of a single storm event resulting from the total storm kinetic energy and rainfall volume, and the maximum 30-minutes intensity of a storm event (BROWN and FOSTER, 1987; RENARD ET AL., 1997). Numerous

studies from different regions worldwide found that the *R* factor correlates the strongest with the soil loss (e.g., RENARD and FREIMUND, 1994). It is the most commonly used index for rainfall erosivity (e.g., WANG ET AL., 2002; SHAMSHAD ET AL., 2008; DIODATO and BELLOCCHI, 2009). However, according to the empirical nature of the RUSLE, the *R* factor is regionally variable and must be determined for each region separately.

To account for area-specific pattern of rainfall erosivity in the subtropical Xiangxi catchment, ***Manuscript 3*** aims at finding the best approximation for the *R* factor. As only daily precipitation data were available for five stations (c.f., Section 3.3), neither the comprehensive demands on the precise calculation requiring long-term precipitation data of single storm events nor on the spatially explicit determination of *R* factors based on a sufficient number of rainfall gauging stations could be met. Thus, *Manuscript 3* presents a method that overcomes these restrictions by

(i) approximating the *R* factor based on erosivity indices and regressions functions, and

(ii) regionalizing the *R* factor using the elevation as a spatially explicit covariable interacting with the rainfall erosivity.

To overcome the restriction of data scarcity in terms of temporal resolution, many approaches have been developed to calculate the *R* factor for specific regions based on erosivity indices, such as the Modified Fournier Index (F_{mod}), and based on regression functions (e.g., LAL, 1976; ARNOLDUS, 1977; KAVIAN ET AL., 2011; ALIPOUR ET AL., 2012). The regressions are mostly based on annual precipitation P_a (e.g., VAN DER KNIJFF ET AL., 1999), precipitation per month P_m (FU ET AL., 2005), precipitation per day P_d (YU and ROSEWELL, 1998; MEN ET AL., 2008), and on single rainfall events or precipitation per hour P_e (e.g., MANNAERTS and GABRIELS, 2000). Those alternative approaches can be very effective according to their correlation with the soil loss due to their regional or scale-dependent determination approach (RENARD ET AL., 1997). They further show that monthly and daily precipitation data already offer a useful and valid approximation of rainfall erosivity when used for the region of origin (e.g., STOCKING and ELWELL, 1976, ARNOLDUS, 1977; LO ET AL., 1985; RENARD and FREIMUND, 1994).

In total, 15 regression functions were tested in *Manuscript 3* to approximate the *R* factors. These regressions incorporate the (i) MAP (ROOSE, 1976; BOLINNE ET AL., 1980; ROGLER and SCHWERTMANN, 1981; LO ET AL., 1985; VAN DER KNIJFF ET AL., 1999), (ii) precipitation per day P_d (ELSENBEER ET AL., 1993; BAGARELLO and D'ASARO, 1994; YU and ROSEWELL, 1998; MANNAERTS and GABRIELS, 2000; DE SANTOS LOUREIRO and DE AZEVEDO COUTINHO, 2001; SHAMSHAD ET AL., 2008; MEN ET AL., 2008) and (iii) F_{mod} (ARNOLDUS, 1977); BOLINNE ET AL., 1980; DVWK, 1990; MEN ET AL., 2008). They all fulfill the requirement of a sufficient discussion in literature in terms of units and can be calculated with the available data. For evaluating their power, the resulting *R* factors were compared with reference data based on high-resolution rainfall data according to WISCHMEIER

and SMITH (1978) for study sites in the TGA (SHI ET AL., 2004; LIU and LUO, 2005; WU ET AL., 2011b, SHI ET AL., 2012) that are directly comparable to the Xiangxi catchment in terms physio-geographic settings.

All available climate stations used in the study presented in *Manuscript 3* belong to the low to medium mountain range between 134 and 950 m a.s.l. With 1,132 mm, Yichang station exhibits the highest mean annual precipitation (MAP). MAP at Badong, Xingshan, and Zigui are 1,074, 991, and 992 mm, respectively. Shennongjia shows the lowest MAP of all stations with 961 mm (c.f., Section 3.3).

The resulting *R* factors are highly variable and range from the lowest of approximately 26 to the highest of approximately 434,491 MJ mm ha^{-1} h^{-1} a^{-1} (Table 7). Except the *R* factors derived from the regressions by MEN ET AL. (2008), all other *R* factors were considered as not applicable to the Xiangxi catchment as discussed in *Manuscript 3*. They were excluded from further analyses as they do not adequately reveal the rainfall erosivity for the sub-humid climate and the orographic effect on the precipitation in the Xiangxi catchment. For instance, the *R* factors calculated according to ROOSE (1976) are distinctly higher (8,149-9,225 MJ mm ha^{-1} h^{-1} a^{-1}) than the evaluation data. The regression by Roose (1976) was originally developed for tropical West Africa with two rainy seasons. Thus, the relation between the *R* factor and the total annual precipitation is considered as not valid for mountainous regions like the TGA and other transition areas with unimodal annual rainfall patterns. Additionally, *R* factors based on the regressions by BOLINNE ET AL. (1980) and LO ET AL. (1985) can be interpreted as extreme outliers compared to all other *R* factors (Table 7).

The regression by MEN ET AL. (2008) integrates F_{mod}, the maximum daily precipitation of days with more than 12 mm and the mean, annual summed precipitation from days with more than 12 mm precipitation. The threshold value of 12 mm is close to the threshold value of 12.7 mm as suggested by WISCHMEIER and SMITH (1978) and was reported as practical for separating erosive and nonerosive storms for the Yellow River basin in China (XIE ET AL., 2002). Thus, F_{mod} combines the precipitation totals of all single erosive storm events within one year and correlates with MAP. Consequently, the analyses were continued with the *R* factors calculated according to MEN ET AL. (2008) as this method fits best to the objectives regarding sparse data considering the precipitation characteristics in the Xiangxi catchment.

Given the causal relation between precipitation and elevation in the Xiangxi catchment (WU ET AL., 2006; c.f., Section 3.2.2), the rainfall-dependent *R* factors are also assumed to increase with the elevation. Thus, *R* factors were spatially regionalized based on elevation bands taking into account (1) R_a in each elevation band and (2) the increase of R_a within each elevation band. Based on the linear, high correlation (r^2=0.94) between MAP and R_a calculated according to MEN ET AL. (2008) for the

available climate stations, R_a factors for each elevation band were derived according to the division method by WU ET AL. (2006).

As explained in *Manuscript 3*, R_a progressively increases from about 1,986 MJ mm ha^{-1} h^{-1} a^{-1} at the outlet to 7,547 MJ mm ha^{-1} h^{-1} a^{-1} at the highest elevation in the Xiangxi catchment. Based on the information of R_a at the upper and lower limit of each elevation band, the increase in rainfall erosivity per 100 meters was calculated according to the division method by WU ET AL. (2006) as shown in *Manuscript 3*. This allowed for the elevation-based, spatially explicit regionalization of R_a factors by assigning *R* factors to each pixel in the DEM (Table 1) according to their increase within the elevation band using GIS techniques.

Table 7 *Approximated R factors (MJ mm ha^{-1} h^{-1} a^{-1}) for the Xiangxi catchment calculated from 1971 to 2000 based on regression equations.*

Type of approximation/Author(s)	Climate station				
	Badong	Shennongjia	Xingshan	Yichang	Zigui
R factors based on regression equations using the mean annual precipitation MAP					
ROOSE (1976)	9,225.2	8,149.1	8,483.7	9,684.5	8,482.3
BOLINNE ET AL. (1980)	44.3	41.0	42.0	42.0	42.0
ROGLER and SCHWERTMANN (1981)	882.0	777.1	809.7	809.7	809.6
LO ET AL. (1985)	415,709.4	371,702.0	385,388.1	434,490.9	385,327.8
VAN DER KNIJFF (1999)	1,409.2	1,244.8	1,296.0	1,479.4	1,295.7
R factors based on regression equations using precipitation per day P_d					
ELSENBEER ET AL. (1993)	5,093.2	3,130.7	4,091.7	5,575.1	4,168.6
BAGARELLO and D'ASARO (1994)	1,853.0	1,231.6	1,546.9	2,001.4	1,562.3
YU and ROSEWELL (1998)	4,895.2	3,285.0	4,121.2	5,400.6	4,142.0
MANNAERTS and GABRIELS (2000)	4,784.9	3,345.5	4,009.0	5,276.4	4,079.4
DE SANTOS LOUREIRO and DE	2,977.5	1,972.9	2,505.2	3,179.7	2,520.6
SHAMSHAD ET AL. (2008)	5,417.9	4,266.3	4,908.6	5,791.3	4,838.4
R factors based on regression equations using the Modified Fournier Index F_{mod}					
ARNOLDUS (1977)	4,898.5	3,919.1	4,215.2	5,573.7	4,223.9
BOLINNE ET AL. (1980)	32.5	25.7	27.8	36.9	27.9
DVWK (1990)	1,075.7	948.5	988.0	1,158.5	989.1
MEN ET AL. (2008)	2,157.9	1,821.4	1,981.3	2,579.3	1,983.7

With approximately 530 MJ mm ha^{-1} h^{-1} a^{-1}, the highest increase in R_a per 100 m can be observed within the elevation band from 500 to 800 m a.s.l. This is due to the high increase of P_a from 1,200 to 1,600 mm in the humid northern subtropics in the Xiangxi catchment with intensive convective precipitation (HE ET AL., 2003). The lowest increase in R_a (~85 MJ mm ha^{-1} h^{-1} a^{-1}) per 100 m can be observed for altitudes above 1,200 m a.s.l. in the mid- and northern temperate zone of the Xiangxi catchment. A close link between MAP and the elevation is typical for climates with intensive convective precipitation such as in the Xiangxi catchment (HE ET AL., 2003). Subsequently, precipitation is mainly erosive with high rainfall intensities. Comparable ranges of *R* factors from elevation-based regionalization were given by GOOVAERTS (1999) for a study area in Portugal with a *R* factor range of 600 MJ mm ha^{-1} h^{-1} a^{-1} per 100 m increase in elevation, which is comparable with an

increase of R_a of approximately 530 MJ mm ha^{-1} h^{-1} a^{-1} per 100 m for the elevation band from 500 to 800 m a.s.l. in the Xiangxi catchment.

In the Xiangxi catchment, the long-term (1971-2000) R_a amounts to 5,222 MJ mm ha^{-1} h^{-1} a^{-1}, generally showing enormous rainfall erosivity. The rainfall erosivity pattern clearly reflects the altitudinal layers in the Xiangxi catchment due to the regionalization based on elevation bands (Figure 13). A narrow strip of comparably low rainfall erosivity characterizes the steep topography of the lower reaches of the Xiangxi River belonging to the Mid Subtropics below 500 m a.s.l. According to the global assessment of land vulnerability to water erosion by BATJES (1996), *R* factors > 1,250 MJ mm ha^{-1} h^{-1} a^{-1}, however, already account for high rainfall erosivity. This, in fact, means high to extreme rainfall erosivity to a hundred per cent for the Xiangxi catchment as the lowest rainfall erosivity at the outlet is *R* = 1,986 MJ mm ha^{-1} h^{-1} a^{-1} (Figure 13).

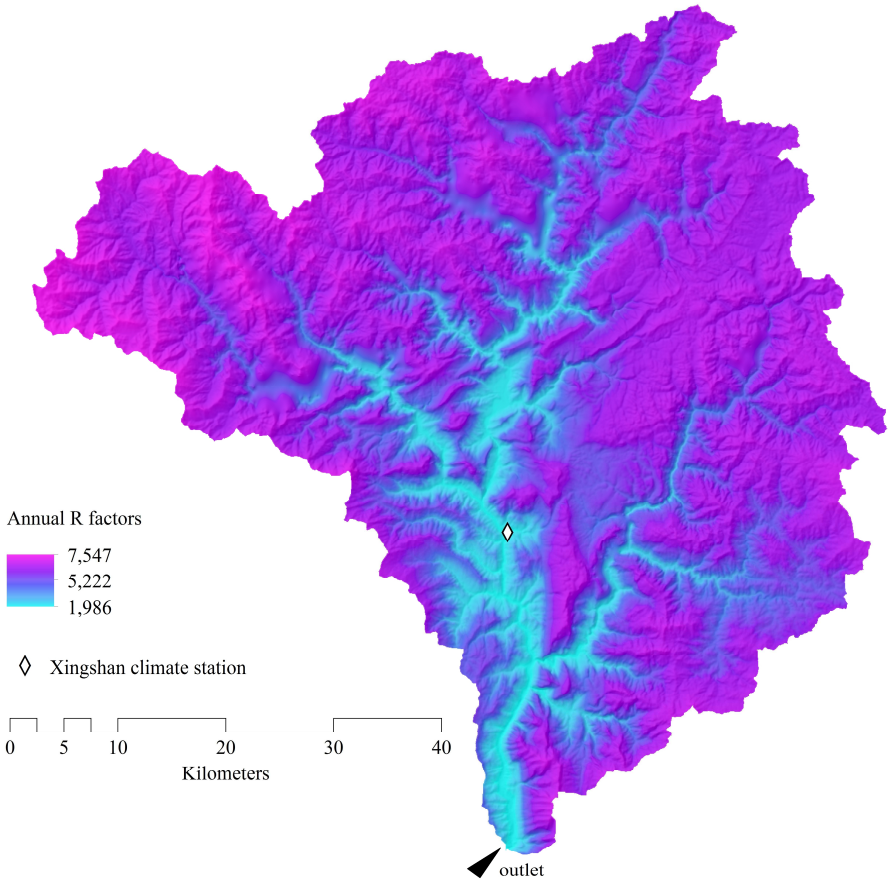

Figure 13 *Spatial distribution of R factors in the Xiangxi catchment based on mean annual R factors according to MEN ET AL. (2008). R factors are in SI unit (MJ mm ha^{-1} h^{-1} a^{-1}). Note: Incorrect figure published in Manuscript 3. The above figure shows the correct color ramp and labeling.*

Finally, *Manuscript 3* shows that, considering the superimposed role of the climate regime for the rainfall erosivity, the approximation of *R* factors using the regression by MEN ET AL. (2008) is

adequate for the conditions in the Xiangxi catchment. The results are in agreement with findings from other studies using higher temporal resolution rainfall data under comparable climate conditions (SHI ET AL., 2004; LIU and LUO, 2005; WU ET AL., 2011b; SHI ET AL.; 2012). Due to the low spatial density of rainfall data, common regionalization methods, such as regression kriging as used by MEUSBERGER ET AL. (2012) for 71 gauging stations or inverses distance weighting based on 121 gauging stations as reported by ALIPOUR ET AL. (2012), could not be applied. Yet, under the given situation of data scarcity in terms of spatial resolution, the spatial regionalization of *R* factors also offers optimal results. According to WEILGUNI (2006), *R* factors from spatially sparse data can be regionalized using a spatial explicit feature as long as they interact with each other. Since the Xiangxi catchment causes a vertically zoned climate, the elevation can be used as an additional feature. Already BIEGER ET AL. (2012) used the altitudinal pattern in the Xiangxi catchment as benefit and sufficiently adjusted the low annual precipitation and volume of discharge through a regionalization using elevation bands. Thus, the division method by WU ET AL. (2006) serves as superior advantage in spatially regionalizing the *R* factors. The applied approach is able to overcome the limited data and to address the highly mountainous topography in the Xiangxi catchment.

4.4 DEGRADATION OF CULTIVATED BENCH TERRACES IN THE THREE GORGES AREA - FIELD MAPPING AND DATA MINING

(Manuscript 4, published in ECOLOGICAL INDICATORS 34, pp. 478-493, November 2013, DOI: 10.1016/j.ecolind.2013.06.010)

Much is known about terrace degradation due to agricultural abandonment (c.f., Section 1.1.3). However, until now no attention was paid to terrace degradation in areas experiencing agricultural intensification and rapid ecosystem changes. Since the widely terraced reservoir of the TGA currently belongs to the most dynamic large-scale anthropogenic influenced regions in the world (c.f., Section 1.2.2), rapid land use changes are expected to likewise impact terracing (Figure 9). In order to minimize soil erosion, e.g., through well-adapted land management and conservation practices, information on soil loss and its spatial and temporal variability is required. This of course, also includes the effect of terraces on soil erosion, especially, since bench terraces are widely-applied in the TGA (SHI ET AL., 2012).

Manuscript 4 broaches the above issue and undertakes an initial attempt to account for the degradation of cultivated terraces in the highly dynamic TGA. *Manuscript 4* aims at identifying the relevant indicators affecting terraces characterized by land use change in order to emphasize the understanding of the processes triggering the degradation and thus, influencing the terraced landscape in the mountainous TGA.

Since there has been no terrace inventory and no further data available, and access to the mountainous terrain was limited, the model framework of *TerraCE* (Terrace Condition Erosion) was developed to overcome these restrictions. *TerraCE* consists of a two-step approach (Figure 14) aiming at

(i) collecting data on terrace degradation by considering different conditions of terraces using field surveys and

(ii) explaining the terrace degradation by embedding environmental and anthropogenic indicators as well as surveyed terrace condition classes into a spatial data mining framework.

Therefore, *TerraCE* is based on the following two fundamental assumptions that enable the development of environmental and anthropogenic indicators as proxy-drivers for the effects of terrain and human impact on terrace degradation:

(i) generally, bench terraces are the product of human activity driven by terrain settings (e.g., INBAR and LLERENA, 2000), and

(ii) the spatial distribution of the degree of degradation of bench terraces is driven by the distance to settlements and to the reservoir as well as their accessibility (e.g., by roads).

The applied field survey scheme, introduced by *Manuscript 4*, was based on an initial survey in the Backwater area and the findings achieved by COMOLLI (2005) and BAZZOFFI and GARDIN (2011). A detailed terrace survey (n=158) for precise measurements of the terrace design and for categorizing the terrace maintenance conditions into four hypothesized classes (i.e., 'well maintained', 'fairly maintained', 'partially collapsed', and 'completely collapsed'), as well as cultivation and erosion pattern was conducted in the sub-catchments Xiangjiaba and Quyuan. Terrace design was assessed by measuring the height of the terrace wall, the width and slope angle of the terrace riser, and the slope angle of the terrain as these parameters are considered to determine the geometry of a terrace (HUDSON, 1981). The terrace' state of maintenance was assessed by focusing on the frequency and intensities of different types of structural wall disorders (i.e., bulges, upsetting, wall failures, complete wall collapses) based on the work by BRANCUCCI and PALIAGA (2006). The final step in the field mapping approach was a less time-consuming and less complex 'remote' survey with major focus on dominant terrace condition but for larger areas to provide a bigger dataset for data mining. Thus, along a strip of approximately 35 km length that is directly adjacent to the Xiangxi Bay in the Backwater area and is easy to access, each terrace plot referring to a homogenous land use was mapped at a scale of 1:10,000. The classification of the terrace plots (n=829) into the given, predefined classes was done according to the detailed terrace survey.

Local, regional and combined geomorphometric terrain features (e.g., elevation, slope, projected distance to the stream, aspect, relative profile curvature, topographic roughness, local

elevation, mean and relative horizontal curvature, and waxing and waning slopes), were derived from the DEM (c.f., Section 3.3). They served as environmental indicators on the condition of terraces. To account for the influence of multiple scales, all terrain attributes were averaged on the basis of local moving window filters with sizes of 7 × 7 as well as 17 × 17 pixels. This allows capturing more general trends in terrain as additional indicators for terrace condition analysis (BEHRENS ET AL., 2010a).

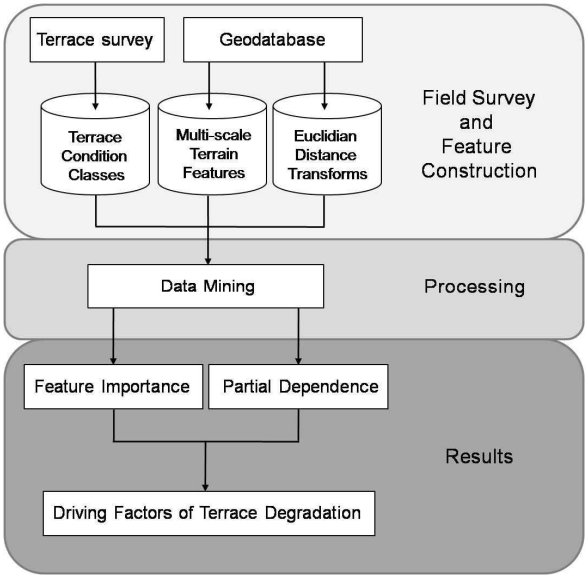

Figure 14 *Model framework of TerraCE.*

Spatial distance transforms mainly served as anthropogenic indicators on the terrace conditions by quantifying relationships between objects (i.e., road and river network, and settlements) according to Tobler's First Law of Geography where "everything is related to everything, but near things are more related than distant things" (TOBLER, 1970). Thus, grids, distances of certain locations can be extracted that are assumed to indicate different human impacts on the terrace conditions. Those grids were calculated for classified, combined road and river network classes to account for the accessibility of the terraces conditions classes via continuous changes in traffic density and via navigable rivers as demonstrated and discussed in *Manuscript 4*. Additionally, the Euclidean distance to the Xiangxi shoreline after the impoundment based on the SPOT5 scene was used as a potential anthropogenic indicator on human influence on terrace condition. Further Euclidian distance transforms were calculated based on 4,420 grouped settlements that were considered as local, regional, and central markets having high local and regional influence as economic trading areas. Settlement areas as well as the road network are based on SPOT5 and Google Earth (c.f., Section 3.3).

In total, 81 environmental and anthropogenic indicators on the terrace conditions were derived as spatial grid datasets. Together with the merged maps from the detailed and the remote terrace inventory, they were embedded into a spatial data mining approach to assess the driving factors of the spatial distribution of the terrace condition classes (Figure 14).

The basic data mining algorithm used is random forests (BREIMAN ET AL., 1984; BREIMAN, 2001). The mean increase in accuracy (MDA) was provided as a measures of the importance of each indicator, respectively, feature. The partial dependence according to CUTLER ET AL. (2007) and LIAW

and WIENER (2011) was applied in *Manuscript 4* to allow for interpretations of the effects of an indicator contributing to the model on the terrace degradation.

In total, 987 bench terraces were mapped covering 10.6 km² of the Backwater area. The terraces are spatially distributed all-over the hillslopes adjacent to the Xiangxi Bay on almost the whole range of altitudes from lowest 137 to 1,402 m a.s.l. The general slope gradient of the terraced hillslopes ranges from 0° to 40°. According to percentage of occurrence, the terrace condition classes are 'fairly maintained' (44.3%; *n*=437), 'partially collapsed' (23.4%, *n*=231), 'well maintained' (21.0%; *n*=207), and 'completely collapsed' (11.3%; *n*=112). Contrary to the common knowledge (e.g., HUDSON, 1981), the heights of the supporting dry-stone walling of the bench terraces do not increase with higher slope angles of the terrain (Figure 14). However, a heightening of the walls is required as the slope angle is the most relevant limiting factor for the construction of bench terraces, particularly when slopes exceed an angle of 25-30° (HUDSON, 1981). This is especially true for ‘partially’ and ‘completely collapsed’ terraces with average slope angles of the original terrain of 27-28° showing the lowest terrace walls (Figure 15). Generally, the shortening of the terrace risers combined with the increases of the terrain slope result in a slight to distinct over-steepening of the terraces as all terrace condition classes predominantly exhibit outward sloping terrace risers (Figures 15 and 16B). As HUDSON (1981) described the terrace risers in steep sloping areas typically to be inward sloping or level and also SHI ET AL. (2012) report of level terraces as only soil conservation measure in the Wangjiiaqiao watershed close to the Xiangxi catchment, the surveyed bench terraces’ design are assumed to be not adequately adapted to the terrain in the Backwater area.

As shown in *Manuscript 4*, a distinct worsening of the supporting walls characterizes the ‘partially collapsed’ and ‘completely collapsed’ terraces while ‘well maintained’ terraces show intact and ‘fairly maintained’ terraces typically show relatively intact terrace structures (Figure 16A). The bulges and upsetting observed for 'well' and 'fairly maintained' terraces are considered to present only slight disturbances and to be "precursors" of a more complex destruction with numerous wall failures and collapses. Already INBAR and LLERENA (2000) described the bulges and upsetting to develop prior to more serious wall failures and complete wall collapses due to increasing pressure on the terrace wall by saturated soil and their shearing effect, and lack of constant maintenance.

Based on the term of terrace degradation (BAZZOFFI and GARDIN, 2011) and following the above findings, the bench terraces in the study area clearly show a sequence of degradation terraces from ‘well maintained’ to ‘completely collapsed’ terrace conditions. The increase in soil erosion fits the degradation of terraces (Table 8).

It is assumed that due to the intact structure and the comparably lowest slope of terrace risers no rills could be observed for ‘well maintained’ terraces, whereas the worsening of the terrace walls with an increasing average number of wall failures and collapses and increasing steepness of terrace

risers distinctly affect the removal of sediment for the other terrace condition classes (Table 8). However, even if the ‘completely collapsed’ terraces show the worst structure that might induce a higher concentrated runoff according to KOULOURI and GIOURGA (2007), there is no increase in the average frequency of rills compared to ‘partially collapsed’ terraces. In this case the worse terrace condition is considered to not affect the frequency of rills, but rather their magnitude. Thus, the worsening from 'partially' to ‘completely collapsed’ terraces becomes obvious when looking at the increases in average depth and width of rills, and the distinct increase in average lengths of rills by more than twice (Table 8).

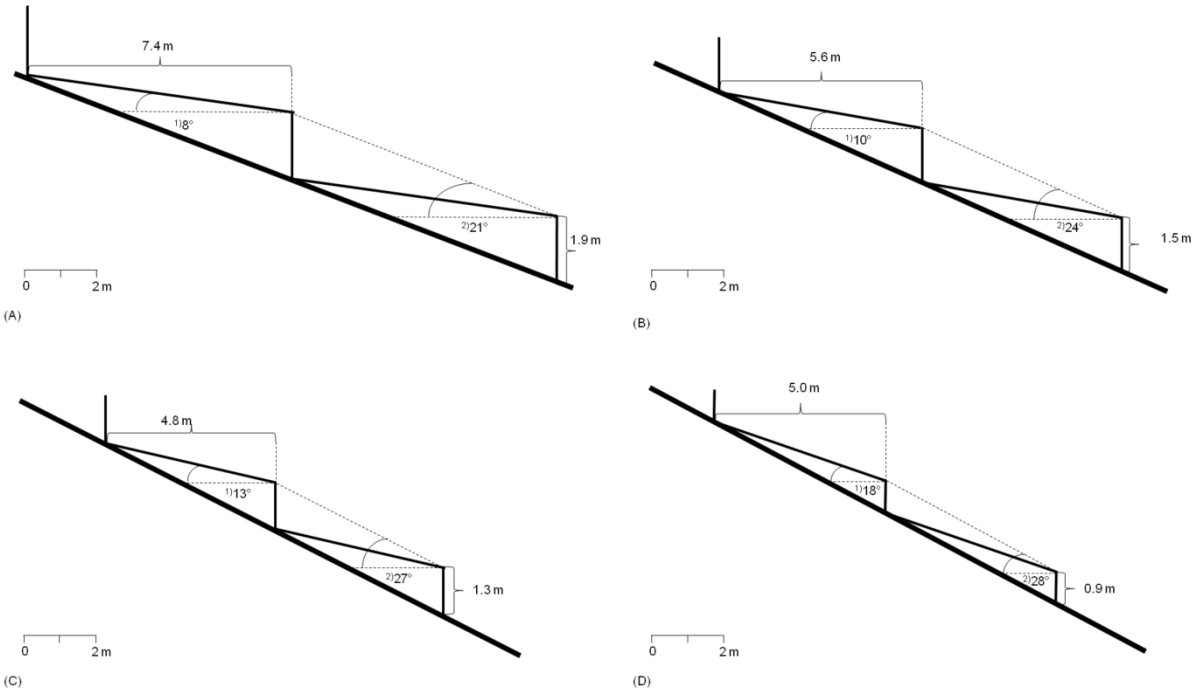

Figure 15 *Typical cross-section of the terrace design of ‘well maintained’ (A), ‘fairly maintained’ (B), ‘partially collapsed’ (C), and ‘completely collapsed’ terraces (D). Shown are the (1) average terrace slope (°), the (2) average terrain slope (°), the average height of the terrace wall (m), and the average width of the terrace riser (m). Results are based on n=158.*

Table 8 *Average frequency and magnitude (depth, width, and length) of soil erosion rills per surveyed terrace plot (from the detailed terrace survey) and terrace condition class.*

	Terrace condition class			
	Well maintained	Fairly maintained	Partially collapsed	Completely collapsed
Frequency	—	2.3 (SD 0.6)	5.0 (SD 3.6)	5.0 (SD 1.4)
Depth (cm)	—	2.7 (SD 0.6)	2.8 (SD 1.3)	3.0 (SD 0.0)
Width (cm)	—	3.0 (SD 0.0)	3.1 (SD 1.3)	3.5 (SD 0.7)
Length (m)	—	1.5 (SD 0.5)	1.6 (SD 0.9)	3.8 (SD 0.4)

SD = standard deviation

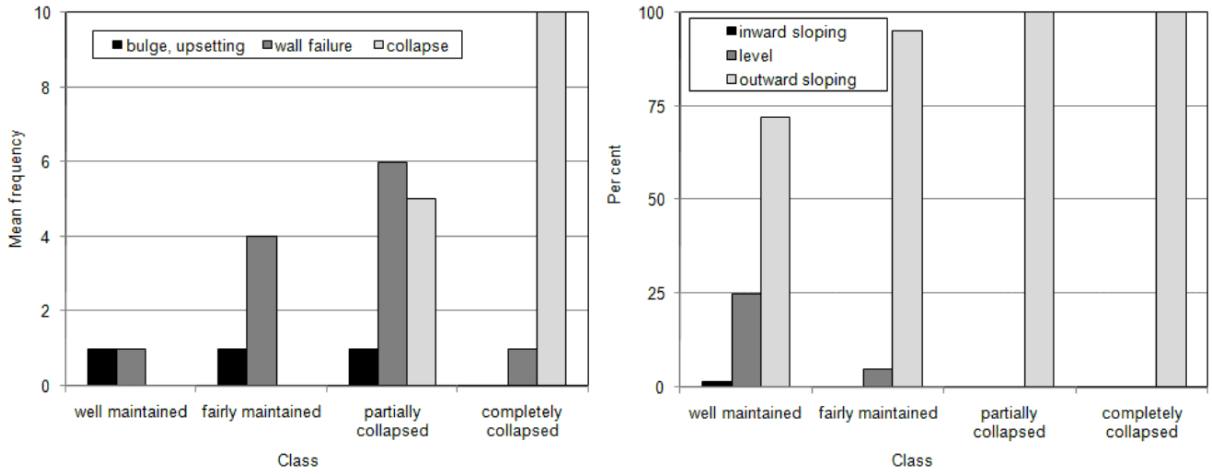

Figure 16 *Average frequency of wall disorders in each terrace condition class (A). Due to few observations of bulges and upsetting these wall disorders are grouped into one category. Percentage of different sloping terrace risers in each terrace condition class (B).*

In *Manuscript 4*, the influences on the terraced landscape in the study area are extensively discussed to be highly complex and to result from multiple decisions and various human-environmental interactions. The multi-factorial influence is clearly indicated by the results from the data mining approach. The data mining approach based on a total of 81 features and using regression reveals a high modeling accuracy of R^2=79% allowing for subsequent analysis as well as interpretations.

The 30 topmost indicators influencing the terrace degradation are given in Table 9. Generally, the higher the MDA the more important the corresponding indicator. The 10 topmost ranking positions (MDA 0.091-0.036) are solely occupied with anthropogenic indicators (Table 9). The most important indicators are those directly related to the major settlements and to the Xiangxi River (distance of stream lines of 1st order) followed by distances to smaller settlements and to the road network. Below rank 10 (MDA 0.031-0.016) mainly terrain attributes (Table 9). The distance transforms of the major centers have the highest importance on the prediction of the terrace degradation (Table 9). In terms of the partial dependence, as shown in *Manuscript 4*, the worse terrace conditions were predicted in close distance to the major centers Gufu and Gaoyang. The distance to settlements of 6-12 ha size show a similar direction of influence, however the area surrounding the settlements that shows worst terrace conditions is smaller compared to the major settlements (about 7 km vs. 3.5 km). For the distance to the Xiangxi River, the worst conditions of terraces were also predicted close to the river. However, better conditions occur at much smaller distances compared to the settlements (i.e., < 1 km). The distance to the major roads shows a very non-linear pattern. The worst terrace conditions occur in distances below 500 m to the road network. The best terrace conditions occur around 1.5 km and around 8 km. The range between 5 km and 7 km is again characterized by worse terrace conditions.

The terrace degradation is assumed to be a direct consequence of complex cause-effect relationship of the rapid land use changes in the TGA, for instance, resulting from the massive dam-induced forced, rural and urban resettlements in Zigui and Xingshan counties associated with the Xiangxi River impoundment by the TGD (HEMING ET AL., 2001; MCDONALD ET AL., 2008).

The steep sloping up-hill-sites close to the new Xiangxi Bay are characterized by land use changes on 26% of the Backwater area (SEEBER ET AL., 2010). As shown in *Manuscript 4*, this is exactly the area of the worst terrace conditions (‘partially’ and ‘completely collapsed’). Comparing the terraces of worse conditions close to larger settlements, and the main road and river network to those terraces of better conditions ('well' and 'fairly maintained') more distant to this dynamic areas, the forced resettlement is supposed to play an important role in the mismanagement of bench terraces leading to their degradation. Possibly, the resettled peasants get confronted by challenges with farming steep sloping land after the impoundment. Farming those uphill-sites requires first of all time-consuming terracing generally necessitating high investments in material and labor (INBAR and LLERENA 2000; SHI ET AL., 2012). According to HEMING ET AL. (2001) and PONSETI and LÓPEZ-PUJOL (2006), the loss of the traditional connection to the land after resettlement causes a lack of familiarity with the new farming environment and techniques. For instance, 66% of the relocates in the TGA were observed to refuse farming due to severe physical settings (HEMING ET AL., 2001). Also aging of the rural population and governmental-driven settling of younger rural migrants in industrial jobs in the TGA as stated by HEMING ET AL. (2001) and STEIL and DUAN (2002) are considered to hinder an adequate terrace construction and constant, but labor-intense maintenance to sustain long-term soil conservation.

The shift of agriculture in the Backwater area, especially toward the cash crop production of oranges (c.f., Sections 1.2.2.1 and 3.2.5) are expected to further affect the terraced landscape. In the Xiangxi catchment orange orchards distinctly predominate on terraces close to large settlements and main transportation routes such as trafficable main roads and rivers (SEEBER ET AL., 2010). According to the findings from the partial dependence analysis, this area adjacent to the river banks of the Xiangxi refers to the location of terraces of higher degree of degradation (‘partially’ and ‘completely collapsed’ terraces). A cause-effect relationship between the governmental-driven implementation of orange orchards and the condition of terraces is discusses in *Manuscript 4*. The farmers' expenses for orange production (e.g., fertilizers, pesticides) are assumed to often exceed their income resulting from decreasing market prices, labor-intensive and costly harvesting, and a non-adequate governmental financial support. In this context, the lack of a cost and time-consuming maintenance of terraces would be a logical consequence of a simple cost-benefit-calculation. This is especially true for slope gradients above 10% (SHI ET AL., 2012), where the spacing between the terraces decreases to such a point that their construction and maintenance is expensive and lack of investments limits their adoption.

Table 9 *The 30 out of 81 most important indicators in predicting the terrace condition classes.*

Ranking position	MDA	Indicator
1	0.0910	Distance to major centers
2	0.0646	Distance of stream lines of 1st order
3	0.0602	Distance to settlements of 6-12 ha area size
4	0.0499	Distance to settlements of 12-18 ha area size
5	0.0386	Distance to major and side roads
6	0.0368	Distance of stream lines of 3rd order
7	0.0365	Distance to major and side roads, and paths
8	0.0365	Distance of stream lines of 2nd order
9	0.0360	Distance to major roads
10	0.0342	Distance to stream lines of 4th order
11	0.0312	Aspect deviance to 90° (17×17 pixel average)
12	0.0308	Aspect deviance to 90° (7×7 pixel average)
13	0.0288	Aspect deviance to 45° (7×7 pixel average)
14	0.0280	Aspect deviance to 45° (17×17 pixel average)
15	0.0249	Aspect deviance to 135° (17×17 pixel average)
16	0.0230	Mean curvature (17×17 pixel average)
17	0.0226	Distance to the Xiangxi River after impoundment
18	0.0225	Distance of settlements of a total of 4420
19	0.0222	Aspect deviance to 90°
20	0.0213	Distance to settlements of 0-6 ha area size
21	0.0207	Distance to stream lines of 6th order
22	0.0205	Distance to stream lines of 5th order
23	0.0192	Aspect deviance to 0° (17×17 pixel average)
24	0.0183	Aspect deviance to 45°
25	0.0177	Aspect deviance to 0° (7×7 pixel average)
26	0.0176	Topographic roughness (17×17 pixel average)
27	0.0176	Relative profile curvature (17×17 pixel average)
28	0.0174	Aspect deviance to 135° (7×7 pixel average)
29	0.0165	Relative richness (17×17 pixel average)
30	0.0160	Aspect deviance to 0°

MDA is the mean decrease accuracy. Due to a higher differentiation of MDA, the numbers are given with four decimal places.

While the immediate reservoir area is considered to present an area of fast access, the uphill-sites in higher altitudes distinctly show less accessibility. The newly constructed paved roads and navigable rivers after impoundment are supposed to exhibit important infrastructural connections and to favor the governmental-driven production of oranges. Also larger settlements, acting as local and regional markets are discussed in *Manuscript 4* to be more attractive for the high quality cash crop production (i.e., in terms of processing, marketing, and transport) than difficult to access small settlements and markets without any trading potential. Furthermore, big cars cannot drive along unpaved and narrow side roads and paths, transportation by ship is impossible and larger settlements do not develop. Thus, the steep sloping uphill-site is concluded to be utterly not attractive for large-scale orange production and to be, in some parts, better protected as revealed by the partial dependence to curvature. A more difficult access to larger settlements via side roads and paths in a region of higher altitudes would further imply that uphill-peasants depend more on their farming products and thus properly maintained terraces. Available capital and efforts for maintaining terraces seem to be better invested.

Besides the effect of resettlements, cultivation, and accessibility, also the geomorphic settings affect the terrace conditions, albeit with less importance of the environmental indicators referring to the terrain (Table 9). As shown in *Manuscript 4*, terraces of worse condition are potentially located on slopes inclining between ENE and ESE. This is supposed to be a typical proxy effect since those slopes mostly occur on Jurassic strata, and to a slightly less extent on Silurian and the top formation of the Triassic strata characterized by low resistance to weathering and prone to water saturation and (EHRET ET AL., 2010). Terraces of better condition mostly occur on south, north, and west exposing slopes referring to Precambrian to Cambrian and Devonian to Permian strata with more stable parent material such as sandstones and limestones (EHRET ET AL., 2010). It is assumed that the terraces built on compact and permeable bedrock are less vulnerable to the destruction by mass movements than terraces built on incoherent materials exhibiting higher risk of deep seated and translational landslides (EHRET ET AL., 2010). In the case of the Backwater area this would imply that water storage, high soil erosion susceptibility, and the occurrence of landslides can induce the process of terrace destruction, and thus have an impact on terrace degradation. In turn, destroyed terraces do not offer enough control to combat soil erosion as damage spots of the ruined terraces' structure exhibit weak points vulnerable to concentrated runoff and sediment removal (KOULOURI and GIOURGA, 2007).

As demonstrated in *Manuscript 4*, the Backwater area where TGD-induced infrastructure construction, the resettlements, the agricultural land reclamation, and shifts in agriculture are closely related to each other, is characterized by a high complexity of interactions affecting the terraced landscape. Thus, an interpretation of the influences and their strengths might not be sufficient enough when addressing an individual indicator, but rather when considered in combination. The knowledge on the process of terrace degradation shown in *Manuscript 4* is new, in that in not only agricultural abandonment explains the terrace degradation, for instance as observed by KOULOURI and GIOURGA (2007), LESSCHEN ET AL. (2008), and EL ATTA and AREF (2010) for bench terraces in the Mediterranean. As the surveyed bench terraces are cultivated to almost a hundred per cent and SEEBER ET AL. (2010) could not detect abandoned farmland to a meaningful extent in the Backwater area, *Manuscript 4* proofs terrace degradation as an effect of land cultivation, as well. Particularly against the background of the bench terraces being reported to exhibit a well-known technique with a long tradition throughout the TGA (e.g., SHEN ET AL., 2010; SHI ET AL., 2012), *Manuscript 4* gains high relevance on addressing their adaption to the new situation in the TGA in order to keep their effectiveness in terms of soil conservation in the highly-dynamic, terraced environment.

5 CONCLUSIONS AND OUTLOOK

This thesis is part of the interdisciplinary joint research project 'YANGTZE GEO' on the sustainable management of the newly created ecosystem at the Three Gorges Dam and the environmental-related consequences resulting from the land use changes, soil erosion, mass movements, and diffuse matter inputs into the reservoir. Within the subproject 'Soil Erosion', the present thesis aimed to substantially contribute to the enhanced understanding of the trigger mechanisms and processes of soil erosion by water, and the effect of the Three Gorges Dam on the soil erosion risk potential and its spatial variability in a highly dynamic, terraced environment.

For the purpose of hydropower generation, flood control, and navigation, China constructed the Three Gorges Dam at the outlet of the upper reaches of the Yangtze River. After nine years of construction and an enormous large-scale transformation process in the Three Gorges Area, the river impoundment started in 2003. The Xiangxi River as a first class tributary to the Yangtze River in the eastern Three Gorges Area became inundated, too. At a length of approximately 35 kilometers, the Xiangxi River was impounded in a narrow valley bordered by steep slopes with shallow and highly erodible soils. The newly created Xiangxi Bay has submerged an estimated area of 9.4 km² (SEEBER ET AL., 2010). Subsequently, the catchment of the Xiangxi River is characterized by rapid land use changes associated to the Three Gorges Dam project. Comparable to the entire Three Gorges Area, this new land reclamation affected the steep sloping up-hill sites adjacent to the new reservoir of the Xiangxi River. Comparing the total Xiangxi catchment and its immediate reservoir area - the Backwater area - in terms of land use changes; urban and rural resettlements, infrastructure construction as well as land reclamation for cultivation and shifts in agriculture from arable land to orange orchards are more pronounced in the Backwater area. Beyond this area of high land use dynamics, the dam-induced land use changes in the northern, largely forested headwater zone of the Xiangxi catchment are much less pronounced. Here, mainly the conversion of marginal farmlands into woodland, driven by the governmental 'Grain for Green Program', controlled the land use change.

The resulting high land use dynamics in the Xiangxi catchment, and in particular in its Backwater area, are concluded to meet unfavorable prerequisites in terms of a high physical vulnerability that is expected to limit the catchment's environmental carrying capacity.

HIGH NATURAL SOIL EROSION RISK POTENTIAL IN THE XIANGXI CACTHMENT

The high physical vulnerability to soil erosion is mainly due to the steep to extremely steep sloping mountainous topography, accounting for more than 70% of the total catchment area, as well as the Qinling mountain range, serving as a climatic border, and the impact of the subtropical monsoon climate. In combination with the range of elevation of more than 3,000 m, the abundant precipitation,

ranging from average annual 961 to 1,132 mm in the catchment and its surrounding area, are typically convective. This orographic pattern of the precipitation is closely linked to high and extreme high rainfall erosivities ranging from 1,986 MJ mm ha^{-1} h^{-1} a^{-1} at the catchment's outlet in the Mid subtropics to 7,547 MJ mm ha^{-1} h^{-1} a^{-1} in the zone of the Northern temperate in the high Qinling mountain range. Additionally, the soil erodibility is concluded to strongly contribute to the high natural soil erosion risk potential in the Xiangxi catchment. In the Backwater area, the mountainous topography and high rainfall erosivities coincide with moderate to extreme high soil erodibilities of the shallow Limestone soils and predominantly shallow Purple soils of more than 0.32 t ha h ha^{-1} MJ^{-1} mm^{-1}. In the Xiangjiaba sub-catchment at the western riverbank of the Xiangxi Bay, the Purple soils of the highly weatherable Jurassic strata occasionally show extreme low topsoil's resistance to particle detachment and transport by water of 0.64 t ha h ha^{-1} MJ^{-1} mm^{-1}.

Assuming the entire Xiangxi catchment as completely forested without any human interventions (e.g., settlements, agriculture, and soil conservation measures) and resulting from the above physical settings, the soil erosion modeling revealed an average annual natural soil erosion risk potential of 10.3 t ha^{-1} that is likely to exceed more than 100 t ha^{-1} in places. Considering the multi-scale approach, the natural disposition to soil erosion in the Backwater area is estimated to be in average 9.6 t ha^{-1} a^{-1}. With an average of 10.7 t $ha^{-1}a^{-1}$, the potential soil loss in the Quyuan sub-catchment in the eastern Backwater area is even higher. Here, average annual soil losses are highest under natural conditions on the catchment scale which is generally considered to result from the higher terrain energy of the Triassic formation.

As PIMENTEL (2006) reports of a natural average annual soil loss ranging from 1 to 5 t ha^{-1} to be typical for mountainous regions completely covered with vegetation, the natural disposition to soil erosion in the Xiangxi catchment is concluded to be already very high. The human influence, and in particular, the interferences into the environment of the Xiangxi catchment associated to the Three Gorges Dam result in a complex system of natural and anthropogenic processes. Under the massive human influences the effects of the controlling factors are concluded to subsume and to strongly foster the natural disposition to soil erosion to considerable higher levels resulting in a distinct spatial distribution of the soil loss.

THE THREE GORGES DAM HAS AN AMBIGIOUS EFFECT ON THE SOIL EROSION RISK POTENTIAL

Compared to the natural soil erosion risk potential, the soil erosion risk potential under human impact in 2007 was estimated to be higher by a factor of about 18 accounting for an annual average soil loss of approximately 188 t ha^{-1} on the catchment scale. In contrast to the generally very few areas exhibiting moderate to extreme (> 25 to > 89 t ha^{-1} a^{-1}) soil erosion risk potential under natural

conditions, accounting for only approximately 6% of the Backwater area, the seriously affected area under human impact is distinctly higher. According to the Chinese Soil Erosion Rate Standard, almost 41% of the total Backwater area exhibited moderate to extreme high soil erosion risk potential in 2007. This is mainly due to the crucial effect of the vegetation cover. Whereas, under natural conditions the high protection effectiveness of the closed forest vegetation cover alleviates the effect of high rainfall erosivity, high soil erodibility, and the mountainous terrain, the vegetation cover is strongly altered under land use conditions.

Besides the distinct differences between potential soil erosion under natural conditions and under land use, a shift between potential soil erosion risk under former conditions in pre-construction times of the dam (1987) and under current land use conditions in post-construction times of the dam (2007) are detectable. Before dam construction and resettlements started, the annual average soil loss in the Xiangxi catchment was estimated to be approximately 264 t ha^{-1} and to vary by a factor of 1.4 between annually 344.9 t ha^{-1} and 245.5 t ha^{-1} in 1987. For post-construction times of the dam, the empirical soil erosion modeling with the RUSLE revealed a distinct decrease of about 29% on the catchment scale. For the sub-units considered the soil losses vary by a factor of 1.8 between average 229.3 t ha^{-1} a^{-1} and 128.2 t ha^{-1} a^{-1} in 2007. Whereas in pre-construction times of the dam almost 45% of the Backwater area exhibited moderate to extreme soil erosion risk potential, this area percentage slightly decreased by 10% in 2007 accounting for an area of 227 km². Though, the Three Gorges Dam and associated land use changes were expected to dramatically increase the soil erosion risk potential, this impact cannot be generally concluded for the Xiangxi catchment. Here, the 'Grain for Green Program', launched in 2002 (LIU and WU, 2010), is regarded to have had a mitigating effect on the soil erosion risk potential. At least this is true for the area exhibiting extreme soil erosion that could be reduced by 36% from approximately 100 km² in 1987 to almost 64 km² in 2007. At the same time, the area under moderate to high soil erosion risk potential (> 25 to 80 t ha^{-1} a^{-1}) increased by 7% from 152 to 163 km².

Against the background of the mitigation of soil erosion by the 'Grain for Green Program' that ended in 2008 (LIU and WU, 2010), the observed time period from 1987 to 2007 is considered to not entirely account for the rapid land use changes of the Three Gorges Dam. Looking at the temporal variability of the predicted potential soil losses from 2005 to 2007 based on the analysis of the fractional vegetation cover and linked crop and vegetation cover during the months of September, a distinct increase of about 24% from average 9.3 to 11.5 t ha^{-1} a^{-1} on the catchment scale can be observed. In the Backwater area the increases in average annual soil losses of about 29% during the same period are even higher. Both are assumed to indicate an accelerating effect of the Three Gorges Dam on the soil erosion risk potential. As expected, the increases are higher in the immediate reservoir area of the Xiangxi Bay where river impoundment, and thus, loss of valuable land and land use changes on the steep sloping uphill-sites are directly linked to each other. A definite proof for the

effect of the Three Gorges Dam on the soil erosion risk potential and its spatial and temporal variability, however, would require continuous analyses and monitoring with a much more 'narrow time frame' of the observation period.

Although, a minimum of at least 1,090 ha of slopes directly adjacent to the Xiangxi Bay are terraced and a distinct amount of arable land has been converted to orange orchards considered as suitable land use on steep slopes, soil erosion is a serious threat in the immediate reservoir area of the Xiangxi catchment. With approximately 128 t ha^{-1} a^{-1} in 2007, the average annual soil loss in the predominantly agriculturally used Xiangjiaba sub-catchment in the western highly dynamic Backwater area is distinctly above the average annual soil loss of 30 to 40 t ha^{-1} a^{-1} on cropland in Asian countries (PIMENTEL, 2006).

Particularly, farmland sloping greater than 5° is considered to contribute to the high soil erosion risk potential as it accounts for approximately 94% of the total cultivated area in the Xiangxi catchment and for about 98% in the Backwater area in 2007. Approximately 35 to 36% of the farmland in the Xiangxi catchment and Backwater area even occurs on slopes above the critical threshold of 25° over which cultivation and land reclamation is actually prohibited according to the Chinese Water Soil and Conservation Law (LIU, 2012). Thus, those slopes and their appropriate management are of pivotal relevance for the agricultural productivity and the sustainability in the Xiangxi catchment. Insofar, bench terraces as major recommended type of soil conservation in mountainous regions are of outstanding importance for the alleviation of the high physical vulnerability, and the cultivation of row crops, such as maize.

TERRACE DEGRADATION AS A CONSEQUENCE OF THE THREE GORGES DAM

Terraces are typical soil erosion control measures in the Xiangxi catchment. Despite environmental restoration programs, such as the 'Rebuilding Terrace and Defarming Mode', in order to break the vicious circle of 'sloping land reclamation - environmental deterioration - farmer's poverty - reclaimed expansion' (XU ET AL., 2005), soil erosion on terraces is or is again a widely detectable phenomenon in the Xiangxi catchment. In places with wall disorders (i.e., wall failures, complete wall collapses) and/or technically poor design of terraces that are not adapted to the local terrain situation (i.e., over-steepening of the terrace risers), distinctly higher soil losses by rill erosion were observed than in places with well maintained terraces. This is mainly concluded to result from the process of terrace degradation that leads to a distinct reduction of the terrace' capability to protect the soil against surface erosion by water (BAZZOFFI and GARDIN, 2011). In the Backwater area of the Xiangxi catchment terrace degradation under cultivation is obvious. The sequence of terrace conditions, as indicators on the process of terrace degradation, ranges from ‘well maintained’ (21.0%), ‘fairly maintained’ (44.3%), and ‘partially collapsed’ (23.4%) to ‘completely collapsed’ terraces (11.3%).

Influences on the systematically spatial distribution of those terrace condition are multi-factorial. The effect of the terrain, which can be regarded as the major natural driver for terrace degradation by erosive action, is tributary but altered and overlaid by the high land use dynamics associated to the Three Gorges Dam. Thus, foremost, anthropogenic indicators such as the distances to settlements and roads affect the spatial distribution of terrace conditions and thus, terrace degradation. With increasing distances to main settlements, acting as local and regional markets for farming products, and transportation routes via paved, main roads and navigable rivers, the terraces exhibit better conditions. This is *inter alia* supposed to be an effect of a higher farmer's motivation to constantly maintain terraces. The closer the terraces to new settlements, to the new Xiangxi River shoreline, and to the new major roads, the worse are their conditions. The newly developed larger settlements and roads for a better infrastructural connection serve as preferential routes for claiming new agricultural land and existing terraced farmland for cash crop production as observed by SEEBER ET AL. (2010) for the Xiangxi catchment. Hence, a fast access to terraced farmland via main transportation routes is furthermore assumed to be a reason for the terrace degradation, whereas remote terraces in higher elevations and more distant to the new infrastructure are less attractive farmland for cash crops because of the difficult access. Moreover, it is concluded that the tempo of the land use dynamics hardly considers available capital and labor for the constant maintenance of terraces. Thus, the motivation of maintaining terraces is assumed to be also driven by economic decisions. Moreover, a lack of familiarity with the new farming system hinders an adequate terracing by former downhill peasant that were previously used to farm the now impounded valley bottoms.

Under the above considerations, the 'equilibrium state' (BRANCUCCI and PALIAGA, 2006) of the terraces in the highly dynamic environment of the Xiangxi catchment is concluded to be strongly disturbed by the complex interactions of forced resettlement (HEMING ET AL., 2001), accessibility, and cultivation resulting from the dam-induced land use changes. This should be urgently addressed by politics since the cultivated bench terraces have to be adapted to this new situation in order to keep their effectiveness in terms of soil conservation.

Using a multi-scale approach, this thesis further sought to develop an integrative data-based methodology for the assessment of soil erosion and its factors by means of GIS-based modeling using relevant digital terrain data and environmental covariates on soil erosion factors, field investigations, and data mining approaches. As the studies were largely constrained by data scarcity and limited access to the mountainous terrain, remote sensing data served as a fast and available supplier for the derivation of area-wide and spatially explicit data as input into the modeling approaches on the landscape level.

SOIL EROSION MODELING WITH THE RUSLE MODEL PROVED AS VALID AND RELIABLE

Against the background of the model constraints (i.e., data scarcity, limited access to terrain) and sheet and rill erosion detected as principal mechanisms of water erosion in the Xiangxi catchment, the RUSLE, as a predictive tool on the soil erosion by water, was considered applicable for modeling the soil erosion risk potentials on the catchment scale.

The application of the RUSLE based on available data remote sensing images, legacy data (i.e., soil map), and literature data from comparable study sites in the Three Gorges Area is concluded to reflect the general situation and the spatial distribution of areas highly prone to soil erosion in the Xiangxi catchment and to give results comparable to other studies from the Upper Yangtze River Basin (YAO, 1993; QUINE ET AL., 1999; LU and HIGGITT, 2000; GUO ET AL., 2001; SHI ET AL., 2004).

The RUSLE proved to be sufficient enough to identify hotspots of soil erosion risk potential and to highlight the dam-induced effects on the soil erosion risk potential in the entire Xiangxi catchment and, in particular, in the highly dynamic Backwater area. However, the spatial validity of the modeling results strongly depends on the coarse spatial resolution of the input data. For instance, due to the fact that the soils are classified according to the Chinese Soil Taxonomy with a limited number of soil types and representative soil profiles that were analyzed, a small-scale variability in erosion-relevant soil texture, soil organic carbon, and soil structure could not be extracted from the available maps. Moreover, the rough estimates on the crucial soil erosion factors 'crop type and management', 'rainfall erosivity', and 'soil conservation practice', expressed as *C*, *R*, and *P* factors in the modeling approach, are concluded to limit the spatial validity of the modeling results. Particularly, in mountainous regions these factors require spatially explicit measurements in order to determine the area-specific patterns of rainfall erosivity and vegetation cover, and to avoid local over- or underestimations resulting from not adequately parameterized soil conservation measure, i.e., bench terraces.

Strictly speaking, the modeling results of the RUSLE only enable statements as to what extent soil is potentially lost by erosive action on the scale of the individual pixels. The integral erosive processes of particle redistribution and deposition by water are not considered in modeling. But as the amount of sediment entering the reservoir is also of interest, for instance for evaluating the off-site effects of soil erosion (e.g., reservoir siltation) and for analyzing the water pollution by diffuse matter input of particle-bounded agro-chemicals into the stream network, the results are only conditionally satisfactory. The integration of the sediment delivery ration (SDR) as introduced by ZHOU and WU (2008) for different study sites in China would definitely improve the applicability of the results for further analyses on the interactions of water, sediment, and contaminants in the Xiangxi catchment.

For a future soil erosion modeling, also calibration and validation data, for instance from runoff plots studies, should be taken into consideration to enhance the spatial validity and thus, the

modeling accuracy. As both were neither conducted within the project framework nor were available from other soil erosion studies in the Three Gorges Area, additional research is needed to improve the significance of the soil erosion modeling throughout the Three Gorges Area and in highly dynamic environments in general.

C FACTORS TAKEN FROM LITERATURE PROVED AS ADEQUATE IN THE MODELING

As the normalized differenced vegetation index, based on the Landsat-TM scenes used, only reflect the date of survey (date of scan flight) of each of the multi-spectral images, also the derived fractional vegetation cover and *C* factor values only present a snapshot. This is certainly sufficient for short-term considerations, however, in the case of the RUSLE expressing the long-term average annual conditions, this approach is concluded as not capable to predict the soil erosion risk potential in the Xiangxi catchment. Here, values on *C* factors taken from studies from comparable subtropical areas, and fitting to the land use classes in the Xiangxi catchment (e.g., arable land, orange orchard, woodland) are considered to offer optimal results against the background of data scarcity and unfeasible *in situ* precise measurement of vegetation properties. As they represent the annual crop cycle in the Three Gorges Area, they are concluded to contribute to reliable results of the potential average annual soil loss in the Xiangxi catchment.

VALUABLE APPROXIMATION OF THE RAINFALL EROSIVITY BASED ON SPARSE DATA

In the present thesis, a further attempt on the approximation of the rainfall erosivity and its spatial regionalizing onto the large catchment scale for gridded analysis has been made. Various studies indicate the crucial role of the climate regime to cover the characteristics of rainfall events that control rainfall erosivity. By testing a large number of regression equations to approximate the *R* factor for the Xiangxi catchment, the function by MEN ET AL. (2008), incorporating the Modified Fournier Index, is concluded to perform best to calculate the *R* factor. Moreover, the barrier effect of the Qinling mountain range, the monsoon climate, and the mountainous terrain of the Xiangxi catchment exhibits a vertically zoned climate, which allows for a regionalization of rainfall erosivity using elevation bands. Thus, the spatial regionalization of *R* factors using the equation by MEN ET AL. (2008) is assumed to be most adequate for the Xiangxi catchment considering that a larger number of gauging stations with less spacing would enhance the accuracy of regionalization. The results of the applied approach based on sparse data are within the same range of the *R* factors from other studies in the Three Gorges Area. Thus, the approach fulfills the requirements to overcome limited data, both in space and time, and to address the mountainous topography in the subtropical Xiangxi catchment. The resulting grid-based *R* factors allow for modeling a area-specific soil erosion risk potential in the

Xiangxi catchment. Consequently, in a next step, the orographic pattern of rainfall erosivity will be considered in soil erosion modeling in order to enhance the spatial validity of the modeling accuracy.

THE MODEL FRAMEWORK *TERRACE* ENABLES FOR THE IDENTIFICATION AND SPATIAL ANALYSIS OF DIFFERENT TERRACE CONDITIONS AND THEIR CAUSES

The developed model framework *TerraCE* (Terrace Condition Erosion) enables for the identification and spatial analysis of different terrace conditions and their causes. It considers the sparse data availability and limited access to terrain and thus, improves the knowledge on terrace degradation by conducting the first inventory of bench terraces in the Three Gorges Area and throughout China. The classification of terrace conditions by combining their design and state of maintenance proved as sufficient as the whole range of wall disorders was assessed.

For the first time, it was proven that spatial data mining tools in combination with specifically derived descriptive data on the effect of human activity and terrain can be used to derive the strength and direction of the effect of the rapid agricultural changes mainly due to forced resettlements on terrace degradation. Applying random forests classification and regression models by embedding environmental and anthropogenic indicators mainly based on remote sensing data performed strongly and proved as valid approach in modeling terrace conditions. Strength and direction of the effect of the forced rapid agricultural changes and massive resettlement on terrace degradation can be clearly derived using analyses on the indicator importance and partial dependence.

With 79%, the modeling accuracy of *TerraCE* is high; however it is concluded that its significance on the effect on the terrace degradation can be still enlarged by incorporating more indicators affecting the development of terraces such as land tenure, ownership, cropping cycle and many more. Here, the model framework of *TerraCE* offers an open structure and therefore, the possibility to incorporate more indicators.

Since such an inventory on bench terraces was conducted the first time in the Three Gorges Area and was not based on any previous qualitative and quantitative information; the approach, however, is certainly capable of further improvements in terms of higher differentiation of terrace conditions. Moreover, direct measurements of soil loss and runoff would help to gain precise information on the effect of the terrace degradation on the soil erosion. An increase in sample sizes, especially of those classes that are yet underrepresented (e.g., 'completely collapsed'), would improve the statistical analysis and its explanatory power on the spatial distribution of terrace conditions. As no information on the time of the construction of the bench terraces was available, a specific terrace condition cannot currently be assigned to the age of a terrace in order to consider its influence on terrace degradation independent from the maintenance. Here, the monitoring of bench terraces over a longer period would eventually improve the understanding of the process of terrace degradation.

Further limitations of this approach unequivocally lie in the low spatial coverage of the mapping area. Especially, the hinterland of the Backwater area could not be covered. The mapping approach was constrained by the limited access to the highly mountainous terrain and the time-consuming detailed survey on bench terraces. The absence of remote sensing data in a satisfactory high spatial resolution exhibits another limiting factor regarding the clear identification of the condition of bench terraces and their area-wide inventory in the study area. In this context, the field mapping approach within the framework of *TerraCE* is considered to be the best affordable method. The 'quasi-remote' inventory on the terrace conditions proved as a fast survey scheme covering a large area compared to the detailed inventory and gained a large training data set.

Indeed, *TerraCE* does not serve as universal model in terms of describing global generalities for terrace degradation. It rather improves the understanding of the phenomenon of terrace degradation under forced resettlement in the Three Gorges Area (HEMING ET AL., 2001) since it is considered to act as a driving factor for land use dynamics affecting the terrace conditions. The relation between the terraces' state of maintenance and the cost and profit is valid for a free-market economy, however, in the Three Gorges Area also the motivation to maintain terraces and the familiarity with the farming system strongly affect the 'treatment of terraces' in a region that accounts for a 'socio-ecological landscape' characterized by various human-environmental interactions as described by BEVAN ET AL. (2012).

In the present thesis, the application of *TerraCE* aimed at a locally adapted model in order to assess the terrace conditions and their driving factors as well as to explain their effect on the terrace degradation. In this context, the costs and benefits of the mostly new installed cash crop oranges are discussed as one reason for the lack of motivation of the farmers to maintain their terraces. As *TerraCE* has an open structure, it is readily transferable to other regions when the requirements on the data are fulfilled. Thus, the model framework of *TerraCE* might be interesting for environmental planning as the results are expected to be helpful for improving the terrace planning in the mountainous Three Gorges Area and its future development.

Furthermore, the consideration of terraces is an essential precondition in soil erosion risk evaluation. Thus, the incorporation of the local-specific variability of soil erosion due to terrace degradation is an important next step in soil erosion modeling incorporating the *TerraCE* approach. Here, precise and spatial information on the characteristics of terrace degradation would help to avoid over- or underestimations of the soil erosion risk potential. Moreover, further analyses intend to extend the modeling approach toward areas beyond the Backwater area, as the hinterland is expected to be reclaimed in the future.

Concluding from the above considerations, the results of the present thesis allow for statements on the status and dynamic of soil erosion and its processes in a highly dynamic

environment. By focusing on the catchment scale of a major tributary to the Yangtze River and thus, covering by far a much larger scale than most of the previous soil erosion studies in the Three Gorges Area, the results can be helpful for further research planning. By choosing an application-based approach and integrating spatially explicit, area-wide remote sensing data, typical field settings could be addressed with best knowledge and available data. Particularly, against the background of a limited environmental carrying capacity in the Three Gorges Area, the results emphasize the relevance of balanced human-environmental interactions for a sustainable land management. They provide a scientific basis for decision making for a sustainable use of a terraced landscape, for instance by identifying key prevention and key rehabilitation areas. Without reducing soil erosion and particularly considering the terrace degradation, agriculture on the steep sloping hillsides in the mountainous Xiangxi catchment and beyond is likely to become hard to sustain.

In a global comparison of large dam projects and their effects on soil erosion, The Three Gorges Dam certainly behaves as expected, as land use changes, triggering soil erosion, are an unavoidable consequence of such large-scale encroachments into the environment. However, in the case of the Three Gorges Dam, the dimensions and the duration of the project definitely make the difference. The benefit of such a project of the century may be left open; in the medium and long-term the main focus should be on how to arrange the physical settings and anthropogenic demands to keep any potential geo-risk to a minimum.

6 SUMMARY

Worldwide, soil erosion is one of the most pressing environmental problems of present times. Particularly, soil erosion triggered by overland flow and runoff seriously affects the productivity and stability of ecosystems. The loss of fertile topsoil and soil's water storage capacity, and the discharge of sediments and associated contamination of waterbodies due to diffuse matter transport of particle-bounded agrochemicals from cropland highly elicit call a for action to combat soil erosion for a future securing of food supply and high drinking water quality. Globally, China belongs to one of those countries most affected by soil erosion. Technical problems as well as high economic off-site damages and costs resulting from reservoir siltation and thus, reduced project's lifespan due to soil erosion are typical for numerous large-scale dam projects in China. In addition to the natural disposition to soil erosion, especially, anthropogenic impacts associated to the dam construction distinctly affect the soil erosion risk potential in the adjacent ecosystems.

This can be exemplarily seen at the currently worldwide largest dam project, the Three Gorges Dam at the Yangtze River in Central China. This megaproject has been controversially discussed since its planning, and most recently since its construction and full operation in 2007. It contains the largest installed hydropower capacity worldwide, and is supposed to distinctly improve the river navigation and to secure the water supply to the northern country in the long-term. The realization of the dam project has already required massive resettlements of rural and urban population of more than one million people long before its start of operation. Additionally, large-scale land use changes, e.g., land reclamation for the road and settlement construction, for small scale subsistence farming and for cash crop production as well as shifts in land uses, on the steep sloping uphill-site above the impounded area are expected to considerably foster the soil erosion in the short- to long-term. Due to their partially direct connection to the stream network agriculturally used land with high soil erosion potential affects the water quality. Precise knowledge on the quality and quantity of soil loss, and its spatial and temporal variability can help to control the soil erosion by developing an adapted land use management and identifying conducive soil conservation measures, such as contour-aligned bench terraces. Under optimum conditions, bench terraces balance the geomorphic settings and anthropogenic use and can present a fair and sound basis for economic growth in mountainous areas.

The focus of the present thesis lies on the risk potential of soil erosion by water in the newly created reservoir of the Three Gorges Dam. Therefore, the central research questions aimed at the natural soil erosion risk potential and the effect of the dam-induced land use dynamics on the dimension and spatial and temporal distribution of soil losses. Due to the data scarcity and limited access to the terrain, a further focus of the research conducted lied on the data-based regionalization of soil erosion factors to use as input in soil erosion modeling.

The research was conducted in the subtropical Xiangxi catchment (3,200 km²) that was considered to adequately represent the Three Gorges Area in terms of physical settings and human interventions attributing to the dam project. The Xiangxi River joins the Yangtze River as a first class tributary approximately 40 km upstream the Three Gorges Dam. Due to the dam construction, the widely terraced landscape of the Xiangxi catchments is also affected by rapid, high land use dynamics with consequences on the slope stability. Particularly, the backwater area in the southern catchment area with the impounded lower reach of the Xiangxi River is characterized by steep to extremely steep sloping terrain and predominantly shallow soils with moderate to very high soil erodibility. Additionally, the very high rainfall erosivity increases the high physical vulnerability of the entire Xiangxi catchment. Between 1987 and 2007, a governmental-driven decrease of arable land and an increase of woodland and shrubland affected the northern headwater zone of the catchment. In the immediate reservoir area, the land use change from 1987 to 2007 was mainly controlled by a distinct conversion of arable land to orange orchards.

Within the framework of this thesis, methods for data survey and data processing were tested and adapted in order to evaluate the risk potential of soil erosion. In addition, comprehensive field investigations focusing on soil erosion processes and on pedological properties and further erosion-relevant factors were conducted. Relevant parameters derived from remote sensing data and land use classifications as well as the documented land use change from 1987 to 2007 were used for the parameterization of the empirical soil erosion model RUSLE. This model was applied to estimate and evaluate the spatial distribution and dynamic of the soil erosion risk potential, and to spatially localize high-risk areas. The new conceptual model *TerraCE* was developed and tested for the identification and spatial analysis of different terrace conditions and their causes. By means of data mining approaches, a prediction of the spatial distribution of the identified terrace conditions was computed. By integrating environmental and anthropogenic indicators on the impact of the terrain and the human influence, the causes and the strength of disturbances on the terrace conditions, and thus terrace degradation were analyzed.

During the observation period from 1987 to 2007, the Xiangxi catchment is generally characterized by a decrease of average annual soil losses and their maxima due to implemented environmental programs. However, a very high soil erosion risk potential in the entire catchment must be assumed. Frequency and intensity of soil erosion mainly concentrate in the backwater area at the lower reaches of the Xiangxi River. Here, land use changes, resettlements, and infrastructure construction have the highest impact. An inadequate construction of terraces that is not adapted to the local terrain conditions and an insufficient maintenance of the farming terraces can further strongly affect the soil erosion dynamic. Moreover, rapid ecosystem changes and an associated intensification and reclamation of terraces can lead to their degradation. The tempo of the land use dynamics hardly considers available capital and labor for the cost and time-consuming restoration and maintenance of

terraces, mainly cultivated with oranges. The high increase of the reclaimed area for the orange production within very short term caused a surplus production and thus, a price decline on the local and regional markets. Due to the not very profitable sale of oranges, a lack of farmers' motivation and little or no capital are made responsible for the gradual worsening of the terrace conditions. As many of the resettled peasants, that were formerly used to farm the flat valley bottoms, are often not familiar with the new and difficult terrain settings and farming techniques, there is also a lack of knowledge on adequate terrace cultivation. Subsequently, inappropriate management of those terraces leads to an increase in the soil erosion

The findings of the present thesis suggest designating the terraces as important, sensitive ecosystem service as they present - if properly maintained - a very effective soil erosion control and enable for a sustainable land use in the mountainous Xiangxi catchment and throughout the entire Three Gores Area. Considering the data scarcity in terms of spatial and temporal resolution, the results further show that soil erosion factors can be successfully regionalized and used for a valid soil erosion modeling. Against the background of ongoing research within the 'Yangtze Project' as well as further projected large dam projects at the Yangtze River and worldwide, the research conducted offers an important starting point for further research on the soil erosion risk potential and associated environmental threats, such as water pollution.

6 ZUSAMMENFASSUNG

Bodenerosion zählt weltweit zu den größten Umweltproblemen der Gegenwart. Insbesondere die durch Oberflächenabfluss ausgelöste Bodenerosion wirkt sich direkt auf die Produktivität und Stabilität von Ökosystemen aus. Der Verlust an fruchtbarem Oberboden und an Bodenwasserspeicher sowie die Erosionsprozesse selbst, gekennzeichnet durch Sedimentausträge verbunden mit dem Austrag partikulär im Boden gebundener Agrochemikalien und Belastung angrenzender Gewässer, stellen Politik und Ökonomie vor enorme politische und planerische Herausforderungen, angefangen bei der Ernährungssicherung bis hin zur Trinkwasserqualität. Global betrachtet gehört China zu den am stärksten von Bodenerosion betroffen Ländern. Durch Bodenerosion ausgelöste technische Probleme verbunden mit hohen Kosten treten vor allem bei den zahlreichen großen Staudammprojekten in China auf, wo infolge hoher Sedimenteinträge in die Reservoirs mit der Abnahme der Staukapazität und somit auch mit Abnahme der Energiegewinnung durch Wasserkraft gerechnet werden muss. Neben der natürlichen Erosionsdisposition spielen vor allem die mit dem Bau und Betrieb von Staudämmen einhergehenden, anthropogenen Eingriffe in die angrenzenden Ökosysteme eine entscheidende Rolle für die Höhe des Bodenabtrags.

Das aktuell weltweit größte Staudammprojekt, der Drei-Schluchten-Staudamm am Yangtze-Fluss in Zentralchina, zeigt dies exemplarisch. Dieses Megaprojekt wurde bereits seit seiner Planung, spätestens jedoch seit seiner Umsetzung und Inbetriebnahme im Jahr 2007 kontrovers diskutiert. Es beinhaltet das größte Wasserkraftwerk der Welt, und soll neben der Verbesserung der Schiffbarkeit des Yangtze-Flusses und seiner Hauptzuflüsse langfristig auch die Wasserversorgung für Gebiete im Norden des Landes sichern. Die Umsetzung des Staudammprojekts erforderte bereits lange vor seiner Fertigstellung großräumige Umsiedelungsmaßnahem der städtischen und ländlichen Bevölkerung von weitaus mehr als einer Million Menschen. Weiterhin stehen großräumige Landnutzungsänderungen, verbunden mit der Neulandgewinnung für den Straßen- und Siedlungsbau, den kleinbäuerlichen Subsistenzanbau und den flächenintensiven, marktorientierten Anbau von Orangen auf stark geneigten Flächen hangaufwärts der ursprünglichen Uferlinie im Verdacht, die Bodenerosion um den Staubereich kurz- bis langfristig erheblich zu verstärken. Aufgrund der teilweise direkten Anbindung landwirtschaftlicher Flächen an das Gewässernetz können gerade diejenigen Flächen mit hohem Erosionspotenzial einen großen Einfluss auf die Wasserqualität ausüben. Kenntnisse zur Qualität und Quantität des Bodenabtrags und dessen räumliche sowie zeitlich Variabilität können helfen, die Ausmaße der Bodenerosion mit Hilfe eines angepassten nachhaltigen Landmanagements und der Identifizierung von Schutzmaßnahmen zu minimieren. Hangparallel angelegte Bankterrassen stellen eine solche Schutzmaßnahme dar. Im Optimalfall gleichen sie die Topographie aus und ermöglichen eine ökonomisch profitable ackerbauliche Nutzung von Gebirgsregionen.

Das Risikopotenzial von Bodenerosion durch Wasser im neu gebildeten Reservoir des Drei-Schluchten-Staudamms bildet den inhaltlichen Schwerpunkt dieser Arbeit. Die zentralen Forschungsfragen galten dem natürlichen Erosionsrisikopotenzial sowie dem Einfluss der Landnutzungsdynamik auf die Höhe der Bodenabträge und deren räumlichen Verteilung und Variabilität. Infolge der generell geringen Datenverfügbarkeit und unzureichenden Zugänglichkeit des Geländes lag ein weiterer Schwerpunkt der Arbeiten auf der datenbasierten Regionalisierung von Erosionsfaktoren für eine anschließende Bodenerosionsmodellierung.

Als exemplarisches Untersuchungsgebiet diente das 3.200 km² große, subtropische Einzugsgebiet des Xiangxi-Flusses, der dem Yangtze-Fluss 40 Kilometer oberhalb des Staudamms direkt zufließt. Infolge des Staudammbaus ist auch das Einzugsgebiet des Xiangxi in diesem hoch-dynamischen Ökosystem von der Flussaufstauung und rapiden Landnutzungsänderungen mit Auswirkungen auf die Hangstabilität in der großflächig terrassierten Landschaft betroffen. Insbesondere das direkt von der Aufstauung betroffene südliche Einzugsgebiet ist durch steile bis extrem steile Hänge mit größtenteils flachgründigen Böden mittlerer bis sehr hoher Boden-erodierbarkeit gekennzeichnet. Zusätzlich erhöht die sehr hohe Regenerosivität die physische Vulnerabilität des gesamten Einzugsgebiets. Zwischen 1987 bis 2007 kennzeichnete ein deutlicher Rückgang von ackerbaulicher Nutzung und eine Zunahme von Wald und Buschland insbesondere den Norden des Einzugsgebietes. In direkter Nähe zum Rückstaubereich im Süden äußerte sich die Landnutzungsänderung von 1987 bis 2007 vor allem durch eine deutliche Umwandlung von Ackerland zu Orangenanbau als Cash crop.

Im Rahmen der vorliegenden Arbeit wurden Methoden im Bereich der Datenerhebung und Datenverarbeitung mit dem Ziel der Entwicklung eines Systems zur Risikoabschätzung von Bodenerosion erarbeitet und angepasst. Neben umfangreichen bodenkundlichen Arbeiten im Gelände wurden Fernerkundungsdaten sowie Landnutzungskarten und der dokumentierte Landnutzungswandel im Zeitraum von 1987 bis 2007 zur Parametrisierung des empirischen Erosionsmodells RUSLE herangezogen. Dieses diente der Abschätzung und Bewertung der räumlichen Verteilung und Dynamik des Bodenerosionsrisikos und der räumlichen Lokalisierung von Hochrisikogebieten. Zusätzlich wurde das neue konzeptionelle Modell *TerraCE* zur Ableitung des Terrassenzustands entwickelt und erstmals getestet. Mittels Data Mining-Verfahren wurde eine flächenkonkrete Prognose zur räumlichen Verteilung der identifizierten Terrassenzustandsklassen berechnet. Durch die Integration von umweltbezogenen sowie anthropogenen Indikatoren, die Rückschlüsse auf den Einfluss des Reliefs und des menschlichen Wirkens in diesem Gebiet zulassen, konnten weiterhin Art sowie Umfang der Störungen auf die Terrassenzustände und damit Terrassendegradation erfasst werden.

Generell ist das Xiangxi-Einzugsgebiet im Beobachtungszeitraum von 1987 bis 2007 durch eine Abnahme der mittleren jährlichen Bodenabträge und der absoluten Maxima infolge implementierter Umweltprogramme gekennzeichnet. Dennoch muss von einem gegenwärtig immer noch sehr hohen Erosionsrisikopotenzial ausgegangen werden. Häufigkeit und Intensität von Bodenerosion konzentrieren sich dabei vor allem auf den Rückstaubereich des Staudamms am Unterlauf des Xiangxi. Landnutzungsänderungen, Umsiedlung und Infrastrukturmaßnahmen wirken hier am stärksten. Eine an das lokale Relief unangepasste Konstruktion der Terrassen sowie deren unzureichende Instandhaltung können dabei durch Herabsetzung der Erosionsschutzwirkung der Terrassen die Erosionsdynamik stark beeinträchtigen. Rapide ökosystemare Veränderungen und eine einhergehende rasche Intensivierung und Inwertsetzung von Terrassenflächen können zu deren Degradation führen. Das Tempo dieser dynamischen Veränderungen berücksichtigt dabei selten vorhandenes Kapital und verfügbare Arbeitskraft zur kosten- und zeitintensiven Instandhaltung der Terrassenflächen. Auf den Terrassen werden hauptsächlich Orangen angebaut. Die starke Zunahme der erforderlichen Anbaufläche für den Orangenbau in sehr kurzer Zeit führt oft zur Überproduktion und damit zum Preisverfall auf den lokalen und regionalen Märkten. Durch den wenig gewinnbringenden Absatz der Orangen werden vor allem eine fehlende Motivation und zu geringes Kapital der Bauern für die sukzessive Verschlechterung des Zustands vieler Terrassenflächen verantwortlich gemacht. Da viele der umgesiedelten Bauern, die vormals in den flachen Talbereichen wirtschafteten, oft nicht mit den für sie erschwerten Anbaubedingungen auf den steilen Hangbereichen vertraut sind, fehlt es oft auch an Wissen zur aufwendigen Terrassenbewirtschaftung. Die Folge ist eine unangepasste Nutzung der Terrassen und Zunahme des Bodenabtrags.

Die Ergebnisse dieser Arbeit legen eine Ausweisung der Terrassenflächen als wichtige, zu erhaltene Ökosystemdienstleistung nahe, da sie bei guter Pflege eine sehr effektive Erosionskontrolle im stark reliefierten Xiangxi-Einzugsgebiet und darüber hinaus im Reservoir des Drei-Schluchten-Staudamms darstellen und eine nachhaltige Bewirtschaftung der Region erlauben. Des Weiteren zeigen die Ergebnisse der Arbeit, dass auch vor dem Hintergrund einer geringen zeitlichen und räumlichen Datenauflösung, Erosionsfaktoren erfolgreich flächendeckend regionalisiert und zur validen Bodenerosionsmodellierung herangezogen werden können. Vor dem Hintergrund weiterer Arbeiten im Rahmen des Yangtze-Projekts, sowie weiterer geplanter Staudammprojekte am Yangtze-Fluss und weltweit, stellt der geleistete Forschungsbeitrag somit einen wichtigen Ausgangspunkt für aufbauende Forschungen zum Erosionsrisikopotenzial und damit einhergehender Umweltgefahren, wie der Gewässerverschmutzung, dar.

7 REFERENCES

ADAMS, W.M., 1993. Development's deaf ear: downstream users and water releases from the Bakolori Dam, Nigeria. *World Development* 2, 1405-1416.

ALDHOUS, P., 1993. Tropical deforestation: not just a problem in Amazonia. *Science* 259, 1390.

ALEXANDRATOS, N., BRUINSMA, J., 2012. World agriculture towards 2030/2050, The 2012 Revision. ESA Working Paper No. 12-13, Agricultural Development Economics Division Food and Agriculture Organization of the United Nations, pp. 147. http://www.fao.org/docrep/016/ap106e/ap106e.pdf (05/31/2013).

ALIPOUR, Z.T., MAHDIAN, M.H., PAZIRA, E., HAKIMKHANI, S., SAEEDI, M., 2012. The determination of the best rainfall erosivity index for Namak Lake Basin and evaluation of spatial variations. *Journal of Basic and Applied Scientific Research* 2, 484-494.

ALIXANDRINI, M., 2010. Land cover change analysis from historical remote sensing images: case study Itaipú. PhD thesis, Karlsruhe Institute of Technology-Karlsruhe, Germany, pp. 104. http://digbib.ubka.uni-karlsruhe.de/volltexte/1000024197 (05/28/2013).

ARNAEZ, J., LASANTA, T., ERREAN, M.P., ORTIGOSA, L., 2010. Land abandonment, landscape evolution, and soil erosion in a Spanish Mediterranean mountain region: the case of Camero Viejo. *Land Degradation and Development* 22 (6), 537-550.

ARNOLDUS, H.M.J., 1977. Methodology used to determine the maximum potential average annual soil loss due to sheet and rill erosion in Morocco. *FAO Soils Bulletin* 34, 39-51.

ARVELA, A.S., PANAGOPOULUS, T., CAKULA, A., FERREIRA, V., AZEVEDO, J.C., 2012. Analysis of landscape change following the construction of the Alqueva dam, southern Portugal - approach and methods. Recent Researches in Environmental Science and Landscaping, 42-47. http://biblioteca.universia.net/html_bura/ficha/params/title/analysis-of-landscape-change-following-the-construction-of-the-alqueva/id/55534789.html (05/25/2013).

AW-HASSAN, A., ALSANABANI, M., BAMATRAF, A.R., 2000. Impact of land tenure and other socioeconomic factors on mountain terrace maintenance in Yemen. CAPRi Working Paper No. 3, CGIAR System-wide Program on Property Rights and Collective Action, International Development Research Center (IDRC), Ottawa, Canada, pp. 42, http://www.capri.cgiar.org/pdf/CAPRIWP03.pdf (08/16/2013).

BAGARELLO, V., D'ASARO, F., 1994. Estimating single storm erosion index. *Transactions of the American Society of Agricultural Engineers* 37, 785-791.

BARTHÈS, B., ROOSE, E., 2002. Aggregate stability as an indicator of soil susceptibility to runoff and erosion; validation at several levels. *Catena* 47, 133-149.

BATJES, N.H., 1996. Global assessment of land vulnerability to water erosion on a ½° by ½° grid. *Land Degradation and Development* 7, 353-365.

BAZZOFFI, P., GARDIN, L., 2011. Effectiveness of the GAEC standard of cross compliance retain terraces on soil erosion control. *Italian Journal of Agronomy*, DOI: 10.4081/ija.2011.6.s1.e6.

BEATTIE, J., 2002. Dam building, dissent, and development: The emergence of the Three Gorges Project. *New Zealand Journal of Asian Studies* 4, 138-158.

BEHRENS, T., ZHU, A.X., SCHMIDT, K., SCHOLTEN, T., 2010a. Multi-scale digital terrain analysis and feature selection in digital soil mapping. *Geoderma* 155, 175-185.

BEHRENS, T., SCHMIDT, K., ZHU, A.X., SCHOLTEN, T., 2010b. The ConMap approach for terrain-based digital soil mapping. *European Journal of Soil Science* 61, 133-143.

BEHRENS, T., SCHMIDT, K., SCHOLTEN, T., 2008. An approach to remove uncertainties in nominal environmental covariates and soil class maps. in: Hartmenink, A.E., McBratney, A., Mendoca-Santos, M.L. (Eds.), Digital soil mapping for regions and countries with sparse soil data infrastructure, Springer-Verlag, New York, pp. 213-224.

BELLIN, N., VAN WESEMAEL, B., MEERKERK, A., VANACKER, V., BARBERA, G.G., 2009. Abandonment of soil and water conservation structures in Mediterranean ecosystems - a case study from east Spain. *Catena* 76, 114-121.

BENNETT, S.J., RHOTON, F.E., 2007. Reservoir sedimentation and environmental degradation: Assessing trends in sediment-associated trace elements in Grenada Lake, Mississippi. *Journal of Environmental Quality* 36, 815-825.

BERGMANN, A. , BI, Y., CHEN, L., FLOEHR, T., HENKELMANN, B., HOLBACH, A., HOLLERT, H., HU, W., KRANZIOCH, I., KLUMPP, E., KÜPPERS, S., NORRA, S., OTTERMANNS, R., PFISTER, G., ROß-NICKOLL, M., SCHÄFFER, A., SCHLEICHER, N., SCHMIDT, B., SCHOLZ-STARKE, B., SCHRAMM, K.W., SUBKLEW, G., TIEHM, A., TEMOKA, C., WANG, J., WESTRICH, B., WILKEN, R.D., WOLF, A., XIANG, X., YUAN, Y., 2012. The Yangtze-Hydro Project: a Chinese - German environmental program. *Environmental Science and Pollution Research* 19, 1341-1344.

BEVAN, A., CONOLLY, J., COLLEDGE, S., FREDERICK, C., PALMER, C., SIDDALL, R., STELLATOU, A., 2012. The long-term ecology of agricultural terraces and enclosed fields from Antikythera. *Human Ecology* 41 (2), 255-272.

BIEGER, K., 2013. Assessing the impact of land use change on hydrology and sediment yield in the Xiangxi Catchment (China) using SWAT. Dissertation, University of Kiel, Kiel, pp. 179.

BIEGER, K., HÖRMANN, G., FOHRER, N., 2012. Simulation of streamflow and sediment with the Soil Water Assessment Tool in a data scarce catchment in the Three Gorges Region, China. *Journal of Environmental Quality*, DOI:10.2134/jeq2011.0383 (online).

BOETTINGER, J.L., RAMSEY, R.D., BODILY, J.M., COLE, N.J., KIENAST-BROWN, S., NIELD, S.J., SAUNDERS, A.M., STURM, A.K., 2008. Landsat spectral data for digital soil mapping. in: Hartemink, A.E., McBratney, A., Mendoca-Santos, M.L. (Eds.), Digital Soil Mapping with Limited Data. Springer-Verlag, New York, pp. 193-202

BOLINNE, A., LAUANT, A., ROSSEAU, P., PAUWELS, J.M., GABRIELS, D., AELTERMANN, J., 1980. Provisional rain erosivity map of Belgium, in: DeBoodt, M., Gabriels, D. (Eds.), Assessment of Erosion. John Wiley and Sons, Chichester, pp. 111-120.

BOT, A.J., NACHTERGAELE, F.O., YOUNG, A., 2000. Land resource potential and constraints at regional and country levels. World Soil Resources Report 90, Land and Water Development Division, FAO, Rome, pp. 122, ftp://ftp.fao.org/agl/agll/docs/wsr.pdf (05/22/2013).

BRADY, N.C., WEIL, R.R., 2007. The nature and properties of soil. 14th edition, Prentice Hall, New Jersey, pp. 980.

BRANCUCCI, G., PALIAGA, G., 2006. The hazard assessment in a terraced landscape: preliminary result of the liguria (Italy) case study in the Interreg III Alpter Project. in: Nadim, N., Pöttler, R., Einstein, H., Klapperich, H., Kramer, S. (Eds.), Geohazards. ECI Symposium Series, Volume P07 (2006), pp.10, http://dc.engconfintl.org/geohazards/16 (01/15/2009).

BRANTLEY, S.L., 2008. Understanding soil time. *Science* 321, 1454-1455.

BREIMAN, L., FRIEDMAN, J.H., OLSHEN, R.A., STONE, C.J., 1984. Classification and regression trees. Wadsworth International Group: Belmont, California, pp. 43-49.

BREIMAN, L., 2001. Random forests. Machine Learning 45, 5-32.

BRESHEARS, D.D., WHICKER, J.J., PINDER, J.E., JOHANSEN, M.P., 2002. A comparison of wind and water erosion rates among grassland, shrubland, and forest ecosystems. in: Lee, J., Zobeck, T.M. (Eds.), Proceedings of ICAR5/GCTE-SEN Joint Conference, International Center for Arid and Semiarid Lands Studies, Texas Tech University, Lubbock, Texas, USA Publication 02-2, p. 152.

BROWN, P.H, MAGEE, D., XU, Y., 2008. Socioeconomic vulnerability in China's hydropower development. *China Economic Review* 19, 614-627.

BROWN, L.C., FOSTER, G.R., 1987. Storm erosivity using idealized intensity distributions. *Transactions of the American Society of Agricultural Engineers* 30, 379-386.

china.org.cn[1] Law of The People's Republic of China on Water and Soil Conservation. http://www.china.org.cn/environment/2007-08/20/content_1034358.htm (01/22/2013).

china.org.cn[2]. Yangtze River. http://www.china.org.cn/english/travel/40876.htm# (05/22/2013).

China's national report on sustainable development, 2012. http://www.china-un.org/eng/zt/sdreng/ (05/19/2013).

CAI, G.G., WANG, H., CURTIN, D., ZHU, Y., 2005. Evaluation of the EUROSEM model with single event data on steeplands in the Three Gorges Reservoir Area, China. *Catena* 59, 19-33.

CAO, S., CHEN, L., FENG, Q., LIU, Z., 2007. Soft-riser bench terrace design for the hilly loess region of Shaanxi Province, China. *Landscape and urban planning* 80, 184-19.

CHEMIN, A., VAROTTO, M., 2008. Veneto. The “masiere” of the Brenta Valley. in: Scaramellini, G., Varotto, M. (Eds.), Terraced landscapes of the Alps - Atlas, pp. 97-101, ALPTER Project, Marsilio, Venice, Italy, http://www.alpter.net/ALPTER-Project-final-publications.html (04/11/2011).

CHEN, Z.Y., LI, J.F., SHEN, H.T., WANG, Z.H., 2001. Yangtze River of China: historical analysis of discharge variability and sediment flux. *Geomorphology* 41, 77-91.

CHENG, C.T., SHEN, J.J., WU, X.Y., CHAU, K.W., 2012. Operation challenges for fast-growing China’s hydropower systems and respondence to energy saving and emission reduction. *Renewable and Sustainable Energy Reviews* 16, 2386-2393.

CHORLEY, R.J., 1978. The hillslope hydrological cycle. in: Kirkby, M.J. (Ed.), Hillslope hydrology. Wiley, Chichester, pp. 1-42.

CHU, M., LI, X., LU, J., HOU, X., WANG, X., 2012. Stability of Huangtupo I# landslide under Three Gorges Reservoir operation. Applied Mechanics and Materials 170-173; 1116-1123.

COCHRANE, T.A., NORTON, L.D., CASTRO-FILHO, C., CAVIGLIONE, J.H., 2004. Development of a river sediment transport monitoring system for large reservoirs. *Applied Engineering in Agriculture* 20 (6), 771-781.

COCHRANE, T.A., CASTRO-FILHO, C., CAVIGLIONE, J.H., NORTON, D.L., FREDERIGI BENASSI, S., 2003. Identification of high risk erosion areas within the Itaipu basin by watershed modeling through RUSLE. II World Congress on Conservation Agriculture, Foz do Iguaçu, Brazil. http://www.agteca.com/publications/poster_cons_Foz3.pdf (05/28/2013).

COCHRANE, T.A., CASTRO-FILHO, C., JOHANSSON, L.P., MARENDA, L.D., CAVIGLIONE, J.H., NORTON, D.L., TEIXEIRA, P.H., LIMONS, C.A., 2002. Reduction of Sediment Delivery to the Itaipu Reservoir: A new vision through the implementation of monitoring techniques and watershed management. International Commission on Large Dams. Symposium on Reservoir Management in Tropical and Sub-Tropical Regions, September, 2002, Iguassu, Brazil. http://www.ars.usda.gov/research/publications/publications.htm?seq_no_115=138247 (05/28/2013).

COMOLLI, R., 2005. Soils and man-made terraces in Sondrio Region: pilot area of Pianazzola. ALPTER Terraced Landscapes of the Alpine Arc, Meeting Internazionale, 3-4 Novembre 2005, Sondrio SO, Italy. http://www.alpter.net/Documents-from-research-activities.html (01/15/2009).

CORBEELS, M., SHIFERAW, A., HAILE, M., 2000. Farmers' knowledge of soil fertility and local management strategies in Tigray, Ethopia. Managing Africa's Soil No. 1, pp. 24. IIED, London. http://pubs.iied.org/pdfs/7421IIED.pdf (11/01/2011).

CUI, P., GE, Y., LIN, Y., 2011. Soil erosion and sediment control effects in the Three Gorges Reservoir Region, China. *Journal of Resources and Ecology* 2(4), 289-297.

CUTLER, D.R., EDWARDS, T.C. JR., BEARD, K.H., CUTLER, A., HESS, K.T., GIBSON, J., LAWLER, J.J., 2007. Random forests for classification in ecology. *Ecology* 88, 2783-2792.

DA SILVA, A.M., ALVARES, C.A., WATANABE, C.H., 2011. Natural potential for erosion for Brazilian territory. in: Godone, D., Stanchi, S. (Eds.), Soil erosion studies. InTech, pp. 23, ISBN: 978-953-307-710-9, http://www.intechopen.com/books/soil-erosion-studies/natural-potential-for-erosion-for-brazilian-territory (06/27/2013).

DAI, H., ZHENG, T., LIU, D., 2010. Effects of reservoir impounding on key ecological factors in the Three Gorges Region. *Procedia Environmental Sciences* 2, 15-24.

DAI, S.B., LU, X.X., YANG, S.L., CAI, A.M., 2008. A preliminary estimate of human and natural contributions to the decline in sediment flux from the Yangtze River to the East China Sea. *Quaternary International* 186, 43-54.

DAI, H., WANG, L., WANG, R., 2006. The Three Gorges Project and eco-environmental monitoring system. *Environmental Informatics Archives* 4, 419-426.

DAI, D., TAN, Y., 1996. Soil erosion and sediment yield in the Upper Yangtze River basin. Erosion and sediment yield: Global and Regional Perspectives. Proceedings of the Exceter Symposium, July 1996, IAHS Publ. no. 236, 191-203.

DAMENE, S., TAMENE, L., VLEK, P.L.G., 2012. Performance of farmland terraces in maintaining soil fertility: a case of Lake Maybar watershed in Wello, Northern Highlands of Ethiopia. *Journal of Life Sciences* 6, 1251-1261.

DE ASIS, A.M., OMASA, K., 2007. Estimation of Vegetation Parameter for Modeling Soil Erosion Using Linear Spectral Mixture Analysis of Landsat ETM Data. ISPRS *Journal of Photogrammetry and Remote Sensing* 62 (4), 309-324.

DE JONG, S.M., 1994. Derivation of Vegetative Variables from a Landsat TM Image for Modelling Soil Erosion. *Earth Surface Processes and Landforms* 19 (2), 165-178.

DE LIMA, J.L.M.P., TAVARES, P., SINGH, V.P., DE LIMA, M.I.P., 2009. Investigating the importance of rainstorm direction on overland flow and soil loss in a laboratory circular soil-flume. *Geoderma* 152, 9-15.

DE SANTOS LOUREIRO, N., DE AZEVEDO COUTINHO, M., 2001. A new procedure to estimate the RUSLE EI30 index based on monthly rainfall data and applied to the Algarve region, Portugal. *Journal of Hydrology* 250, 12-18.

DEININGER, K., JIN, S., 2006. Tenure security and land-related investments: evidence from Ethiopia. *European Economic Review* 50, 1245-1277.

DENG, L., SHANGGUAN, Z., LI, R., 2012. Effects of the grain-for-green program on soil erosion in China. *International Journal of Sediment Research* 27(1), 120-127.

DIODATO, N., BELLOCCHI, G., 2009. Assessing and modelling changes in rainfall erosivity at different climate scales. *Earth Surface Processes and Landforms* 34, 969-980.

DUFKOVA, J., TOMAN, J., 2004. Influence of climate change on soil erosion in the Czech Republic, Europe. ISCO 2004 - 13th International Soil Conservation Organisation Conference - Brisbane, July 2004, pp. 4. http://tucson.ars.ag.gov/isco/isco13/PAPERS%20AE/DUFKOVA%202.pdf (05/31/2013).

DVWK, 1990. Grundlagen der Verdunstungsermittlung und Erosivität von Niederschlägen. Deutscher Verband für Wasserwirtschaft und Kulturbau (Eds.) Parey-Verlag, Hamburg (in German).

EHRET, D., ROHN, J., DUMPERTH, C., ECKSTEIN, S., ERNSTBERGER, S., OTTE, K., RUDOLPH, R., WIEDENMANN, J., XIANG, W., BI, R., 2010. Frequency ratio analysis of mass movements in the Xiangxi catchment, Three Gorges Reservoir area, China. *Journal of Earth Science* 21 (6), 824-834.

EL ATTA, H.A., AREF, I., 2010. Effect of terracing on rainwater harvesting and growth of Juniperus Procera Hchst. ex Endlicher. *International Journal of Environmental Science and Technology* 7, 59-66.

EL-SWAIFY, S.A., 1997. Factors affecting soil erosion hazards and conservation needs for tropical steeplands. *Soil Technology* 11, 3-16.

EL-SWAIFY, S.A., DANGLER, E.W., ARMSTRONG, C.L., 1982. Soil erosion by water in the tropics. Research Extension Series 024, Department of Agronomy and Soil Science, College of Tropical Agriculture and Human Resources, University of Hawaii Honolulu, Hawaii, , pp. 173.

ELSENBEER, H., CASSEL, D.K., TINNER, W., 1993. A daily rainfall erosivity model for Western Amazonia. *Journal for Soil and Water Conservation* 48, 439-444.

ERENCIN, Z., 2000. C-factor mapping using remote sensing and GIS - a case study of Lom Sak/Lom Kao, Thailand. Dissertation, Institute of Geography of the University of Giessen and Soil Science Devision, International Institute for Aerospace Survey and Earth Sciences (ITC), pp. 25. http://geb.uni-giessen.de/geb/volltexte/2004/1537/pdf/ErencinZihni-2000-08-15.pdf (03/17/2010).

ESTEVE, J.F., IMESON, A., JARMAN, R., BARBERIS, R., RYDELL, B., CASTILLO SÁNCHEZ, V., VANDEKERCKHOVE, L., 2004. Pressures and drivers causing soil erosion. in: Van-Camp, L., Bujarrabal, B., Gentile, A.R., Jones, R.J.A., Montanarella, L., Olazabal, C., Selvaradjou, S.K. (Eds.), Reports of the Technical Working Groups Established Under the Thematic Strategy for Soil Protection. Volume II Erosion. EUR 21319 EN/2, Office for Official Publications of the European Communities, Luxembourg. http://ec.europa.eu/environment/soil/pdf/vol2.pdf (01/27/2013).

ESWARAN, H., LAL, R., REICH, P.F., 2001. Land degradation: an overview. in: Bridges, E.M., Hannam, I.D., Oldeman, L.R., Pening de Vries, F.W.T., Scherr, S.J., Sompatpanit S. (Eds.), Responses to Land Degradation. Proc. 2nd. International Conference on Land Degradation and Desertification, Khon Kaen, Thailand. Oxford Press, New Delhi, India.

FERREIRA, V., PANAGOPOULOS, T., 2012. Predicting soil erosion at the Alqueva dam watershed: seasonal variations. *Recent Researches in Environment, Energy Systems and Sustainability*, 99-104. http://www.wseas.us/e-library/conferences/2012/Algarve/EEESD/EEESD-14.pdf (05/25/2013).

FERREIRA, V., PANAGOPOULOS, T., 2010. Soil erodibility assessment at the Alqueva dam watershed, Portugal. *Advances in Climate Changes, Global Warming, Biological Problems and Natural Hazards*, pp.112-118. http://www.wseas.us/e-library/conferences/2010/Faro/NAGB/NAGB-17.pdf (05/25/2013).

FERRO, V., PORTO, P., YU, B., 1999. A comparative study of rainfall erosivity estimation for southern Italy and southeastern Australia. *Hydrological Sciences Journal* 44, 3-24.

FIGUEIREDO, M. DO A., AUGUSTIN, C.H.R.R., FABRIS, J.D., 1999. Mineralogy, size, morphology and porosity of aggregates and their relationship with soil susceptibility to water erosion. *Hyperfine Interactions* 122 (1-2), 177-184.

FLANAGAN, D.C., NEARING, M.A., 1995. USDA Water erosion prediction project: hillslope profile and watershed model documentation. USDA-ARS National Soil Erosion Laboratory Report No. 10, pp. 141, http://www.ars.usda.gov/Research/docs.htm?docid=18073

FOURNIER, F., 1960. Climat et erosion; la relation entre l'erosion du sol par l'eau et les precipitations atmospheriques. Presses universitaires de Frances, Paris, pp. 201.

FU, B.J., ZHAO, W.W., CHEN, L.D., ZHANG, Q.J., LÜ, Y.H., GULINCK, H., POESEN, J., 2005, Assessment of soil erosion at large watershed scale using RUSLE and GIS: a case study in the Loess Plateau of China. *Land Degradation and Development* 16, 73-85.

GEIßLER C, NADROWSKI K, KÜHN P, BARUFFOL M, BRUELHEIDE H, SCHMID, B., SCHOLTEN, T., 2013. Kinetic energy of throughfall in subtropical forests of SE China - effects of tree canopy

structure, functional traits, and biodiversity. *PLoS ONE* 8 (2): e49618. DOI:10.1371/journal.pone.0049618

GEIßLER, C., KÜHN, P., BÖHNKE, M., BRUELHEIDE, H., SHI, X.Z., SCHOLTEN, T., 2012. Measuring splash erosion under vegetation using sand-filled splash cups. *Catena* 91, 85-93.

GEIßLER, C., KÜHN, P., SHI, X.Z., SCHOLTEN, T., 2010. Estimation of throughfall erosivity in a highly diverse forest ecosystem using sand-filled splash cups. *Journal of Earth Science* 21 (6), 897-900.

GHAHRAMANI, A., YOSHIHARU, I., MUDD, S.M., 2011. Field experiments constraining the probability distribution of particle travel distance during natural rainstorms on different slope gradients. *Earth Surface Processes and Landforms* 37, 473-485.

GILLEY, J.E., FLANAGAN, D.C., 2007. Early investments in soil conservation research continues to provide dividends. *American Society of Agricultural and Biological Engineers* 50 (5), 1595-1601.

GILLEY, J.E., 2004. Erosion water-induced, in: Hillel, D., Rosenzweig, C., Powlson, D., Scow, K., Singer, M., Sparks, D. (eds.), Encyclopedia of soils in the environment. Academic Press, 1 edition, four-volume set, 2,200 pages, pp. 463-469.

GLEICK, P.H., 2009. Three Gorges Dam Project, Yangtze River, China. in: Gleick, H.P. (Ed.), The World's Water 2008-2009: The Biennial Report on Freshwater Resources. Water Brief 3, Island Press, pp. 432.

GOOVAERTS, P., 1999. Using elevation to aid the geostatistical mapping of rainfall erosivity. *Catena* 34, 227-242.

GOVERS, G., 2011. Misapplications and misconceptions of erosion models. in: Morgan, R.P.C., Nearing, M.A. (Eds.), 2011. Handbook of soil erosion modelling. 1st edition, Blackwell Publishing Ltd., pp. 416.

GROHMANN, C.H., 2006. Resampling SRTM 03" data with kriging. *GRASS/OSGeo-News Open Source GIS and Remote Sensing information* 4, 21-25.

GUO, G., 2010. Environmental security concerns and the Three Gorges Reservoir Basin in China. Issue Brief of the Foundation for Environmental Security and Sustainability (FESS), USAID, pp. 12, http://www.fess-global.org/Publications/issuebriefs/ES_Three_Gorges_Reservoir_Basin_in_China.pdf (12/17/2012).

GUO, Z., XIAO, X., GAN, Y., ZHENG, Y., 2001. Ecosystem functions, services and their values - a case study in Xingshan County of China. *Ecological Economics* 38, 141-154.

GUO, Z., XIAO, X., LI, D., 2000. An assessment of ecosystem services: Water flow regulation and hydroelectric power production. *Ecological Applications* 10, 925-936.

HAMMAD, A.A., HAUGEN, L.E., BØRRESEN, T., 2004. Effects of stonewalled terracing techniques on soil water conservation and wheat production under Mediterranean conditions. *Environmental Management* 34, 701-710.

HANCOCK, G.R., MARTINEZ, C., EVANS, K.G., MOLIERE, D.R., 2006. A comparison of SRTM and high-resolution digital elevation models and their use in catchment geomorphology and hydrology: Australian examples. *Earth Surface Processes and Landforms* 31, 1394-1412.

HAO, F., CHANG, Y., NING, D., 2004. Assessment of China's economic loss resulting from the degradation of agricultural land in the end of the 20th century. *Journal of Environmental Sciences* 16, 199-203.

HE, K., LI, X., YAN, X., GUO, D., 2008. The landslides in the Three Gorges Reservoir Region, China and the effects of water storage and rain on their stability. *Environmental Geology* 55, 55-63.

HE, L., KING, L., JIANG, T., 2003. On the land use in the Three Gorges Reservoir area. *Journal of Geographical Sciences* 13, 416-422.

HEGGELUND, G., 2006. Resettlement programmes and environmental capacity in the Three Gorges Dam Project. *Development and Change* 37, 179-199.

HEMING, L., WALEY, P., REES, P., 2001. Reservoir resettlement in China: past experience and the Three Gorges Dam. *The Geographical Journal* 167, 195-212.

HER, Y., HEATWOLE, C.D., 2008. Assessment of interpolation methods for refining SRTM and DEM. American Society of Agricultural and Biological Engineers, An ASABE Meeting Presentation Paper Number: 085214, Rhode Island Convention Center Providence, Rhode Island June 29 - July 2, 2008.

HEYWOOD, V.H., 1995. Global biodiversity assessment. Cambridge, UK, Cambridge University Press, pp. 1152.

HIGGITT, D.L., LU, X.X., 2001. Sediment delivery to the three gorges: 1. Catchment controls. *Geomorphology* 41, 143-156.

HONG, Q., CHEN, P., 1990. Soils of China. Science Press, Beijing, China, pp. 873.

HOWARD, A.D., 1999. Simulation of gully erosion and bistable landforms. in: Darby, S.E., Simon, A. (Eds.), Incised river channels. pp. 277-299 and Annex, John Wiley & Sons Ltd.

HU, B.Q., YANG, Z.S., WANG, H.J., SUN, X.X., BI, N.S., 2009. Sedimentation in the Three Gorges Dam and its impact on the sediment flux from the Changjiang (Yangtze River), China. *Hydrology and Earth System Sciences* 6, 5177-5204.

HUANG, J.Q., LU, D.S., LI, J., WU, J.S., CHEN, S.Q., ZHAO, W.M., GE, H.L., HUANG, X.Z., YAN, X.J., 2012. Integration of remote sensing and GIS for evaluating soil erosion risk in northwestern Zhejiang, China. *Photogrammetric Engineering and Remote Sensing* 78 (9), 935-946.

HUANG, H., YAN, Z., 2009. Present situation and future prospects of hydropower in China. *Renewable and Sustainable Energy Reviews* 13, 1652-1656.

HUANG, B.W., 1987. Slopeland utilization and amelioration: importance and feasibility. *Geographical Research* 6, 1-5.

HUDSON, N., 1981. Soil conservation. Cornell University Press, London, pp. 324.

HURNI, H., GIGER, M., MEYER, K. (Eds.), 2006. Soils on the global agenda. Developing international mechanisms for sustainable land management. Prepared with the support of an international group of specialists of the IASUS Working Group of the International Union of Soil Sciences (IUSS). Centre for Development and Environment, Bern, pp. 64.

IECA, 1991. Erosion control - a global perspective. Proceedings of Conference XXII, International Erosion Control Association, Steamboat Springs, CO, USA, pp. 561.

IUSS Working Group WRB. 2007.World Reference Base for Soil Resources 2006, first update 2007. World Soil Resources Reports No. 103. FAO, Rome, pp. 128.

INBAR, M., LLERENA, C.A., 2000. Erosion processes in high mountain agricultural terraces in Peru. *Mountain Research and Development* 20, 72-79.

INTERNATIONAL RIVERS, 2007. Damming statistics (Date: Monday, October 22, 2007). http://www.internationalrivers.org/damming-statistics (05/24/2013).

JACKSON, S., SLEIGH, A., 2000. Resettlement for China's Three Gorges Dam: socio-economic impact and institutional tensions. *Communist and Post-Communist Studies* 33, 223-241.

JARVIS, A., REUTER, H.I., NELSON, A., GUEVARA, E., 2008. Hole-filled seamless SRTM data V4, International Centre for Tropical Agriculture (CIAT), available from http://srtm.csi.cgiar.org.

JENSEN, J.R., 2000. Remote Sensing of the Environment: An Earth Resource Perspective. Prentice Hall, New Jersey, pp. 544.

JETTEN, V.G., MANETA, M.P., 2011. Calibration of erosion models. in: Morgan, R.P.C., Nearing, M.A. (Eds.), 2011. Handbook of soil erosion modelling. 1st edition, Blackwell Publishing Ltd., pp. 416.

JIM, C.Y., YANG, F.Y., 2006. Local Responses to Inundation and De-Farming in the Reservoir Region of the Three Gorges Project (China). *Environmental Management* 38, 618-637.

JONES, A., PANAGOS, P., BARCELO, S., BOURAOUI, F., BOSCO, C., DEWITTE, O., GARDI, C., ERHARD, M., HERVÁS, J., HIEDERER, R., JEFFERY, S., LÜKEWILLE, A., MARMO, L., MONTANARELLA, L., OLAZÁBAL, C., PETERSEN, J.E., PENIZEK, V., STRASSBURGER, T., TÓTH, G., VAN DEN EECKHAUT, M., VAN LIEDEKERKE, M., VERHEIJEN, F., VIESTOVA, E., YIGINI, Y., 2012.The State of Soil in Europe. A contribution of the JRC to the European Environment Agency's Environment State and Outlook Report-SOER 2010. Report EUR 25186 EN.

KACHINSKY, N.A., 1965. Soil Physics, Part I. Kolos Publishers. Moscow, pp. 132-139 (in Russian).

KAVIAN, A., FATHOLLAH NEJAD, Y., HABIBNEJAD, M., SOLEIMANI, K., 2011. Modeling seasonal rainfall erosivity on a regional scale: a case study from Northeastern Iran. *International Journal of Environmental Research* 5, 939-950.

KEERATIKASIKORN, G., TRISIRISATAYAWONG, I., 2008. Reconstruction of 30m DEM from 90m SRTM DEM with bicubic polynomial interpolation method. The International Archives of the Photogrammetry, *Remote Sensing and Spatial Information Sciences* Vol. XXXVII. Part B1. Beijing 2008.

KOLB, R.T., 2003. About figures and aggregates: some arguments for a more scrupulous evaluation of quantitative data in the history of population and agriculture in Chin (1644-1949). Agriculture, Population and economic development in China and Europe I, pp. 200-275, Breuninger Stiftung, Stuttgart.

KONZ, N., SCHAUB, M., PRASUHN, V., BAENNINGER, D., ALEWELL, C., 2009. Caesium-137-based erosion-rate determination of a steep mountainous region. Journal of Plant Nutrition and Soil Science 172, 615-622.

KOULOURI, M., GIOURGA, C., 2007. Land abandonment and slope gradient as key factors of soil erosion in Mediterranean terraced lands. *Catena* 69, 274-278.

KOVDA, V.A., 1959. Outline of soils and natural conditions of China. Nayku Press, Publishing House of the Academy of Sciences of the U.S.S.R., Moscow (in Russian).

LAL, R., PIMENTEL, D., 2008. Soil erosion: a carbon sink or source? *Science* 22, 1040-1042.

LAL, R., 2004. Soil carbon sequestration impacts on global climate change and food security. *Science* 304, 1623-1627.

LAL, R., 2003. Soil erosion and the global carbon budget. *Environment International* 29, 437-450.

LAL, R., 2001. Soil degradation by erosion. *Land Degradation & Development* 12, 519-539.

LAL, R., STEWART, B.A., 1990. Soil degradation. Advances in Soil Science, 1st edition, New York, Springer-Verlag, pp. 368.

LAL, R., 1976. Soil erosion problems on an alfisol in western Nigeria and their control. Communications and Information Office, IITA Monograph no. 1, Ibadan, Nigeria, pp. 208, available from http://library.wur.nl/isric.

LASANTA, T., ARNÁEZ, J., OSERÍN, M., ORTIGOSA, L.M., 2001. Marginal lands and erosion in terraced fields in the Mediterranean mountains - a case study in the Camero Viejo (Northwestern Iberian System, Spain). *Mountain Research and Development* 21, 69-76.

LEHNER, B., REIDY LIERMANN, C., REVENGA, C., VÖRÖSMARTY, C., FEKETE, B., CROUZET, P., DÖLL, P., ENDEJAN, M., FRENKEN, K., MAGOME, J., NILSSON, C., ROBERTSON, J.C., Rödel, R., Sindorf, N., Wisser, D., 2011. High resolution mapping of the world's reservoirs and dams for sustainable river flow management. *Frontiers in Ecology and the Environment* 9 (9), 494-502.

LESSCHEN, J.P., CAMMERRAT, L.H., NIEMANN, T., 2008. Erosion and terrace failure due to agricultural abandonment in a semi-arid environment. *Earth Surface Processes and Landforms* 33, 1574-1584.

LI, H., CHEN, X., KYOUNG, J.L., CAI, X., MYUNG, S., 2010. Assessment of soil erosion and sediment yield in Liao watershed, Jiangxi Province, China Using USLE, GIS, and RS. *Journal of Earth Science* 21, 941-953.

LI, Y., NGUYEN, M.L., 2008. Effectiveness of soil conservation measures in reducing soil erosion and improving soil quality in China, assessed by using fallout radionuclides. in: Zdruli, P., Costantini, E. (Eds.), "Moving ahead from assessments to action: could we win the struggle with land degradation?" 5th Int. Conference on Land Degradation. Valenzano Bari, Italy 18-22 September 2008, pp. 287-290, Book of abstracts. ISBN 2-85352-399-3, II.

LI, W., YANG, D.T., 2005. The Great Leap Forward: an anatomy of a central planning disaster. *Journal of Political Economy* 113 (4), 840-877.

LI, Y., LINDSTROM, M.J., 2001. Evaluating soil quality - soil redistribution relationship on terraces and steep hillslope. *Soil Science Society of America Journal* 65, 1500-1508.

LI, H., ZHANG, X., CHEN, X., LU, W., 1999. Soil and water strategies on the red and yellow soils of South China. in: Stott DE, Mohtar, R.H., Steinhardt, G.C. (Eds.), 2001. Sustaining the global farm. Selected papers from the 10th International Soil Conservation Meeting held May 24-29, 1999 at Purdue University and the USDA-ARS National Soil Erosion Laboratory and Purdue University, pp. 6, http://topsoil.nserl.purdue.edu/nserlweb-old/isco99/pdf/iscodisc/Sustaining%20the%20Global%20Farm/P074-Huaxing%20Li.pdf (03/16/2010).

LIAW, A., WIENER, A., 2011. Package 'randomForest'. http://cran.r-project.org/web/packages/randomForest/randomForest.pdf (08/12/2011).

LILLESAND, T.M., KIEFER, R., CHIPMAN, J.W., 2007. Remote Sensing and Image Interpretation. 6th Edition. John Wiley and Sons, New York, pp. 768.

LIU, N., 2012. People's Republic of China: Water and Soil Conservation Law. *IUCN Academy of Environmental Law e-Journal* 1, 69-74.

LIU, C., WU, B., 2010. 'Grain for Green Programme' in China: policy making and implementation? Briefing Series - Issue 60, China Policy Institute, University of Nottingham, pp. 17. http://www.nottingham.ac.uk/cpi/documents/briefings/briefing-60-reforestation.pdf (01/12/2013).

LIU, Y., LUO, Z., 2005. A study on estimation of the amount of soil erosion in small watershed based on GIS: a case study in the Three Gorge Area of China. *Geoscience and Remote Sensing (IGARSS), IEEE International Geoscience and Remote Sensing Symposium* 3, 1859-1863.

LIU, S.M., ZHANG, J., CHEN, H.T., WU, Y., XIONG, H., ZHANG, Z.F., 2003. Nutrients in the Changjiang and its tributaries. *Biochemistry* 62, 1-18.

LO, A., EL-SWAIFY, S.A., DANGLER, E.W., SHINSHIRL, L., 1985. Effectiveness of EI30 as an erosivity index in Hawaii, in: El-Swaify, S.A., Moldenhauer, W.C., Lo, A. (Eds.), Soil Erosion and Conservation. *Soil Conservertaion Society of America*, Ankeny, pp. 384-392.

LONG, H., WU, X., WANG, W., DONG, G., 2008. Analysis of Urban-Rural Land use Change during 1995-2006 and Its Policy Dimensional Driving Forces in Chongqing, China. *Sensors* 8, 681-699.

LONG, H.L., HEILIG, G.K., WANG, J., LI, X.B., LUO, M., WU, X.Q., ZHANG, M., 2006. Land use and soil erosion in the upper reaches of the Yangtze River: some socio-economic considerations on China's Grain-For-Green Programme. *Land Degradation & Development* 17, 589-603.

LÓPEZ-PUJOL, J., REN, M.X., 2009. Biodiversity and the Three Gorges Reservoir: a troubled marriage. *Journal of Natural History* 42, 2765-2786.

LU, X.X., HIGGITT, D.L., 2000. Estimating erosion rates on sloping agricultural land in the Yangtze Three Gorges, China, from caesium-137 measurements. *Catena* 39, 33-51.

LU, X.X., HIGGITT, D.L., 1999. Sediment yield variability in the Upper Yangtze, China. *Earth Surface Processes and Landforms* 24, 1077-1093.

LYNN USERY, E., FINN, M.P., SCHEIDT, D.J., RUHL, S., BEARD, T., BEARDEN, M., 2004. Geospatial data resampling and resolution effects on watershed modeling: A case study using the agricultural non-point source pollution model. *Journal of Geographical Systems* 6, 289-306.

MAINSTONE, C.P., DILS, R.M., WITHERS, P.J.A., 2008. Controlling sediment and phosphorus transfer to receiving water - a strategic management perspective for England and Wales. *Journal of Hydrology* 350, 131-143.

MANNAERTS, C.M., GABRIELS, D., 2000. Rainfall erosivity in Cape Verde. *Soil and Tillage Research* 55, 207-212.

MCCOOL, D.K., BROWN, L.C., FOSTER, G.R., MUTCHLER, C.K., MEYER, L.D., 1987. Revised slope steepness factor for the Universal Soil Loss Equation. *Transactions of the American Society of Agricultural Engineers* 30, 1387-1396.

MCDONALD, B., WEBBER, M., DUAN, Y., 2008. Involuntary resettlement as an opportunity for development: the case of urban resettlers of the Three Gorges Project, China. *Journal of Refugee Studies*. DOI: 10.1093/jrs/fem052

MEN, M., YU, Z., XU, H., 2008. Study on the spatial pattern of rainfall erosivity based on geostatistics in Hebei Province, China. *Frontiers of Agriculture in China* 2, 281-289.

MENG, Q. H., FU, B. J., YANG, L.Z., 2001. Effects of land use on soil erosion and nutrient loss in the Three Gorges Reservoir Area, China. *Soil Use and Management* 17, 288-291.

MEP, 2010. Bulletin on the ecological and environmental monitoring results of the Three Gorges Project 2010. Ministry of Environmental Protection of the People's Republic of China, 2010, pp. 47. http://english.mep.gov.cn/down_load/Documents/201104/P020110407569629279171.pdf (05/28/2013).

MEP, 2009. Bulletin on the ecological and environmental monitoring results of the Three Gorges Project 2009. Ministry of Environmental Protection of the People's Republic of China, 2008, pp. 84. http://english.mep.gov.cn/down_load/Documents/201002/P020100225376514651439.pdf (05/28/2013).

MEP, 2008. Bulletin on the ecological and environmental monitoring results of the Three Gorges Project 2008. Ministry of Environmental Protection of the People's Republic of China, 2009, pp. 53. http://english.mep.gov.cn/down_load/Documents (05/28/2013).

MEUSBERGER, K., STEEL, A., PANAGOS, P., MONTANARELLA, L., ALEWELL, C., 2012. Spatial and temporal variability of rainfall erosivity factor for Switzerland. *Hydrology and Earth System Sciences* 16, 167-177.

MIDDLETON, N., THOMAS, D., 1997. World Atlas of Desertification. Published for UNEP by Arnold Publ. 2nd. Edition. London, pp. 182.

MIKHAILOVA, E.A., BRYANT, R.B., SCHWAGER, S.J., SMITH, S.D., 1997. Predicting rainfall erosivity in Honduras. *Soil Science Society of America Journal* 61, 273-279.

MONTGOMERY, D.R., 2007a. Dirt: The erosion of civilizations. University of California Press, Ltd., London, pp. 285.

MONTGOMERY, D.R., 2007b. Soil erosion and agricultural sustainability. PNAS 104(33), 13268-13272.

MORGAN, R.P.C., 2011. Model development: a user's perspective. in: Morgan, R.P.C., Nearing, M.A. (Eds.), 2011. Handbook of soil erosion modelling. 1st edition, Blackwell Publishing Ltd., pp. 416.

MORGAN, R.P.C., NEARING, M.A. (Eds.), Handbook of erosion modelling. 1st edition 2011, Blackwell Publishing Ltd., pp. 416.

MORGAN, R.P.C., 2005. Soil erosion and conservation. Third edition, Blackwell Publishing, pp. 316.

MORGAN, R.P.C., QUINTON, J.N., SMITH, R.E., GOVERS, G., POESEN, J.W.A., AUERSWALD, K., CHISCI, G., TORRI, D., STYCZEN, M.E., 1998. The European Soil Erosion Model (EUROSEM): a dynamic approach for predicting sediment transport from fields and small catchments. *Earth Surface Processes and Landforms* 23 (6), 527-544.

MORMUL, R.P., FERREIRA, F.A., MICHELAN, T.S., CARVLHO, P., SILVEIRA, M.J., THOMAZ, S.M., 2010. Aquatic macrophytes in the large, sub-tropical Itaipu Reservoir, Brazil. *Revista de Biologia Tropical (International Journal on Tropical Biology)* 58 (4), 1437-1452.

MOSS, A.J., GREEN, P., HUTKA, J., 1982. Small channels: their formation, nature and significance. *Earth Surface Processes and Landforms* 7, 401-415.

MUSGRAVE, G.W., 1947. The quantitative evaluation of factors in water erosion – A first approximation. *Journal of Soil and Water Conservation* 2, 133-138.

NEARING, M.A., PRUSKI, F.F., O'NEAL, M.R., 2004. Expected climate change impacts on soil erosio nrates: a review. *Journal of Soil and Water Conservation* 59 (1), 43-50.

NEARING, M.A., 1997. The mechanisms of soil detachment by raindrops and runoff. *Eurasian Soil Science* 30 (5), 552-556.

NEUBERT, M., MEINEL, G., 2005. Atmosphärische und Topographische Korrektur von IKONOS-Daten mit ATCOR. in: Strobl, J., Blaschke, T., Griesebner, G. (Eds.), Angewandte Geoinformatik 2005. Beiträge zum 17, AGIT-Symposium, Salzburg, Heidelberg, Wichmann, pp. 503-512 (in German).

NG, S., CAI, Q., DING, S., CHAU, K., QIN, J., 2008. Effects of contour hedgerows on water and soil conservation, crop productivity and nutrient budget for slope farmland in the Three Gorges Region (TGR) of China. *Agroforestry Systems* 74, 279-291.

NILSSON, C., REIDY, C.A., DYNESIUS, M., REVENGA, C., 2005. Fragmentation and flow regulation of the world's large river systems. *Science* 308, 405-408.

NING, D., CHANG, Y., 2002. An assessment of economic loss resulting from the degradation of agricultural land in China. Consulting report, ADB TA-3548 PRC.

NORTON, L.D., CASTRO FILHO, C., COCHRANE, T.A., CAVIGLIONE, J.H., FONTES JR., H.M., JOHANSON, L.P., MARENDA, L.D., 2001. Monitoring the sediment loading of Itaipu Lake and modeling sheet and rill erosion hazards in the watershed of Parana River: an outline of the project. in: Mohtar, R.H., Steinhardt, G.C., (Eds.), Sustaining the global farm. Selected papers from the 10th International Soil Conservation Meeting held May 24-29, 1999 at Purdue University and the USDA-ARS National Soil Erosion Research Laboratory, pp. 321-323.

OSTER, S., 2007 (October 12th). China dam project to uproot millions more. Wall Street Journal. http://online.wsj.com/article/SB119212305140656176.html (08/26/2010).

OUD, E., MUIR, T.C., 1997. Engineering and economic aspects of planning, design, operation and construction of large dam projects. in: Dorcey, T., Steiner, A., Acreman, M., Orlando, B. (Eds.), Large dams. Learning from the past. Looking at the future. Part II: Overview papers. Proceedings of the Gland (Switzerland) Workshop. Gland, IUCN–The World Conservation Union & The World Bank Group, pp. 159. http://www-wds.worldbank.org/external/default/WDSContentServer/IW3P/IB/1999/09/17/000178830_98101912310448/Rendered/PDF/multi_page.pdf (12/17/2008).

PANG, G.W., YAO, Z.H., XIE, H.X., YANG, Q.K., LI, R., XIE, M.L., 2013. Soil erosion dynamic changes and its impact factors in Zhifanggou watershed of the Loess Plateau, China. Journal of Food Agriculture & Environment 11 (1), 822-831.

PIMENTEL, D., 2006. Soil erosion: a food and environmental threat. *Environment, Development and Sustainability* 8, 119-137.

PIMENTEL, D., KOUNANG, N., 1998. Ecology of soil erosion in ecosystems. *Ecosystems* 1, 416-426.

PIMENTEL, D., HARVEY, C., RESOSUDARMO, P., SINCLAIR, K., KURZ, D., MCNAIR, M., CRIST, S., SPHPRITZ, L., FITTON, L., SAFFOURI, R., BLAIR, R., 1995. Environmental and economic costs of soil erosion and conservation benefits. *Science* 267, 1117-1123.

PIMENTEL, D., STACHOW, U., TAKACS, D.A., BRUBAKER, H.W., DUMAS, A.R., MEANEY, J.J., O'NEIL, J., ONSI, D.E., CORZILIUS, D.B., 1992. Conserving biological diversity in agricultural/forestry systems. *BioScience* 42, 354-362.

PITTOCK, J., XU, M., 2011. World resources report case study. controlling Yangtze River floods: a new approach. World Resources Report, Washington DC. http://www.worldresourcesreport.org (05/22/2013).

POESEN, J., 2011. Challenges in gully erosion research. *Landform Analysis* 17, 5-9.

PONSETI, M., LÓPEZ-PUJOL, J., 2006. The Three Gorges Dam project in China: history and consequences. ORIENTATS-2006, *Revista HMiC Nr. IV*, 151-188.

POSTHUMUS, H., STROOSNIJDER, L., 2010. To terrace or not: the short-term impact of bench terraces on soil properties and crop response in the Peruvian Andes. *Environment, Development and Sustainability* 12, 263-276.

QUINE, T.A., WALLING, D.E., CHAKELA, Q.K., MANDIRINGANA, O.T., ZHANG, X., 1999. Rates and patterns of tillage and water erosion on terraces and contour strips: evidence from caesium-137 measurements. *Catena* 36, 115-142.

QUINTON, J.N., CATT, J.A., WOOD, G.A., STEER, J., 2006. Soil carbon losses by water: experimentation and modeling at field and national scales in the UK. *Agriculture, Ecosystems and Environment 112* (1), 87-102.

RENARD, K.G., FOSTER, G.R., WEESIES, G.A., MCCOOL, D.K., YODER, D.C., 1997. Predicting soil erosion by water: a guide to conservation planning with the Revised Universal Soil Loss Equation (RUSLE), U.S. Department of Agriculture, Agriculture Handbook No. 703, USDA, Washington, DC., pp. 385.

RENARD, K.G., FREIMUND, J.R., 1994. Using monthly precipitation data to estimate the R-factor in the revised USLE. *Journal of Hydrology* 157, 287-306.

RENARD, K., FOSTER, G.R., WEESIES, G.A. PORTER, J.P., 1991. RUSLE Revised universal soil loss equation. *Journal of Soil and Water Conservation* 46, 30-33.

REYNOLDS, I., 2011. Impact of the Three Gorges Dam. *JCCC Honors Journal* Vol. 2, Issue 2, Article 3, pp. 23, http://scholarspace.jccc.edu/honors_journal/vol2/iss2/3 (12/05/2012).

RICHARDS, J.A., JIA, X., 2006. Remote Sensing Digital Image Analysis: An Introduction. 4th Edition, Springer-Verlag, Berlin. pp. 439.

RICHTER, R., 2010. Atmospheric/Topographic Correction for Satellite Imagery (ATCOR 2/3 User Guide, Version 7.1, January 2008). 165. http://atcor.ch/pdf/atcor3_manual.pdf

ROGLER, H., SCHWERTMANN, U., 1981. Erosivität der Niederschläge und Isoerodentkarte Bayerns. *Zeitschrift für Kulturtechnik und Flurbereinigung* 22, 99 -112 (in German).

ROOSE, E.J., 1976. Use of the universal soil loss equation to predict erosion in West Africa. *Soil Conservation Society of America*, Ankeny, Iowa, pp. 60-74.

ROUSE, J.W., HAAS, R. W., SCHELL, J.A., HARLAN, J.C., 1974. Monitoring the vernal advancement and retrogradation (greenwave effect) of natural vegetation. NASA/GSFCT Type III Final Report, Greenbelt, MD, USA.

ROZELLE, S., HUANG, J., ZHANG, L., 1997. Poverty, population and environmental degradation in China. *Food Policy* 22 (3), 229-251.

SANG-ARUN, J., MIHARA, M., HORAGUCHI, Y., YAMAJI, E., 2006. Soil erosion and participatory remediation strategy for bench terraces in northern Thailand. *Catena* 65, 258-264.

SCHMIDT, J., WERNER, M.V., MICHAEL, A., 1999. Application of the EROSION3D model to the Catsop watershed, The Netherlands. *Catena* 37 (3-4), 449-456.

SCHÖNBRODT-STITT, S., BEHRENS, T., BIEGER, K., EHRET, D., FREI, M., XIA, Y., HÖRMANN, G., SEEBER, C., SCHLEIER, M., BI, R., WIEGAND, M., SCHMALZ, B., FOHRER, N., CAI, Q., KAUFMANN, H., KING, L., ROHN, J., SUBKLEW, G., WEI, X., SHI, X., SCHOLTEN, T., 2012. Umweltforschung im Drei-Schluchten-Ökosystem in China – Eine Synthese. in: Scholten, T., Schönbrodt-Stitt, S. (Hrsg.), Umweltforschung im Drei-Schluchten-Ökosystem in China - Ergebnisse der Forschungsarbeiten zur Risikoabschätzung von Bodenerosion, Hangrutschungen, diffusen Stoffeinträgen und Landnutzungswandel. Tübinger Geographische Studien 151, 283-291. ISBN 978-3-88121-089-8.

SEEBER, C., WIEGAND, M., XIANG, W., KING, L., 2012. Landnutzungsklassifizierung und Analyse der Vulnerabilität von Risikoelementen im Einzugsgebiet des Xiangxi. in: Scholten, T., Schönbrodt-Stitt, S. (Hrsg.), Umweltforschung im Drei-Schluchten-Ökosystem in China - Ergebnisse der Forschungsarbeiten zur Risikoabschätzung von Bodenerosion, Hangrutschungen, diffusen Stoffeinträgen und Landnutzungswandel. Tübinger Geographische Studien 151, pp. 84-139, ISBN 978-3-88121-089-8, (in German).

SEEBER, C., HARTMANN, H., XIANG, W., KING, L., 2010. Land Use Change and Causes in the Xiangxi Catchment, Three Gorges Area Derived from Multispectral Data. *Journal of Earth Science* 21 (6), 846-855.

SEPA, 2006. Bulletin on the ecological and environmental monitoring results of the Three Gorges Project 2006. State Environmental Protection Administration, 2006, pp. 41. http://english.mep.gov.cn/down_load/Documents/200712/P020071226462929438115.pdf (05/28/2013).

SERAFIM, A., MORAIS, M., GUILHERME, P., SARMENTO, P., RUIVO, M., MAGRIÇO, A., 2006. Spatial and temporal heterogenity in the Alqueva reservoir, Guadiana river, Portugal. *Limnetica* 25 (3), 771-786.

SHAMSHAD, A., AZHARI, M.N., ISA, M.H., WAN HUSSIN, W.M.A., PARIDA, B.P., 2008. Development of an appropriate procedure for estimation of RUSLE EI30 index and preparation of erosivity maps for Pulau Penang in Peninsular Malaysia. *Catena* 72, 423-432.

SHEN, Z., GONG, Y., LI, Y., LIU, R., 2010. Analysis and modeling of soil conservation measures in the Three Gorges Reservoir Area in China. *Catena* 81, 104-112.

SHI, Z.H., AI, L., FANG, N.F., ZHU, H.D., 2012. Modeling the impacts of integrated small watershed management on soil erosion and sediment delivery: a case study in the Three Gorges Area, China. *Journal of Hydrology* 438-439, 156-167.

SHI, X.Z., YU, D.S., XU, S.X., WARNER, E.D., WANG, H.J., SUN, W.X., ZHAO, Y.C., GONG, Z.T., 2010. Cross-reference for relating Genetic Soil Classification of China with WRB at different scales. *Geoderma* 155, 344-350.

SHI, Z.H., CAI, C.F., DING, S.W., WANG, T.W., CHOW, T.L., 2004. Soil conservation planning at the small watershed level using RUSLE with GIS. A case study in the Three Gorges Area of China. *Catena* 55, 33-48.

SHI, D.M., 1999. Analysis of relationship between soil and water loss and flood disasters in Yangtze River basin. *Journal of Soil and Water Conservation* 5, 1-7 (in Chinese with an English Abstract).

SHI, L.R., 1998. Characteristics of soil and water loss, control measures and their effects in the upper reaches of the Yangtze River. *Yangtze River* 29, 41-43 (in Chinese with English abstract).

SHI, D.M., YANG, Y.S., LU, X.X., 1992. Analysis of soil erosion characteristics and sediment sources for the Yangtze Three Gorges region. *International Journal of Sediment Research* 7(2), 1-22.

SHIRAZI, M.A., BOERSMA, L., 1984. A unifying quantitative analysis of soil texture. *Soil Science Society of America Journal* 48, 142-147, DOI: 10.2136/sssaj1984.03615995004800010026x

SHRESTRA, D.P., ZINCK, J.A., VAN RANST, E., 2004. Modeling land degradation in the Nepalese Himalaya. *Catena* 57, 135-156.

SIDLE, R.C., ZIEGLER, A.D., NEGISHI, J.N., RAHIM NIK, A., SIW, R., TURKELBOOM, F., 2006. Erosion processes in steep terrain - truths, myths, and uncertainties related to forest management in Southeast Asia. *Forest Ecology and Management* 224, 199-225.

SIX, J., FELLER, C., DENEF, K., OGLE, S.M., DE MORAES SA, J.C., ALBRECHT, A., 2002. Soil organic matter, biota and aggregation in temperate and tropical soils - effect of no-tillage. *Agronomie* 22, 755-775.

SONG, Y., LIU, L., YAN, P., CAO, T., 2005. A review of soil erodibility in water and wind erosion research. *Journal of Geographical Sciences* 15 (2), 167-176.

SOUTHGATE, D., WHITAKER, M., 1992. Promoting resource degradation in Latin America: Tropical deforestation, soil erosion, and coastal ecosystem disturbance in Ecuador. *Economic, Development and Cultural Change* 40(4), 787-807.

STEIL, S., DUAN, Y., 2002. Policies and practice in the Three Gorges resettlement: a field account. *Forced Migration Review* 12, 10-13.

STOCKING, M.A., ELWELL, H.A., 1976. Rainfall erosivity over Rhodesia. *Transactions of the Institute of British Geographers New Series 1,* 231-245.

STONE, R., 2008. Three Gorges Dam: Into the Unknown. *Science* 321, 628-321.

STONE, R., JIA, H., 2006. Going against the flow. *Science* 313, 1034-1037.

STONE, R.P., MOORE, N., 1997. Control of soil erosion. http://www.omafra.gov.on.ca/english/engineer/facts/95-089.htm (01/23/2013).

SUBKLEW, G., XIANG, W., SCHÖNBRODT-STITT, S., SCHOLTEN, T., 2012. Der Drei-Schluchten-Staudamm am Yangtze und seine ökologischen Implikationen - Eine Einführung. in: Scholten, T., Schönbrodt-Stitt, S. (Hrsg.), Umweltforschung im Drei-Schluchten-Ökosystem in China - Ergebnisse der Forschungsarbeiten zur Risikoabschätzung von Bodenerosion, Hangrutschungen, diffusen Stoffeinträgen und Landnutzungswandel. Tübinger Geographische Studien 151, pp. 1-10, ISBN 978-3-88121-089-8 (in German).

SUBKLEW, G., ULRICH, J., FÜRST, L., HÖLTKEMEIER, A., 2010. Environmental impacts of the Yangtze Three Gorges Project - an overview of the Chinese-German research cooperation. *Journal of Earth Science* 21 (6), 817-823.

SUN, X.X., ZHANG, J.X., LIU, Z.J., 2008. Vegetation cover annual changes based on MODIS/TERRA NDVI in the Three Gorges Reservoir Area. *The International Archives of the Photogrammetry, Remote Sensing and Spatial Information Sciences* 37(Part B7), 1397-1400.

SUN, G., MCNULTY, S.G., MOORE, J., BUNCH, C., NI, J., 2002. Potential impacts of climate change on rainfall erosivity and water availability in China in the next 100 years. Proceedings of the 12th International Soil Conservation Organization. Beijing, China, pp. 244-250, http://efetac4.sref.info/www/efetac4/efetac4/products/publications/sun02c.pdf/view (06/01/2013).

SURIYAPRASIT, M., SHRESTHA, D.P., 2008. Deriving land use and canopy cover factor from remote sensing and field data in inaccessible mountainous terrain for use in soil erosion modelling. *The International Archives of the Photogrammetry, Remote Sensing and Spatial Information Sciences* 37 (Part B7), 1747-1750.

SUTTON, A., 2004. The Three Gorges Project on the Yangtze river in China. *Geography* 89, 111-126.

TAN, Y., GUO, F., 2007. Environmental concerns and population displacement in West China. 8th International Conference of Asian Pacific Migration Research Network (APMRN): Migration, Development and Poverty Reduction, 2007. http://piasdgserver.usp.ac.fj/apmrn/conferences/8thAPMRNconference/26.Tan%20Guo.pdf (05/24/2013).

TAN, Y., BRYAN, B., HUGO, G., 2005. Development, land-use change and rural resettlement capacity: a case study of the Three Gorges Project, China. *Australian Geographer* 36, 201-220.

TARBOTON, D.G., 1997. A new method for the determination of flow directions and upslope areas in grid digital elevation models. *Water Resources Research* 33, 309-319.

TE BOEKHORST, D.G.J., SMITS, T.J.M., YU, X., LI, L., LEI, G., ZHANG, C., 2010. Implementing integrated river basin management in China. *Ecology and Society* 15 (2): 23, pp. 18.

THORP, J., 1936. The geography of soils in China. Edited by the Institute of Geology and Survey of China. Nanjing, China.

TIAN, Z., CHEN, W., ZHAO, C., ZHENG, B., 2007. Plant biodiversity and its conservation strategy in the inundation and resettlement districts of the Yangtze Three Gorges, China. *Acta Ecologica Sinica* 27, 3110-3118.

TOBLER, W.R., 1970. A computer movie simulating urban growth in the Detroit region. *Economic Geography* 46, 234-240.

TOY, T.J., RENARD, K.G., 1998. Chapter 1 - Introduction. in: Toy, T.J., Foster, G.R. (Eds.), Guidelines for the use of the Revised Universal Soil Loss Equation (RUSLE) version 1.06 on mined land, construction sites, reclaimed land. Office of Surface Mining, Reclamation, and Enforcement, pp.149, http://www.greenfix.com/Channel%20Web /pdfs/RUSLE%20Guidelines.pdf.

TOY, T.J., FOSTER, G.R., RENARD, K.G., 2002. Soil erosion: processes, prediction, measurement, and control. John Wiley & Sons, 1st edition, New York, pp. 352.

UNITED NATIONS, 2011. World Economic and Social Survey 2011 - the great green technological transformation. Department of Economic and Social Affairs, E/2011/50/Rev.1, United Nations Publication, New York, pp. 251.

USDA-ARS; United States Department of Agriculture, Agricultural Research Service (2010). Revised Universal Soil Loss Equation (RUSLE). http://www.ars.usda.gov/Research/docs.htm?docid =5971 (07/17/2013).

VALERIANO, M.M., KUPLICH, T.M., STORINO, M., AMARAL, B.D., MENDES JR, J.N., LIMA, D.L., 2006. Modeling small watersheds in Brazilian Amazonia with shuttle radar topographic mission-90 m data. *Computers and Geosciences* 32 (8), 1169-1181.

VAN DER KNIJFF, J.M., JONES, R.J.A., MONTANARELLA, L., 1999. Soil erosion risk management in Italy. European Comission, European Soil Bureau, pp. 52.

VAN DIJK, A.I.J.M., 2002. Water and sediment dynamics in bench-terraced agricultural steeplands in West Java, Indonesia. Amsterdam, Thesis, pp.378.

VAN LYNDEN, G.W.J., OLDEMAN, L.R., 1997. The assessment of the status of human-induced soil degradation in south and south-east Asia. United Nations Environment Programme (UNEP), Food and Agricultural Organization of the United Nations (FAO), International Soil Reference and Information Centre (ISRIC), Wageningen (digital map and data sets).

VAN OOST, K., QUINE, T.A., GOVERS, G., DE GRYZE, S., SIX, J., HARDEN, J.W., RITCHIE, J.C., MCCARTY, G.W., HECKRATH, G., KOSMAS, C., GIRALDEZ, J.V., MARQUES DA SILVA, J.R., MERCKX, R., 2007. The impact of agricultural soil erosion on the global carbon cycle. *Science* 318, 626-629.

VRIELING, A., 2007. Mapping erosion from space. Doctoral Thesis Wageningen University, pp. 167.

VRŠČAJ, B., DAROUSSIN, J., MONTANARELLA, L., 2007. SRTM as a possible source of elevation information for soil-landscape modelling. Digital Terrain Modelling, Lecture Notes in Geoinformation and Cartography 2007, 99-120

WACHS, T., THIBAULT, M. (Eds.), 2009. Benefits of sustainable land management. World overview of sustainable conservation approaches and technologies WOCAT, Centre for Development and Environment (CDE), University of Berne, Swiss, pp. 15, http://www.ais.unwater.org/ais/ plug-infile.php/516/course/section/175/CSD_Benefits_of_Sustainable_Land_Management%20.pdf (01/15/2013).

WANG, X., LU, C., FANG, J., SHEN, Y., 2007. Implications for development of grain-for-green policy based on cropland suitability evaluation in desertification-affected north China. *Land Use Policy* 24, 417-424.

WANG, Y., 2004. Environmental degradation and environmental threats in China. *Environmental Monitoring and Assessment* 90, 161-169.

WANG, G., WENTE, S., GERTNER, G.Z., ANDERSEN, A., 2002. Improvement in mapping vegetation cover factor for the Universal Soil Loss Equation by geostatistical methods with Landsat Thematic Mapper Images. *International Journal of Remote Sensing* 23 (18), 3649-3667.

WCD (World Commission on Dams), 2000. Dams and development. A new framework for decision-making: the report of the World Commission on Dams, Earthscan Publications Ltd, London and Sterling: VA, pp. 404, http://www.internationalrivers.org/files/attached-files/world_commission_on_dams_final_report.pdf (04/05/2009).

WEILGUNI, V., 2006. Regionalisierung des Niederschlags. Wiener Mitteilungen Band 197, Methoden der hydrologischen Regionalisierung, pp. 71-92 (in German).

WEN, D., 1997. Agriculture in China: water and energy resources. Shenyang Institute of Applied Ecology, China, Chinese Academy of Sciencea, Forthcoming.

WILLIAMS, L.S., 1990. Agricultural terrace evolution in Latin America. Ohio University. http://sites.maxwell.syr.edu/clag/yearbook1990/williams.pdf (02/27/2013).

WISCHMEIER, W.H., SMITH, D.D., 1978. Predicting rainfall erosion losses - a guide to conservation planning. Agriculture Handbook No. 537, USDA, Washington, DC, pp. 58, available from http://naldc.nal.usda.gov/download/CAT79706928/PDF.

WISCHMEIER, W.H., SMITH, D.D., 1965. Predicting rainfall-erosion losses from cropland east of the Rocky Mountains - Guide for Selection of Practices for Soil and Water Conservation. Agriculture Handbook No. 282, USDA, Washington, DC, pp. 47, available from http://naldc.nal.usda.gov/download/CAT87208342/PDF.

World Bank, 2013. World Development Indicators 2013. Washington, DC: World Bank. DOI: 10.1596/978-0-8213-9824-1. License: Creative Commons Attribution CC BY 3.0, pp. 152. http://de.scribd.com/doc/135966817/World-Development-Indicators-2013

WU, D.M., YU, Y.C., XIA, L.Z., YIN, S.X., YANG, L.Z., 2011a. Soil fertility indices of citrus orchards land along topographic gradients in the Three Gorges Area of China. *Pedosphere* 21, 782-792.

WU, C., ZHOU, Z., XIAO, W., WANG, P., TENG, M., HUANG, Z., 2011b. Estimation of soil erosion in the Three Gorges Reservoir Area of China using RUSLE, remote sensing and GIS. *Journal of Food, Agriculture and Environment* 9, 728-734.

WU, P., CAO, F.S., XIAO, X., 2010. Yangtze River: China's golden waterway. *Proceedings of the ICE - Civil Engineering* 163 (5), 15-18.

WU, Y., LIAO, W., KING, L., YUAN, X., 2009. Analysis and utilization of the climatic resources in Xiangxi River basin. International Conference on Environmental Science and Information Application Technology, ESIAT 2009, Wuhan, China, 3 Volumes, 217-220, DOI: 10.1109/ESIAT.2009.177

WU, Y.J., KING, L., JIANG, T., 2006. Climatic vertical graduation and its use in the Xiangxi River catchment, in: Cai, Q., Fohrer, N. (Eds.), Sino-German Workshop on Environmental Impacts of Large-scale Hydraulic Engineer. Programme and Abstracts, March 2006, Xingshan, pp. 104-108.

WU, F., LUO, Y., 2006. Cutting slope reinforcement in reconstructed migrants cities in the Three Gorges area of China. The Geological Society of London, IAEG2006 Paper number 714, 1-5. http://iaeg2006.geolsoc.org.uk/cd/PAPERS/IAEG_714.PDF (07/01/2013).

WU, J., HUANG, J., HAN, X., GAO, X., HE, F., JIANG, M., JIANG, Z., PRIMACK, R.B., SHEN, Z., 2004. The Three Gorges Dam: an ecological perspective. *Frontiers in Ecology and the Environment* 2, 241-248.

WWF China, 2013. Living Yangtze. http://en.wwfchina.org/en/what_we_do/living_yangtze/ (05/25/2013).

XIE, Y., LIU, B., NEARING, M.A., 2002. Practical thresholds for separating erosive and non-erosive storms. *Transactions of the American Society of Agricultural Engineers* 45, 1843-1847.

XINHUA, 2012. Tower columns for Three Gorges shiplift to be built. Xinhua News Agency February 27, 2012. http://english.peopledaily.com.cn/90882/7741118.html (05/29/2013).

XINHUA, 2008. 40% of China's territory suffers from soil erosion. Xinhua News Agency November 21, 2008. http://www.china.org.cn/environment/news/2008-11/21/content_16803229.htm (05/24/2013).

XU, K., MILLIMAN, J.D., 2009. Seasonal variations of sediment discharge from Yangtze River before and after impoundment of the Three Gorges Dam. *Geomorphology* 104, 276-283.

XU, Y., PENG, J., SHAO, X., 2009. Assessment of soil erosion using RUSLE and GIS: a case study of the Maotiao River watershed, Guizhou Province, China. *Environmental Geology* 56, 1643-1652.

XU, Y., SHAO, X., KONG, X.B., PENG, J., YUN, Y.L., 2008. Adapting the RUSLE and GIS to model soil erosion in a mountainous karst watershed, Guizhou Province, China. *Environmental Monitoring Assessment* 141, 275-286.

XU, K.Q., BROWN, C., KWON, H., LALL, U., ZHANG, J., HAYASHI, S., CHEN, Z., 2007. Climate teleconnections to Yangtze River seasonal streamflow at the Three Gorges Dam, China. *International Journal of Climatology* 27 (6), 771-780. DOI:10.1002/joc.1437.

XU, Z., XU, J., DENG, X., HUANG, J., UCHIDA, E., ROZELLE, S., 2006. Grain for green versus grain: conflict between food security and conservation set-aside in China. *World Development* 34 (1), 130-148.

XU, Y., GUO, T., YANG, G., 2005. A comparison between different ecological de-farming modes in the loess hilly-gully region in China. *Journal of Geographical Sciences* 15 (1), 53-60.

XU, J., 2000. Some problems and research requirements concerning eco-environmental construction on Loess Plateau. *Research of Soil and Water Conservation* 7 (2), 10-13 (in Chinese).

YANG, X., LU, X.X., 2012. Model of water regulation in the Yangtze River Basin and its effects using remote sensing techniques. Erosion and Sediment Yields in the Changing Environment (Proceedings of a symposium held at the Institute of Mountain Hazards and Environment, CAS-Chengdu, China, 11–15 October 2012) (IAHS Publ. 356, 2012), 235-243.

YANG, S.L., ZHANG, J., DAI, S.B., LI, M., XU, X.J., 2007. Effect of deposition and erosion within the main river channel and large lakes on sediment delivery to the estuary of the Yangtze River. *Journal of Geophysical Research* 112, DOI:10.1029/2006jf000484

YANG, Z., WANG, H., SAITO, Y., MILLIMAN, J.D., XU, K., QIAO, S., SHI, G., 2006. Dam impacts on the Changjiang (Yangtze) River sediment discharge to the sea: the past 55 years and after the Three Gorges Dam. *Water Resources Research* 42, W04407, DOI: 10.1029/2005WR003970

YANG, S.L., ZHANG, J., ZHU, J., SMITH, J.P., DAI, S.B., GAO, A., LI, P., 2005. Impact of dams on Yangtze River sediment supply to the sea and elta intertidal wetland response. *Journal of Geophysical Research 10: F03006*, pp. 12, DOI: 10.1029/2004JF000271

YANG, Z.S., LIANG, L.H., LIU, Y.S., HE, Y.M., 2004. land use change during 1960-2000 period and its eco-environmental effects in the Middle and Upper Reaches of the Yangtze River: a case study in Yiliang County, Yunnan, China. *Journal of Mountain Science* 1, 250-263.

YANG, D., KANAE, S., OKI, T., KOIKE, T., MUSIAKE, K., 2003. Global potential soil erosion with reference to land use and climate changes. *Hydrological Processes* 17 (14), 2913-2928.

YANG, S.L., ZHAO, Q.Y., BELKIN, I.M., 2002. Temporal variations in the sediment load of the Yangtze river and the influences of human activities. *Journal of Hydrobiology* 263, 56-71.

YANG, Y.S., SHI, D.M., 1994. Study on Soil Erosion in the Three Gorges Area of the Changgjiang River. Southeast Univ. Press, Nanjing (in Chinese).

YAO, H., 1993. Characteristics and control of soil erosion in Hubei Province, China. Sediment problems: strategies for monitoring, prediction and control (Proceedings of the Yokohama Symposium, July 1993). *International Association Hydrological Sciences (IAHS) Publication*. No. 217, 23-27.

YIN, H., LIU, G., PI, J., CHEN, G., LI, C., 2006. On the river-lake relationship of the middle Yangtze reaches. *Geomorphology* 85, 197-207.

YIN, H., LI, C., 2001. Human impact on floods and flood disasters on the Yangtze River. *Geomorphology* 41, 105-109.

YU, B., ROSEWELL, C.J., 1998. RECS: A program to calculate the R-factor for the USLE/RUSLE using BOM/AWS Pluviograph data. ENS Working Paper No. 8/98, pp. 15.

ZANDBERGEN, P., 2008. Applications of Shuttle Radar Topography Mission Elevation Data. *Geography Compass* 2 (5), 1404-1431.

ZHANG, H., CHEN, T.T., LIU. L.J., WANG, Z.Q., YANG, J.C., ZHANG, J.H., 2013. Performance in grain yield and physiological traits of rice in the Yangtze River basin of China during the last 60 yr. *Journal of Integrative Agriculture* 12 (1), 57-66.

ZHANG, Y.G., NEARING, M.A., LIU, B.Y., VAN PELT, R.S., STONE, J.J., WEI, H., SCOTT, R.L., 2011. Comparative rates of wind versus water erosion from a small semiarid watershed in southern Arizona, USA. *Aeolian Research* 3, 197-204.

ZHANG, J., LIU, Z., SUN, X., 2009. Changing landscapes in the Three Gorges Reservoir Area of the Yangtze River from 1977 to 2005: Land use/land cover, vegetation cover changes estimated using multi-source satellite data. *International Journal of Applied Earth Observation and Geoinformation* 11, 403-412.

ZHANG, B., 2008. Impact on mountainous agricultural development in the Three Gorges Reservoir Area forced by migrants of the Three Gorges Project. *Chinese Journal of Population, Resources and Environment* 6, 83-89.

ZHANG, B., ZEPP, H., JU, M., 2002. Soil erosion in southeastern China of red soil area - causes, effects, and countermeasures. 12th ISCO Conference, Beijing 2002, pp. 229-236.

ZHANG, S., ZHU, C., 2001. Soil loss and its effect on flooding catastrophe in Yangtze drainage basin, *Journal of Soil and Water Conservation* 15, 9-16.

ZHANG, Y., 2000. Deforestation and forest transition: theory and evidence in China. in: Palo, M., Vanhanen, H. (Eds.), World Forests from Deforestation to Transition? Forest Transition II, pp. 41-65.

ZHANG, X., WALLING, D.E., QUINE, T.A., WEN, A., 1997. Use of reservoir deposits and caesium-137 measurements to investigate the erosional response of a small drainage basin in the rolling loess plateau region of China. *Land Degradation and Development* 8, 1-16.

ZHAO, S., 1986. Physical Geography of China. 1st edition, Wiley, New York, pp. 244.

ZHOU, P., 2008. Landscape-scale erosion modeling and ecological restoration for a mountainous watershed in Sichuan, China. Academic dissertation, Tropical Forestry Reports 35, University of Helsinki Viikki Tropical Resources Institute VITRI, Helsinki, Finland, pp. 95 https://www.doria.fi/ bitstream/handle/10024/37384/landscap.pdf?sequence=1 (05/29/2013).

ZHOU, P., LUUKKANEN, O., TOKOLA, T., NIEMINEN, J., 2008. Effect of vegetation cover on soil erosion in a mountainous watershed. *Catena* 75 (3), 319-325.

ZHOU, W., WU, B., 2008. Assessment of soil erosion and sediment delivery ratio using remote sensing and GIS: a case study of upstream Chaobaihe River catchment, north China. *International Journal of Sediment Research* 23, 167-173.

ZHOU, J., ZHOU, Q., HUANG, Z., 2006. Monitoring the cultivated slope land in the Three Gorges Reservoir Area based on remote sensing and GIS. Wuhan University Journal of Natural Sciences 11, 915-921.

ZHU, A.X., WANG, P., ZHU, T., CHEN, L., CAI, Q., LIU, H., 2013. Modeling runoff and soil erosion in the Three-Gorge Reservoir drainage area of China using limited plot data. *Journal of Hydrology* 492, 163-175.

ZINGG, A.W., 1940. Degree and length of land slope as it affects soil loss in runoff. *Agricultural Engineering* 21, 59-64.

CHINA'S HISTORY OF HUMAN-INDUCED SOIL EROSION

China has a long history of human-induced soil erosion. Already in pre-modern China, climate change, population increase, migration movements and settling of 'ecological fragile areas' such as the Yangtze and Yellow River Basins caused large-scale deforestation and environmental degradation (ZHANG, 2000; KOLB, 2003; LIU and WU, 2010). According to ZHANG (2000) significant deforestation in China started around 3000 BC at the origin of Chinese civilization in the Loess Plateau and Guangzhong region and moved towards the south, east, and north as land deterioration progressed and population increased. Massive deforestation caused by agricultural expansion and logging strongly reduced the vegetation cover around 1,000 to 500 BC and caused enormous sedimentation loading into the Wei and Yellow (Huang He) Rivers. As stated by ZHANG (2000) the origin of the rivers' names probably first date back to this time. They indicate those acute soil erosion and high silt inputs that steadily increased to recently 2 billion tons per year transported downstream to the Yellow Sea (ZHANG ET AL., 1997).

New land reclamation east of the Loess region led to extensive logging and agricultural expansion around 500 to 0 BC and also did not stop in the mountain ranges in the southern and northern regions (ZHANG, 2000). Resulting soil erosion, land deterioration, and migration movements still continued to modern times as population density steadily increased. In the late 19th and early 20th century, logging, forest land conversion to agriculture, and 'urban uses' significantly attributed to the early stage of economic development with railway construction and political development such as the foundation of the People's Republic of China in 1949 (ZHANG, 2000). Forest land was reduced by estimated more than 6 million hectares (LIU and SUN 1985 quoted in ZHANG, 2000). With the start of the nationwide 'Great Leap Forward' in 1958 (LI and YANG, 2005) a new dimension of deforestation increase, due to rapid industrialization and the raise of agricultural productivity, exhibited a tipping point towards exacerbated soil erosion in China (YANG ET AL., 2005).

Particularly, the Yangtze River Basin (YRB) was affected (YANG ET AL., 2005). According to their findings based on literature review, YANG ET AL. (2005) further differentiate two phases of largely 'pulsed' increases in soil erosion in the YRB, especially in the Upper Yangtze River Basin (UYRB). These phases of enhanced soil erosion during the early 1980s and the begin of the 21th century (Table 10) referred to full modernization and economic innovation in China mainly associated with intensifications in cropland cultivation, deforestation, mining, and road construction (SHI, 1999; ZHANG and ZHU, 2001; YANG ET AL., 2005).

Table 10 *Areas (in 10^3 km²) of soil erosion and soil erosion control in the Upper Yangtze River Basin (UYRB) and Yangtze River Basin (YRB) from the 1950s to 2002 (after YANG ET AL., 2005).*

	Soil erosion		Soil erosion control	
Year	UYRB	YRB	UYRB	YRB
1951	—	350	—	—
1985	352	562	—	—
1992	346	572	54	157
1993	347	573	52	160
1994	347	572	66	177
1996	380	613	81	199
1997	368	600	74	197
1998	368	600	58	186
1999	370	603	90	240
2000	370	603	97	243
2001	460	707	103	243
2002	472	711	110	251

CHINA'S EFFORTS ON COMBATING SOIL EROSION

First governmental efforts to combat soil erosion in China include the *Soil and Water Provisional Outlines* (1957) and *Methods of Soil and Water Conservation for Small Watersheds* (1980) which finally led to the *Regulations on Water and Soil Conservation* in 1982 (LI ET AL., 1999; LIU, 2012). On 29th of June 1991, at the 20th Standing Committee of the Seventh National People's Congress, soil erosion was declared nationwide a top priority (china.org.cn[1]; LIU, 2012). The same day, the central government adopted the *Law of The People's Republic of China on Water and Soil Conservation* (WSCL) ensuring enforced "[…] preventive and rehabilitative measures taken against soil erosion which is caused by natural factors or human activities." (Chapter I, Article 2; china.org.cn[1]). More concretely, the law includes central aspects at the prevention (Chapter II), rehabilitation (Chapter III), supervision (Chapter IV), and legal responsibility (Chapter V) such as in extracts:

- Facilitation of afforestation, preservation of the vegetation, and prohibition of logging and burning for the purpose of **land reclamation** (Chapter II, Article 13)
- Prescription of **'reclamation-forbidden' slopes** with inclinations greater than 25 degrees, prohibition of reclamation of those slopes for the cultivation of crops, gradual stop of already existing cultivation on 'reclamation-forbidden' slopes, restoration of vegetation or construction of farming terraces (Chapter II, Article 14)
- Overall planning and comprehensive rehabilitation for the soil erosion prevention and control in **river basins in water-eroded regions** (Chapter III, Article 22)
- Installation and **management of cultivated slopes** between 5 to 25 degrees by means of conducive water and soil conservation measures and farming techniques as drainage systems and **farming terraces** (Chapter III, Article 24)
- Establishment of a **monitoring network for WSC and prediction** of the nation-wide soil erosion, publication of the results by the department of water administration under the State Council (Chapter IV, Article 29)
- Cessation of the reclamation, **adoption of remedial measures**, and imposition of a penalty in the case of any violation of the provisions in Article 14 (Chapter V, Article 32).

In 2011, a revised version of the WCSL entered the legislation in order to adequately address the current issues of 'one of China's Top 10 Environmental Problems' (WWF China, 2013) and to strengthen the legislative tools on soil erosion control and combat (LIU, 2012). Basically, the revised law equals the WSCL from 1991, however amendments have been made in terms of better planning and rehabilitation measures (e.g., identification and designation of *Key Preventions Areas* and *Key Rehabilitation Areas*), greater involvement of responsibilities, and increased penalties against violations of the WCSL (LIU, 2012).

The *Relieving and De-farming* (RD) and *Rebuilding Terrace and De-farming* (RTD) *modes* are part of the governmental action plan in the eco-environmental restoration in order to break the vicious circle of "sloping land reclamation - environmental deterioration - farmer's poverty - reclaimed expansion" (XU, 2000; XU ET AL., 2005) and have been implemented in the UYRB of the Yangtze River and the Loess Plateau in the Yellow River Basin as both regions are priority areas in the nation-wide development (XU ET AL., 2005).

In 2002, China additionally launched one of the largest conservation projects worldwide for the protection and improvement of the ecological environment in the major river basins and ecological vulnerable regions (LIU and WU, 2010; WANG ET AL., 2007; XU ET AL., 2006). The 'Grain for Green Program' (GFG) was in particular designed to reduce processes exacerbating soil erosion and to strengthen the framework conditions of ecological protection including deforestation, over-logging, over-cultivation, and rural poverty alleviation (LIU and WU, 2010). As GFG is especially based upon the slope steepness criterion determining the cropland suitability, the program also got known as *Sloped Land Conversion Program* (XU ET AL., 2006; WANG ET AL., 2007). By the end of GFG in 2008, 8.22 million hectares of sloping land accounting for approximately 6.8%

of China's total arable land had been converted to forestland (LIU and WU, 2010). By doing so, runoff and soil erosion could considerably be reduced about 18% and 45% with further ecological benefits such as of reduction in siltation of reservoirs and downstream flooding (DENG ET AL., 2012; XU ET AL., 2006). The economic losses due to soil loss by erosion were reduced to more than 50 billion Yuan (NING and CHANG, 2002).

According to the People's Republic of China's national report on sustainable development from 2012, China has kept approximately 1.07 million km² of nationwide soil erosion under control by 2010. 150 million people directly benefit from this soil erosion management and annual soil loss could be reduced by 1.5 billion tons.

THE YANGTZE RIVER

With a length of 6,380 kilometer, the Yangtze River (Chángjiāng, 长江) ranks as third longest river in the world, as fifth in terms of annual water discharge (920 km³), and historically as fourth in terms of annual sediment load (480 Mt; HU ET AL., 2009). The Yangtze as a 'world class' river (HU ET AL., 2009) originates at the Jianggendiru glacier at Mount Geladandong (6,621 m a.s.l.) in the Qinghai Tibetan Plateau (china.org.cn[2]) and flows into the East China Sea near the million-strong metropolis Shanghai. The river's enormous draining area of 1,810,000 km² accounts for 19% of China's territory (CHEN ET AL., 2001) and counts more than 700 major and minor tributaries (china.org.cn[2]).

The Yangtze River mainly crosses the provinces Quinghai, Sichuan, Chongqing Municipality, Hubei, Anhui, and Jiangsu (from west to east) being amongst the most populous provinces in China (Figure 17). In total, the Yangtze River basin (YRB) is home to more than 400 million people (HU ET AL., 2009; XU and MILLIMAN, 2009) accounting for 35% of the national total, and producing 40% of the gross domestic product (DAI and TAN, 1996; PITTOCK and XU, 2011). The YRB is the main rice planting area in China and approximately half of the national total crop harvest originates from this region. It further contributes about one third of the national grain and gross domestic product (TE BOEKHORST ET AL., 2010; ZHANG ET AL., 2013).

The Yangtze River can be divided into three sections according to their physical settings and drainage area; the Upper Yangtze River (UYR) from the source region to Yichang (Figure 17), the middle Yangtze River from Yichang to Hukou close to Poyang Lake, and Lower Yangtze River from Hukou to the river estuary in the Yangtze River delta in Shanghai Municipality (DAI and TAN, 1996; YANG ET AL., 2006; XU and MILLIMAN, 2009). According to its physical settings and spatial dimension, the UYR distinctly dominates the YRB. The mountainous landscape of the UYR basin is strongly characterized by the Parallel Ridges and Valleys (2,000-4,000 m), the Yunan-Guizhou Plateau (1,000-2,000 m) and the Sichuan Plain (500-1,000 m) located at the geological contact zone between the rising géosynclinal area to the west and the stable plateau to the east (DAI and TAN, 1996).

The UYR drains an area of approximately 100 x 10^4 km² (DAI and TAN, 1996; XU ET AL., 2007; HU ET AL., 2009) accounting for nearly 56% of the total Yangtze River basin (YANG ET AL., 2002). The flow length is 4,500 km from the source region through mainly narrow and steep valleys with an average gradient of 1.1% (YANG ET AL., 2007; HU ET AL., 2009) towards Yichang (Hubei Province; Figure 17). Its average annual discharge from 1950 to 2002, recorded at the gauging station in Yichang, is 440 km³ (YANG ET AL., 2006). With an average annual sediment load of approximately 500 million tons, the UYR basin accounts for the principal area of sediment production in the entire Yangtze River basin (DAI and TAN, 1996; YANG ET AL., 2006).

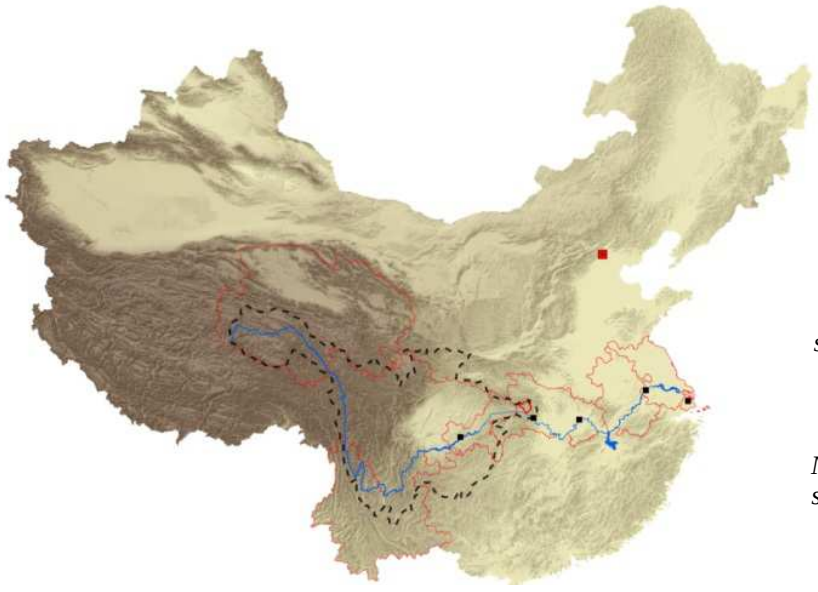

Figure 17 *The river course of the Yangtze (blue line) and the Upper Yangtze River Basin (framed by dashed black line). The red lines show the borders of the provinces where the Yangtze River mainly passes through. The black squares symbolize from west to east the cities Chongqing, Yichang, Wuhan, Nanjing, and Shanghai. The blue colored area between Wuhan and Nanjing shows Poyang Lake. The red square shows Beijing (after SUBKLEW ET AL., 2012).*

ON LARGE DAM PROJECTS AND THEIR EFFECT ON SOIL EROSION

The increasing need to supply the growing world population and steadily expanding economy with water, food, and energy particularly determines political and economic decisions on constructing dam projects and hydropower engineering schemes not only in China but worldwide. According to the *World Commission on Dams* (WCD, 2000) and INTERNATIONAL RIVERS (2007) more than 800,000 dam projects (mostly small dams) exist worldwide. They provide approximately 19% of the global energy supply and provide water to 30-40% of worldwide irrigated land of 271 million hectares (WCD, 2000).

Estimated 12-16% of the global food production is directly linked to reservoirs of large dams (WCD, 2000). The number of large and major dams worldwide is estimated to range from more than 45,000 to more than 50,000 (WCD, 2000; LEHNER ET AL., 2011). According to the criteria of the *International Commission of Large Dams* (ICOLD), dams of a height of more than 15 m or a height of 5-15 m and a storage volume of more than 3 million m³ constitute large dams, while major dams are higher than 150 m (ICOLD). Both are mainly located in major river networks in North and South America and China (Figure 18). In China alone, approximately 45% of the world's large dams (~22,000) and more than 85,000 dams in total are located (WCD, 2000; PONSETI and LOPÉZ-PUJOL, 2006).

Large dam projects attract worldwide scientific and media interest due to their serious upstream and downstream environmental impacts and socio-economic consequences in space, time, and costs (e.g. WU ET AL., 2004; NILSSON ET AL., 2005; STONE and JIA, 2006), inasmuch, as they strongly fragment more than 50% of large river systems worldwide (NILSSON ET AL., 2005).

Within the framework of the *International Union for Conservation of Nature* (IUCN), OUD and MUIR (1997) reported on a myriad of key potential environmental and social impacts caused by large dam projects differentiated into upstream and downstream effects mainly resulting from the loss of settlements and infrastructure, biomass, habitats of flora and fauna, mineral resources and numerous more (OUD and MUIR, 1997). The land use changes mainly account for large-scale shifts in agriculture, land reclamation, and construction of new roads and settlements to compensate the inundation of valuable land.

By looking at the globally 400,000 km² of land that were lost by flooding and the estimated 40 to 80 million people that were resettled since 1958 (WCD, 2000; INTERNATIONAL RIVERS, 2007) it seems logical to perceive soil erosion in the surrounding of large dams and their reservoirs as a serious environmental threat. Caused dredging costs of annually US$100-150 billion (INTERNATIONAL RIVERS, 2007) due to reservoir siltation also illustrate the relevance of soil erosion and sediment production as economic threat to the lifespan of reservoirs (e.g., BENNETT and RHOTON, 2007).

One prominent European example is the multipurpose (i.e., hydropower generation, water storage and supply, tourist attraction) large Alqueva dam at the Guadiana River in the semiarid south of Portugal. Its reservoir presents the largest artificial lake (250 km²) in Europe. However, post-construction shifts in land use and human activities in combination with erosion-prone soils, high rainfall erosivity during periods of poor vegetation cover, and steep terrain enhanced the soil erosion risk potential and sediment production in the Alqueva dam watershed and lead to distinct decreases in storage capacity due to silting up (SERAFIM ET AL., 2006; FERREIRA and PANAGOPOULUS, 2010; 2012). Applying empirical soil erosion modeling using RUSLE combined with Geographic Information Systems, FERREIRA and PANAGOPOULUS (2012) revealed an average annual soil loss by water erosion of approximately 29 t ha^{-1} which constitutes the threefold of what is considered as severe soil loss in entire Europe (JONES ET AL., 2012). Dam-induced rapid intensification of agriculture and irrigated area, biomass production, and development of tourism promoted by regional development plans as well as climate change are assumed to even raise the soil erosion risk in the affected watershed and to boost the reservoir siltation (ARVELA ET AL., 2012; FERREIRA and PANAGOPOULOS, 2012).

A second prominent example is the binational Itaipú dam impounding Rio Paraná at the border of Brazil and Paraguay. The subtropical reservoir of Itaipú Lake has an area of 1,350 km² at the normal operation water level of 220 m a.s.l. (MORMUL ET AL., 2010). The drainage area

upstream the dam is 820,000 km² (NORTON ET AL., 2001). The Itaipú dam construction was completed in 1982 for the main purpose of hydropower generation. After the Three Gorges Dam at the Yangtze River in China, it is the second largest in world in terms of installed capacity. The Itaipú hydroelectric facility provides more than 24% of Brazil's and 95% of Paraguay's electricity needs (COCHRANE ET AL., 2004). Since the start of its construction in 1975 and as a consequence of poor environment-related planning and follow-up of the aggressive policies of agricultural expansion in Brazil since the 1950s, intense land use changes are attributed to the project (NORTON ET AL., 2001; ALIXANDRINI, 2010). By conducting land cover change analysis from remote sensing images for the period from 1973 to 2009, ALIXANDRINI (2010) reveals a progressive and drastic reduction of woodland area by approximately 74% from 4,666 km² to 1,206 km² in both, Brazil and Paraguay, mainly for the benefit of agricultural land that increased by approximately 76% from 3,062 km² to 5,393 km². Urban area increased more than fivefold from 30 km² to 152 km² within the same period. Those shifts dramatically increased soil losses by water erosion and enhanced sediment production from the major tributaries of Rio Paraná River by draining these areas of high erosion risk (NORTON ET AL., 2001; COCHRANE ET AL., 2002).

High to extremely high rates of soil loss by water erosion in the Itaipú reservoir basin of annually more than 20, respectively, 50 t ha^{-1} refer to areas under conventional tillage directly adjacent to the impounded backwater area (COCHRANE ET AL., 2003). Initially, during the feasibility study of the dam, no risk of sedimentation was expected and the lifespan of the project was assumed to be more than 300 years (NORTON ET AL., 2001). However, the enhanced sedimentation loading into the reservoir is expected to dramatically shorten the dam's long-term safe operation by premature filling and to affect the water ecology (MORMUL ET AL., 2010).

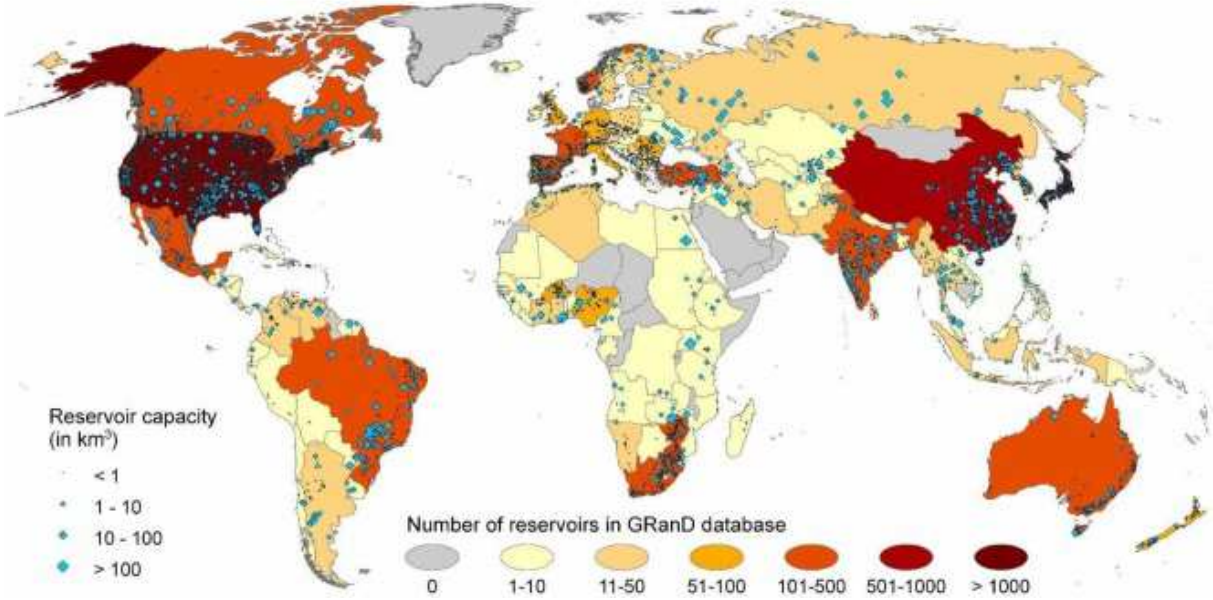

Figure 18 *Global spatial distribution of large dam projects by country (after LEHNER ET AL., 2011).*

THE THREE GORGES DAM AND ITS RESERVOIR

First proposals for the regulation of the discharge and hydropower generation by damming the Yangtze river in the area of the 'Three Gorges' date back to 1919 and to the 1930s. Various political and financial reasons, however, caused a postponement of the ambitious plan (PONSETI and LOPÉZ-PUJOL, 2006). After a severe series of floods, the original plans were re-examined in the mid 1950s and further reviewed in the mid 1980s. The plans were finally checked for their technical and financial feasibility in 1988 by the Canadian Yangtze Joint Venture (CYJV). In 1992, the CYJV feasibility study was approved through the Chinese National People's Congress (BEATTIE, 2002; DAI ET AL., 2006). The TGD project was then declared a chief task and a key strategic component in the development of the whole YRB (SUTTON, 2004). In 1993, the comprehensive construction project including the dam and the preparatory actions along the future reservoir started.

After its closure in 2003, the TGD started to impound the Yangtze River upstream of Sandouping close to Yichang, the outlet of the UYR (Figures 19 and 20). Geologically, the zone of the 'Three Gorges' stretches from *Qutang Gorge* (downstream of Fengdu towards Wushan), and *Wu Gorge* (from Wushan towards Badong) towards *Xiling Gorge* (from Zigui towards Yichang; Figure 20).

Figure 19 *The Three Gorges Dam in 2008 (above) and the sediment-choked, impounded Yangtze River right upstream the dam in 2010 (below). Pictures were taken by S. Schönbrodt-Stitt.*

Six years later in 2009, the dam itself, the installation of the hydropower plan, and two ship-locks were completed. The design water level of 175 m a.s.l. at the dam was reached the first time and full operation started. Additional construction works at the dam, such as the ship-lift, still continued to at least 2012 (XINHUA, 2012).

With a surface area of 1.084 km² (PONSETI and LOPÉZ-PUJOL, 2006), the Three Gorges Reservoir (TGR) is approximately the fourfold of the largest dam reservoir in Europe (Alqueva lake) and approximately 1.2-fold less of the largest dam in South America, the Itaipú lake (c.f., Annex IV). Due to the narrow valley bordered and steep sloped topography, the newly created reservoir stretches on a length of 660 km. At the scheduled water level of 175 dam (full operation level), the storage capacity of the reservoir is 39.3 km³ accounting for 8.7% of annual discharge at the dam site and 4.5% of the Yangtze River's annual discharge (DAI ET AL., 2006; HU ET AL., 2009; XU and MILLIMAN, 2009).

By realizing this project of the century, the Chinese government aims at following multiple purposes to strengthen the role of the Yangtze River as China's 'Golden Waterway' (WU ET AL., 2010):

- **Flood control and reduction of peak discharge downstream the TGD** in order to prevent nearly 80 million people from death and 60,000 km² of farmland as well as the dense industrial network in the middle and lower Yangtze River from monsoon flooding (PONSETI and LÓPEZ-PUJOL, 2006, PITTOCK and XU, 2011).
- **Energy generation by hydropower** in order to cover the increasing demand of energy and making the hydropower the first priority amongst all types of electricity generation in China (CHENG ET AL., 2012). The TGD is currently the largest hydroelectric dam in the world in terms of installed capacity with 26 hydro-turbines generating a total capacity of 18.2-22.5 gigawatts amounting to 11% of China's total hydropower capacity (CHENG ET AL., 2012; HUANG and YAN, 2009; BBC China, 05 July 2012).
- **Improvement of the Yangtze River's (and tributaries') navigation** due to deepening and widening of the river channel after river impoundment that lead to a better infrastructural connection of remote areas, an increase of one-way shipping river's capacity,

and boost of tourism in the region via a navigable length of more than 70,000 km (china.org.cn[2]; PONSETI and LÓPEZ-PUJOL, 2006);

- **Securing and facilitation of water supply and water transfer** by realizing the 'South-to-North Water Diversion Project' and bringing water from the TGR toward the north to the Huang-Huai-Hai Plain by linking the Yangtze River with the rivers Huang He, Huaihe, and Haihe (Water-Technology.Net, 29 May 2013).

The impoundment of the Yangtze River and the associated backwater creation in the tributaries currently lead to far-reaching and drastic changes in the affected landscapes and ecosystems. A central effect of the TGD is the required seasonal adoption of the water level of 30 m at the dam in order to realize the above goal settings by considering as far as possible the characteristics of the natural watercourse flow (SUBKLEW ET AL., 2012).

Until the start of the Southeast Asian summer monsoon, the reservoir's water level is lowered to 145 m a.s.l. at the dam in order to provide a sufficient upstream compensating volume for abundant precipitation and thus, flood retention volume during the rainy season from May to September. In October when the peak flow passed through, the water level is raised to a maximum scheduled water level of 175 m a.s.l. for peak load energy production. From January to May, the water level is again lowered to 145 m a.s.l. to compensate the very low precipitation and thus, to increase the water flow downstream the TGD. Furthermore, existing sediment deposits shall partly be washed away in order to keep the reservoir siltation on a low level during rainy season when highest precipitation is associated with an increased solid matter transport (SUBKLEW ET AL., 2012).

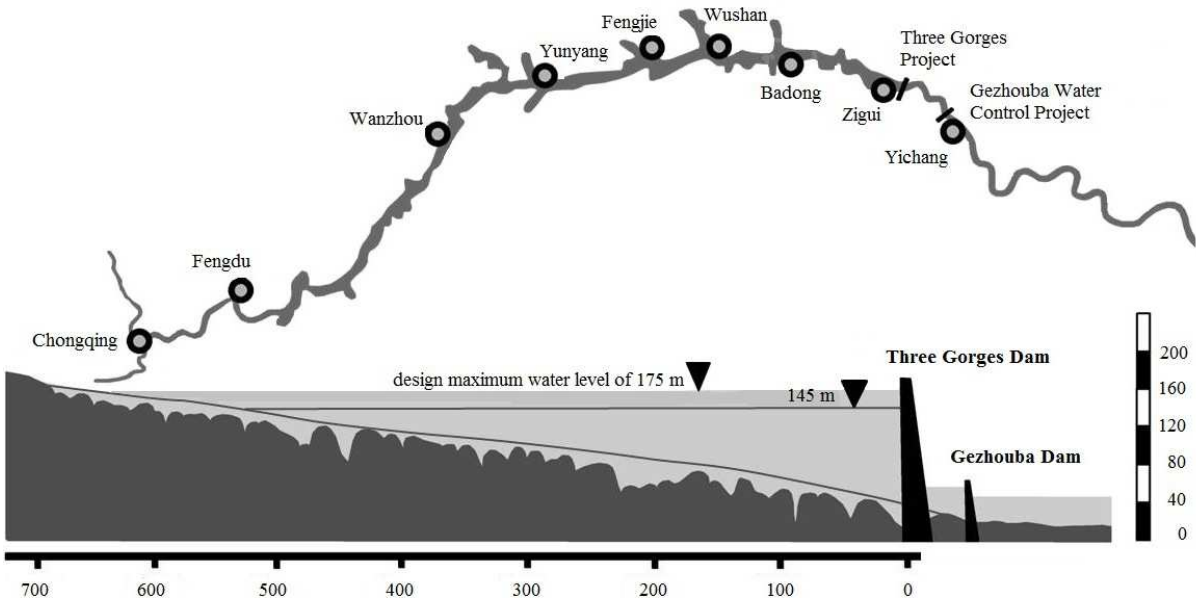

Figure 20 *Location of the Three Gorges Dam close to Yichang at the outlet of the Upper Yangtze River Basin and the newly created Three Gorges Reservoir after river impoundment in 2007 upstream from Yichang towards Chongqing (above), and design of the scheduled water levels (below; after Three Gorges Project; modified by S. Schönbrodt-Stitt).*

MANUSCRIPT 1

GIS-basierte Erfassung und Analyse der Bodenerosion durch Wasser im Drei-Schluchten-Ökosystem

Veröffentlicht in: Scholten, T., Schönbrodt-Stitt, S. (Hrsg.), 2012. Umweltforschung im Drei-Schluchten-Ökosystem in China - Ergebnisse der Forschungsarbeiten zur Risikoabschätzung von Bodenerosion, Hangrutschungen, diffusen Stoffeinträgen und Landnutzungsvulnerabilität. Tübinger Geographische Studien Heft 151, Selbstverlag des Geographischen Instituts der Universität Tübingen, Seiten 27-83, ISBN 978-3-88121-089-8

Sarah Schönbrodt-Stitt[1)], Thorsten Behrens[1)], Xuezheng Shi[2)], Thomas Scholten[1)]

1) Institute of Geography, Department of Physical Geography and Soil Science, University of Tübingen, Tübingen, Germany

2) Department for Soil Resources and Remote Sensing Application, Institute of Soil Science, Chinese Academy of Sciences, Nanjing, China

ZUSAMMENFASSUNG

Mit der Entwicklung eines integrativen, datenbasierten Modellierungsansatzes verfolgte diese Studie die räumliche hochaufgelöste Erfassung und Vorhersage von Bodenerosion in das Reservoir des Drei-Schluchten-Staudamms (*Three Gorges Dam*; TGD). Die zentralen Forschungsfragen galten (a) der Art und dem Umfang der Auswirkungen veränderter Rahmenbedingungen am TGD auf die Bodenerosion durch Wasser, (b) den Veränderungen der Ressource Boden durch die Bodenerosion, (c) den durch die Bodenerosion ausgelösten Geo-Risiken bzw. Risikopotenziale und (d) deren räumliche und zeitliche Variabilität.

Infolge des Baus des TGD ist auch das Einzugsgebiet des Xiangxi in diesem hoch-dynamischen Ökosystem von der Flussaufstauung, saisonalen Wasserstandsschwankungen und rapiden Landnutzungsänderungen mit Auswirkungen auf die Hangstabilität und Bodenerosion betroffen. Das Risikopotenzial von Bodenerosion in das Reservoir bildete den inhaltlichen Schwerpunkt dieser Studie. Das Einzugsgebiet des Xiangxi ist gekennzeichnet durch steile bis extrem steile, größtenteils terrassierte Hänge und die künstliche Verlagerung von Oberbodenmaterial von den gefluteten Uferbereichen hangaufwärts. Das Ziel der Untersuchungen bestand in der Entwicklung einer integrativen und datenbasierten Methode zur Erfassung und Analyse von Bodenerosion mittels eines mehrstufigen und multiskaligen Ansatzes. Die Kombination von GIS-basierter empirischer und

einzugsgebietsbezogener Erosionsmodellierung basierend auf Reliefanalysen mit Geländearbeiten und Fernerkundung bildete den konzeptionellen Aufbau der Arbeiten.

Die wesentlichsten Ergebnisse sind die Kartierung bodenerosionsrelevanter Prozesse in den Intensivuntersuchungsgebieten, die erfolgreiche Parametrisierung des Bodenerosionsmodells RUSLE und die Entwicklung des konzeptionellen Modells *TerraCE*, sowie die Regionalisierung erosionssteuernder Faktoren auf Basis von *TerraCE* mittels Data Mining-Verfahren und Berechnung der flächenkonkreten Bodenerosionsgefährdungskarte.

1 EINLEITUNG

Bodenerosion zählt nach wie vor zu den größten Umweltproblemen weltweit. In den 1990er Jahren sind allein in Europa 105 Millionen ha oder 16% der gesamten Landfläche (ohne Russland) betroffen (EEA, 2003). Neuere Berechnungen des *Joint Research Centre* der EU (JRC, JONES ET AL., 2012) schätzen die Fläche aktuell auf 1,3 Millionen km² für die EU-27, wovon annähernd 20% einen Bodenabtrag von mehr als 10 t ha^{-1} a^{-1} aufweisen. Im wissenschaftlichen Diskurs wird der Verlust fruchtbaren Bodens durch Erosion gar als *silent global crisis* mit Auswirkungen auf die Nahrungsmittelproduktion, Wasserverfügbarkeit und auf den Klimawandel verstanden (u.a. MONTGOMERY, 2007). Eine Bodendegradation durch Bodenerosion wirkt sich direkt auf die Produktivität landwirtschaftlicher Ökosysteme und Forstökosysteme aus. Ebenso bedroht der Bodenverlust die Stabilität von Ökosystemen und sozioökonomischer Strukturen (PIMENTEL, 2006). Der Verlust an fruchtbaren Oberboden und an Bodenwasserspeicher ebenso wie die Erosionsprozesse selbst, gekennzeichnet durch Sedimentausträge, Austräge partikulär im Boden gebundener Agrochemikalien und Belastung angrenzender Gewässer, stellen Politik und Ökonomie damit vor enorme politische und planerische Herausforderungen, angefangen bei der Ernährungssicherung bis hin zur Trinkwasserqualität. Global betrachtet gehört China zu den Ländern, die am stärksten von Bodenerosion betroffen sind (HUANG, 1987; ALDHOUS, 1993; VAN LYNDEN und OLDEMANN, 1997; KOLB, 2003; CAI ET AL., 2005; Abbildung 1). Aktuelle fernerkundungsbasierte Studien zeigen, dass 3,56 Millionen km² Chinas ernste Bodenerosionsschäden aufweisen (PEOPLE DAILY, März 2010). Dies sind ungefähr 37% der gesamten Landesfläche.

Durch Bodenerosion ausgelöste technische Probleme verbunden mit hohen Kosten treten u.a. bei großen Staudammprojekten auf, wo infolge hoher Sedimenteinträge in die Reservoirs mit der Abnahme der Staukapazität und damit der Energiegewinnung durch Wasserkraft gerechnet werden muss. Neben der natürlichen Erosionsdisposition, determiniert durch die Topographie, die Erosivität der Niederschläge und Erodierbarkeit der Böden, spielen vor allem die mit dem Bau und Betrieb von Staudämmen einhergehenden, anthropogenen Eingriffe in die angrenzenden Ökosysteme, z.B. durch

Straßen- und Siedlungsbau sowie Bodenverdichtung und Flächenversiegelung, eine entscheidende Rolle für die Höhe des Bodenabtrags.

Die Errichtung und der Betrieb des weltweit größten Staudammprojekts am Yangtze in Zentralchina zeigt dies exemplarisch. Der Drei-Schluchten-Staudamm (*Three Gorges Dam*, im Folgenden TGD) am Oberlauf des Yangtze verursacht kurzfristige, massive Landschafts- und Umweltveränderungen in einer Region, die die höchsten Bodenerosionsraten in ganz China aufweist (ZHOU, 2008). Ungefähr 33% (560.000 km²) des Yangtze-Einzugsgebietes (Yangtze-EZG), eine Fläche fast 1,5 Mal so groß wie Deutschland, ist bereits ernsthaft durch Bodenerosion, speziell am Unter- und Mittellauf des Yangtze, betroffen. Die sich infolge des TGDs rapide ändernden und hochdynamischen Ökosystemeigenschaften können die Bodenerosion dabei noch verstärken. Durch den Aufstau des Yangtze verlagert sich die lokale Erosionsbasis. Infolge künstlicher Wasserstandschwankungen im Jahresgang werden die angrenzenden Hänge destabilisiert und Massenbewegungen induziert.

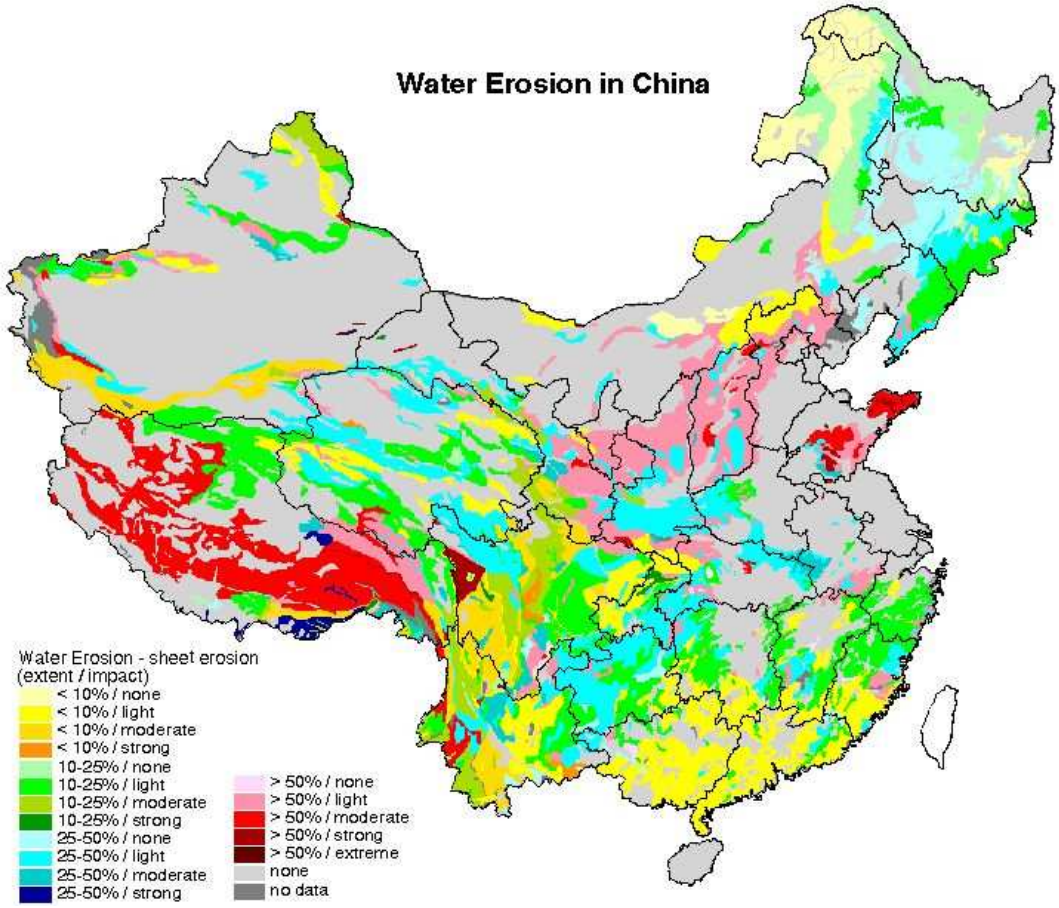

Abbildung 1 *Durch den Menschen verursachte Bodenerosion in China und deren Ausmaß (nach VAN LYNDEN und OLDEMANN, 1997).*

Großräumige Landnutzungsänderungen, verbunden mit der Neulandgewinnungen für Infrastruktur, Subsistenzanbau und den flächenintensiven Anbau von Marktfrüchten (*Cash crops*) auf stark geneigten Flächen hangaufwärts der ursprünglichen Uferlinie (CAI ET AL., 2005; HUANG ET AL., 2006) können ebenfalls ein Zunahme der Bodenerosion bewirken. Es wird erwartet, dass der TGD und die damit zusammenhängenden, sich rapide ändernden und hochdynamischen Ökosystembedingungen, die Bodenerosion in einer unerwarteten Dimension forcieren. Infolge der Flussaufstauung wurden die Auen und mithin der überwiegende Teil landwirtschaftlich genutzter Flächen überflutet. Mehr als eine Million Menschen wurden umgesiedelt (TAN ET AL., 2005; MCDONALD ET AL., 2008). Einige Studien weisen eine Umsiedlung weiterer vier Millionen Menschen bis zum Jahr 2020 aus (u.a. OSTER, 2007). Die neuen Siedlungsgebiete befinden sich oberhalb der neuen Uferlinie des Aufstaubereichs auf stark geneigten Hängen, die durch flachgründige, erosionsempfindliche Böden gekennzeichnet sind (HE ET AL., 2008). Weitere erosionsrelevante Faktoren sind eine erhöhte Hanginstabilität infolge der künstlichen, saisonalen Wasserspiegelschwankungen sowie die Entwaldung und nachfolgende Intensivierung der Landwirtschaft an den Hängen kombiniert mit unangepassten Managementpraktiken (CAI ET AL., 2005; HUANG ET AL., 2006).

Mittel- bis langfristig werden daher im Einzugsgebiet des Yangtze und seiner Nebenflüsse beträchtliche ökologische Folgen und sozioökonomische Konsequenzen der Bodenerosion erwartet (MENG ET AL., 2001). Unter der Prämisse einer nachhaltigen Nutzung der natürlichen Ressourcen Wasser und Boden stellt sich damit die Frage nach (a) den Reaktionen der Landschaft auf die veränderten Rahmenbedingungen und (b) der räumlichen und zeitlichen Dynamik der Reaktionen im neu geschaffenen Ökosystem Drei-Schluchten-Staudamm. Kenntnisse zur Qualität und Quantität des Bodenabtrags und dessen räumliche sowie zeitlich Variabilität können helfen, die Ausmaße der Bodenerosion mit Hilfe eines angepassten Managements und Schutzmaßnahmen zu minimieren. Hangparallel angelegte Ackerterrassen stellen eine solche Schutzmaßnahme dar, die im Bereich des TGD großflächig zur Anwendung kommt. Im Optimalfall gleichen die Terrassen die Topographie aus und ermöglichen eine ökonomisch profitable ackerbauliche Nutzung von Gebirgsregionen (z.B. BRANCUCCI und PALIAGA, 2006; CAO ET AL., 2007).

Bereits in der Antike und frühen Neuzeit erkannten die Kulturen im Mittelmeerraum, in China und in Mittel- und Südamerika die Bedeutung eines optimal an die physio-geographischen Bedingungen angepassten und konstruierten Terrassensystems für den Erosionsschutz und die Bodenfruchtbarkeit (LAL, 1976; TOY ET AL., 2002; MONTGOMERY, 2007). Durch die quer zum Hang gerichtete Terrassierung werden steil geneigte Hänge in mehrere kürzere Abschnitte mit relativ flachen Oberflächen überführt. Dies bewirkt eine deutliche Herabsenkung der erosiven Hanglänge und des Oberflächenabflusspotenzials. Jedoch ermöglicht die verbleibende Hangneigung der einzelnen Terrassenstufen in Abhängigkeit von der Topographie und der Konstruktionsweise der Terrassen immer noch Bodenabtrag (HUDSON, 1981; KOULOURI und GIOURGA, 2007). HAMMAD ET AL. (2004)

haben für Trockensteinterrassen (*dry-stone walls*) unter mediterranen Bedingungen eine Verringerung des Runoff-Koeffizienten (Menge des Oberflächenabflusses im Verhältnis zur Niederschlagsmenge) von 20% für nicht terrassierte Plots auf 4% für terrassierte Plots gemessen. Untersuchungen von ZHANG ET AL. (2008) im montanen Sichuan-Becken in Westchina zeigen einen Anstieg des Runoff-Koeffizienten um circa 22 bis 70% auf nicht-terrassierten Flächen gegenüber terrassierten Plots. Die Bodenerosion auf nicht-terrassierten Plots ist dabei um circa 35 bis 400% erhöht.

Eine inadäquate Konstruktion und Missmanagement von Terrassen können die Erosionsschutzwirkung stark beeinträchtigen. Verschiedene Studien in Peru (INBAR und LLERENA, 2000), Italien (BRANCUCCI und PALIAGA, 2006) und Thailand (SANG-ARUN ET AL., 2006) zeigen einen Zusammenhang zwischen der beobachteten Höhe des Bodenabtrags und des Zustands der Terrassen. Insbesondere die Aufgabe bzw. Stilllegung von Terrassenflächen können zu einem erneuten Anstieg der Erosionsraten führen. Gründe für eine Aufgabe der Flächen liegen häufig in der Extensivierung der Landwirtschaft und/oder mangelnden Kapitals zur Unterhaltung der Flächen. Ebenso kann der umgekehrte Fall eintreten. Rapide ökosystemare Veränderungen und eine einhergehende rasche Intensivierung und Inwertsetzung bzw. Reaktivierung von Terrassenflächen, wie es in der Drei-Schluchten-Region großflächig zu beobachten ist, können zur Degradation von Terrassenflächen führen (SCHÖNBRODT-STITT ET AL., 2011; *under review*). Im Xiangxi-Einzugsgebiet (Xiangxi-EZG) zeigt sich eine Degradation der Terrassenlandschaft insbesondere im Aufstaubereich (Abbildung 2). Bislang ungenutzte Flächen werden im Zuge der Umsiedlung rasch in Wert gesetzt und brachliegende Flächen reaktiviert. Das Tempo dieser dynamischen Veränderungen berücksichtigt dabei nur zu selten vorhandenes Kapital zur Instandsetzung alter Terrassenflächen. Auf den neuen Terrassen werden hauptsächlich Orangen angebaut. Die starke Zunahme der Anbaufläche in sehr kurzer Zeit führt zur Überproduktion und zum Preisverfall auf den lokalen und regionalen Märkten, der mangelnde Absatz der Orangen ist wenig gewinnbringend. Dadurch fehlen die Motivation und das Kapital zur Pflege und Instandhaltung der Terrassen und es kommt sukzessive zu einer Verschlechterung des Zustands vieler Terrassenflächen.

Quantitative Abschätzungen zum Bodenabtrag auf Terrassen mit starken Degradationserscheinungen fehlen in der Literatur bisher bzw. beziehen sich nur auf vorsichtige Schätzungen ohne Kalibrierung und Validierung durch direkte Abtragsmessungen. Dies liegt unter anderem darin begründet, dass die Integration von Terrassen sowie die Berücksichtigung ihres Zustands in der Erosionsmodellierung bislang nur ansatzweise gelungen sind. Fehlt einer prozessorientierten Erosionsmodellierung auf Terrassen, wie sie z.B. mit dem TEST Modell auf West Java vorgenommen wurde (VAN DIJK, 2002), die Parametrisierung auf Plotebene, lassen sich die Ergebnisse nicht auf Einzugsgebietsebene übertragen. In der empirischen Erosionsmodellierung auf Einzugsgebietsebene wurde die Wirkung der Terrassen auf den Bodenabtrag bislang in einem Maß für Erosionsschutzmaßnahmen widergegeben. Bei der Modellierung mit der USLE bzw. RUSLE (WISCHMEIER

und SMITH, 1965; RENARD ET AL., 1997) ist dies der *P*-Faktor. Die durch Terrassierung modifizierten, erosiven Hangneigungen und Hanglängen als prozessrelevante Größen werden dabei nur indirekt berücksichtigt. Ein Maß für den Terrassenzustand fehlt. Es gehen lediglich Angaben zum Terrassendesign ein, abgeleitet aus Terrassenneigung und Breite der Terrassenstufe.

Abbildung 2 *Diversität terrassierten Farmlands im Einzugsgebiet des Xiangxi. Fotos aufgenommen von S. Schönbrodt (09/2008, 04/2009).*

Angesichts der Beobachtungen im Bereich des TGD vermuten wir, dass der Zustand der Terrassen einen prozessbestimmenden Faktor der Bodenerosion darstellt. Die Kausalität zwischen Auftretenswahrscheinlichkeit sowie Intensität des Bodenabtrags und dem Pflegezustand der Terrassen war bereits zu Beginn der ersten Projektphase offensichtlich und scheint in dem stark reliefierten Xiangxi-EZG eine der zentralen Steuergrößen der Bodenerosion zu sein. Es zeigte sich, dass dort wo Störungen der Trockensteinmauern, z.B. eingestürzte und/oder verschlämmte Terrassenwände, und/oder an die lokale Reliefsituation unangepasstes, ingenieurtechnisches Terrassendesign auftreten, ein deutlich höherer Bodenabtrag und Oberflächenabfluss austritt als bei gut gepflegten Terrassen. Wir nehmen daher an, dass die Höhe sowie die zeitliche und räumliche Verteilung der Bodenerosion im Gebiet des TGD in erster Linie eine Funktion des Terrassenzustands ist und weniger durch die

natürliche Erosionsdisposition bestimmt wird. Wir betrachten den Terrassenzustand dabei als eine Funktion aus reliefbasiertem Terrassendesign und Pflegezustand. Ursächlich stehen sozioökonomische Faktoren und naturräumliche Gegebenheiten nebeneinander und bedingen in Wechselwirkung den jeweiligen Terrassenzustand.

2 ANSATZPUNKT DER ARBEITEN UND FORSCHUNGSFRAGEN

Ziel der Arbeiten war die Entwicklung eines integrativen, datenbasierten Modellierungsansatzes zur hochaufgelösten Erfassung und Vorhersage von Bodenerosion und diffusen Stoffeinträgen in das Reservoir des Drei-Schluchten-Staudamms. Die zentralen Forschungsfragen zielen auf (a) Art, Umfang und Auswirkungen veränderter Rahmenbedingungen am TGD auf die Bodenerosion durch Wasser, (b) Veränderungen der Ressource Boden durch die Bodenerosion, (c) durch die Bodenerosion ausgelöste Geo-Risiken bzw. Risikopotenziale und (d) deren räumliche und zeitliche Variabilität ab.

In einem schrittweise und rekursiv angelegten Ansatz (Abbildung 3) wurden dabei im Einzugsgebiet des Xiangxi und der Teileinzugsgebiete Quyuan und Xiangjiaba (*nested approach*) die bodenkundlichen und geomorphologischen Grundlagen sowie die Bodenerosion und deren steuernden Eigenschaften erfasst. Darauf aufbauend erfolgte die Erstellung und Validierung einer hochauflösenden, flächenkonkreten Gefahrenkarte zur Bodenerosion. Die zentralen Forschungsfragen lauten:

- Wie lassen sich die Erosionsgefährdung und das Erosionsrisikopotenzial im Xiangxi-EZG erfassen und bewerten?
- Welches Erosionsmodell eignet sich zur Vorhersage des Bodenerosionsrisikos?
- Wie lassen sich die Hotspots des Erosionsrisikopotenzials identifizieren und wo befinden sie sich?
- Wie kann die Rolle der Terrassen als wirksamer Erosionsschutz im Untersuchungsgebiet berücksichtigt werden?

Die Arbeiten zur Beantwortung der Forschungsfragen gliedern sich in Kartierungsarbeiten und Bodenprobenahme im Gelände, laboranalytischen Arbeiten und GIS-gestützten Modellierungen der Bodenerosion unter Berücksichtigung des Terrassenzustands. Basierend auf der Analyse von Felddaten und der Regionalisierung erosionssteuernder Faktoren erfolgt zunächst die Parametrisierung des Erosionsmodells RUSLE mit dem erste flächenkonkrete Bodenerosionsgefährdungskarten gerechnet werden. Weitere Geländearbeiten dienten der Parametrisierung des neu entwickelten Terrassenzustandsmodells *TerraCE*. Abschließend erfolgt die Integration der Ergebnisse von *TerraCE* in die Erosionsmodellierung und die Neuberechnung des Erosionsrisikopotenzials unter Berücksichtigung des Terrassenzustands als erosionssteuernder Faktor.

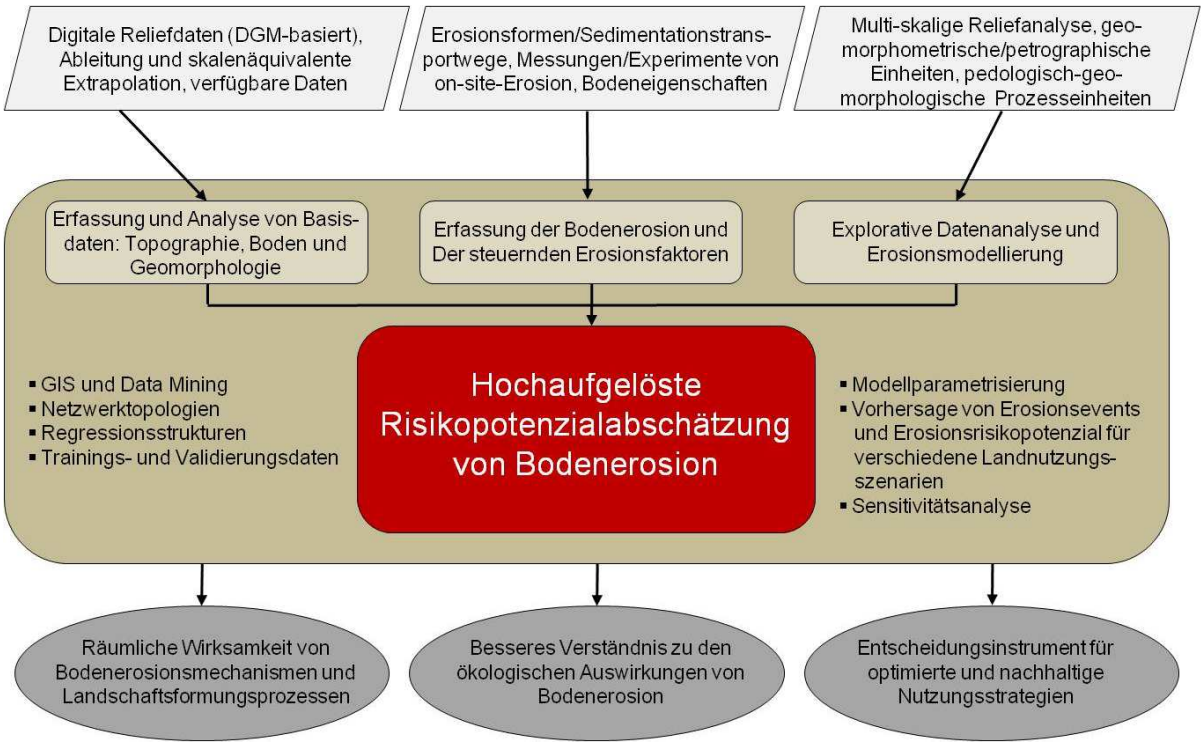

Abbildung 3 *Ablauf und Koppelung der Arbeitsschritte für die Erstellung und Validierung einer hochauflösenden, flächenkonkreten Gefahrenkarte zur Bodenerosion.*

3 MATERIAL UND METHODEN

3.1 Geländearbeiten

Die erste mehrwöchige Geländephase im Xiangxi-EZG in 2008 diente der Erfassung bodenkundlicher und geomorphologischer Charakteristika sowie der Klassifikation aktueller Erosionserscheinungen und deren steuernden Faktoren (Tabelle 1). Aufbauend auf den Erkenntnissen der Übersichtsbegehungen zur Abgrenzung der Teileinzugsgebiete Xiangjiaba und Quyuan wurden Standorte mit repräsentativen Landnutzungstypen und Reliefformen als Typlokalitäten ausgewiesen. Ein weiterer zentraler Arbeitsschritt in der ersten Geländephase war die genaue Positions-bestimmungen, die Lokalisierung der Typlokalitäten auf der Topographischen Karte, die Relief-korrektur sowie die Georeferenzierung der Kartengrundlage. Dieses war notwendig, da die zur Verfügung stehenden Karten teils verzerrt sind und teils keine absolute Positionsbestimmung erlauben. Die topographischen Vermessungsarbeiten umfassten tägliche Trackaufzeichnungen der Straßen und Wege sowie die wiederholte Lokalisierung von Städten und Dörfern sowie markanten Plätzen (Brücken, Staumauern, Uferlinie, Mündungsbereiche von Nebenflüssen in den Xiangxi, markante Bauten, z.B. Tempel).

Die zweite mehrwöchige Geländephase im Xiangxi-EZG in 2009 diente der weiterführenden Erfassung bodenkundlicher und geomorphologischer Charakteristika von Typlokalitäten. Diese Typlokalitäten entsprechen in ihrer Funktionalität denen der ersten Geländephase. Als eine weitere

funktionale Landnutzungsgruppe wurden Waldflächen kartiert. Weiterhin wurden rezente Erosionserscheinungen klassifiziert und deren steuernde Faktoren erfasst.

Aufbauend auf den Erkenntnissen der starken Kausalität zwischen der Auftretenshäufigkeit von Erosionserscheinungen und dem Zustand landwirtschaftlich genutzter terrassierter Flächen, lag ein zweiter inhaltlicher Schwerpunkt der Geländearbeiten in 2009 und 2010 auf der Klassifizierung und Kartierung von Terrassenzuständen sowie der Erfassung rezenter Erosionsformen im Aufstaubereich und in den Teileinzugsgebieten Xiangjiaba und Quyuan. Von besonderer Bedeutung waren Charakteristika des Terrassendesigns und die Qualität des Pflegezustandes sowie Erosionsformen und deren Ausprägung. Des Weiteren wurden topographische Vermessungsarbeiten durchgeführt.

Rezente Erosionsformen wurden in ihrer Ausdehnung (Länge, Breite, Tiefe) vermessen und in Anlehnung an die Richtlinien des DVWK-Fachausschuss Bodenerosion (1996) nach *Sheet erosion*, *Interrill erosion*, *Rill erosion* und *Gully erosion* klassifiziert. Die Schätzung des Bodenabtrags erfolgte im Gelände nach HUDSON (1981, Tabelle 3). Während der ersten Geländekampagne (2008) wurden insgesamt 27 Standorte (E_1 bis E_27), verteilt auf das Xiangxi-EZG, den Aufstaubereich und die Teileinzugsgebiete Xiangjiaba und Quyuan, auf aktuelle Erosionserscheinungen und bodenkundliche, morphologische und landnutzungsbedingte Erosionsfaktoren untersucht. In 2009 und 2010 kamen weitere 218 Standorte hinzu (Abbildungen 4 und 5). Flächen ohne Erosionserscheinungen wurde der Erosionsklasse 1 zugeordnet. Ein allgemein mäßiger Verlust des Oberbodens und ein geringfügiges Einschneiden durch Abflussrinnen kennzeichnen die Standorte der Erosionsklasse 2, während Erosionsklasse 3 einen deutlich höheren Oberbodenverlust und eine stärkere Zergliederung durch Abflussrinnen beinhaltet. In die Erosionsklasse 4 eingestufte Standorte sind durch eine sehr starke Abtragung des Oberbodens bis zur Bloßlegung des Unterbodens bzw. selten auch des Ausgangsgesteins und eine tiefe (20 bis vereinzelt 50 cm Tiefe) und verhältnismäßig breite (20-30 cm) Zerschneidung durch Rinnen und Gräben gekennzeichnet.

Die Erhebung des Pflegezustands von Terrassen erfolgte mittels eines eigens entwickelten standardisierten Aufnahmebogens in Anlehnung an COMOLLI (2005), SFONDRINI ET AL. (2005) und BRANCUCCI und PALIAGA (2006). Die Bestimmung des Bodentyps (Abbildung 6) erfolgte nach WRB (2007) an Leitbodenprofilen und mittels Bohrstockkartierung (Pürckhauer-Bohrstock). Für eine Analyse bodenphysikalischer und bodenchemischer Parameter wurden von jeder Typlokalität gestörte Bodenproben aus dem Oberboden (0-20 cm) und an den Leitprofilen horizontweise gestörte und ungestörte Bodenproben entnommen. Alle bodenkundlich und geomorphologisch untersuchten und im Hinblick auf Erosionsformen kartierten Typlokalitäten wurden mit täglich variierenden Genauigkeit zwischen ± 4-12 m GPS-lokalisiert (UTM WGS 1984, Zone 49N).

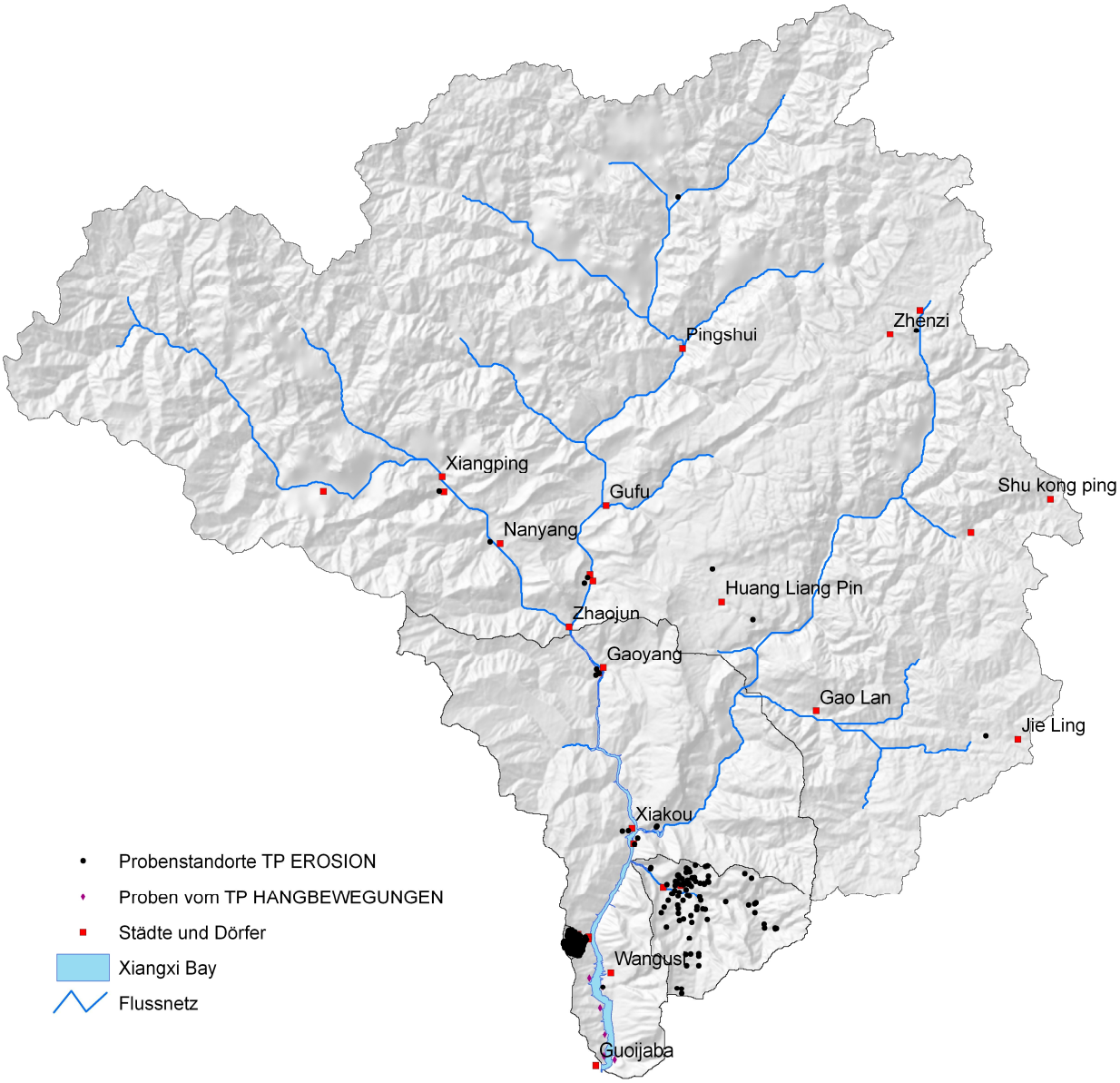

Abbildung 4 *Standorte der Probenentnahmen und Kartierungsflächen im Einzugsgebiet des Xiangxi. GIS und Layout von S. Schönbrodt.*

3.2 Laboranalysen

Die Bestimmung der Lagerungsdichte erfolgte gravimetrisch in dreifacher Wiederholung an Volumenproben nach Trocknung bei 105 °C bis zur Gewichtskonstanz im Labor der *Faculty of Engineering* (CUG) in Wuhan. Ebenfalls erfolgte hier die Probenvorbehandlung (Lufttrocknung, Siebung < 2 mm, Mörsern, Ermittlung des Masseanteils der Grobbodenkomponente > 2 mm). Im Labor für Bodenkunde und Geoökologie am Lehrstuhl für Physische Geographie und Bodenkunde (Universität Tübingen) wurden Korngrößenzusammensetzung (7 Fraktionen, kombinierte Sieb-Pipett-Methode nach Köhn, DIN 19683 1/2), Karbonatgehalt (gasvolumetrisch an gemahlenen Teilproben, Calcimeter, Eijkelkamp), pH-Wert (potentiometrisch in deionisiertem Wasser und in 1 M KCl-Lösung

bei einem Boden:Lösungs-Verhaltnis von 2,5:1 mit einer Sentix 81-Glaselektrode im Lösungsüberstand, WTW pH 340) und C- und N-Gesamtgehalte (an gemahlenen Teilproben mittels flammenloser Verbrennung am CNS-Analyzer, Vario EL III, Elementar GmbH, Hanau) bestimmt.

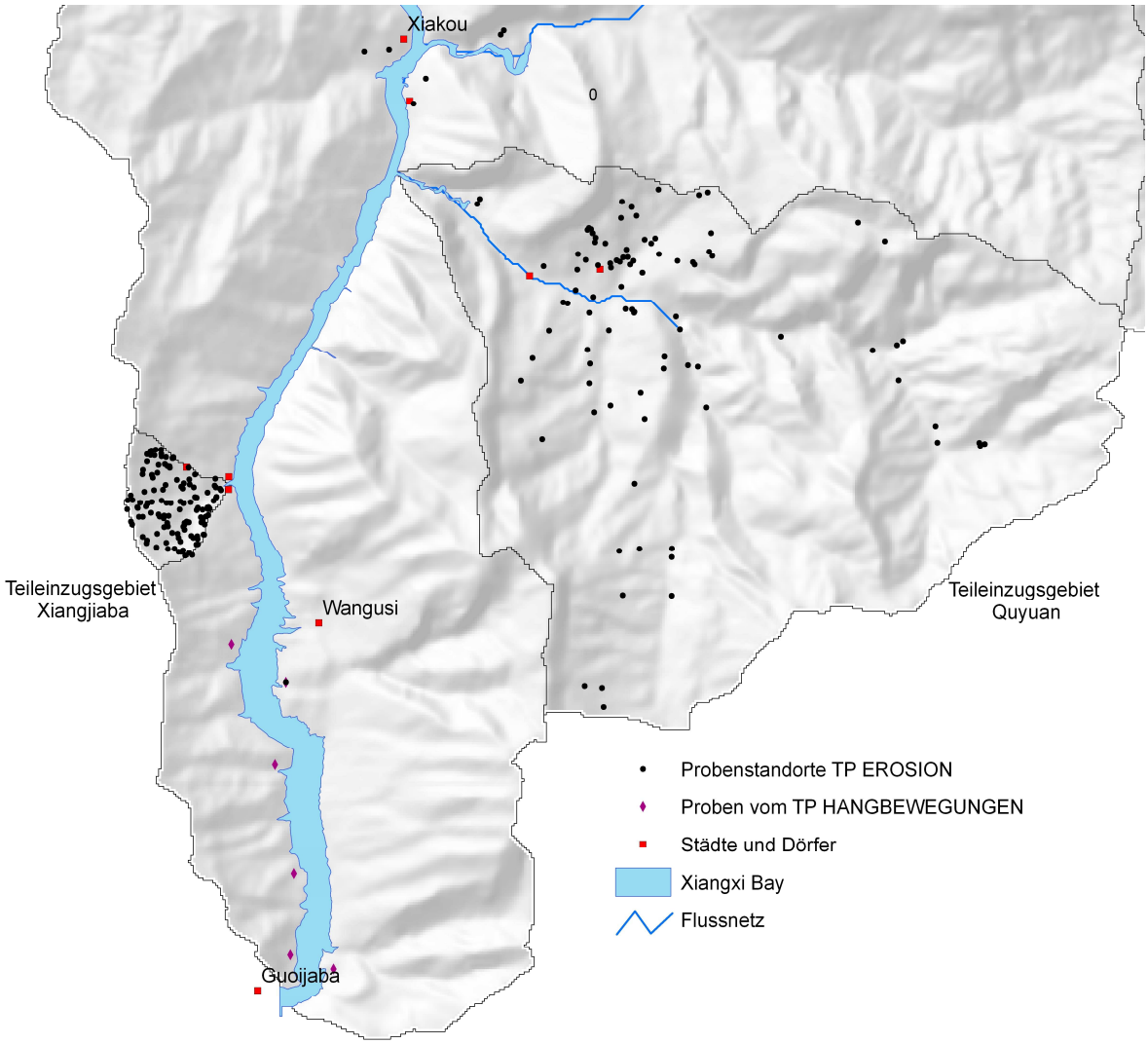

Abbildung 5 *Standorte der Probenentnahmen und Kartierungsflächen im Aufstaubereich im südlichen Einzugsgebiet des Xiangxi. GIS und Layout von S. Schönbrodt.*

Tabelle 1 *Parameter zur Erfassung der Faktoren der Bodenerosion im Einzugsgebiet des Xiangxi (KA5: Bodenkundliche Kartieranleitung, Ad-hoc-AG Boden der Geologischen Landesämter und der Bundesanstalt für Geowissenschaften und Rohstoffe der Bundesrepublik Deutschland; WRB 2006: World Reference Base of Soil Resources, IUSS Working Group WRB; RUSLE: Revised Universal Soil Loss Equation, RENARD ET AL., 1997).*

Faktor	Parameter
Boden	Textur des Feinbodens (Fingerprobe nach KA5)
	Bodentyp (WRB 2006)
	Steinanteil auf Bodenoberfläche (Flächen-%)
	Karbonat (Test mit HCl 10%)
Relief	Hangneigung (Neigungsmesser)
	Hangform (KA5)
	Lage am Hang (KA5)
Landnutzung	Dominierende Landnutzung und Größe der landwirtschaftlich genutzten Fläche (Breite und Läge in m)
	Zwischenfruchtanbau (Kartierung und Befragung der Bauern)
	Grad der Bodenbedeckung (Flächen-%), Mulchfaktor (RUSLE)
	Anbautechnik (Aufnahmebogen: terrassiert/nicht terrassiert)
	Terrassen (Aufnahmebogen: Typ, Höhe, Breite, Neigung)
	Zustand der Terrassen (Aufnahmebogen: qualitativ)
Management	Erosionsschutzmaßnahmen (RUSLE)

Abbildung 6 *Beschreibung pedologischer Eigenschaften im Einzugsgebiet des Xiangxi mittels Profilgrabungen (links) und Bohrstockkartierung (rechts). Fotos aufgenommen von S. Schönbrodt (04/2009).*

3.3 Datenaufbereitung und Erstellung der Datensätze für die Erosionsmodellierung und für *TerraCE*

Die Ableitung des hydrologischen Xiangxi-EZGs erfolgte mittels ArcGIS. Die dafür erforderlichen digitalen Höhendaten basieren auf den Daten der *Shuttle Radar Topographic Mission* (SRTM 3, Version 4; JARVIS ET AL., 2008) in 90-m-Auflösung der CGIAR-CSI. Im Preprozessing wurden die SRTM-Daten von Geographische Koordinaten in UTM WGS 84, Zone 49N umgerechnet. Anschließend wurde der Datensatz mit dem Open-Source-Programm 3DEM (Version 20, *Terrain Visualization And Flyby Animation*; Richard Horne) auf die Untersuchungsgebietsgröße zugeschnitten. Die Berechnung der Einzugsgebietsgrenzen erfolgte mit ArcGIS 9 (ArcMap Version 9.3) mittels *Spatial Analyst*, *Extension ArcHydro Tools* (Version 1.0).

Es wurde eine Korrektur des SRTM-DGMs durch manuelle Bearbeitung der Tiefenlinien zur Vermeidung von Artefakten im Oberflächenabfluss und anschließendes Resampling des SRTM-DGMs von 90 m auf 45 m Auflösung vorgenommen. Die digitale Reliefanalyse erfolgte auf Basis des korrigierten SRTM-DGMs und Berechnung der Hangneigung nach TARBOTON (1997). Abschließend wurden das hydrologische Xiangxi-EZGs und die hydrologischen Teileinzugsgebiete Xiangjiaba und Quyuan auf Basis des korrigierten SRTM-DGMs neuberechnet. Die Geologischen Karte und die Topographischen Karte wurden digitalisiert (Grenzen der Legendeneinheiten, Isohypsen) und georeferenziert. Die Georeferenzierung der Punktdatensätze aus der Erosionskartierung, der Bodenprofilaufnahme und Übertragung der kartierten landwirtschaftlichen Nutzflächen aus der Fernaufnahme von Terrassen (Abbildung 7) erfolgte auf Basis von SPOT-Bildern (5 m).

Die Berechnung der Niederschlagserosivität (*R*-Faktor) und Erstellung der Isoerodentenkarten für das Xiangxi-EZG erfolgte anhand von Stationsdaten in täglicher Auflösung von sechs Klimastationen sowie einer höhendifferenzierten Regionalisierung mittels *Elevation bands* auf Basis des SRTM-DGM.

Die Erstellung einer digitalen Bodenkarte als Grundlage zur flächenkonkreten Ableitung der Bodenerodierbarkeit erfolgte auf der Grundlage digitalisierter Bodenkarte des *2nd National Soil Survey of China* (SHI ET AL., 2010). Die Ergebnisse der Kartierung sind nach Landkreisen (*Counties*) gegliedert im Yellow Book veröffentlicht. Die entsprechenden, analog vorliegenden Karten zur Verteilung der Bodentypen in den Landkreisen Shennongjia, Xingshan und Zigui wurden als gescannte, georeferenzierte (UTM WGS 1984, Zone 49N) Karten entsprechend der Bodentypenzuordnung als Polygone digitalisiert und miteinander verschnitten. Basierend auf den ermittelten Profildaten des *2nd National Soil Survey* wurden die bodentypenspezifischen Parameter den jeweiligen Bodentypen der digitalen Bodenkarten in der Attributtabelle zugewiesen. Eine Plausibilitätsprüfung der Bodentypenverteilung erfolgte während des mehrtägigen Aufenthaltes am *Institute of Soil Science* der CAS in Nanjing, China.

Die flächendeckende Ermittlung der erosiven Hanglänge und erosiven Hangneigung (Topographiefaktor) wurde mit dem korrigierten SRTM-DGMs in 45-m-Auflösung vorgenommen. Die Erfassung der erosionswirksamen Oberfläche (*Fractional Vegetation Cover, Normalized Differenced Vegetation Index*) erfolgte mittels optischer, multitemporaler relief- und atmosphärenkorrigierter Fernerkundungsdaten. Hieraus wurde auch der *C*-Faktor der RUSLE abgeleitet.

Die Erfassung von Straßen und Siedlungsflächen erfolgte auf Basis hochaufgelöster GoogleEarth-Aufnahmen (Stand: Januar 2003). Insgesamt wurden 4400 Siedlungspolygone mit dem entsprechenden Vermerk zur Anzahl der in den einzelnen Polygonen enthaltenen Gebäude digitalisiert.

Alle GIS-bezogenen Arbeiten und Digitalisierungen erfolgten mit ArcGIS 9. Alle Datensätze wurden als ESRI Shapefiles (*point shapefiles* für Punkdatensätze, *polygon shapefiles* für flächenbezogene Datensätze, *polyline shapefiles* für Liniendatensätze) georeferenziert oder als Rasterdaten im ESRI-Format für generierte Reliefparameter in 45-m-Auflösung entsprechend der Auflösung des SRTM-DGMs abgelegt. Die Projektion der digitalisierten und generierten Daten ist UTM WGS 1984, Zone 49N und entspricht der Projektion der im Feld erhobenen Daten. Die Datensätze wurden auf dem Server in Gießen abgelegt und so allen beteiligten Wissenschaftlern zugänglich gemacht.

3.4 Parametrisierung der RUSLE

Auf der Landschafts- und Einzugsgebietsebene kann der Bodenabtrag durch Wassererosion quantitativ mit der etablierten und weltweit angewandten, empirischen *Universal Soil Loss Equation* USLE (WISCHMEIER und SMITH, 1965; RENARD ET AL., 1997) bzw. mit der überarbeiteten *Revised* USLE (RUSLE) modelliert und abgeschätzt werden. Die USLE wurde von WISCHMEIER und SMITH (1965) auf der Grundlage statistischer Analyseverfahren konzipiert. Die Untersuchungen stützen sich auf langjährige Messreihen von Bodenabträgen und Studien von ZINGG (1940) und MUSGRAVE (1947). Entwickelt wurde dieses empirische Modell für Bedingungen im Mittleren Westen der USA, aufbauend auf Untersuchungen auf Standardparzellen mit saatbettbereiter Schwarzbrache und 22,13 m Hanglänge und 9% Hangneigung. Infolge zahlreicher Anwendungen und räumlich-spezifischer Modifikationen (vgl. MCCOOL ET AL., 1987; EL-SWAIFY, 1997) eignet sich die USLE bzw. RUSLE auch und insbesondere für Gebiete mit geringer Datendichte und Datenauflösung wie es in China die Regel ist (vgl. SHI ET AL., 2004; LIU und LUO, 2005; XU ET AL., 2008, 2009; LI ET AL., 2010).

Abbildung 7 *Kartierte (1: 5.000) terrassierte Farmlandflächen (oben) und digitalisierte Terrassenflächen (unten) im Aufstaubereich des Einzugsgebiets des Xiangxi (oben). GIS und Layout von S. Schönbrodt.*

Unter Berücksichtigung der Erosivität des Niederschlags (*R*-Faktor), der Erodierbarkeit des Bodens (*K*-Faktor), der Topographie (*LS*-Faktor), der Bodenbearbeitung (*C*-Faktor) und des Erosionsschutzfaktors *P* lässt sich der langjährige, mittlere Bodenabtrag *A* pro Jahr mit folgender Gleichung errechnen:

$$A = R \times LS \times K \times C \times P \qquad (4.1)$$

mit:

A = langjähriger, mittlerer Bodenabtrag (t ha a^{-1})

R = Niederschlagserosivität (MJ mm^{-1} ha^{-1} a^{-1})

K = Bodenerodierbarkeit (t ha h ha^{-1} MJ^{-1} mm^{-1})

LS = Topographiefaktor (*L* = erosive Hanglänge; dimensionslos, *S* = Hangneigungsfaktor; dimensionslos)

C = Erosionswirksame Bodenoberfläche und Bodenbearbeitungsfaktor (dimensionslos)

P = Erosionsschutzfaktor (dimensionslos)

Die RUSLE arbeitet parametrisch und rasterbezogen und erlaubt somit die Integration fernerkundungsbasierter, flächenkonkreter Daten. Dies ermöglicht eine akzeptable Parametrisierung auch von schwer zugänglichen Gebieten bei Verfügbarkeit hochaufgelöster Eingangsdatensätze. Die RUSLE ermöglicht jedoch keine Aussagen zu den ablaufenden Erosionsprozessen und betrachtet infolge der statischen Parametrisierung keine dynamischen Abläufe. Diesen Umstand kann jedoch mit der Integration einer zeitlichen Komponente, z.B. durch eine Parametrisierung mit annuellen und/oder interannuellen Änderungen der Landnutzung begegnet werden. Für die Ausweisung von Erosionsrisikogebieten bzw. der Identifizierung der Gefährdung durch Erosion unter Berücksichtigung der langjährigen, mittleren Bodenabträge erlaubt die RUSLE insgesamt zufriedenstellende Aussagen. Zudem ermöglicht die RUSLE eine Bewertung von Managementpraktiken und Dimensionierung von Bodenschutzmaßnahmen (RENARD ET AL., 1997).

3.4.1 Niederschlagserosivität (*R*-Faktor)

Die Niederschlagserosivität (*R*-Faktor) in der RUSLE ist als kinetische Erosionsenergie des Niederschlags definiert (WISCHMEIER und SMITH, 1965) und berechnet sich als Produkt aus der kinetischen Energie eines Niederschlagsereignisses und seiner maximalen 30-minütigen Intensität. Da es für das Untersuchungsgebiet keinen Datensatz mit *R*-Faktoren gab, wurde dieser neu erstellt. Insgesamt lagen für sechs Klimastationen Daten zum Niederschlag vor (Abbildung 8 und Tabelle 2). Die Rohdaten wurden mittels Kolgomorov-Smirnov-Test, Standard-Normal-Homogenity-Test (ALEXANDERSON, 1986), Neumann-Ratio-Test, kumulativer Abweichungsanalyse und Bayesian procedures (BUISHAND, 1982) auf Homogenität und Normalverteilung getestet. Mit Ausnahme der Station Yichangxian (Abbildung 8) war die Qualität der Daten für alle Klimastationen ausreichend. Allerdings benötigt eine präzise, gebietsspezifische Berechnung des *R*-Faktors unter Berücksichtigung der Topographie im stark reliefierten Xiangxi-EZG einen räumlich hoch aufgelösten ereignisbezogenen Datensatz. Beide Bedingungen sind für das Xiangxi-EZG mit lediglich sechs bzw. nur fünf Stationen mit aufgezeichneten Tageswerten der Niederschlagshöhe nicht erfüllt.

Tabelle 2 *Geographische Position (Projektion UTM WGS 1984, Zone 49N), Höhenlage und Zeitraum der täglichen Niederschlagsaufzeichnungen für die sechs Klimastationen (H: Höhe über NN).*

Station	Rechtswert	Hochwert	H (m)	Aufzeichnungsperiode
Badong	442491	3437891	295	01.07.1952 - 31.12.2007
Shennongjia	469423	3512773	950	01.01.1975 - 31.12.2007
Xingshan	477772	3455484	275	01.01.1958 - 31.12.2007
Yichang	528850	3396689	134	01.08.1951 - 31.12.2007
Yichangxian	530978	3404291	116	01.01.2003 - 31.12.2007
Zigui	469765	3429644	151	01.04.1959 - 31.12.2007

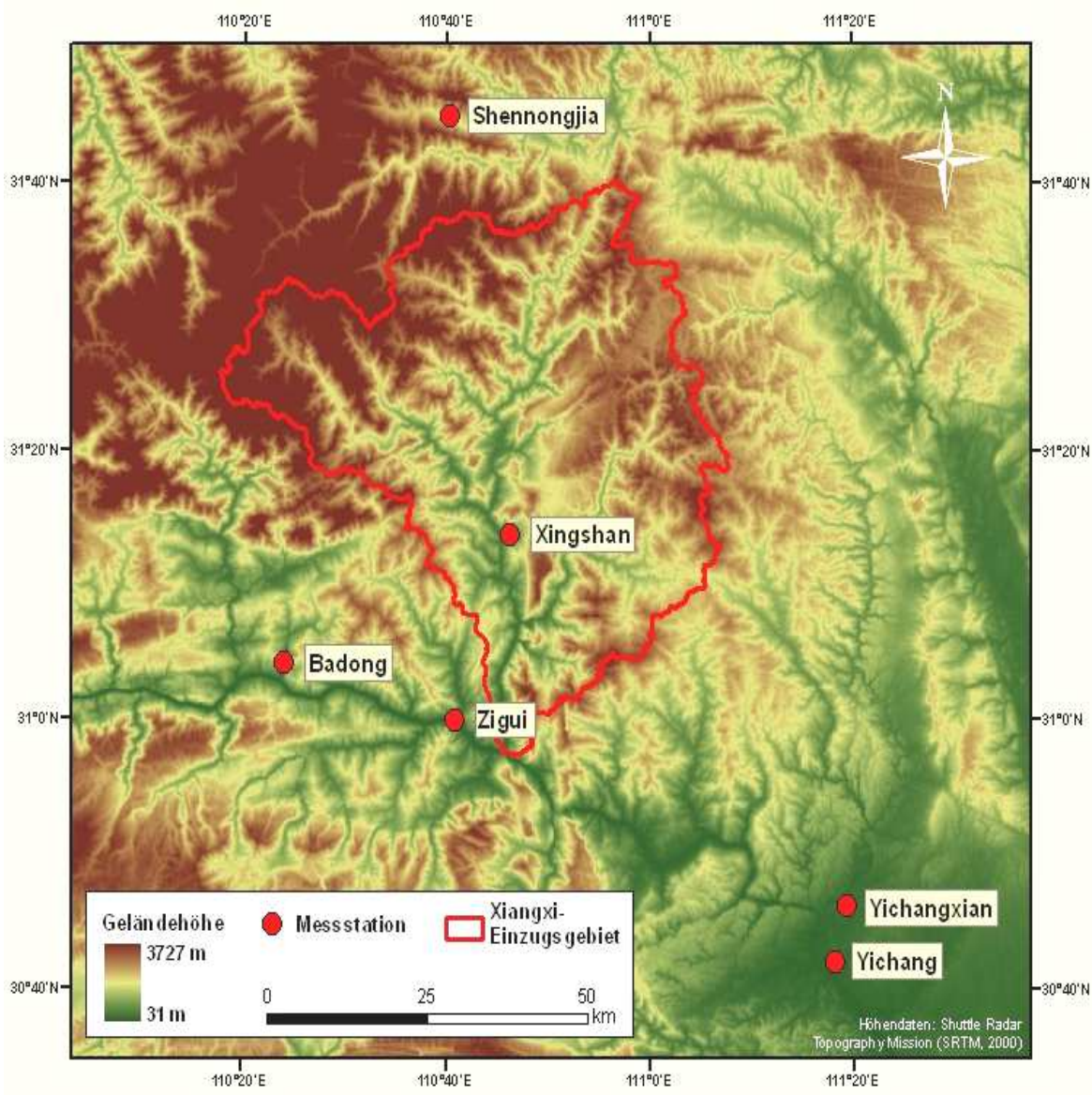

Abbildung 8 *Lage der Klimastationen Xingshan, Shennongjia und Zigui. GIS und Layout von A. Bosch und S. Schönbrodt.*

Alternativ können regressionsanalytische Annäherungsverfahren zur Ermittlung des *R*-Faktor verwendet werden, die auf Grund ihrer spezifisch regionalen oder maßstäblichen Ausrichtung in der Lage sind, die von der RUSLE geforderte Korrelation mit dem Bodenabtrag abzubilden (RENARD ET AL., 1994). Hierzu wurden verschiedene Verfahren getestet, wobei der Algorithmus nach MEN ET AL. (2008) für das Xiangxi-EZG sowie die mit GIS abgeleitete Isoerodenten die besten Ergebnisse zeigte und angewendet wurde. Die flächendeckende Extrapolation der Stationsdaten und die Isoerodentenkarte für das gesamte Xiangxi-EZG wurde mit einer höhenbasierten Regionalisierung (BOLINNE ET AL., 1980; MIKHAILOVA ET AL., 1997; WANG ET AL., 2002) erreicht. Als geeignet erwies sich eine vertikale Klimazonierung mittels *elevations bands* (GOOVAERTS, 1999).

3.4.2 Bodenerodierbarkeit (*K*-Faktor)

Die Berechnung der Bodenerodierbarkeit (*K*-Faktor der RUSLE) erfolgte anhand der digitalen Bodenkarte, basieren auf dem *2nd National Soil Survey* (SHI ET AL., 2010) in China. Basierend auf der digitalen Bodenkarte und den zugewiesenen Attributen wurden die vorhandenen Daten zur Korngrößenzusammensetzung mittels Transferfunktionen nach SHIRIZA (1984) in die spezifische Bodenerodierbarkeit umgerechnet. Die Auflösung des flächendeckenden Rasterdatensatzes beträgt 45 m. Des Weiteren wurden *K*-Faktoren aus den laboranalytisch ermittelten Daten zur Korngrößenzusammensetzung der Oberbodenproben nach WISCHMEIER und SMITH (1965) berechnet. Diese Daten wurden zur Validierung der Berechnungen nach SHIRAZI and BOERSMA (1984) auf Basis der Bodenkarte des Xiangxi-EZG verwendet.

3.4.3 Topographie (*LS*-Faktor)

Der Einfluss der Topographie auf den Bodenabtrag (*LS*-Faktor) berechnet sich aus der erosiven Hanglänge *L* und der erosiven Hangneigung *S* (WISCHMEIER und SMITH, 1965). Hohe Hangneigungen und zunehmende Hanglänge bewirken hohe Fließgeschwindigkeiten des Oberflächenabflusses und begünstigen stark dessen Abscher- und Transportkapazität. *L* und *S* wurden auf Basis der einzelnen Landnutzungsklassen, dem Hanglängenexponent, dem Verhältnis von Rillenerosion zu flächenhafter Erosion sowie dem Radians des Sinus der Hangneigung basierend auf dem SRTM-DGM in 45-m-Auflösung berechnet (RENARD ET AL., 1997). Dem *S*-Faktor liegt die Berechnung nach RENARD ET AL. (1997) und KONZ ET AL. (2009) für steil geneigte Gebiete zugrunde. Die Hangneigung wurde nach TARBOTON (1997) berechnet, der entgegen des in ArcGIS integrierten Algorithmus zur Berechnung der mittleren Hangneigung vom steilsten erosiven Wert ausgeht. Die Berechnung des *L*-Faktors erfolgte unter Berücksichtigung von Landnutzungsgrenzen schlagbezogen für jede einzelne Landnutzungsklasse auf Basis der Fließlänge mittels Monte-Carlo-Aggregation (BEHRENS ET AL., 2008). Durch Multiplikation der Rasterdatensätze ergibt sich der Topographiefaktor (kombinierter *LS*-Faktor).

3.4.4 Erosionswirksame Bodenoberfläche und Bodenbearbeitung (*C*-Faktor)

Der *C*-Faktor beschreibt das Verhältnis des Bodenabtrages bestimmter Fruchtarten oder Fruchtfolgen gegenüber dem Bodenabtrag unter Standardbedingungen. Die benötigten Informationen wurden mittels Fernerkundungsdaten und Literaturstudien erhoben. Als Kovariaten der Vegetation und damit der erosionswirksamen Bodenoberfläche wurde der *Normalized Differenced Vegetation Index* (NDVI) auf Basis von Landsat-TM-Daten (vgl. LILLESAND ET AL., 2007; BOETTINGER ET AL., 2008; SUN ET AL., 2008) verwendet. Als Funktion aus dem NDVI lässt die *Fractional Vegetation Cover* (FVC) Aussagen zur prozentualen Vegetationsbedeckung zu und dient bei Verwendung

räumlich-spezifischer Regressionsgleichungen als Grundlage zur Ableitung des dimensionslosen *C*-Faktors (BOETTINGER ET AL., 2008; ZHOU ET AL., 2008; SCHÖNBRODT ET AL., 2010b). Basierend auf drei Landsat-TM-Szenen von 2005, 2006, und 2007 wurde der Bodenbearbeitungsfaktor *C* auf Basis der FVC für das gesamte Xiangxi-EZG abgeleitet. Als Referenzwerte dienen die *C*-Faktoren aus der Literatur für das TGD-Gebiet (SCHÖNBRODT ET AL., 2010b). Diese sind 0,13 für Orangenhaine (SHI ET AL., 2004), 0,18 für Reisfelder (LIU und LUO, 2005), 0,46 für Trockenflächen (LIU und LUO, 2005), 0,1 für Gartenland (LIU und LUO, 2005), 0,08 für besiedelte Flächen mit kleinen Gärten (LIU und LUO, 2005) und 0,2 für Brache bzw. Gebiete mit geringer Vegetationsbedeckung (ERENCIN, 2000).

3.4.5 Erosionsschutz (*P*-Faktor)

Da zu Beginn der Untersuchungen keine Geländebefunde und Kartengrundlagen zur Berücksichtigung spezieller Schutzmaßnahmen, z.B. Terrassierung und Kontur- oder Streifennutzung, vorlagen, wurde mit der generalisierten Annahme gearbeitet, dass alle landwirtschaftlichen Nutzflächen im Xiangxi-EZG flächendeckend mit flachen Terrassenstufen auf Hängen von 20 bis 25° Neigung terrassiert sind. Der *P*-Faktor wurde auf einen Wert von 0,55 gesetzt (SHI ET AL., 2004).

3.5 Erosionsmodellierung

Neben den statischen Angaben zu Boden, Relief und Klima im Xiangxi-EZG wurde eine zeitliche Komponente in die Modellierung integriert. Diese Dynamisierung zielt auf die Analyse der Folgen der geänderten Landnutzung auf den potenziellen Bodenabtrag ab. Zur Modellparametrisierung wurden die Landnutzungsklassifikationen von 1987 und 2007 verwendet (SCHÖNBRODT ET AL., 2010b). Diese Zeitscheiben repräsentieren die post-konstruktive Phase des TGD (1987) und die Zeit nach seiner Errichtung und des Aufstau des Yangtze und seiner Nebenflüsse (2007).

Eine vergleichende Betrachtung des natürlichen Erosionspotenzials wurde für das nahegelegene Taipingxi-EZG vorgenommen (SHI ET AL., 2004). Der *R*-Faktor wurde hierzu auf 2880 MJ mm ha^{-1} h^{-1} a^{-1} und der Erosionsschutzfaktors *P* auf 0,55 gesetzt.

Die Modellierung der natürlichen Erosionsdisposition erfolgte unter der Annahme einer gleichmäßigen Bewaldung (Primärvegetation) sowie keines anthropogenen Einflusses und im Xiangxi-EZG. Der *C*-Faktor wurde auf 0,005 für Waldfläche (LIU und LUO, 2005) und der *P*-Faktor auf 1.

3.6 Konzeption und Parametrisierung von *TerraCE*

Die Bedeutung der Terrassen als erosionssteuernder Faktor wurde bereits in der Einleitung herausgestellt. Als prozessbestimmend hinsichtlich des Bodenabtrags zeigte sich bereits zu Projektbeginn der Zustand der in landwirtschaftlichen genutzten Bereichen überwiegend anzutreffenden Bankterrassen mit Trockensteinmauern. Die Kausalität zwischen der Auftretenshäufigkeit und Intensität des Bodenabtrags und dem Pflegezustand der Terrassen sowie dem reliefbeeinflussten Terrassendesign war offensichtlich. Vor diesem Hintergrund wurde das Terrassenzustandsmodel *TerraCE* (*Terrace Condition Erosion Model*) entwickelt. Das Modell basiert auf einen empirisch-konzeptionellen Ansatz und integriert sozioökonomische und reliefbasierte Parameter zur räumlich expliziten Vorhersage des Terrassenzustands (Abbildung 9). Es dient der Identifizierung der räumlichen Verteilung und Qualität von Bankterrassen basierend auf Felduntersuchungen und der räumlichen Quantifizierung der Steuerfaktoren des Terrassenzustands. *TerraCE* soll weiterhin klären, wie und warum das Ausmaß der Bodenerosion vom Zustand der Terrassen und mithin der landwirtschaftlichen Nutzflächen abhängt. Die Berechnungen zum Terrassenzustand wurden mit dem Data-Mining-Verfahren Random Forests (BREIMAN, 2001) durchgeführt. Random Forests ist ein Ensembleverfahren welches den CART-Entscheidungsbaumalgorithmus (BREIMAN ET AL., 1984) verwendet. Zur Anwendung kam das „Random Forest“ Paket (LIAW und WIENER, 2011) für 'R' als objektorientierte Statistiksprache (R DEVELOPMENT CORE TEAM, 2011).

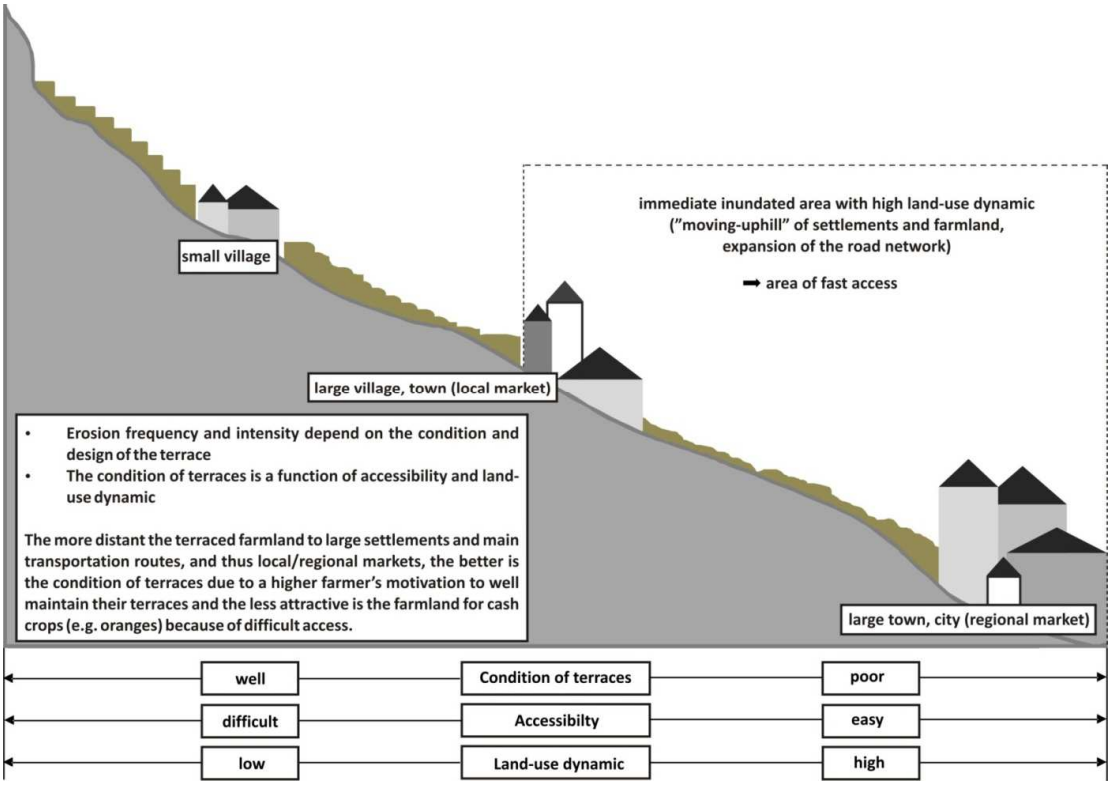

Abbildung 9 *Schematische Darstellung des konzeptionellen Terrassenzustandsmodells TerraCE für das Einzugsgebiet des Xiangxi. Layout von S. Schönbrodt.*

3.6.1 Erfassung des Terrassenzustandes

Für die Generierung eines ausreichenden großen Datensatzes für die Anwendung von Random Forest wurde zunächst ein Protokoll zur Dokumentation und Beschreibung von Terrassen in Anlehnung an BRANCUCCI und PALIAGA (2006), COMOLLI (2005) und SFONDRINI ET AL. (2005) entwickelt. Die Erfassung der Parameter zur Terrassengeometrie und zum Pflegezustand der Terrassen sowie die Erfassung der rezenten Bodenerosion auf den Terrassenflächen erfolgten anhand von Vermessungen und qualitativen Einschätzung im Gelände mit einem standardisierten Aufnahmebogens (Abbildung 10). Zunächst wurde die Terrasseneigenschaften im den Teileinzugsgebieten Xiangjiaba und Quyuan aufgenommen. Für die Kartierung wurden 158 Terrassen zufällig auf Grundlage der Landnutzungsklassifikation für 2007 mit einer Auflösung von 45 m (SEEBER ET AL., 2010) verwendet, wobei alle landwirtschaftlichen Nutzflächen berücksichtigt wurden. In einem zweiten Schritt wurde eine visuelle Fernaufnahme von 829 Flächen mit homogener Landnutzung und einer Mindestgröße von 45 × 45 m entlang des Xiangxi vom jeweils gegenüberliegenden Ufer durchgeführt (Abbildung 11). Der Vorteil dieses Verfahrens lag in der schnellen Erhebung eines umfangreichen Datensatzes. Räumlich konzentrierte sich die Arbeit im Aufstaubereich ausgehend von der Ortschaft Xiakou bis etwa 2 km nördlich der Mündung des Xiangxi in den Yangtze.

Data sheet for assessment of terrace condition for supported GIS-analysis

Qualitative and quantitative erosion inventory (45 m x 45 m)

ID: _____ Coordinates: X _____ Y _____ Size:_____ Photo ID:_____

Parameter \ ID	**A**	**B**	**C**
Wall: Height	m	m	m
Condition	☐well maintained ☐partially collapsed features:	☐badly maintained ☐collapsed	
Disorders	☐ bulge/upsetting _____ ☐ wall failure _____ ☐ collapsed _____		
Geometry: Land slope			
Terrace Slope	☐inward ☐outward _____ °	☐inward ☐outward _____ °	☐inward ☐outward _____ °
Width (slope length)	m	m	m
Length	m	m	m
Parallel Alignment	☐ YES ☐NO		
Landuse:	☐paddy field [11] ☐dry land (sesame) [12] ☐orchard (oranges) [21/22] ☐ _____	☐dry land (maize) [12] ☐ garden land [14] ☐ orchard/vegetable [23]	
Grass cover	_____%	_____%	_____%
Soil: Texture			
Stone cover	☐embedded ☐loose _____%	☐embedded ☐loose _____%	☐embedded ☐loose _____%
Erosion: Akkumulation	☐ YES ☐ NO		
Sheet erosion	☐wash down ☐micro rills (<2cm)		
Rill erosion	☐shallow rills ____ ☐deep rills ____ ☐gullies ____ due to: ☐ wall failure ☐ inflow ☐ other		
	average size: D _____cm W _____cm L _____m		
Run-off Disposal:	☐YES ☐NO ☐stone/concrete ☐soil ☐grass		

Comment:

Abbildung 10 *Protokoll zur Inventarisierung und Beschreibung von Terrassen im Einzugsgebiet des Xiangxi.*

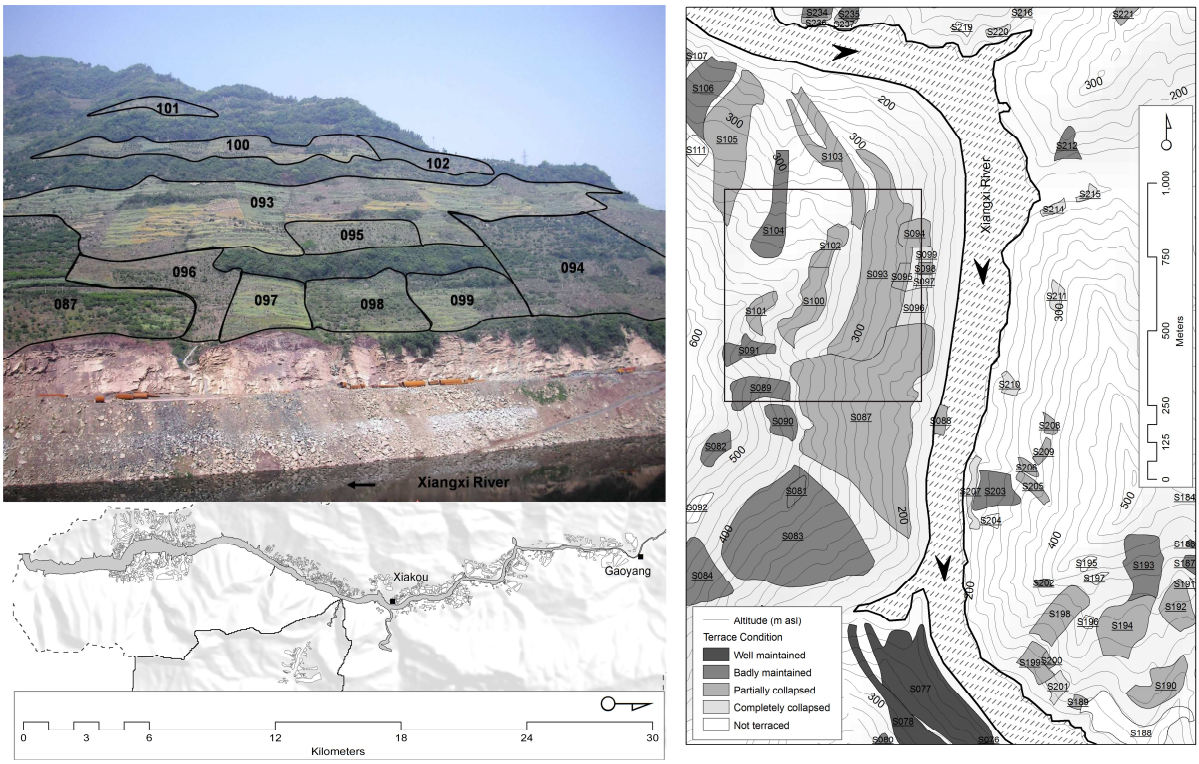

Abbildung 11 *Räumliche Ausdehnung des Kartiergebietes im südlichen Einzugsgebiet des Xiangxi für die Fernaufnahme von terrassierten Hangabschnitten mit homogener Landnutzung und einer Mindestgröße von 45 × 45 m entlang des Flusslaufs (links unten) und deren Einordnung in verschiedene Zustandskategorien (links oben) sowie digitalisierte Terrassengrenzen (rechts). GIS und Layout von S. Schönbrodt.*

3.6.2 Parametrisierung von *TerraCE*

TerraCE integriert reliefbasierte und sozioökonomische Parameter, die aus digitalen Höhenmodellen und Satellitenbildern abgeleitet werden können. Zur Beschreibung des Reliefs wurde ebenso wie für die RUSLE das SRTM-DGM in 45-m-Auflösung verwendet. Grundlage zur Ableitung der sozioökonomischen Parameter bilden die Digitalisierungen der Straßen und Siedlungsflächen anhand von GPS-Trackaufzeichnungen, SPOT-Bildern (5 m) und GoogleEarth-Daten.

Als Kovariablen für das Relief zur Bestimmung deren Einflusses auf die Terrassenzustände und deren räumlicher Verteilung wurden lokale und komplexe morphometrische Reliefparameter u.a. Geländehöhe, lokale Höhe (vgl. MACMILLAN ET AL., 2000; BEHRENS, 2003) steilste Hangneigung (TARBOTON, 1997), mittlere, minimale und maximale Hangwölbung (SHARY ET AL., 2001), relative Profilkrümmung (BEHRENS, 2003), relative horizontale Krümmung (KLEEFISCH und KÖTHE, 1993), topographische Rauhigkeit, Abweichung von der Exposition (*Aspect deviance*; um 0°, um 45°, um 90° und um 135°; BEHRENS ET AL., 2003 basierend auf HORN, 1981), projizierte Distanz zum Gewässernetz (vgl. BEHRENS, 2003), relative hemispherische Dispersion (HODGSON und GAILE, 1999), *Relative Richness* sowie *Waxing* und *Waning Slope* (HUBER, 1994) berechnet.

Zur Ermittlung des gegenseitigen Einflusses sich nicht überlagernder räumlicher Objekte wurde die Euklidische Distanz der relevanten, fernerkundungsbasierten anthropogenen bzw. sozioökonomischen abgeleitet. Die somit ermittelten distanztransformierten Indikatoren liefern eine komplette räumliche Abdeckung und damit wesentliche Grundlage für eine weitere GIS-basierte Prozessierung (Euklidische Distanz zu jedem relevanten, raumbezogenen Objekt als Pixel im Rasterdatensatz des Untersuchungsgebietes) und kombinierten Analyse und Visualisierung mit den rasterbasierten Reliefdaten als Proxy für den physiogeographischen Einfluss auf die variierenden Terrassenzustände.

Als sozioökonomische Kovariablen, die als Proxy zur Ermittlung des anthropogenen Einfluss auf die Terrassenzustände und deren räumliche Verteilung herangezogen wurden, dienten das Straßennetz, die Lage der Siedlungen, die Distanz zu den Flüssen und die Entfernung zur neuen Uferlinie des Xiangxi im Bereich des Aufstaus (SCHÖNBRODT-STITT ET AL., 2011; *under review*).

Das Straßennetz wurde in drei Klassen eingeteilt: asphaltierte Hauptstraßen, asphaltierte bzw. für Kraftfahrzeuge befahrbare Nebenstraßen und nicht befahrbare Pfade. Aufgrund der zeitlichen Aktualität der SPOT5-Szene vom September 2007 und der Trackaufzeichnungen während der Geländearbeiten bezieht sich das Straßennetz auf die gegenwärtige Situation nach der Flussaufstauung durch den Drei-Schluchten-Staudamm und die damit zusammenhängende Ausweitung der Infrastruktur. Zur Berechnung der distanztransformierten Kovariaten wurden nicht die einzelnen Klassen des klassifizierten Straßennetzes sondern deren Kombination betrachtet: (i) asphaltierte Hauptstraßen, (ii) asphaltierte Hauptstraßen und befahrbare Nebenstraßen und (iii) asphaltierte Hauptstraßen und befahrbare Nebenstraßen plus Pfade. Dieses Verfahren vermeidet Artefakte aufgrund einzelner, isolierter (Straßen-) Abschnitte und erlaubt die Berücksichtigung kontinuierlicher Veränderungen im Verkehrsfluss und der Verkehrsdichte.

Des Weiteren wurden insgesamt 4420 Siedlungspolygone in der *Backwater area* auf Basis der SPOT5-Szene und *GoogleEarth*-Bildern mit Raumbezug digitalisiert. Dabei entspricht ein Siedlungspolygon einer zusammenhängenden Anordnung von Gebäuden und Höfen mit einem jeweiligen Abstand von weniger als 100 m. Einzelne Gebäude bzw. Höfe mit einer Distanz von mehr als 100 m zum nächsten Gebäude wurden einzeln betrachtet. Die Siedlungspolygone wurden entsprechend ihrer Flächengröße in (i) Siedlungen von 0 bis 6 ha, (ii) Siedlungen von 6 bis 12 ha, (iii) Siedlungen von 12 bis 18 ha und (iv) Hauptzentren (Gaoyang mit 79 ha und Gufu mit 109 ha) gruppiert und vom Vektor- ins Rasterformat zur weiteren Generierung der distanztransformierten Indikatoren überführt. Die Siedlungen werden als lokale, regionale und zentrale Märkte mit hohem lokalen und regionalen Einfluss als Wirtschaftshandelsgebiete verstanden.

Im konzeptionellen *TerraCE*-Ansatz wird ebenfalls das Flussnetz berücksichtigt. Dabei wird dem Gewässernetz als schiffbares Verkehrsnetz die Bedeutung als soziökonomischer als auch als

reliefbasierter Indikator mit einem indirekten Einfluss auf den variierenden Terrassenzustand beigemessen. Das Flussnetz als Basis zur computergestützten Ableitung distanztransformierter Indikatoren wurde basierend auf dem DGM mittels D8-Fließakkumulation-Algorithmus berechnet und anschließend entsprechend der Fließgewässerordnung von STRAHLER (1957) klassifiziert. Analog zum Straßennetz wurde folgende Gruppierung zur Ableitung der distanztransformierten Indikatoren gewählt: (i) Fließgewässer der 1. Ordnung, (ii) Fließgewässer der 1. und 2. Ordnung, (iii) Fließgewässer der 1., 2. und 3. Ordnung, (iv) Fließgewässer der 1., 2., 3. und 4. Ordnung, (v) Fließgewässer der 1. bis 5. Ordnung, (vi) Fließgewässer der 1. bis 6. Ordnung und (vi) Fließgewässer der 1. bis 7. Ordnung. Zusätzlich wurde die Euklidische Distanz zur neuen Uferlinie des Xiangxi nach dessen Aufstauung als potenzieller Indikator für die Terrassenzustände abgeleitet.

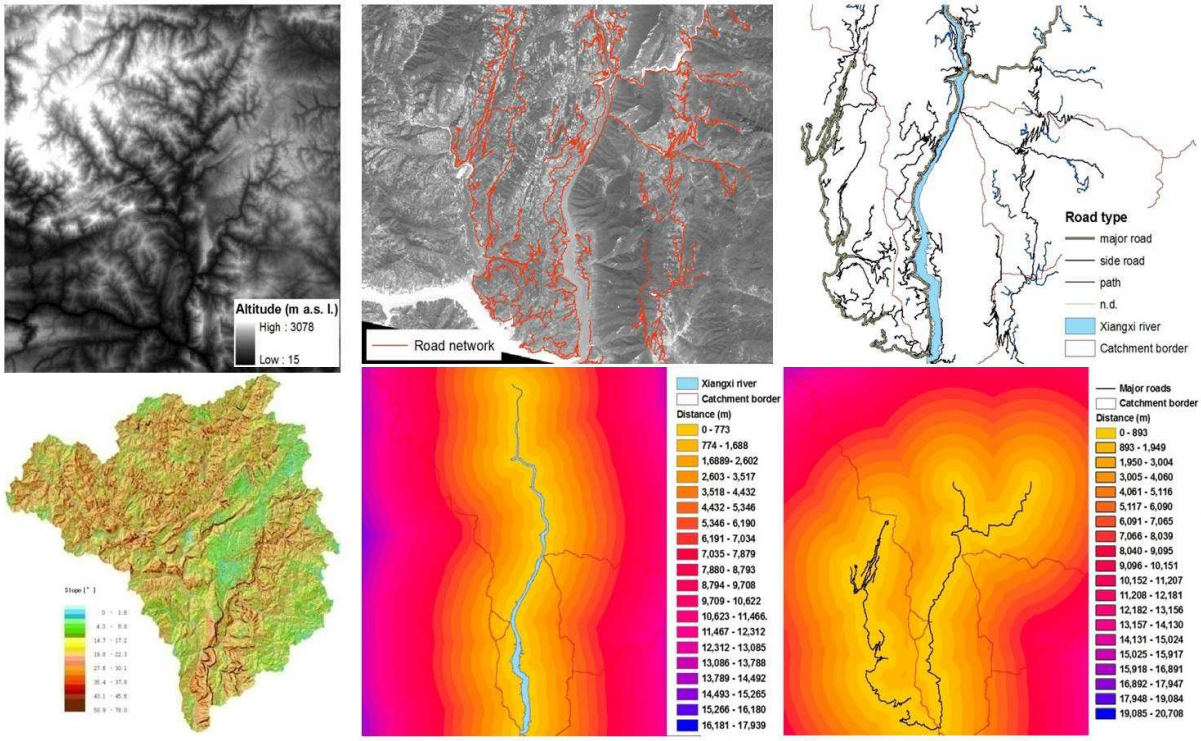

Abbildung 12 *GIS-basierte Ableitung von Kovariaten zur Parametrisierung von TerraCE basierend auf dem Digitalen Geländemodell und SPOT-Bildern (oben links: DGM des Xiangxi-Einzugsgebietes, unten links: steilste Hangneigung, oben Mitte: SPOT-Bild (5 m) mit Straßennetzwerk, unten Mitte: neue Uferlinie des Xiangxi nach Aufstau, unten Mitte: euklidische Distanzkarte für die Xiangxi-Uferlinie, unten rechts: euklidische Distanzkarte des Straßennetzes. GIS und Layout von S. Schönbrodt.*

3.6.3 Prognose des Terrassenzustands

Für die Feature-Importance-Analyse (Maß zum Einfluss einer Variable/Indikators) wurde die *Mean decrease in accuracy* (MDA) herangezogen. Diese berechnet sich aus den "*Out-of-Bag*"- (OOB) Daten. OOB ist diejenige Teilmenge der Daten, die in jeder Bootstrap- (Ladung der Daten)

Wiederholung in Random Forest herausgelassen wird. Zur Ermittlung der MDA wurde jede Variable an jedem Spalt eines Baumes in Random Forest zufällig permutiert und die Änderungsrate des Mittelquadratfehlers im Vergleich zur ursprünglichen Variable als Maß für seine Bedeutung herangezogen (BREIMAN, 2001; GRIMM ET AL., 2008). Da dieser Wert gegen die unabhängigen OOB-Daten geprüft wird, überschätzt dieser Wert nicht (PRASAD ET AL., 2006). Die *Feature Importance*-Analyse gibt ein Ranking des Einflusses der untersuchten Variablen anstelle einer Auswahl der Eigenschaften wieder. Aus diesem Grund wurden verschieden große Teilmengen getestet, um einen minimalen Satz von Eigenschaften, der für die Modellbildung erforderlich ist, abzuleiten. Aus diesem Grund wurden weiterhin die Rangfolgen der Einflüsse resultierend aus Regression und Klassifikation verglichen.

Die *Partial Dependence*-Analyse (Ermittlung der partiellen Abhängigkeit) untersucht dabei den marginalen Effekt einer Variable auf den Terrassenzustand unter Berücksichtigung des mittleren Einfluss aller Variablen im Modell (CUTLER ET AL., 2007; LIAW und WIENER, 2011). Eine Beschränkung infolge der Mittelwertbildung besteht darin, dass die *Partial Dependence*-Analyse nur relative Beziehungen und nicht exakte Werte wiedergibt. Die Darstellung der partiellen Abhängigkeit erfolgt als Graph. Die abgebildete Funktion beschreibt den Effekt der Antworten als kontinuierliche Funktion. Sie ist definiert als:

$$f' = \frac{1}{n}\sum_{i=1}^{n} f\,(x, x_{iC}) \tag{4.2}$$

wobei x die Variable (Terrassenzustand) ist für die die *Partial dependence* gesucht wird und x_{iC} die weiteren Einflussvariablen im Datensatz sind. Der Summand ist die prognostizierte Funktion der Regression (LIAW und WIENER, 2011).

Folglich erlaubt die *Partial dependence* eine einfache und direkte Interpretation der Effekte einer Variablen, die zum Modell beiträgt. Im Vergleich zur Korrelationsanalyse bei linearen Regressionen ermöglicht die *Partial dependence* des Random Forests-Verfahrens die Beschreibung nicht-linearer Einflüsse auf den Terrassenzustand. *Die Partial dependence* kann sowohl für Regressionen als auch für Klassifikationen berechnet werden. Untersucht wurden jedoch nur die Ergebnisse der Regressionsanalyse, da bei der Klassifikation jede Klasse einzeln betrachtet wird und die Beschreibung so unnötig komplex macht.

4 ERGEBNISSE

4.1 Rezente Erosion

Aktuelle On-site-Erosionserscheinungen konnten für jeden der 27 in 2008 untersuchten Standorte beobachtet werden (Abbildung 13). Mit einer Ausnahme zeichnen sich alle untersuchten Standorte durch mäßige Erosion (Erosionsklasse 2) bzw. mäßig bis starke (Erosionsklasse 3) und starke bzw. starke bis sehr starke Erosion (Erosionsklasse 4) aus. Aktuelle On-site-Erosionsschäden konnten auch in 2009 und 2010 für nahezu jeden der weiteren 218 untersuchten Standorte beobachtet werden. Insbesondere Verschlämmung (*Wash down*) und mehrheitlich Mikrorillen (< 2 mm) als Initialstadium linearer Tiefenabtragsformen traten auf jeder der untersuchten Flächen auf. *Gullies* (Abbildung 14) stellen jedoch eine seltene Ausnahme dar. Generell konnten bezüglich der kartierten, rezenten lineareren Abtragsformen und deren Häufigkeit dieselben Beobachtungen wie in 2008 gemacht werden. Sehr häufig anzutreffen waren demnach *wash down* und Mikrorinnen (< 2 cm Tiefe), sowie Rillen- und Rinnenerosion (> 2 cm Tiefe bzw. > 10 cm Tiefe).

Die linearen Abtragsformen treten in der Regel lokal konzentriert an steil geneigten Hängen in Form parallel zueinander verlaufend Rillen auf. Dort wo Hindernisse in Form von Geröll, größeren Gesteinskomponenten auf der Bodenoberfläche bzw. Störungen im Mikrorelief auftreten, werden die Parallelstrukturen durch Konvergenz-Divergenz-Strukturen und fächerartige lineare Strukturen ersetzt. Die erfassten On-site-Schäden lassen sich wie folgt kategorisieren:

- sehr häufig Initialstadium der Erosion (*Splash*, Mikrorinnen < 2 cm Tiefe),
- sehr häufig Rillenerosion (> 2 cm Tiefe),
- sehr häufig Rinnenerosion (> 10 cm Tiefe),
- selten Grabenerosion (*Gullies*, > 40 cm Tiefe),
- häufig Oberflächenspülung mit Profilverkürzung bzw. komplette Bloßlegung des Unterbodens stellenweise bis zum anstehenden Gestein und
- vereinzelt unter Orangen und Mais ausgespülte und freigelegte Pflanzenwurzeln.

Als Akkumulationsformen waren aufgehäufte Erdhügel auf der Luvseite kräftigerer Orangenstämme zu beobachten, sowie mit Bodenmaterial und Pflanzenresten zugespülte und verschlämmte Treppengänge, Ableitungskanäle auf den terrassierten Flächen und verschlämmte Trockensteinmauern. Größere Akkumulationen von Erosionsmaterial zeigten sich entlang der in die steilen Hänge eingeschnittenen Straßenläufe im südlichen Xiangxi-EZG.

4.2 Aktuelle Erosionsprozesse

Die Standorte mit in erster Linie reliefbedingtem Abtrag erstrecken sich vornehmlich entlang von Unter- und Mittelhängen in relativer Nähe zur neuen Uferlinie nach Aufstauung des TGD. Die

mittleren Hangneigungen der Flächen variieren zwischen 15 und 43° (Tabelle 3). Dort wo die Hänge sich durch ein starkes Mikrorelief auszeichneten, wurden innerhalb der Standorte stark variierende Neigungen zwischen 13° und 25° bzw. 25° und 36° ermittelt. Dabei handelt es sich meist um alte terrassierte Strukturen, die der jeweiligen Hangform angepasst wurden.

Abbildung 13 *Lineare Formen der Tiefenerosion im Einzugsgebiet des Xiangxi: Mikrorinne auf Fläche E_10 (links), Erosionsgully auf Fläche E_26 (Mitte) und sehr starke Rinnenerosion auf Fläche E_7 (rechts). Fotos aufgenommen von S. Schönbrodt (09/2008).*

Abbildung 14 *Grabenerosion auf schluffig-tonigen Untergrund bei variierenden Hangneigungen: Gullies auf einem für den Anbau von Orangen genutzten, nicht terrassierten Standorts ohne Unterwuchs im südlichen Teileinzugsgebiet Xiangjiaba (links) und Gullies auf einem ungenutzten Standort im zentralen Teileinzugsgebiet Quyuan (rechts). Fotos aufgenommen von S. Schönbrodt (03/2010, 04/2010).*

Die in situ Ansprache der zumeist kalkfreien bis kalkarmen Oberböden ergab zu 70% schwach tonige Lehme bzw. sandig-tonige Lehme. Seltener wurden lehmige Tone und schwach sandige Lehme und schwach sandige Tone angetroffen. Die stark zur Verschlämmung neigenden Oberböden zeichnen

sich oftmals durch einen sehr geringen Grad der Bodenbedeckung aus. Rund 30% bzw. 40% der untersuchten Standorte wiesen einen Anteil des Steingehalts auf der Bodenoberfläche in Form zumeist lose als Streu aufliegender Grobkomponenten von 5-15% bzw. 15-40% auf. Selten überstieg die Steinbedeckung 80%.

Ein weiterer zentraler erosionssteuernder Prozess im Xiangxi-EZG ist die Art der Landnutzung. Im Aufstauungsbereich um Gaoyang und Xiakou und im Teileinzugsgebiet Xiangjiaba (vgl. Abbildungen 1 und 2) am westlichen Xiangxi-Ufer dominiert großflächig Orangenanbau, zumeist terrassiert. Großflächiger Maisanbau konzentriert sich im Zentrum des Xiangxi-EZGs, z.B. auf der Hochfläche bei Huang Liang Ping, sowie im zentralen Beriech des Teileinzugsgebiet Quyuan. Deutlich geringere Flächenanteile wurden von Tee und Tabak bestanden, deren großflächige Kultivierung auf die Regionen um Huang Liang Ping, Zhenzi, Shu Kong Ping und Jie im Norden und Nordwesten des Xiangxi-EZG (Abbildung 15) begrenzt war.

Auf Basis dieser Ergebnisse wurden funktionale landwirtschaftliche Nutzungsgruppen ausgewiesen, die sich im Hinblick auf ihre Erosionswirksamkeit deutlich voneinander unterscheiden. Die funktionalen Gruppen wurden unterteilt in solche, die typisch für Plantagennutzung sind, und solche, die überwiegend als Gartenland zur Selbstversorgung und für lokale Märkte dienen (Tabelle 4).

Tabelle 3 *Merkmale (Art) funktionaler landwirtschaftliche Nutzungsgruppen untergliedert in Plantagen (P1 bis P6) und Gartenland (G1 bis G6) zur Selbstversorgung.*

Art	Plantage	Art	Gartenland
P1	Großflächiger Anbau mit einer dominierenden Frucht	G1	Anbau verschiedener Kulturen, selten nur eine dominierende Anbaufrucht
P2	Kultivierung überwiegend terrassiert	G2	Kultivierung sowohl terrassiert als auch nicht terrassiert
P3	marktorientierter Anbau (c*ash crop*)	G3	kleinbäuerlicher Anbau für Selbstversorgung
P4	nicht unmittelbar an Siedlungsstruktur gebunden	G4	Anbauflächen in Hof -oder Siedlungsnähe
P5	Zwischenfruchtanbau möglich	G5	meist Kultivierung von Zwischenfrucht
P6	Anbau von (a) immergrünen, mehrjährigen Orangen (und Tee) sowie (b) einjährigem	G6	Anbau von Gemüse (Sesam, Chili, Kürbis, Kräutern, Soja etc.) im Wechsel auch mit

Eine bodennahe Vegetationsbedeckung mit Gräsern und/oder Kräutern wurde ausschließlich an zwei Standorten beobachtet. Diese sind weitgehend frei von Erosionserscheinungen. Es kann ein enger Zusammenhang zwischen dem Grad der Bodenbedeckung und der Auftretenshäufigkeit und Intensität des Bodenabtrags angenommen werden (u.a. HUDSON, 1981). Auf Standorten mit fehlender

bzw. sehr geringer Bodenbedeckung (geringer Mulchfaktor, geringer Steinfaktor) wurde dementsprechend in der Regel stärkerer Bodenabtrag festgestellt (Erosionsklassen 3 und 4; Tabelle 4).

Ebenfalls prozessbestimmend ist der Terrassenzustand. Die Kausalität zwischen der Auftretenshäufigkeit und Intensität des Bodenabtrags und dem Pflegezustand der Terrassen war offensichtlich und scheint in dem stark reliefierten Xiangxi-EZG einer der zentralen Steuergrößen zu sein. Entsprechend wurden in 2008 erste Daten zum Terrassendesign und dem Terrassenzustand erhoben. Die Ergebnisse zeigen, dass dort wo Störungen der Terrassen, z.B. eingestürzte und/oder verschlämmte Terrassenwände, und/oder an die lokale Reliefsituation unangepasstes ingenieurtechnische Terrassendesigns auftreten, deutlich höherer Bodenabtrag und Oberflächenabfluss anzutreffen sind, als bei gut gepflegten Terrassen (Abbildung 15).

Abbildung 15 *Terrassendesign und Erosionsschäden im Einzugsgebiet des Xiangxi. Parallel verlaufende Level bed-Terrassen im guten Zustand in Huang Liang Ping, Fläche E_5 (links) und durch Bodenerosion zerstörte Trockensteinmauern auf einer Terrasse im Teileinzugsgebiet Xiangjiaba, Fläche E_21 (rechts). Fotos aufgenommen von S. Schönbrodt (09/2008).*

4.3 Bodenverbreitung

Acht Hauptbodentypen können im Xiangxi-EZG hinsichtlich ihrer Relevanz für die Bodenerosion und die hydrologische Modellierung unterschieden werden (Abbildung 16). Die Nomenklatur orientiert sich an der *Chinese Soil Taxonomic Classification* (CSTC, SHI ET AL., 2010), die vor allem auf die landwirtschaftliche Nutzung der Böden zielt und sich auf die traditionelle Namensgebung der Farmer stützt. Subtypen werden aufgrund von diagnostischen bodengenetischen Merkmalen zugewiesen.

In den höher gelegenen Bereichen bilden sich typischerweise unter Nadelwaldbedingungen auf kalkfreien Ausgangsgestein saure Braunerden vergesellschaftet mit Podsolen (CSTC: *Brown Soils*, Subtypen: *Mountainous brown soil, Mountainous brown soil-like-soil*). Sie erstecken sich gürtelartig oberhalb der humosen Braunerden (CSTC: *Dark Brown Soils*) sowie im Osten des Xiangxi-EZGs und zeigen eine stark saure Bodenreaktion bei geringer Basensättigung. Mit weniger als 7% gehören die *Brown Soils* im Xiangxi-EZG zu den gering verbreiteten Bodentypen.

Tabelle 4 *Kenngrößen des Erosionsfaktors Landnutzung gegliedert nach funktionalen Landnutzungsgruppen für die 27 in 2008 untersuchten Standorte. Dargestellt ist die dominierende Landnutzung. Dort wo keine Benennung des Terrassenzustands erfolgt, entspricht die Anbautechnik einer entlang der Kontur verlaufenden Kultivierung auf nicht terrassierten Standorten (LNG: Landnutzungsgruppe, HN: Hangneigung in °, LN: Landnutzung, ZwiFr: Zwischenfrucht, BB: Bodenbedeckung, TZ: Terrassenzustand, EK: Erosionsklasse, BB, TZ, EK: Klassen 1 bis 5 mit 1=sehr gering, sehr schlecht, sehr hoch bis 5= sehr dicht, sehr gut, sehr gering).*

LNG	Ort	HN	LN	ZwiFr	BB	TZ	EK
Plantage	E_2	18	Orange	Ja	2	2-3	2-3
	E_3	24	Orange	Ja	3	2-3	3
	E_4	13-25	Mais	Ja	3-4	3	2
	E_5	16-18	Mais	Ja	2-3	4	2
	E_8	10-12	Orange	Ja	1-2	-	2-3
	E_9	17-22	Mais	Ja	3	1	4
	E_10	28-31	Tabak	Nein	3	1-2	2
	E_11	15	Orange	Nein	2	4	2
	E_12	43	Orange	Nein	-	2	3
	E_13	26-32	Orange	Ja	3-4	1-2	4
	E_14	22-24	Tee	Nein	2	3	3-4
	E_16	33	Orange	Ja	5	4	1
	E_17	29-31	Orange	Nein	4	2-3	2
	E_20	19	Orange	Nein	5	5	3-4
	E_24	27	Orange	Nein	-	2-3	4
	E_26	23-25	Orange	Nein	1	-	4
Gartenland	E_1	34	Orange	Ja	2-3	2	2
	E_6	10-12	Orange	Ja	2	-	3
	E_7	18-20	Mais	Ja	4	2	4
	E_15	23-25	Gem.	Ja	5	4	2
	E_18	24	Mais	Ja	3-4	3	2-3
	E_21	24-32	Keine	Ja	2	2	2
	E_22	29	Keine	Ja	2-3	4	4
	E_23	27	Mais	Ja	1	1-2	3
	E_25	32	Mais	Ja	3	1-2	4
	E_27	33	Orange	Ja	3	1-2	2-3
Brache	E_19	29-36	keine	Ja	2-3	4	2-3

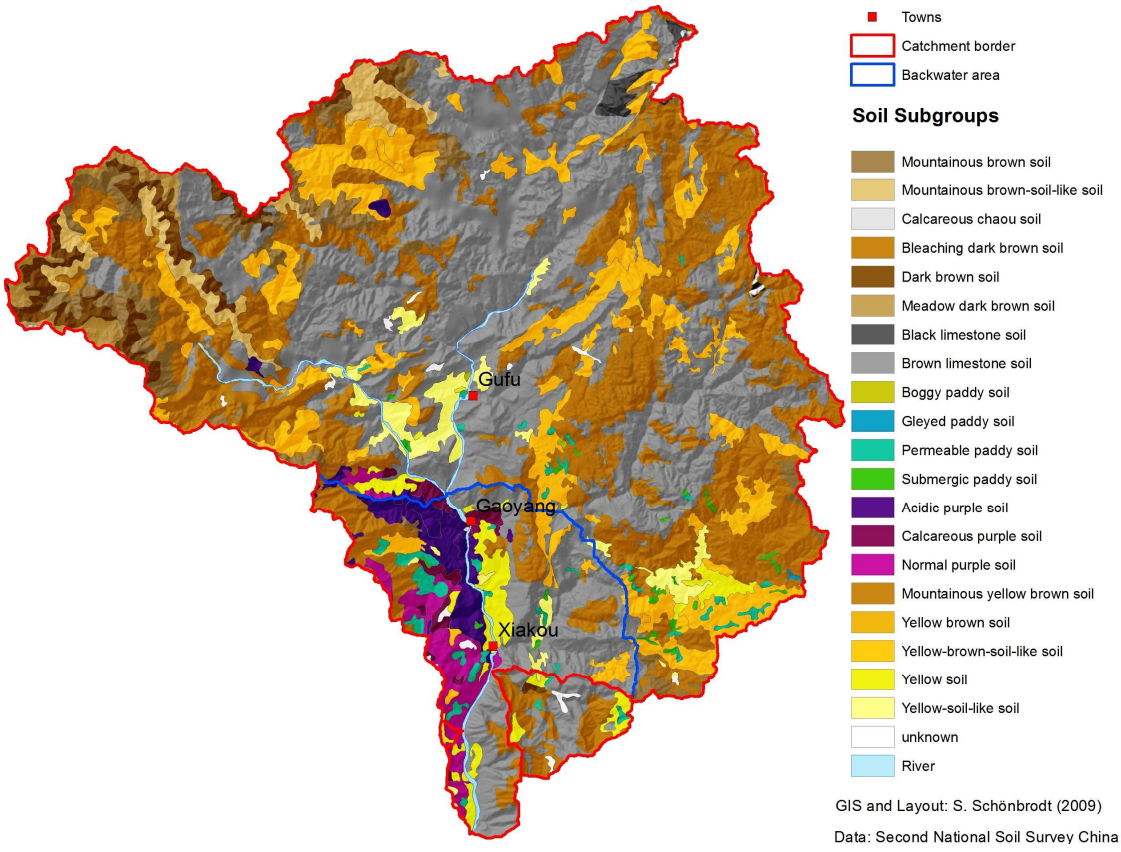

Abbildung 16 *Verbreitung der Hauptbodentypen im Einzugsgebiet des Xiangxi (Bezeichnung der Bodentypen nach Chinese Soil Taxonomic Classification).*

Humose Braunerden (CSTC: *Dark Brown Soil*, Subtypen: *Bleaching dark brown soil*, *Dark brown soil*, *Meadow dark brown soil*) bilden sich unter ganzjährig humid-temperierten Monsunklima. Sie sind durch eine hohe Solumsmächtigkeit, hohe Basensättigung und eine Bodenreaktion im neutralen bis alkalischen Bereich gekennzeichnet. In China sind sie typische Böden der Gebirgsregionen und bilden ideale Standorte für gut wüchsige Waldgebiete. Ihr Verbreitungsgebiet wird daher auch als *Dark brown forest soil belt* bezeichnet. Mit einem Flächenanteil von fast 4% beschränkt sich ihre Verbreitung im Xiangxi-EZG ausschließlich auf die hochgelegenen (2200-3000 m) Gebirgsregion in Landkreis Shennongjia.

Die fersialitischen sauren Böden der nördlichen Subtropen (CSTC: *Yellow brown soil*, Subtypen: *Mountainous yellow brown soil*, *Yellow brown soil*, *Yellow brown soil-like-soil*) sind entlang des Yangtze-Mittellaufs typischer Weise in den Mittelgebirgen und hügeligen Regionen beidseitig des Yangtze anzutreffen. In Abhängigkeit vom Ausgangsgestein und der Nutzung variieren die *Yellow Brown Soils* in ihrer Solummächtigkeit stark. Bei Reis- und Weizenanbau sind zwei Ernten pro Jahr möglich. Im Xiangxi-EZG gehören sie mit einem Flächenanteil von 40% neben Rendzinen, Regosole und kalkreichen humosen Braunerden zu den dominierenden Bodentypen. Ihr Hauptverbreitungsgebiet liegt im Osten und Nordosten, im Nordwesten sowie im zentralen Teil des

Untersuchungsgebiets. Auf etwa zwei Dritteln der Fläche überwiegen die *Mountainous yellow brown soils*, insbesondere in höheren Lagen. In der Regel sehr tonreiche fersialitische saure Böden (CSTC: *Yellow Soil*, Subtypen: *Yellow soil, Yellow soil-like-soil*) kommen auf etwa 4% der Flächen des Xiangxi-EZG vor. Sie haben ihr Hauptverbreitungsgebiet im Aufstaubereich sowie im zentralen und östlichen Teil des Untersuchungsgebiets. In China gelten sie als typische Böden der tropischen und subtropischen Gebirgsregionen (HONG und CHEN, 1990).

Flachgründigen Rendzinen, Regosole und kalkreiche humose Braunerden aus Kalkstein, Dolomit und andere Karbonatgesteine (CSTC: *Limestone Soil*, Subtypen: *Black limestone soil*, *Brown limestone soil*) sind mit 38% der Fläche charakteristisch für weite Teile des Untersuchungsgebiets. Sie reagieren im neutralen bis mittel alkalischen Bereich. Im Aufstaubereich sind sie ausschließlich auf der östlichen Uferseite des Xiangxi anzutreffen, geprägt durch die steil einfallenden Schichten der Trias. Zu fast 100% dominieren hier die *Brown limestone soils* deutlich. In höheren weniger geneigten Bereichen wird u.a. Raps kultiviert.

Reisböden (CSTC: *Paddy Soil*, Subtypen: *Boggy paddy soil*, *Gleyed paddy soil*, *Permeable paddy soil*, *Submergic paddy soil*) als einer der Hauptbodentypen der landwirtschaftlichen Nutzflächen im subtropischen China sind im Untersuchungsgebiet eher untypisch und lediglich auf 2% der Fläche verbreitet. Durch künstliche Landeinebnung und Terrassierung sowie saisonale Bewässerung weisen sie charakteristische Veränderungen in ihren hydrothermischen Regime und typische Oxidations- und Reduktionsprozesse auf. Im Xiangxi-EZG überwiegt ihre Verbreitung auf verstreuten Standorten im gesamten Aufstaubereich, vornehmlich im südöstlichen Teil.

Die schluffreichen *Purple Soils* (CSTC: *Purple Soil*, Subtypen: *Acidic purple soil*, *Calcareous purple soil*, *Normal purple soil*) sind im Untersuchungsgebiet typischerweise als Regosols ausgebildet, die sich hauptsächlich in den niedrigeren Höhenlagen auf hämatitreichen sandigen Schiefern und Sandstein (*purple sandy shale, purple s*andstone) sowie schluffigen Jurakalken ausgebildet haben. In den Unterhangbereichen zeichnen sich die erosionsanfälligen *Purple Soils* durch eine größere Entwicklungstiefe aus als auf den Mittel- und Oberhängen. Die Bodenfruchtbarkeit der *Purple Soils* ist hoch, sie gelten neben den Reisböden als fruchtbarste Böden der Region. Mit etwa 5% Flächenanteil ist ihre Verbreitung im Xiangxi-EZG auf das jurassisch geprägte westliche Xiangxi-Ufer im Aufstaubereich, vor allem im Teileinzugsgebiet Xiangjiaba, beschränkt. Innerhalb der Gruppe der *Purple Soils* dominieren die *Acidic purple soil* (45%) und die *Normal purple soils* (40%).

Die oben aufgeführten Erläuterungen zu den Hauptbodengruppen im Xiangxi-EZG orientieren sich neben den geländebefunden auch am bodenkundlichen Standardwerk „*Soils of China*“ von HONG und CHEN (1990). Aufgrund der stark auf die agrarische Bedeutung der Böden orientierten Klassifizierung lassen sich die Böden nur unter hohen Informationsverlust in den Standard des internationalen Klassifikationssystems *World Reference Base for Soil Resources* 2007 der FAO

überführen (SHI ET AL., 2010). Bezüglich ihrer geomorphologischen Position und ihres Ausgangsgesteins lassen sich die Böden im Xiangxi-EZG grob den Luvisols, Alisols, Cambisols, Regosols, Leptosols, Fluvisols und Gleysols (WRB, 2007) zuordnen.

4.4 Erosionsrisikopotenzial im Einzugsgebiet des Xiangxi

4.4.1 Erosivität der Niederschläge

Unter Berücksichtigung der höhendifferenzierten Klimazonierung im Xiangxi-EZG wurden die *R*-Faktoren nach MEN ET AL. (2008) anhand von Tageswerten des Niederschlags berechnet und Isoerodenten (Linien gleicher Niederschlagserosivität) abgeleitet (Abbildung 17). Die *R*-Faktoren variieren zwischen 1973,9 und 7258,2 MJ mm ha^{-1} h^{-1} a^{-1} und weisen eine sehr hohe Erosivität aus. Die räumliche Verteilung der *R*-Faktoren reflektiert deutlich die einzelnen Höhenstufen. Mit zunehmender Höhe steigt die Niederschlagserosivität. Vergleichbare Werte wurden auch für die ebenfalls in der TGD-Region gelegenen, klimatisch sowie topographisch vergleichbaren Einzugsgebiete Taipingxi mit 4969 MJ mm ha^{-1} h^{-1} a^{-1} (LIU und LUO, 2005) und Wangjiaqiao mit 2880 MJ mm ha^{-1} h^{-1} a^{-1} (SHI ET AL., 2004) berichtet.

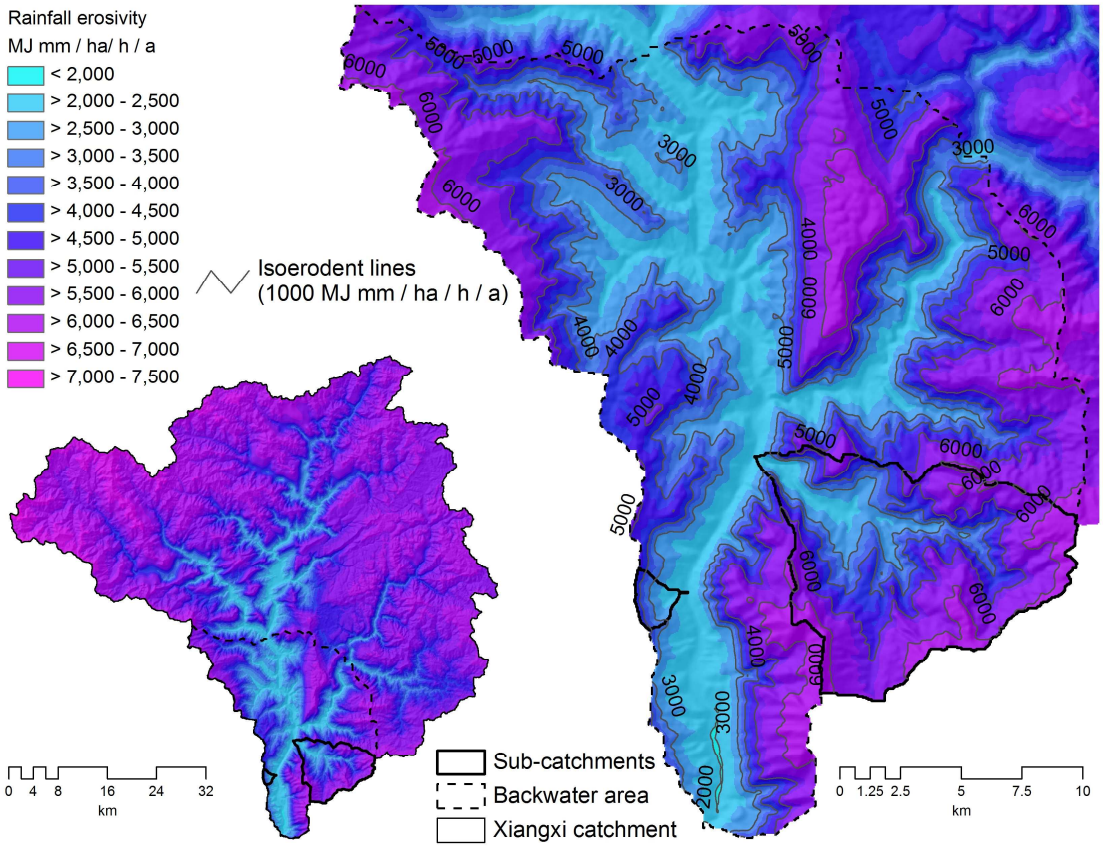

Abbildung 17 *Niederschlagserosivität und Isoerodenten im Aufstaubereich des Xiangxi-Einzugsgebiets (alle Angaben in MJ mm ha^{-1} h^{-1} a^{-1}). GIS und Layout von S. Schönbrodt.*

4.4.2 Erodierbarkeit der Boden

Die Erosionsanfälligkeit der Böden wird in starkem Maße durch ihre Textur bestimmt. Die Korngrößenzusammensetzung der Oberbodenproben (Abbildung 18) bewegt sich im Bereich der Normallehme (Ls2, Ls3, Lt2), Tonschluffe (Lu, Ut4) und Schlufftone (Lt3, Tu3, Tu4) sowie seltener im Bereich der Lehmsande (Sl3), Lehmtone (Tu2, Tl) und Lehmschluffe (Ut2, Ut3, Uls) an. Insgesamt dominieren schluffige Böden. Deutliche Unterschiede zwischen terrassierten und nicht terrassierten Standorten sind nicht feststellbar.

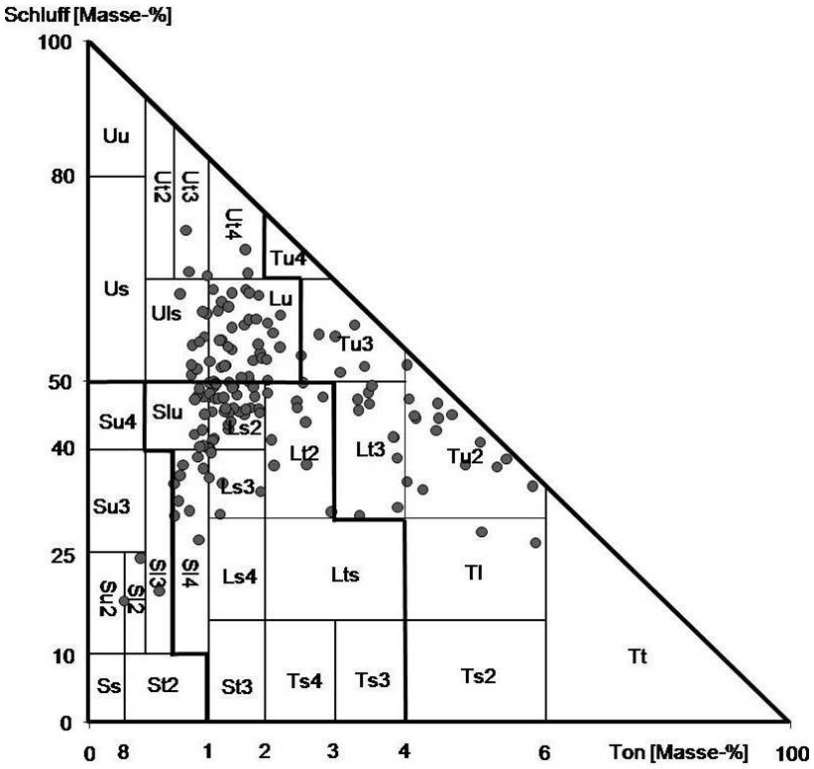

Abbildung 18 *Korngrößenverteilung im Einzugsgebiet des Xiangxi.*

Die Erodierbarkeit der Oberböden wurde nach drei verschiedenen Verfahren berechnet: (i) für das Gesamtgebiet auf Basis der Bodenkarte mit der Transferfunktion nach SHIRIZA (1984; Abbildung 19), die in China landesweit angewendet wird, (ii) für die im Gelände entnommenen und analysierten 245 Oberbodenproben nach den Empfehlungen für die RUSLE (RENARD ET AL., 1997) und (iii) wie (ii) jedoch unter zusätzlicher Berücksichtigung der organischen Substanz. Die Unterschiede zwischen allen drei Verfahren sind gering. Wir können annehmen, dass die Ableitung der *K*-Faktoren aus der Bodenkarte für die Erosionsmodellierung plausible Werte liefert. Infolge der engen Bodenarten-verteilung sind die Wertespannen insgesamt gering. Sie betragen für (i) 0,37 bis 0,40 t ha h ha^{-1} MJ^{-1} mm^{-1}, für (ii) 0,25 bis 0,37 t ha h ha^{-1} MJ^{-1} mm^{-1}, und für (iii) 0,26 bis 0,42 t ha h ha^{-1} MJ^{-1} mm^{-1}. Dies entspricht nach KA5 (Ad-hoc-AG Boden, 2005) eine mittleren (0,2 bis < 0,3

t ha h ha^{-1} MJ^{-1} mm^{-1}) bis hohen (0,3 bis < 0,5 t ha h ha^{-1} MJ^{-1} mm^{-1}) Disposition der Böden gegenüber Wassererosion. Verfahrensbedingt ist die Erodierbarkeit des Oberbodens sind eng an die Verbreitung der Bodentypen im Xiangxi-EZG gekoppelt. Insbesondere im westlichen Teil des Aufstaubereichs weisen die *Purple Soils* aus Jurakalken hohe Erodierbarkeiten auf (Abbildung 19). Die geringste Suszeptibilität der Oberböden gegenüber Wassererosion zeigen die *Yellow Soils* und *Limestone Soils*.

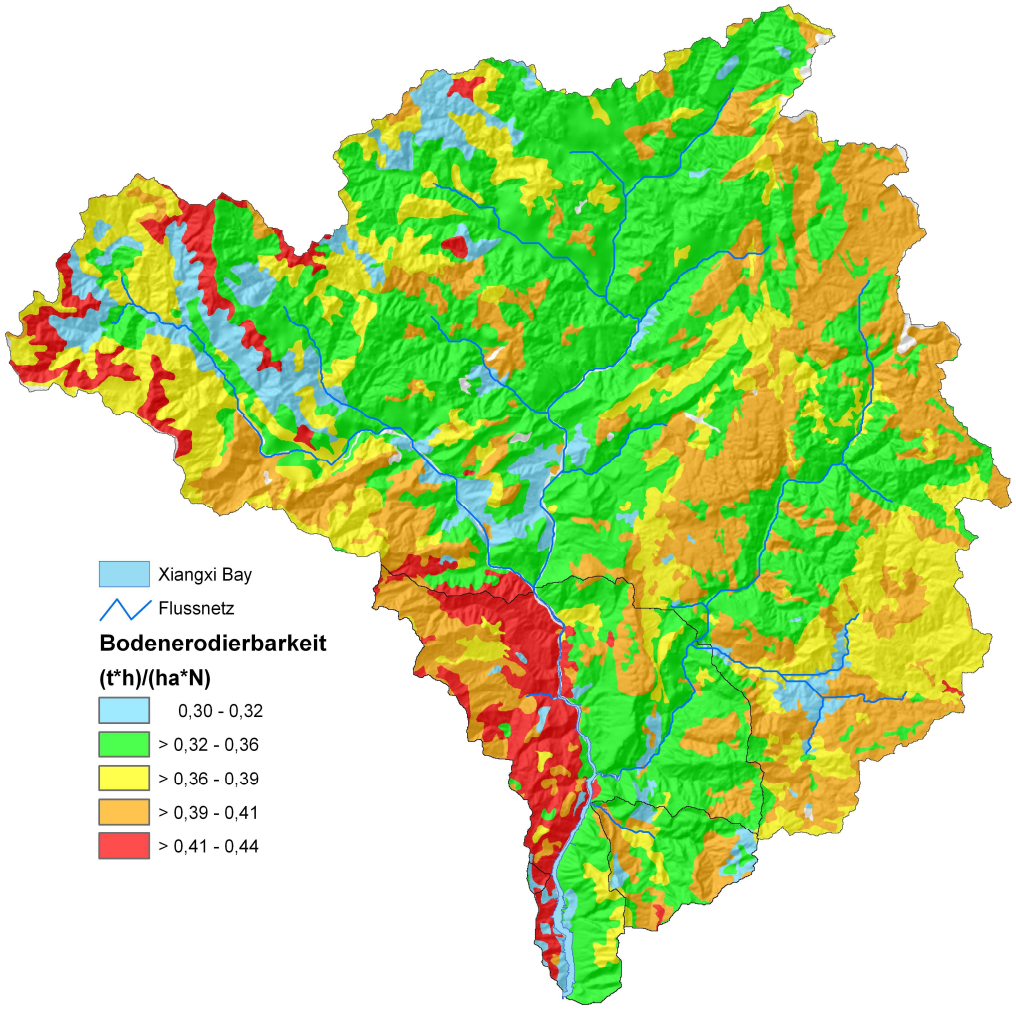

Abbildung 19 *K-Faktoren der Oberböden für das Einzugsgebiet des Xiangxi, abgeleitet aus der Bodenkarte (räumliche Auflösung: 45 m). GIS und Layout von S. Schönbrodt.*

4.4.3 Einfluss der Topographie

Entsprechend der hochgebirgsartigen Topographie im Untersuchungsgebiet werden insgesamt sehr hohe Hangneigungsfaktoren erreicht (Abbildung 20). Für extrem steil geneigte Hänge mit einer maximalen Hangneigung von 78° erreichen der *S*-Faktoren Werte bis 15,7. Typisch für die Gegend um Xiakou sind Hangabschnitte, die bei Nichtberücksichtigung der Terrassierung sehr hohe erosive Hanglängen bis zu 760 m aufweisen (Abbildung 21).

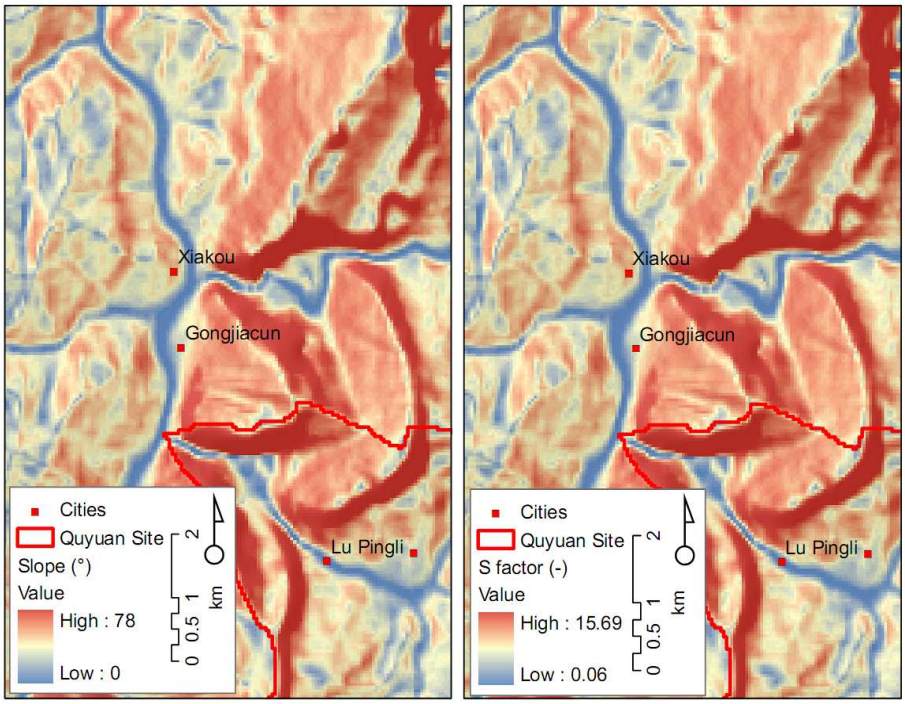

Abbildung 20 *Steilste erosive Hangneigung (links) und Hangneigungsfaktor S (rechts) für die Umgebung von Xiakou im Aufstaubereich im südlichen Einzugsgebiet des Xiangxi Hangneigung in Grad (°) berechnet auf Basis des SRTM-DGM für 45-m-Auflösung nach* TARBOTON *(1997). S-Faktor (dimensionslos) berechnet nach* RENARD ET AL., *(1997). GIS und Layout von S. Schönbrodt.*

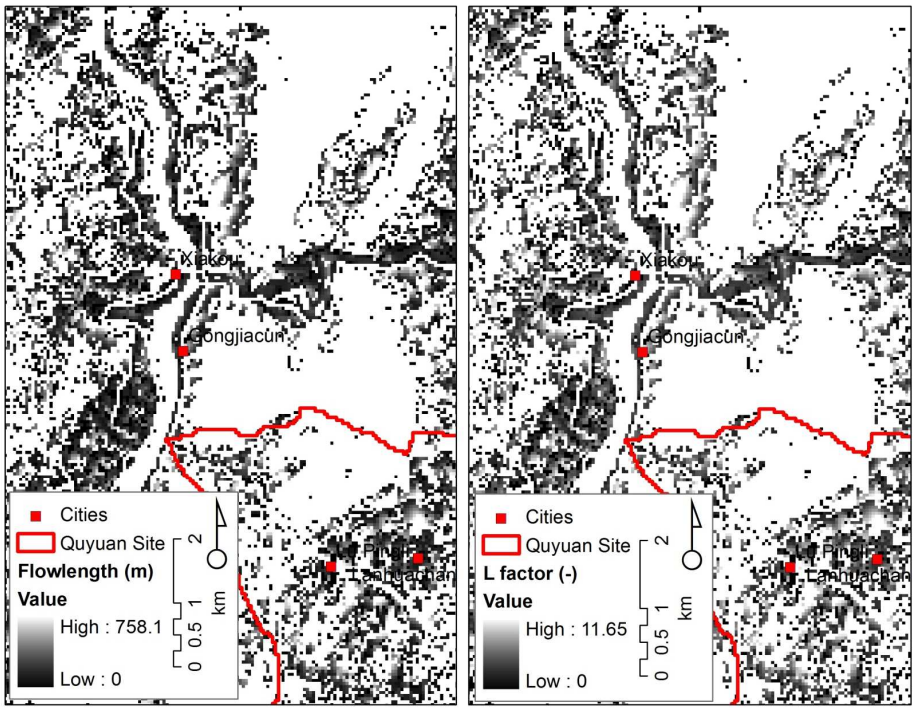

Abbildung 21 *Hanglänge (links) und Hanglängenfaktor L (rechts) für die Umgebung von Xiakou im Aufstaubereich im südlichen Einzugsgebiet des Xiangxi. Hanglänge in m berechnet auf Basis des SRTM-DGM für 45-m-Auflösung. L-Faktor (dimensionslos) abgeleitet mittels Monte-Carlo-Aggregation nach* BEHRENS ET AL. *(2008). GIS und Layout von S. Schönbrodt.*

4.4.4 Bodenbedeckung und Bodenbearbeitung

Die NDVIs der Landsat-TM-Daten jeweils für September der Jahre 2005, 2006 und 2007 zeigen insgesamt nur geringe Unterschiede (Abbildung 22, links). Hohe Werte charakterisieren das nördliche, westliche und östliche Xiangxi-EZG, wo großflächig bewaldeten Gebiete vorherrschen. Niedrige NDVIs charakterisieren vor allem die Flussläufe, an denen zumeist Straßen und Wege entlangführen und Schotterflächen verbreitet sind. Ebenso weisen die Siedlungsflächen um Gufu, Gaoyang und Xiakou niedrige NDVIs auf. Der Aufstaubereich und die beiden Teileinzugsgebiete zeigen ein sehr differenzierteres Bild hinsichtlich der Vegetationsbedeckung. Sehr geringe NDVIs charakterisieren vor allem die landwirtschaftlich genutzten Flächen östlich des Xiangxi. NDVI-Werte von annähernd -1 sind typisch für die engen und schmalen Täler im Teileinzugsgebiet Quyuan.

Die Werte des FVC reichen im gesamten Xiangxi-EZG von 0 bis 100% und entsprechen der räumlichen des NDVIs (Abbildung 22, links und Mitte). Hohe Werte zwischen 90 und 100% sind typisch für die bewaldeten Gebiete im Norden des Untersuchungsgebietes. In der Nähe der Flussläufe nimmt die FVC um 10 bis 20% ab. FVC-Werte von 70 bis 80% charakterisieren weite Bereiche des Aufstaubereichs und der Teileinzugsgebieten Xiangxiaba und Quyuan. Extrem geringe Werte des FVC (< 10%) bis sehr geringe FVC-Werte (10-20%) sind typisch für das Reservoir und die größeren Orte Gufu und Gaoyang. Moderate FVC (30-60%) sind typisch für die Gebiete in der Nähe von Siedlungen und entlang des Xiangxi im Aufstaubereich.

Die *C*-Faktoren der RUSLE (Abbildung 22, rechts) erreichen Werte bis 0,87 für September 2005, über 0,93 für September 2006 und bis 0,98 für September 2007. Diese hohen *C*-Faktoren, die gleichbedeutend mit einer geringen Erosionsschutzwirksamkeit der Bodenoberfläche sind, gelten vor allem für die moderate bis sehr geringe Vegetationsbedeckung im Aufstaubereich. Im Mittel liegen die *C*-Faktoren zwischen 0,04 und 0,05. Hier spiegelt sich vor allem der Einfluss der großen Waldflächen im Norden des Xiangxi-EZGs wider.

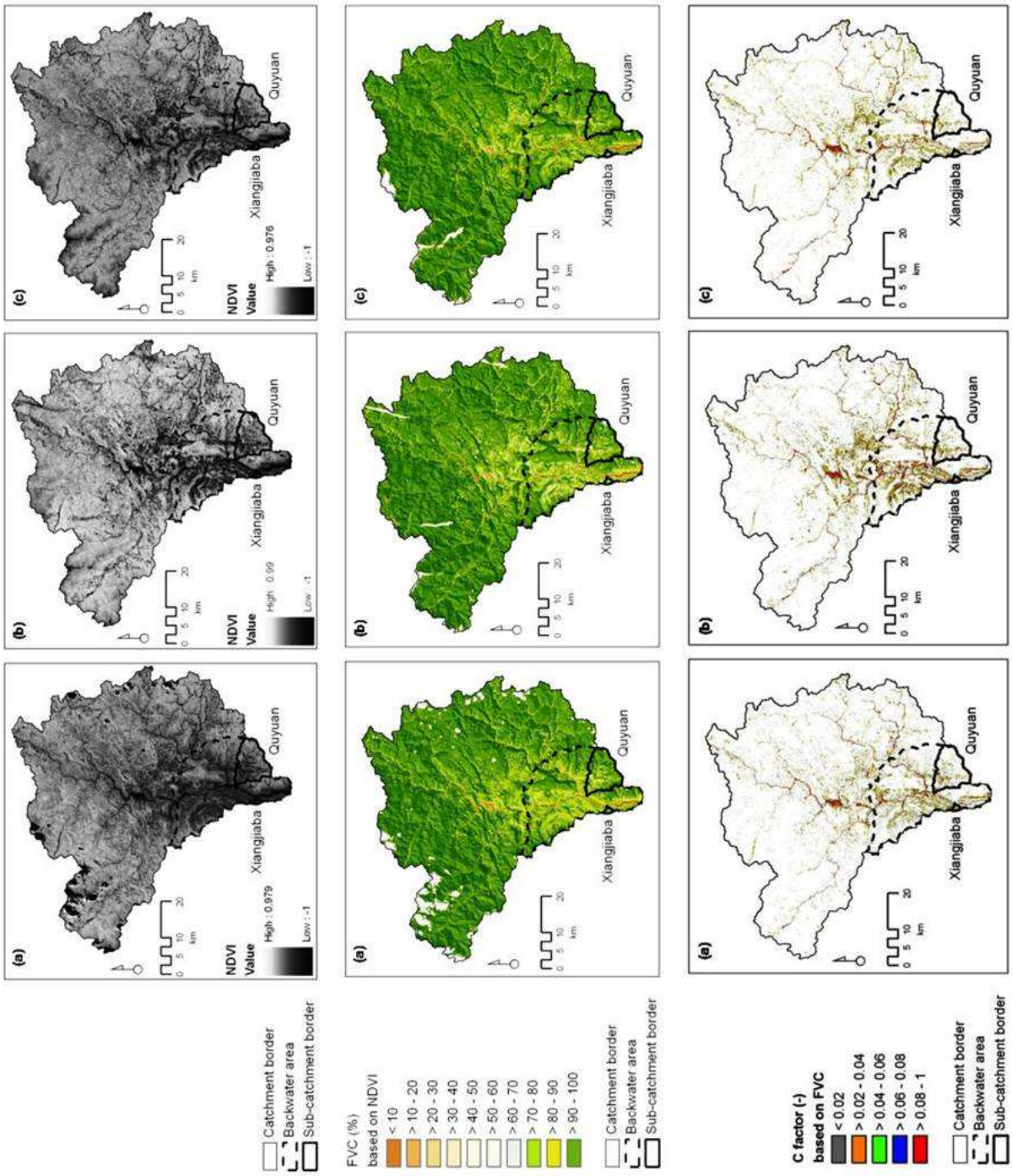

Abbildung 22 *Vergleichende multitemporale Darstellung des Normalized Differenced Vegetation Index (NDVI, links), der Fractional Vegetation Cover (FVC, Mitte) und des C-Faktors der RUSLE (rechts) im Einzugsgebiet des Xiangxi basierend auf Landsat-TM-Szenen für (a) September 2005, (b) September 2006 und (c) September 2007 (nach SCHÖNBRODT ET AL., 2010b).*

4.4.5 Natürliche Erosionsdisposition und Erosionspotenzial unter Berücksichtigung des Landnutzungswandels

Im Mittel variieren die langjährigen, potenziellen Bodenabträge im Xiangxi-EZG, berechnet als natürliche Erosionsdisposition bei vollständiger Bedeckung mit Primärwald, zwischen 6 und 11 t ha^{-1} a^{-1}. Um ein Vielfaches höher sind die potenziellen Bodenabträge unter Berücksichtigung der Landnutzung für 1987 und 2007. Im Mittel werden potenzielle langjährige Bodenabtrag in Höhe von 100 t ha^{-1} a^{-1} erreicht. Interessanterweise wirkt die Landnutzung in 2007 im Vergleich zu 1987 erosionsmindernd. Deutlich wird der erosionsreduzierende Einfluss der Landnutzung in 2007 vor allem bei Betrachtung der Maxima (Tabelle 5). In den Teileinzugsgebieten Xiangjiaba und Quyuan verringern sich die Maxima von 1987 auf 2007 um knapp 300 bis 400 t ha^{-1} a^{-1}. Unabhängig vom betrachteten Zeitraum ist das Erosionsrisiko im Teileinzugsgebiet Quyuan sehr hoch. Infolge der hohen Reliefenergie liegen die potenziellen Bodenabträge dort im Mittel liegen deutlich höher als im gesamten Xiangxi-EZG sowie im Aufstaubereich.

Tabelle 5 *Natürliche Erosionsdisposition (NED) und potenzieller langjähriger Bodenabtrag (t ha^{-1} a^{-1}) unter Berücksichtigung der Landnutzung in 1987 und 2007 für das gesamte Einzugsgebiet des Xiangxi, den Aufstaubereich und die Teileinzugsbiete Quyuan und Xiangjiaba (SD: Standardabweichung).*

	NED (t ha^{-1} a^{-1})	Nutzung 1987 (t ha^{-1} a^{-1})	Nutzung 2007 (t ha^{-1} a^{-1})
Xiangxi-EZG			
Maximum	146,4	5.264,6	5.057,9
Minimum	0,0	0,0	0,0
Mittelwert	10,3	263,8	188,3
SD	8,9	332,2	260,6
Aufstaubereich			
Maximum	104,2	3.898,0	3.812,3
Minimum	0,0	0,0	0,0
Mittelwert	9,6	256,5	169,3
SD	9,0	306,9	227,2
Quyuan			
Maximum	69,4	2.673,2	2.256,9
Minimum	0,0	0,0	0,0
Mittelwert	10,7	344,9	229,3
SD	9,0	376,2	283,2
Xiangjiaba			
Maximum	24,7	1.232,9	945,1
Minimum	0,0	0,0	0,0
Mittelwert	5,9	245,5	128,2
SD	4,8	230,0	142,1

Die modellierten potenziellen Bodenabträge für die Abfolge der Jahre 2005, 2006 und 2007 (Tabelle 6) zeigen für das Xiangxi-EZG und den Aufstaubereich eine deutliche Zunahme von 23 bzw. 29%. In den Teileinzugsgebiete Quyuan und Xiangjiaba sind die Bodenabträge in 2007 ebenfalls deutlich höher als in 2005 (6 bzw. 25%), folgen allerdings keinem linearen Trend sondern zeigen vielmehr deutliche Schwankungen zwischen den Jahren. Landnutzungsänderungen auf einzelnen Flächen oder Teilbereichen wirken sich hier offensichtlich aufgrund der geringen Gebietsgrößen stärker aus als ein mehrjähriger Trend.

Tabelle 6 *Potenzieller langjähriger Bodenabtrag (t ha^{-1} a^{-1}) im Einzugsgebiet des Xiangxi, im Aufstaubereich und in den Teileinzugsgebieten Xiangjiaba und Quyuan für die Jahre 2005, 2006 und 2007 (nach SCHÖNBRODT ET AL., 2010b).*

	2005	2006	2007
Xiangxi-EZG			
Minimum	0,0	0,0	0,0
Maximum	1.133,4	1.498,2	1.646,9
Mittelwert	9,3	11,0	11,5
Standardabweichung	21,9	26,0	28,8
Aufstaubereich			
Minimum	0,0	0,0	0,0
Maximum	607,1	708,6	873,6
Mittelwert	11,0	13,6	14,2
Standardabweichung	23,5	24,5	28,3
Quyuan			
Minimum	0,0	0,0	0,0
Maximum	385,7	180,3	285,6
Mittelwert	10,4	9,1	11,1
Standardabweichung	18,6	14,8	18,9
Xiangjiaba			
Minimum	0,0	0,0	0,0
Maximum	66,7	99,3	109,6
Mittelwert	11,7	16,3	14,6
Standardabweichung	13,1	19,5	16,6

Gebiete mit hohem bis extrem hohem Erosionspotenzial lassen sich aus der Modellierung der natürlichen Erosionsdisposition identifizieren. Diese erstrecken sich im Xiangxi-EZG kleinflächig entlang der steilen Hangbereiche der triassischen Felsformationen westlich des Xiangxi. Eine geringe bis moderate natürliche Erosionsdisposition charakterisiert den Aufstaubereich (Abbildung 23a). Unter Hinzunahme der Landnutzung und der Annahme einer flächendeckenden Terrassierung des Aufstaubereichs zeigt sich ein stärker differenziertes Bild des langjährigen mittleren Bodenabtrags (Abbildung 23b und 23c). Sowohl in 1987 als auch in 2007 lassen sich *Hot Spots* der Bodenerosion deutlich entlang des Unterlaufs des Xiangxi und vor allem auf dessen westlicher Uferseite identifizieren. Vor

der Errichtung des TGD (1987) lag der mittlere Bodenabtrag bei 257 t ha^{-1} a^{-1} (Tabelle 5) deutlich über dem in 2007 nach der Errichtung des TGD (169 t ha^{-1} a^{-1}). Dies geht einher mit dem Rückgang von Ackerland zugunsten von Orangenhainen und kleineren Waldparzellen, ausgelöst durch staatlicher Förderprogramme. Ein geringes Erosionsrisiko weisen vereinzelte Flächen auf den hochgelegenen Mittelgebirgsrücken auf. Dieses kann zum einen auf die staatlich gesteuerte Umwandlung von Ackerland in Wald sowie dem vermehrten Brachfallen von Flächen zurückgeführt werden.

4.5 Zustand und räumliche Verteilung von Terrassen im Einzugsgebiet des Xiangxi

Bei den untersuchten Terrassen handelt es sich um Bankterrassen mit, angepasst an die Reliefsituation, hangparallel angelegten Trockensteinmauern. Diese Art der Terrassierung ist typisch für den Yangtze-Mittellauf. Im Hinblick auf ihre Erosionsschutzwirksamkeit wurden die Terrassen in vier Kategorien gegliedert (Abbildung 24 und 25): *well maintained*, *fairly maintained*, *partially collapsed* und *completely collapsed*. Entsprechend der physischen Ausstattung gegeben durch das Terrassendesign und den Pflegezustand der Terrassen zeichnen sich die vier Klassen durch eine abnehmende Schutzwirksamkeit gegenüber Oberflächenabfluss und Wassererosion aus.

4.5.1 Terrassenzustand

Die im Hinblick auf den Erosionsschutz effektivste Terrassenzustandskategorie *well maintained* macht 21% der kartierten Terrassen aus. Die ursprüngliche künstliche Zergliederung des Hanges in Abschnitte geringerer erosiver Hanglänge ist noch vollständig erhalten (Abbildung 24). Leichte Störungen in den Trockensteinmauern kennzeichnen die Terrassen der Zustandskategorie *fairly maintained*, angetroffen in 44% der kartierten Fälle. An Mauerdurchbrüchen zeigen sich häufig Anzeichen von Rillen- und seltener Rinnenerosion. Die Erosionsschutzfunktion der Terrassen ist nach wie vor erhalten. Dieses ändert sich deutlich in den Klassen *partially collapsed* (23%) und *completely collapsed* (11%), die zusammen etwa ein Drittel aller kartierten Terrassen ausmachen. Während Terrassen der Klasse *partially collapsed* stellenweise noch die ursprünglichen Trockensteinmauern aufweisen, sind diese bei den Terrassen der Klasse *completely collapsed* zerstört (Abbildung 24). Damit stellt sich die ursprüngliche erosive Hanglänge nahezu wieder her und die Effektivität der Terrassen als Erosionsschutz geht gegen Null (SCHÖNBRODT-STITT ET AL., 2011; *under review*).

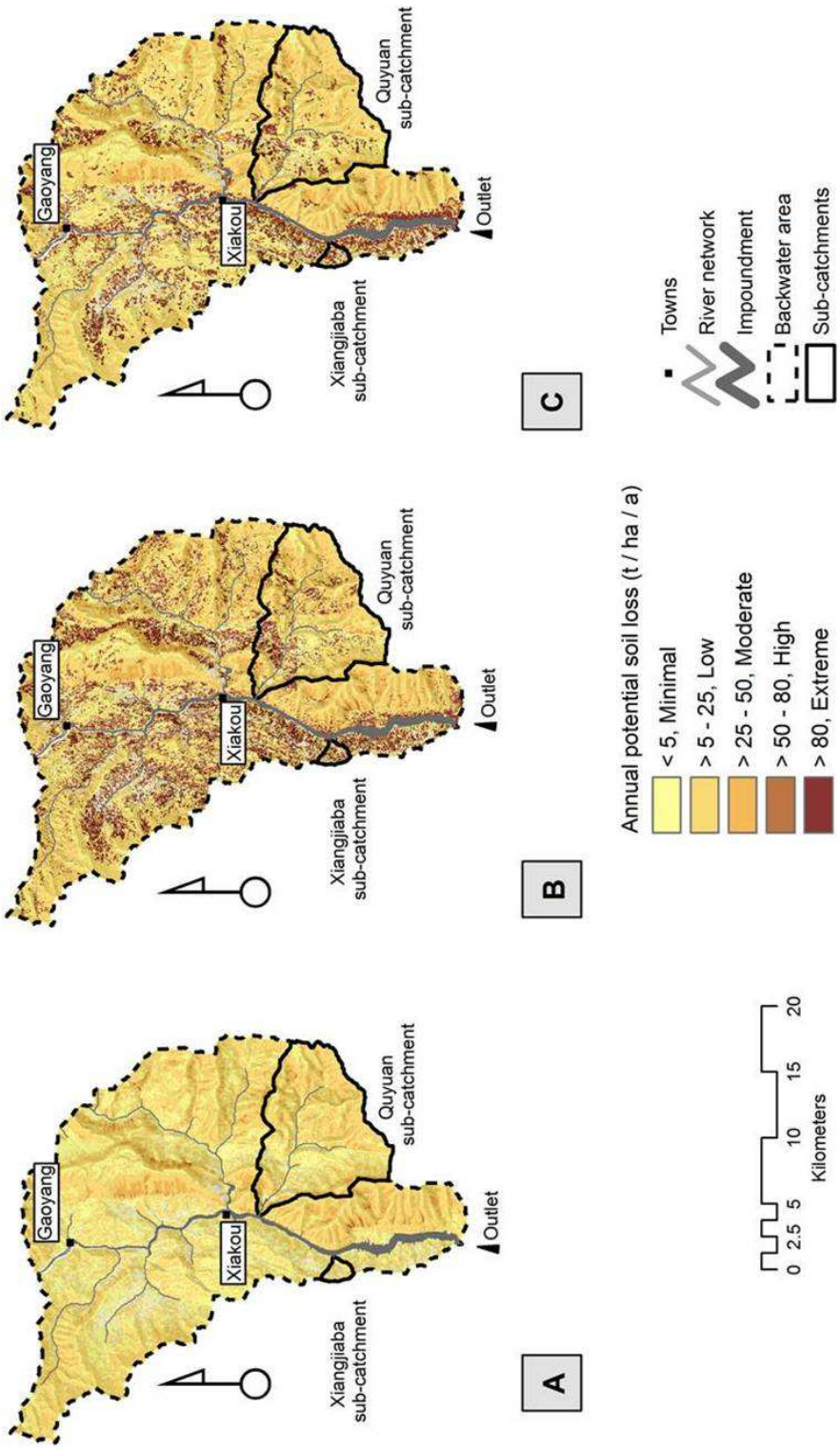

Abbildung 23 *Potenzieller langjähriger Bodenabtrag (t ha^{-1} a^{-1}) unter natürlichen Bedingungen (A) sowie unter Berücksichtigung der Landnutzung von 1987 (B) und 2007 (C) für den Aufstaubereich im südlichen Einzugsgebiet des Xiangxi. Die Klassifikation des modellierten mittleren Bodenabtrag entspricht dem Technological Standard of Soil and Water Conservation SD238-87 des Ministeriums für Wasserressourcen in China (vgl. LU und HIGGITT, 2000; XU ET AL., 2008; XU ET AL., 2009). GIS und Layout von S. Schönbrodt.*

Für die Erosionsschutzfunktion der Terrassen spielt neben dem Terrassenzustand, in erster Linie angezeigt durch Schäden an den Natursteinmauern, das Terrassendesign eine wichtige Rolle. Es lässt sich anhand der Parameter Neigung der Terrassenstufe, Hintergrundneigung bzw. ursprüngliche Hangneigung, Höhe der Trockensteinmauern und Breite der Terrassenstufe differenzieren (Tabelle 7). Während Terrassen der Klasse *well maintained* relative geringe Neigungen des Terrassenbettes aufweisen und sich mehrheitlich auf Hängen mit 20° Hintergrundneigung lokalisieren lassen (Abbildung 25), treten die mit im Mittel 18° deutlich steiler geneigten Terrassenbetten der Klasse *completely collapsed* vornehmlich an Hängen mit 30° Hintergrundneigung auf.

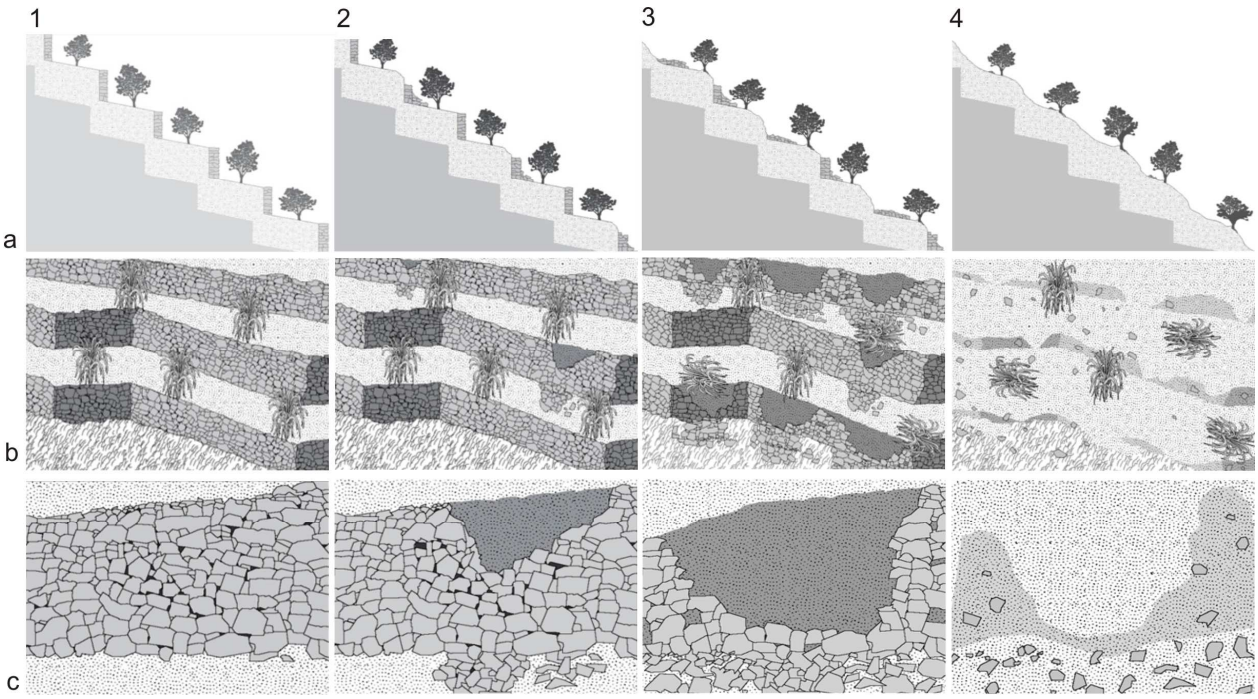

Abbildung 24 *Terrassenzustandskategorien (1) well maintained, (2) fairly maintained, (3) partially collapsed und (4) completely collapsed im (a) Querprofil sowie die Ausprägung von Mauerstörungen (b) über die Terrasseneinheit verteilt und im (c) Detail.*

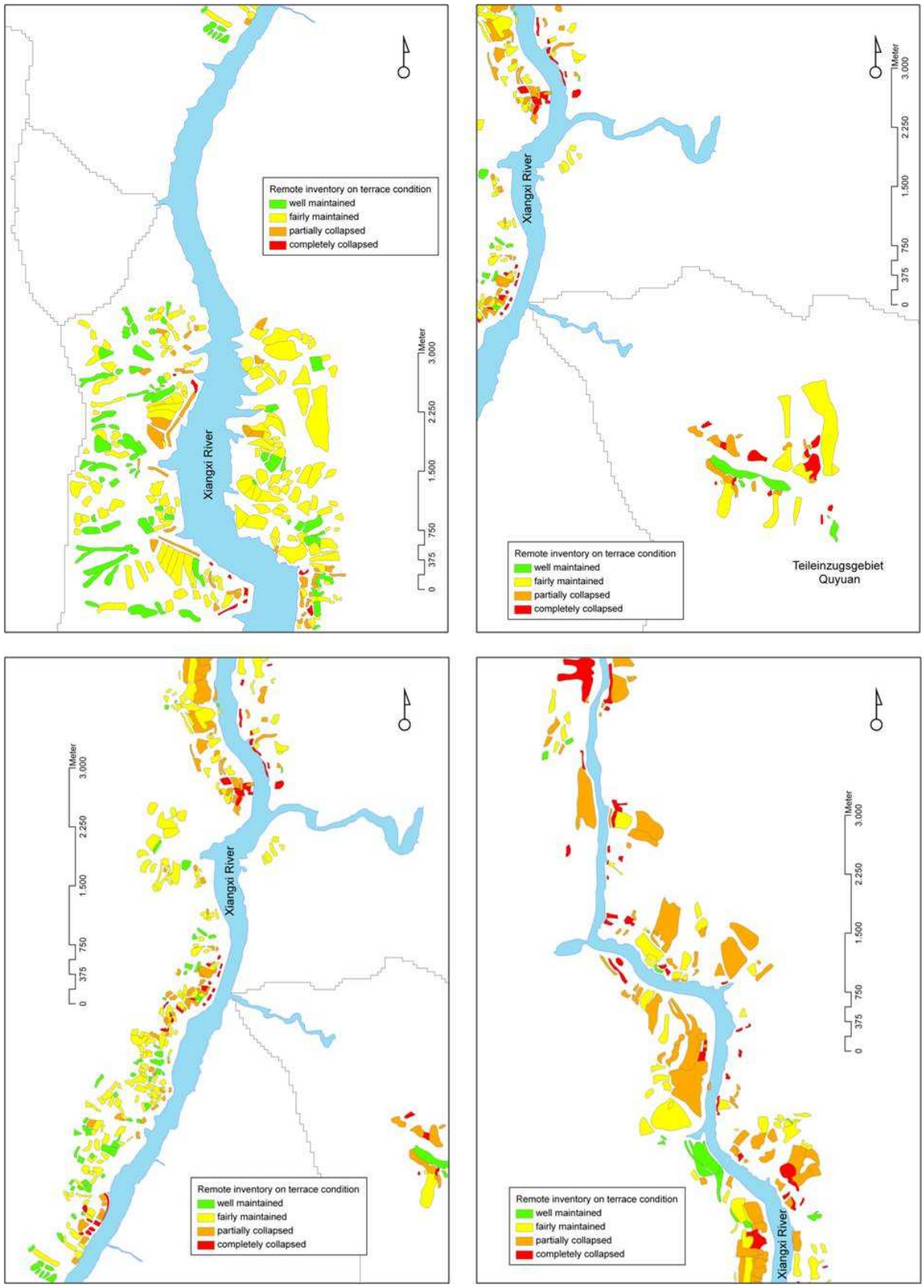

Abbildung 25 *Räumliche Verteilung der mittels Fernaufnahme kartierten 829 Terrassenflächen im Aufstaubereich des Einzugsgebiets des Xiangxi, differenziert nach Zustandskategorien (grün = well maintained, gelb = fairly maintained, orange = partially collapsed, rot = completely collapsed). GIS und Layout von S. Schönbrodt-Stitt.*

Tabelle 7 *Parameter des Terrassendesigns für die vier Terrassenzustandskategorien basierend auf der detaillierten Terrassenaufnahme von 158 Terrassen in den Teileinzugsgebieten Xiangjiaba und Quyuan (nach SCHÖNBRODT-STITT ET AL., 2011; under review).*

Zustandskategorie (n = 158)	Neigung Terrasse (°)	Hangneigung (°)	Höhe Terrassenmauer (m)	Breite Terrasse (m)
Well maintained	8	21	1,9	7,4
Fairly maintained	10	24	1,5	5,6
Partially collapsed	13	27	1,3	4,8
Completely collapsed	18	28	0,9	5,0

4.5.2 Räumliche Verteilung des Terrassenzustands

Mit einer Modellgüte circa 92% können die Vorhersagen des Terrassenzustandes für den Aufstaubereich des Xiangxi-EZG als sehr gut eingestuft werden. Insbesondere die Zustandskategorien *well maintained* und *fairly maintained* zeigen eine hohe Klassifizierungsgüte (Tabelle 8).

Tabelle 8 *Konfusionsmatrix für die Regionalisierungsergebnisse der mit Random Forests berechneten Klassifikations- und Regressionsregeln der Terrassenzustandskategorien für 829 Terrassen im Aufstaubereich des Xiangxi (nach SCHÖNBRODT-STITT ET AL., 2011; under review).*

Beobachtung	Vorhersage				Fehler
	Well maint.	*Fairly maint.*	*Part. coll.*	*Compl. coll.*	
Well maintained	611	88	17	1	0.1478
Fairly maintained	53	2094	71	0	0.0559
Partially collapsed	13	97	1444	3	0.0726
Completely collapsed	8	12	8	21	0.5714

Well maint. well maintained, fairly maint. fairly maintained, part. coll. partially collapsed, compl. coll. completely collapsed

Insbesondere die Entfernungen zu Siedlungsflächen, zur alten Uferlinie und zu den Hauptstraßen erklären die vier Terrassenzustandsstufen (Abbildung 26). Je näher die Terrassenflächen am Xiangxi und an Hauptstraßen liegen, desto schlechter ist deren Zustand. Die schnelle Erreichbarkeit dieser Terrassenflächen durch Haupttransportrouten kann als wesentliche Ursache für deren Degradation betrachtet werden.

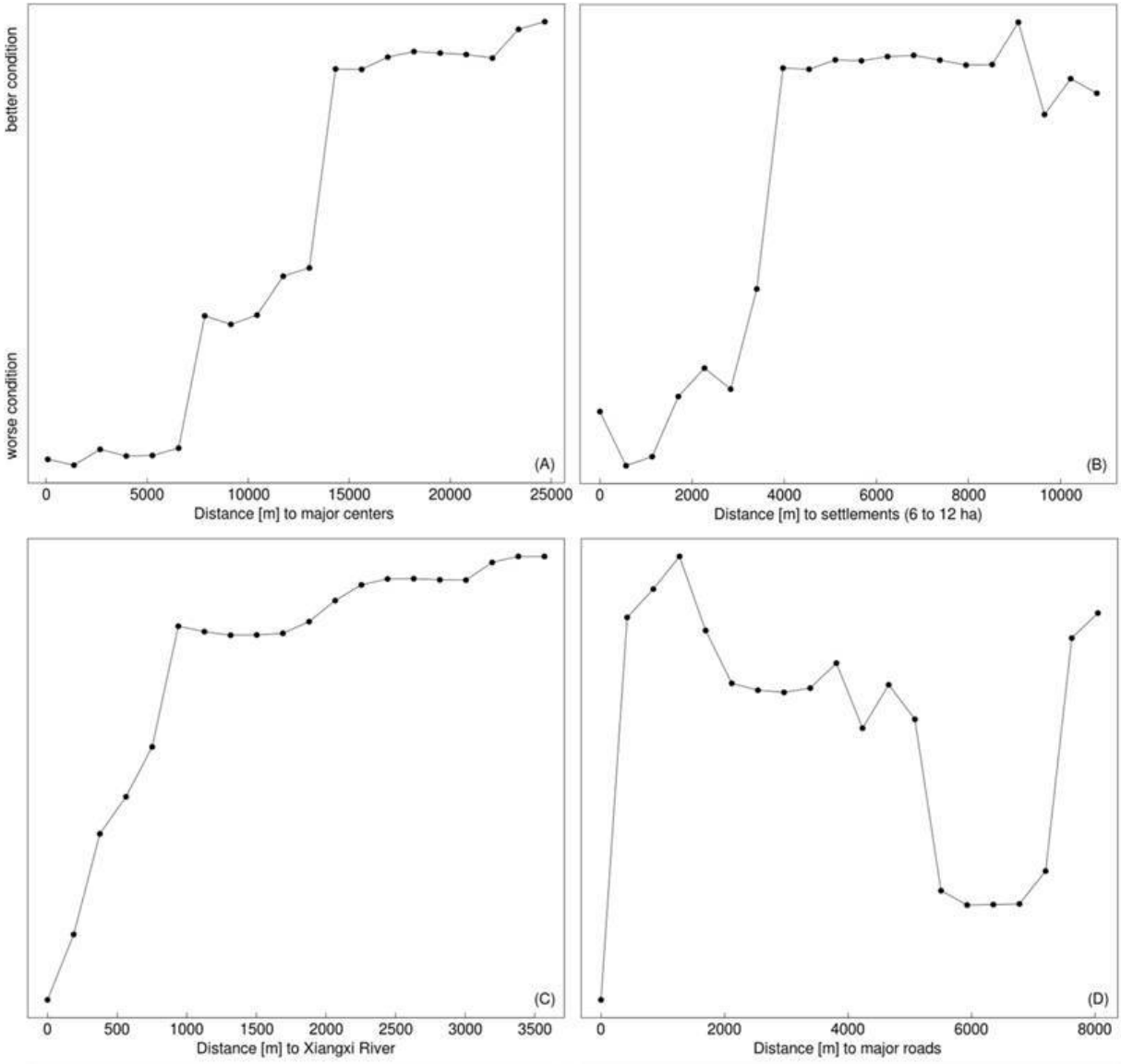

Abbildung 26 *Partielle Abhängigkeiten für die Distanzen (m) zu den Hauptsiedlungszentren (A), den Siedlungsflächen mit einer Größe zwischen 6 bis 12 ha (B), zur neuen Uferlinie des Xiangxi (C) und zu den Hauptstraßen (D) im Aufstaubereich des Xiangxi (nach SCHÖNBRODT-STITT ET AL., 2011; under review).*

Der räumliche Schwerpunkt der als *well maintained* und *fairly maintained* prognostizierten Terrassen liegt deutlich auf den höher gelegenen Flächen an Mittel- und Oberhängen in größerer Entfernung zur neuen Uferlinie des Xiangxi und zu größerer Siedlungen. In unmittelbarer Nähe der Siedlungsbereiche, entlang der Straßen und der neuen Xiangxi-Uferlinie wurden überwiegend Terrassen der Zustandskategorien *partially collapsed* und *completely collapsed* vorhergesagt (Abbildung 27).

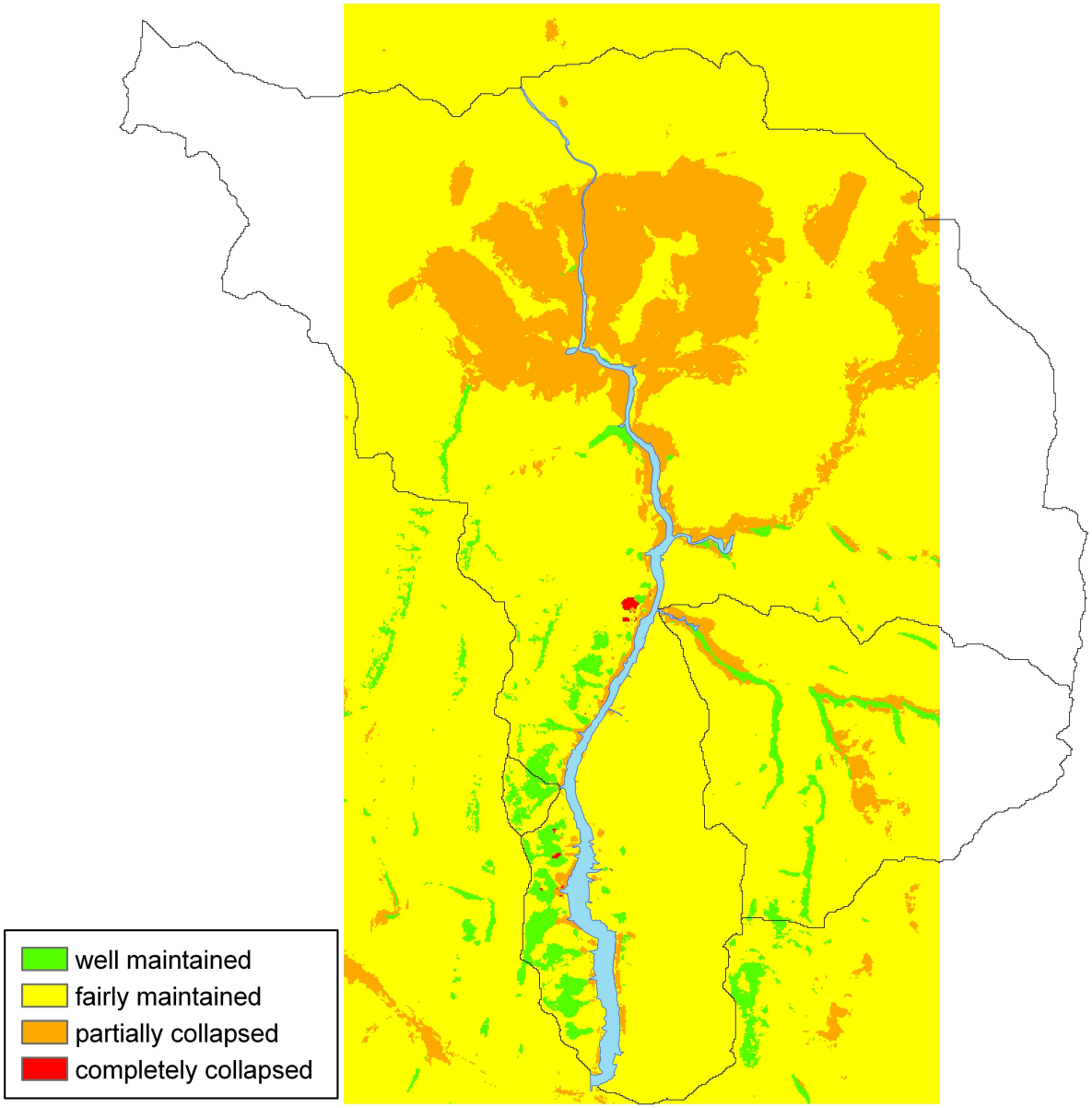

Abbildung 27 *Ergebnisse der Regionalisierung der Terrassenzustandsstufen mit TerraCE. GIS und Layout von S. Schönbrodt-Stitt.*

5 Diskussion und Schlussfolgerungen

Unter der Annahme einer vollständigen Bedeckung mit Primärwald unterscheidet sich die natürliche Erosionsdisposition im Xiangxi-EZG, berechnet mit der RUSLE als langjährige mittlere Bodenabtrage für die ehemalige (1987) sowie aktuelle (2007) Landnutzung erwartungsgemäß erheblich. Entsprechend der generell geringeren Reliefenergie weist das Teileinzugsgebiet Xiangjiaba im Vergleich zum gesamten Xiangxi-EZG, dem Aufstaubereich und dem Teileinzugsgebiet Quyuan dabei die geringsten potenziellen Bodenabträge auf. Offensichtlich erweist sich der Unterschied zwischen aktueller Bodenbedeckung und Wald, ausgedrückt im *C*-Faktor, als wichtigste Regelgröße

für den potentiellen Bodenabtrag. Selbst die schützende Wirkung der Terrassierung kann dies nur eingeschränkt ausgleichen.

In Kontrast zu der mehr oder weniger gleichmäßigen Verteilung der natürlichen potenziellen Bodenabträge bewirkt die aktuelle Landnutzung dementsprechend eine deutliche räumliche Differenzierung des Erosionsrisikos (vgl. Abbildung 22 und 23). Basierend auf Caesium-137-Messungen zum Bodenabtrag ermittelte QUINE ET AL. (1999) für subtropische Bedingungen in der Sichuan Province aktuelle Bodenabträge durch Wasserosion von 51.5 t ha^{-1} a^{-1} für landwirtschaftlich genutzte Flächen auf Hängen mit 6,2° Neigung. Dies ist vergleichbar mit den Ergebnissen für das Xiangxi-EZG, wo mittlere Bodenabträge auf Hängen mit 5-8° Neigung von 54,4 t ha^{-1} a^{-1} in 1987 bis 50,7 t ha^{-1} a^{-1} in 2007 berechnet wurden.

Die räumliche Verteilung der Bodenabträge im Xiangxi-EZG belegt das sehr hohe Erosionsrisikopotenzial im Aufstaubereich des Xiangxi. Gegenüber 6,3% (35,1 km²) der Fläche, die entsprechend der Klassifikation des Erosionsrisikos nach dem *Chinese Technological Standard of Soil and Water Conservation Rules* (SD238-87) als Gebiete mit moderaten Bodenabträge klassifiziert wurden, steigen die Werte unter Berücksichtigung der aktuellen Landnutzung auf 25,3% (141,17 km²) in 1987 und 26,7% (149,1 km²) in 2007. Diese Ergebnisse verdeutlichen das hohe Erosionsrisikopotenzial welches mit der aktuellen Landnutzung einhergeht. Bemerkenswert ist der klare Trend zur Zunahme des Bodenabtrags in den Jahren 2005 bis 2007, obgleich die großflächige Neuanlage und Wiederinbetriebnahme von Terrassen grundsätzlich eine deutliche Erosionsminderung bewirken.

Obwohl die Eingangsparameter für die RUSLE mit 45 m, bezogen auf das eng gekammerte Relief und den kleinräumigen Nutzungswechsel sowie den nach dem Aufstau überwiegenden Anbau auf terrassieren Flächen, eine geringe räumliche Auflösung besitzen, liefert die Modellierung im Vergleich mit anderen Studien aus dem Yangtze-EZG plausible Ergebnisse (u.a. YAO, 1993; QUINE et al., 1999; LU und HIGGITT, 2000; GUO ET AL., 2001; SHI ET AL., 2004). Die räumliche Auflösung der Ergebnisse ist zunächst vorgegeben durch die Zellengröße des SRTM-DGM und den Maßstab der Bodenkarte. Weiterhin wird die Aussagekraft der Modellierungsergebnisse durch die mittels Höhenbändern extrapolierten *R*-Faktoren auf der Grundlage von lediglich fünf Stationen für einen Fläche von etwa 3200 km² geprägt. Gerade in gebirgigen subtropischen Gebieten wäre eine räumlich und zeitlich hoch aufgelöste Bestimmung der Niederschlagserosivität von großer Bedeutung für die Aussagekraft von Bodenerosionsmodellen. Ein weiterer zentraler Qualitätsaspekt betrifft die Berücksichtigung der Terrassierung. Unter der Annahme, dass das gesamte Xiangxi-EZG terrassiert ist und diese Terrassen in ihrem Design, ihrer Hintergrundhangneigung und ihrem Zustand nicht variieren, werden Bodenabträge zunächst zwar deutlich realistischer abgebildet als ohne Berücksichtigung der Terrassierung, jedoch infolge der fehlenden räumlichen Differenzierung stellenweise über- bzw. unterschätzt. Dies gilt insbesondere in Gebieten hoher Reliefenergie (CAO ET AL., 2007; LESSCHEN ET

AL., 2008). Für 31% der Fläche des Xiangxi-EZGs, 23% der Fläche des Aufstaubereichs und 61% bzw. 37% der Fläche der Teileinzugsgebiete Xiangjiaba und Quyuan mit Hangneigungen zwischen 20 und 25° ergibt die Modellannahme für die erosionsschützende Wirkung der Terrassierung mit $P = 0{,}55$ allerdings realistische Ergebnisse.

Im Xiangxi-EZG ist die Terrassierung der steilen Hänge als weitverbreitete Maßnahme zum Schutz des Bodens vor Erosion durchaus wirksam und reduziert den potenziellen Bodenabtrag deutlich. Allerdings zeigen die Terrassen sehr unterschiedliche Pflegezustände von sehr gut erhaltenen und gepflegten Terrassen bis hin zu komplett zerstörten Terrassen. Obwohl bislang keine Zeitreihe der Terrassenzustände vorliegt, kann angenommen werden, dass eine sukzessive Verschlechterung des Terrassenzustands nach deren Einrichtung den Trend zunehmender potenzieller Bodenabträge von 2005 nach 2007, zumindest teilweise, erklärt. Das hier entwickelte Terrassenzustandsmodell *TerraCE* könnte zukünftig ein zentrales Verfahren nicht nur zur Modellierung der räumlichen Verteilung von Terrassenzuständen sein, sondern auch zur Prüfung dieses Zusammenhangs und weiterer Ursachen für den Zustand terrassierter Hänge dienen. Unsere Ergebnisse zeigen, dass höher gelegene Hangbereiche fern des Aufstaubereichs sowie die flacheren Hangbereiche deutlich bessere Pflegezustände aufweisen und sich gut für die Anlage neuen terrassierten Farmlands eignen. Die Errichtung von Terrassen auf Flächen nahe der Uferlinie sowie auf sehr steilen Hängen, z.B. in der Trias auf der Ostseite des Xiangxi, bietet dagegen nur unter sehr hohen Pflegeaufwand einen ausreichenden Erosionsschutz. Um dies zu gewährleisten, müsste das erwirtschaftete Einkommen in diesen Bereichen entsprechend hoch sein.

Eine weitergehende Interpretation der Zusammenhänge und der Ursachen, die den Zustand einer Terrasse und dessen räumliche Anordnung bestimmen, hebt in erster Linie anthropogene Effekte hervor (SCHÖNBRODT-STITT ET AL., 2011; *under review*). Neu gebaute Straße zur infrastrukturellen Anbindung der im Zusammenhang mit dem Aufstau des TGD neu entstehenden und/oder wachsenden Siedlungen in Nähe zur neuen Uferlinie des Xiangxi dienen als präferentielle Pfade der Inwertsetzung neuer landwirtschaftlich genutzter Flächen für die Nahrungsmittelproduktion und den Anbau von Marktfrüchten. Es konnte gezeigt werden, dass der Terrassenzustand mit zunehmender Nähe zu Siedlungsbereichen, der neuen Xiangxi-Uferlinie und Hauptstraßen hinsichtlich des Erosionsschutzes schlechter wird. Rapide ablaufende sozio-ökonomische Umbrüche, wie sie für die TGD-Region typisch sind, begünstigen somit die Bodenerosion.

Mit zunehmender Entfernung zu großen Siedlungsbereichen und Hauptverkehrswegen wie Hauptstraßen und Flüsse weisen die Terrassenflächen bessere Zustände hinsichtlich des Terrassen-designs sowie der Pflege und Erhaltung auf. Dies kann auf eine höhere Motivation der hier siedelnden Familien, ihre Flächen zu pflegen und zu erhalten, zurückgeführt werden. Des Weiteren sind die Flächen in zunehmender Entfernung zum dynamischen Aufstaubereich mit seinen größeren Sielungen

und Hauptstraßen unattraktiver für den Anbau von Marktfrüchten, in erster Linie Orangen. Deren Ertrag unterliegt regionalen Marktentwicklungen und steht in direktem Zusammenhang mit dem Pflegeaufwand zum Erhalt der erosionswirksamen Terrassenfunktionen. Die abnehmende Attraktivität der Flächen für den Marktfruchtanbau kann mit der weniger günstigen Erreichbarkeit der steilen Mittel- und Oberhangbereiche und den ruralen Bedingungen mit eingeschränkten Möglichkeiten zur Weiterverarbeitung und zum Transport der Marktfrüchte erklärt werden (SCHÖNBRODT-STITT ET AL., 2011; *under review*). Eine weitere Ursache der schlechteren Terrassenzustände in unmittelbarer Nähe zum Reservoir ist das hier häufig festgestellte nicht angepasste und nicht nachhaltige Management der Flächen. Während die Farmer vor der Aufstauung die ebenen, fruchtbaren Talböden bewirtschafteten, fehlen ihnen Kenntnisse für die zeitaufwendigen und kostenintensiven Pflege und Unterhaltung der Terrassen.

Es kann abschließend festgehalten werden, dass die Geschwindigkeit der ablaufenden sozioökonomischen und ökosystemaren Veränderungen in der TGD Region die Instandsetzung und den Erhalt neuen ebenso wie vorhandener, alter Terrassen bislang nicht oder nur untergeordnet berücksichtigen. Unsere Ergebnisse legen nahe, dass eine Verbesserung dieser Situation geeignet ist, den Erosionsschutz in Gebieten geringer Tragfähigkeit und knapper werdender Bodenressourcen effektiver und wirkungsvoller zu gestalten.

Die Anwendung der RUSLE zur Vorhersage des potenziellen mittleren langjährigen Bodenabtrags und dessen räumlicher Verteilung sowie die Anwendung und Weiterentwicklung von *TerraCE* zur besseren Einbindung der für gebirgigen Regionen charakteristischen Bewirtschaftung terrassierter Hänge in die Erosionsmodellierung erlauben eine valide Vorhersage des räumlich expliziten Erosionsrisikos und des Effekts von Erosionsschutzmaßnamen für den Bodenabtrag. Die hier für das Einzugsgebiet des Xiangxi erzielten Ergebnisse sind beispielhaft für große Staudammprojekte und können helfen, den Erosionsschutz und insbesondere den Einsatz von Terrassen als nachhaltige Erosionsschutzmaßnahme in gebirgigen Landschaften zu optimieren.

Literatur

ALDHOUS, P., 1993. Tropical deforestation: not just a problem in Amazonia. *Science* 259, 1390.

ALEXANDERSON, H., 1986. A homogenity test applied to precipitation data. *Journal of Climatology* 6, 661-675.

BEHRENS, T., 2003. Digitale Reliefanalyse als Basis von Boden-Landschafts-Modellen - am Beispiel der Modellierung periglaziärer Lagen im Ostharz. Boden und Landschaft 42, pp. 189. Giessen.

BEHRENS, T., SCHMIDT, K., SCHOLTEN, T., 2008. An approach to remove uncertainties in nominal environmental covariates and soil class maps. in: Hartemink, A.E., McBratney, A., Mendoca-Santos, M.L. (Eds.), Digital Soil Mapping for regions and countries with sparse soil data infrastructures, Springer: Netherlands.

BEHRENS, T., ZHU, A.X., SCHMIDT, K., SCHOLTEN, T., 2010. Multi-scale digital terrain analysis and feature selection in digital soil mapping. *Geoderma* 155, 175-185.

Ad-hoc-Arbeitsgruppe Boden der Geologischen Landesämter und der Bundesanstalt für Geowissenschaften und Rohstoffe der Bundesrepublik Deutschland. 2005. Bodenkundliche Kartieranleitung 2005. Schweizerbart'Sche Verlagsbuchhandlung; Auflage: 5., verb. u. erw. A. (12. Mai 2005), pp. 438.

BOETTINGER, J.L., RAMSEY, R.D., BODILY, J.M., COLE, N.J., KIENAST-BROWN, S., NIELD, S.J., SAUNDERS, A.M., STURM, A.K., 2008. Landsat Spectral Data for Digital Soil Mapping. in: Hartemink, A.E., McBratney, A., Mendoca-Santos, M.L. (Eds.), Digital Soil Mapping for regions and countries with sparse soil data infrastructures Springer-Verlag, Netherlands. 193-202.

BOLINNE, A., LAUANT, A., ROSSEAU, P., PAUWELS, J.M., GABRIELS, D., AELTERMANN, J., 1980. Provisional rain erosivity map of Belgium. in: DeBoodt M, Gabriels D. (Eds.), Assessment of Erosion. John Wiley and Sons: Chichester, pp. 111-120.

BRADY, N.C., WEIL, R.R., 2007. The Nature and Properties of Soil. 14th edition, Prentice Hall, New Jersey. 980.

BRANCUCCI, G., PALIAGA, G., 2006. The hazard assessment in a terraced landscape: Preliminary result of the Liguria (Italy) Case Study in the Interreg III Alpter Project. 2006 ECI Conference on Geohazards, Lillehammer, Norway.

BREIMAN, L., 2001. Random forests. *Machine Learning* 45, 5-32.

BUISHAND, T.A., 1982. Some methods for testing the homogenity of rainfall records. *Journal of Hydrology* 58, 11-27.

CAI, G.G., WANG, H., CURTIN, D., ZHU, Y., 2005. Evaluation of the EUROSEM model with single event data on steeplands in the Three Gorges Reservoir Areas, China. *Catena* 59, 19-33.

CAO, S., CHEN, L., FENG, Q., LIU, Z., 2007. Soft-riser bench terrace design for the hilly loess region of Shaanxi Province, China. *Landscape and urban planning* 80, 184-19.

COMOLLI, R., 2005. Soils and man-made terraces in Sondrio Region: pilot area of Pianazzola. ALPTER Terraced Landscapes of the Alpine Arc, Meeting Internazionale, 3-4 Novembre 2005, Sondrio SO, Italy.

CUTLER, D.R., EDWARDS, T.C. JR, BEARD, K.H., CUTLER, A., HESS, K.T., GIBSON, J., LAWLER, J.J., 2007. Random forests for classification in ecology. *Ecology* 88, 2783-2792.

DVWK, Fachausschuss Bodenerosion (1996): Bodenerosion durch Wasser - Kartieranleitung zur Erfassung aktueller Erosionsformen. DVWK-Merkblätter zur Wasserwirtschaft 239, Wirtschafts- und Verl.-Ges. Gas und Wasser, Bonn.

EEA, 2003. Assessment and reporting on soil erosion. EEA Technical Report 94. European Environment Agency, Copenhagen.

EL-SWAIFY, S.A., 1997. Factors affecting soil erosion hazards and conservation needs for tropical steeplands. *Soil Technology* 11, 3-16.

ERENCIN, Z., 2000. C-factor mapping using remote sensing and GIS - A case study of LOM Sak / Lom Kao, Thailand. Unpublished M.Sc. Thesis, ITC, Holland.

GEROLD, R., (Hrsg.) 2001. Bodenerosion. Analyse und Bilanz eines Umweltproblems. Wissenschaftliche Buchgesellschaft, Darmstadt 2001.

GOOVAERTS, P., 1999. Using elevation to aid the geostatistical mapping of rainfall erosivity. *Catena* 34, 227-242.

GRIMM, R., BEHRENS, T., MÄRKER, M., ELSENBEER, A., 2008. Soil organic carbon concentrations and stocks on Barro Colorado Island - digital soil mapping using random forests analysis. *Geoderma* 146, 102-113.

GUO, Z., XIAO, X., GAN, Y., ZHENG, Y., 2001. Ecosystem functions, services and their values - a case study in Xingshan County of China. *Ecological Economics* 38, 141-154.

HAMMAD, A.A., HAUGEN, L.E., BØRRESEN, T., 2004. Effects of stonewalled terracing techniques on soil water conservation and wheat production under mediterranean conditions. *Journal of Environmental Management* 34, 701-710.

HE, K., LI, X., YAN, X., GUO, D., 2008. The landslides in the Three Gorges Reservoir Region, China and the effects of water storage and rain on their stability. *Environmental Geology* 55, 55-63.

HODGSON, M.E., GAILE, G., 1999. A cartographic modeling approach for surface orientation-related applications. *Photogrammetric Engineering und Remote Sensing* 65, 85-95.

HONG, Q., CHEN, P., 1990. Soils of China. Science Press, Beijing, China, pp. 873.

HORN, B.K.P., 1981. Hillshading and the reflectance map. *Proceedings of the IEEE* 69, 14-47.

HUANG, B.W., 1987. Slopeland utilization and amelioration: importance and feasibility. *Geographical Research* 6, 1- 5.

HUANG, Z., ZHOU, W., ZHOU, J., ZHU, M., 2006. Land use of the Three Gorges reservoir Area and the effect on its landscape in the recent 50 years. *Wuhan University Journal of Natural Sciences* 11, 910-914.

HUBER, M., 1994. The digital geo-ecological map - concepts, GIS-methods and case studies: Physiogeographica 20, Basel, pp. 144.

HUDSON, N.W., 1981. Soil conservation. London, Batsford.

LI, H., CHEN, X., KYOUNG, J.L., CAI, X., MYUNG, S., 2010. Assessment of soil erosion and sediment yield in Liao watershed, Jiangxi Province, China Using USLE, GIS, and RS. *Journal of Earth Science* 21, 941-953.

LIAW, A., WIENER, A., 2011. Package 'randomForest'. http://cran.r-project.org/web/packages/randomForest/randomForest.pdf (08/12/2011).

INBAR, M., LLERENA, C.A., 2000. Erosion processes in high mountain agricultural terraces in Peru. *Mountain Research and Development* 20, 72-79.

IUSS WORKING GROUP WRB 2007. World Reference Base for Soil Resources 2006, first update 2007. World Soil Resources Reports No. 103. FAO: Rome.

JARVIS, A., REUTER, H.I., NELSON, A., GUEVARA, E., 2008. Hole-filled seamless SRTM data V4, International Centre for Tropical Agriculture (CIAT), available from http://srtm.csi.cgiar.org.

JONES, A., PANAGOS, P., BARCELO, S., BOURAOUI, F., BOSCO, C., DEWITTE, O., GARDI, C., ERHARD, M., HERVÁS, J., HIEDERER, R., JEFFERY, S., LÜKEWILLE, A., MARMO, L., MONTANARELLA, L., OLAZÁBAL, C., PETERSEN, J.E., PENIZEK, V., STRASSBURGER, T., TÓTH, G., VAN DEN

EECKHAUT, M., VAN LIEDEKERKE, M., VERHEIJEN, F., VIESTOVA, E., YIGINI, Y., 2012.The State of Soil in Europe. A contribution of the JRC to the European Environment Agency's Environment State and Outlook Report-SOER 2010. Report EUR 25186 EN

LILLESAND, T.M., KIEFER, R.W., CHIPMAN, W.C., 2008. Remote sensing and image interpretation. 6th edition, John Wiley and Sons, New York, pp. 768.

KLEEFISCH, B., KÖTHE, R., 1993. Wege zur rechnergestützten bodenkundlichen Interpretation digitaler Reliefdaten. Geol. Jb. F 27, 59-122.

KOLB, R.T., 2003. About figures and aggregates: some arguments for a more scrupulous evaluation of quantitative data in the history of population and agriculture in China (1644-1949). Agriculture, Population and economic development in China and Europe 1, 200-275. Breuninger Stiftung, Stuttgart.

KONZ, N., SCHAUB, M., PRASUHN, V., BAENNINGER, D., ALEWELL, C., 2009. Caesium-137-based erosion-rate determination of a steep mountainous region. *Journal of Plant Nutrition and Soil Science*172, 615- 622.

KOULOURI, M., GIOURGA, C., 2007. Land abandonment and slope gradient as key factors of soil erosion in mediterranean terraced lands. *Catena* 69, 274-278.

LAL, R., 1976. Soil erosion problems on Alisols in western Nigeria and their control. Monograph No. 1, IITA: Ibadan.

LESSCHEN, J.P., CAMMERRAT, L.H., NIEMANN, T., 2008. Erosion and terrace failure due to agricultural abandonment in a semi-arid environment. *Earth Surface Processes and Landforms* 33, 1574-1584.

LIU, Y., LUO, Z., 2005. A Study on Estimation of the amount of Soil erosion in Small watershed based on GIS: a case study in the Three Gorge Area of China. *International Geoscience and Remote Sensing Symposium Proceedings* 3, 1859-1863.

LU, X.X., HIGGITT, D.L., 2000. Estimating erosion rates on sloping agricultural land in the Yangtze Three Gorges, China, from caesium-137 measurements. *Catena* 39, 33-51.

MACMILLAN, R.A., PETTAPIECE, W.W., NOLAN, S.C., GODDARD, T.W., 2000. A generic procedure for automatically segmenting landforms into landform elements using DEMs, heuristic rules and fuzzy logic. *Fuzzy Sets and Systems* 113, 81-109.

MCCOOL, D.K., BROWN, L.C., FOSTER, G.R., MUTCHLER, C.K., MEYER, L.D., 1987. Revised slope steepness factor for the Universal Soil Loss Equation. *Trans. ASAE* 30, 1387-1396.

MCDONALD, B., WEBBER, M., YUEFANG, D., 2008. Involuntary Resettlement as an Opportunity for Development: The Case of Urban Resettlers of the Three Gorges Project, China. *Journal of Refugee Studies*, doi:10.1093/jrs/fem052.

MEN, M., YU, Z., XU, H., 2008. Study on the spatial pattern of rainfall erosivity based on geostatistics in Hebei Province, China. *Frontiers of Agriculture in China* 2, 281-289.

MENG, Q.H., FU, B.J., YANG, L.Z., 2001. Effects on land use on soil erosion and nutrient loss in the Three Gorges Reservoir Area, China. *Soil use and management* 17, 288-291.

MIKHAILOVA, E.A., BRYANT, R.B., SCHWAGER, S.J., SMITH, S.D., 1997. Predicting rainfall erosivity in Honduras. *Soil Science Society of America* 61, 273-279.

MONTGOMERY, D.R., 2007. Dirt: The erosion of civilizations. University of California Press, Ltd., London, pp. 285..

MUSGRAVE, G.W., 1947. The quantitative evaluation of factors in water erosion – A first approximation. *Journal of Soil and Water Conservation* 2, 133-138.

OSTER, S., 2007, 12th October, China dam project to uproot millions more. Wall Street Journal. http://online.wsj.com/article/SB119212305140656176.html (08/26/2010).

PIMENTEL, D., 2006. Soil erosion: a food and environmental threat. *Environment, Development and Sustainability* 8, 119-137.

PRASAD, A.M., IVERSON, L.R., LIAW, A., 2006. Newer classification and regression tree techniques: bagging and random forests for ecological prediction. *Ecosystems* 9, 181-199.

QUINE, T.A., WALLING, D.E., CHAKELA, Q.K., MANDIRINGANA, O.T., ZHANG, X., 1999. Rates and patterns of tillage and water erosion on terraces and contour strips: evidence from caesium-137 measurements. *Catena* 36, 115-142.

RENARD, K.G., FREIMUND, J.R., 1994. Using monthly precipitation data to estimate the R-factor in the revised USLE. *Journal of Hydrology*157, 287-306.

RENARD, K.G., FOSTER, G.R., WEESIES, G.A., MCCOOL, D.K., YODER, D.C., 1997. Predicting Soil Erosion by Water: A Guide to Conservation Planning with the Revised Universal Soil Loss Equation (RUSLE). U.S. Department of Agriculture, Agriculture Handbook No.703, USDA, Washington, DC.

SANG-ARUN, J., MIHARA, M., HORAGUCHI, Y., YAMAJI, E., 2006. Soil erosion and participatory remidation strategy for bench terraces in northern Thailand. *Catena* 65, 258-264.

SCHEFFER, F., SCHACHTSCHABEL, P., 2009. Lehrbuch der Bodenkunde. Spektrum Akademischer Verlag, 15. Auflage, pp. 528.

SCHÖNBRODT, S., BEHRENS, T., IMBERY, S., SCHOLTEN, T., 2010a. Assessing and modeling the soil erosion risk potential in a highly dynamic terraced landscape, Three-Gorges-Area. 19th World Congress of Soil Science, Brisbane, Australia. Published on CDROM (2010).

SCHÖNBRODT, S., SAUMER, P., BEHRENS, T., SEEBER, C., SCHOLTEN, T., 2010b. Assessing the USLE crop and management factor C for soil erosion modeling in a large mountainous watershed in Central China. *Journal of Earth Science* 21, 835-845.

SCHÖNBRODT, S., EHRET, D., SEEBER, C., BEHRENS, T., FREI, M., ROHN, J., KING, L., KAUFMANN, H., XIANG, W., SUBKLEW, G., SCHOLTEN, T., 2010c. Geo-risks in the highly dynamic Three Gorges Reservoir ecosystem: Interactions of soil erosion, mass movements, and land use. *Earth Surface Processes and Landforms* (*under review).*

SCHÖNBRODT, S., BEHRENS, T., SCHMIDT, K., SCHOLTEN, T., 2011. Terrace degradation under forced resettlements - field mapping and data mining. *Ecological Indicators* (*under review*).

SFONDRINI, G., APUANI, T., MAZZOLENI, G., CONFORTO, A., 2005. Terraced slope instability: Controlling factors for the risk definition and evaluation. ALPTER Terraced Landscapes of the Alpine Arc, Meeting Internazionale, 3-4 Novembre 2005, Sondrio SO, Italy.

SHARY, P.A., SHARAYA, L.S., MITUSOV, A.V., 2002. Fundamental quantitative methods of land surface analysis. *Geoderma* 107, 1-35.

SHI, Z.H., CAI, C.F., DING, S.W., WANG, T.W., CHOW, T.L., 2004. Soil conservation planning at the small watershed level using RUSLE with GIS. A case study in the Three Gorges Area of China. *Catena* 55, 33-48.

SHI, X.Z., YU, D.S., XU, S.X., WARNER, E.D., WANG, H.J., SUN, W.X., ZHAO, Y.C., GONG, Z.T., 2010. Cross-reference for relating Genetic Soil Classification of China with WRB at different scales. *Geoderma* 155, 344-350.

SHIRAZI, M.A., BOERSMA, L., 1984. A unifying quantitative analysis of soil texture. *Soil Science Society of America Journal* 48, 142-147, DOI: 10.2136/sssaj1984.03615995004800010026x

SUN, X., ZHANG, J., LIU, Z., 2008. Vegetation cover annual changes based on MODIS/TERRA NDVI in the Three Gorges Reservoir Area. *The International Archives of the Photogrammetry, Remote Sensing and Spatial Information Sciences* 37(Part B7), 1397-1400.

TAN, Y., GRAEME, H., POTTER, L., 2003. Government-organized distant resettlement and the Three Gorges Project, China. *Asia-Pacific Population Journal* 18, 5-26.

TAN, Y., BRYAN, B., HUGO, G., 2005. Development, Land-use Change and Rural Resettlement Capacity: a case study of the Three Gorges Project, China. *Australian Geographer* 36, 201-220.

TARBOTON, D.G., 1997. A new method for the determination of flow directions and upslope areas in grid digital elevation models. *Water Resources Research* 33, 309-319.

TOY, T.J., FOSTER, G.R., RENARD, K.G., 2002. Soil Erosion: Processes, Prediction, Measurement, and Control. New York.

VAN DIJK, A.I.J.M., 2002. Water and Sediment Dynamics in Bench-terraced Agricultural Steeplands in West Java, Indonesia. Amsterdam. Thesis, pp. 378.

VAN LYNDEN, G.W.J., OLDEMAN, L.R., 1997. The assessment of the status of human-induced soil degradation in south and south-east Asia. United Nations Environment Programme (UNEP), Food and Agricultural Organization of the United Nations (FAO), International Soil Reference and Information Centre (ISRIC), Wageningen (digital map and data sets).

WANG, G., GERTNER, G., SINGH, V., SHINKAREVA, S., PARYSOW, P., ANDERSON, A., 2002. Spatial and temporal prediction and uncertainty of soil loss using revised universal soil loss equation: A case study in rainfall and runoff erosivity for soil loss. *Ecological Modeling* 153, 143-155.

WISCHMEIER, W.H., SMITH, D.D., 1965. Predicting rainfall-erosion losses from cropland east of the Rocky Mountains - Guide for Selection of Practices for Soil and Water Conservation. Agriculture Handbook No. 282, USDA, Washington, DC.

XU, Y., SHAO, X., KONG, X.B., PENG, J., YUN, Y.L., 2008. Adapting the RUSLE and GIS to model soil erosion in a mountainous karst watershed, Guizhou Province, China. *Environmental Monitoring Assessment* 141, 275-286.

XU, Y., PENG, J., SHAO, X., 2009. Assessment of soil erosion using RUSLE and GIS: a case study of the Maotiao River watershed, Guizhou Province, China. *Environmental Geology* 56, 1643-1652.

YANGTZE 2008. Erster Zwischenbericht des Verbundprojekts YANGTZE: Landnutzungs-wandel - Erosion - Hangbewegungen. Forschung zur Risikoabschätzung von Hangrutschungen,

Bodenerosion, diffusen Stoffeinträgen und Landnutzungsvulnerabilität im Drei-Schluchten-Ökosystem, VR China. Berichtszeitraum: 01.04.2008 - 31.12.2008, Unveröffentlicht.

YANGTZE 2009. Erster Zwischenbericht des Verbundprojekts YANGTZE: Landnutzungs-wandel - Erosion - Hangbewegungen - Stoffeinträge. Forschung zur Risikoabschätzung von Hangrutschungen, Bodenerosion, diffusen Stoffeinträgen und Landnutzungsvulnerabilität im Drei-Schluchten-Ökosystem, VR China. Berichtszeitraum: 01.04.2009 - 31.12.2009, Unveröffentlicht.

YAO, H., 1993. Characteristics and control of soil erosion in Hubei Province, China. Sediment Problems: Strategies for Monitoring, Prediction and Control (Proceedings of the Yokohama Symposium, July 1993). *IAHS Publ.* No. 217, 23-27.

ZHANG, J.H., SU, Z.A., LIU, G.C., 2008. Effects of Terracing and Agroforestry on Soil and Water Loss in Hilly Areas of the Sichuan Basin, China. *Journal of Mountain Science* 5, 241-248.

ZHOU, P., 2008. Landscape-scale erosion modeling and ecological restoration for a mountainous watershed in Sichuan, China. University of Helsinki, Department of Forest Ecology, VITRI. Tropical Forestry Reports 35. 95

ZINGG, A.W., 1940. Degree and length of land slope as it affects soil loss in runoff. *Agricultural Engineering* 21, 59-64.

MANUSCRIPT 2

Assessing the USLE Crop and Management Factor C for Soil Erosion Modelling in a Large Mountainous Watershed in Central China

Published in JOURNAL OF EARTH SCIENCE, Volume 21, Issue 6, pp. 817-823, December 2010

Sarah Schönbrodt[1)]*, Patrick Saumer[2)], Thorsten Behrens[1)], Christoph Seeber[3)], Thomas Scholten[1)]

1) Institute of Geography, Department of Physical Geography and Soil Science, University of Tübingen, Tübingen, Germany

2) Science Strategy, Coordination and Planning Office, European Space Agency-ESRIN, Frascati, Italy

3) Center for International Development and Environmental Research, Giessen University, Giessen, Germany

* Corresponding author: sarah.schoenbrodt@uni-tuebingen.de

ABSTRACT

Due to the impoundment of the Yangtze River, the Three Gorges Dam in China fosters high land-use dynamics. Soil erosion is expected to increase dramatically. One of the key factors in soil erosion control is the vegetation cover and crop type. However, determining these factors adequately for the use in soil erosion modeling is very time-consuming especially for large mountainous areas, such as the Xiangxi (香溪) catchment in the Three Gorges area. In our study, the crop and management factor C was calculated using the fractional vegetation cover (C_{FVC}) based on Landsat-TM images from 2005, 2006, and 2007 and on literature studies (C_{LIT}). In 2007, the values of C_{FVC} range between 0.001 and 0.98 in the Xiangxi catchment. The mean C_{FVC} value is 0.05. C_{LIT} values are distinctly higher, ranging from 0.08 to 0.46 with a mean value of 0.32 in the Xiangxi catchment. The mean potential soil loss amounts to 120.62 t ha^{-1} a^{-1} in the Xiangxi catchment when using C_{LIT} for modeling. Based on C_{FVC}, the predicted mean soil loss in the Xiangxi catchment is 11.50 t ha^{-1} a^{-1}. Therefore, C_{LIT} appears to be more reliable than the *C* factor based on the fractional vegetation cover.

KEYWORDS

C factor, soil erosion modeling, Universal Soil Loss Equation, fractional vegetation cover, Three Gorges Dam, Yangtze River.

This study was supported by the Federal German Ministry of Education and Research BMBF) (No. 03 G 0669), and coordinated by the German Jülich Research Centre (FZJ).

1 INTRODUCTION

Soil erosion is a severe problem worldwide, and controlling it will be a major challenge in the future (BRADY and WEIL, 2007). Diminishing soil quality by soil erosion highly affects the productivity of natural, agricultural, and forest ecosystems (PIMENTEL, 2006). At the same time, the vegetative soil cover highly contributes to a protection of topsoils against erosive processes. Out of the whole of China, the Yangtze River catchment shows the highest rates of soil erosion by water (ZHOU, 2008). Thirty-three percent (560 000 km^2) of the catchment area is severely affected by soil erosion, mainly alongside the upper and middle reaches of the Yangtze River. The construction of the world's largest dam project, the Three Gorges Project (TGP), and thus rapidly changing and highly dynamic ecosystem conditions, is expected to foster soil erosion by water in an unforeseeable dimension. Due to the river impoundment, large areas became inundated. Consequently, more than one million people had to resettle (MCDONALD ET AL., 2008; TAN ET AL., 2005) mostly to steep sloping uphill-sites with fragile and shallow soils (HE ET AL., 2008). Further factors triggering soil erosion as a major geogene threat lie in the enforced slope instability by artificial water-level fluctuations, deforestation, and increase in agricultural land use on extremely steep sloping areas combined with improper management practices (HUANG ET AL., 2006; CAI ET AL., 2005). Long-term effects of soil erosion in the Yangtze River catchment and its major tributaries are considered to have strong ecological impacts and socio-economic consequences (MENG ET AL., 2001). Information on the quality and quantity of soil erosion is required in order to control soil erosion through well-adapted management and conservation practices.

On the landscape scale, quantities of soil erosion can be modeled with the well-established and worldwide-applied empirical (Revised) Universal Soil Loss Equation (R)(USLE) (RENARD ET AL., 1997; WISCHMEIER and SMITH, 1965). Expressed as crop and management factor *C*, the soil vegetative cover is considered in the USLE. The *C* factor refers to the ratio of soil loss under specific crop conditions to the corresponding soil loss from clean-tilled continuous bare fallow (WISCHMEIER and SMITH, 1965). Its values range between 0 (very high crop cover protecting the topsoil against soil erosion) and 1 (no effect of the crop cover and high soil loss that is comparable to that of bare soil). According to the resulting soil loss ratio, a series of subfactors need to be considered (RENARD ET AL., 1997). These subfactors refer to the previous crop and management practices (prior land-use subfactor), the reduction of soil erosion by the soil cover and soil surface roughness (surface cover subfactor and surface roughness subfactor), the effect of low soil moisture on reduction of runoff from

low intensity rainfall (soil moisture subfactor), and protection of the soil by the vegetation cover (canopy cover subfactor).

However, the assessment of each of those factors in order to calculate the given soil loss ratio is very time-consuming especially in mountainous areas, such as the Xiangxi catchment, where access to terrain is often limited. Thus, large effort has been made on calculating and mapping the *C* factors for use in soil erosion modeling by means of Geographic Information System, remote sensing data, and spectral indices (SURIYAPRASIT and SHRESTHA, 2008; ZHOU ET AL., 2008; DE ASIS and OMASA, 2007; WANG ET AL., 2002; DE JONG, 1994). Remote sensing data are able to provide information on environmental covariates to predict the *C* factor while covering a large scale. This avoids time and cost intensive field investigations and offers the possibility of a multitemporal observation. The normalized differenced vegetation index (NDVI) derived from multispectral images, such as Landsat, is currently one of the most common environmental covariates of vegetation in order to monitor and analyze vegetation, its properties, and spatial and temporal changes (BOETTINGER ET AL., 2008; SUN ET AL., 2008; LILLESAND ET AL., 2007). As a function of the NDVI, the fractional vegetation cover (FVC) provides information on the percentage of vegetation cover (BOETTINGER ET AL., 2008). Thus, FVC can also be used to predict the *C* factor using regression functions considering the soil loss ratio resulting from the specific conditions of the subfactors (ZHOU ET AL., 2008).

In this study, we focus on the capability of the FVC based on Landsat-TM data in order to derive *C* factor values for soil erosion modeling on a large scale in the mountainous Xiangxi catchment. As we have no sufficient database on *C* factor values from field investigations, we further consider *C* factor values from literature assigned to the specific land use classes from a land use classification based on Landsat-TM 2007 as reference. The effect of *C* factors derived on potential soil erosion will be modeled using USLE.

2 MATERIAL AND METHODS

2.1 STUDY AREA

The research area covers the Xiangxi catchment (3,200 km2) located in western Hubei Province, Central China. The Xiangxi River originates in the Shennongjia Forest Nature Reserve region (elevation about 3 000 m) and reaches the Yangtze River almost 40 km westward of the TGP as a first class tributary. Seventy-three percent of the catchment area has slopes with inclinations above 20° (mean slope angle 39°, standard deviation 22.8°). The soils (e.g., brown soil, limestone soil, and yellow soil) are closely linked to the subtropical monsoon climate with an annual precipitation of 1,000 mm, of which 69% fall between May and September, and an annual average temperature of 16.9 °C (1961–1990, Xingshan Climate Station in the central Xiangxi catchment). Land use is characterized by subsistence farming mixed with cash crop production, typically on terraced farmland

with contour cultivation. Typical crops are orange, rice, dry land crops (rape, wheat, and maize), and garden fruits. Due to the TGP, the impoundment of the Xiangxi River reaches from the outlet, approximately 30 km northward to the central catchment. In this backwater area (560 km^2), resettlement, land use change, road construction, landslide, and soil erosion are common features that result in a highly dynamic ecosystem. More detailed studies are conducted with higher spatial resolution in the backwater area of the Xiangxi catchment and in the two subcatchments Xiangjiaba (2.8 km^2) and Quyuan (88 km^2) in order to directly assess the effect of the river inundation on soil erosion.

2.2 DATABASE AND COVARIATES

Data on NDVI and FVC are based on Landsat-TM images. Three Landsat-TM scenes from September 2005, September 2006, and September 2007 showing the lowest cloud and haze cover throughout these years were chosen for this study. Typically, remote sensing images of rugged and steep sloping mountainous regions, such as the Xiangxi catchment, show interfering atmospheric and topographic effects (RICHARDS and JIA, 2006; JENSEN, 2000). These internal and external effects were reduced by means of image preprocessing (atmospheric, radiometric, and geometric corrections) using ATCOR, according to NEUBERT and MEINEL (2005) and RICHTER (2010).

The NDVI was computed for each of the Landsat-TM images preprocessed based on bands 3 (red band; R) and 4 (near infrared; NIR) using equation (1), according to ROUSE ET AL. (1974)

$$NDVI = (NIR - R)/(NIR+R) \quad (1)$$

Based on the three NDVI images derived the FVC was calculated. Therefore, the NDVI values were renormalized, providing an estimated value of vegetation cover (e.g., BOETTINGER ET AL., 2008). Taking into account the NDVI of uncovered, bare ground (minNDVI) and of ground completely covered by vegetation (maxNDVI), the percentage of the FVC was computed using equation (2)

$$FVC\ (\%) = (NDVI - minNDVI)/(maxNDVI + minNDVI) \times 100 \quad (2)$$

In order to provide a correct percentage of vegetation cover, dense clouds were masked (EASTMAN and FULK, 1993) before deriving the FVC. *C* factor values were then calculated taking the logarithm of the percentage of FVC (*c*) using the regression function, according to SHI ET AL. (2004) and ZHOU ET AL. (2008), using equation (3)

$$C = 0.650\ 8\text{-}0.343 \log c \quad (3)$$

The *c* values range between 0 and 78.3%. Thus, a *C* of 1 refers to a *c* of 0 and *C* of 0 equals to a *c* of 78.3%. This function was established by YANG and SHI (1994) for a watershed in the Three Gorges Project (TGP) area using more than 200 soil loss ratios measured from 30 runoff erosion plots under natural as well as simulated rainfall events.

Serving as reference to the *C* factor values derived from the FVC (C_{FVC}), *C* factor values were taken from literature (C_{LIT}) for the land use classes, which were derived from a land use classification based on Landsat-TM data of 2007 (SEEBER ET AL., 2010). As USLE is considered for agricultural used land only, *C* factor values were assigned accordingly. These *C* factors represent common seasonal crop rotation within one year for subtropical agriculture in the TGP area. In detail, these values are 0.13 for orange orchards (SHI ET AL., 2004), 0.18 for paddy field (LIU and LUO, 2005), 0.46 for dry land (LIU and LUO, 2005), 0.1 for garden plots (LIU and LUO, 2005), 0.08 for residential area with homegardens (LIU and LUO, 2005), and 0.2 for fallow land, respectively, land with lower vegetation (ERENCIN, 2000).

Soil erosion was modeled using the USLE (WISCHMEIER and SMITH, 1978). Data on the topography factor *LS* were derived from a digital elevation model in 45 m resolution, according to RENARD ET AL. (1997). The calculation on the erosive slope length *L* was done individually for the land use classes. This refers to agriculturally used land based on a Monte-Carlo-aggregation approach according to BEHRENS ET AL. (2008). The steepest slope algorithm (TARBOTON, 1997) was applied to calculate the erosive slope factor *S*. Data on the soil erodibility *K* are based on the Second National Soil Survey in China (SHI ET AL., 2010). The rainfall erosivity *R* of 2 880 MJ·mm·ha/h/a, according to SHI ET AL. (2004), for the Wangjiaqiao watershed in the TGP area was considered to be valuable for the Xiangxi catchment. Assuming the Xiangxi catchment as totally terraced, a support conservation practice factor of *P* 0.55 (LIU and LUO, 2005) was taken into the calculation of the potential soil loss *A* ($t\ ha^{-1}\ a^{-1}$). The soil loss was modeled in a resolution of 45 m using equation (4)

$$A=R\times LS\times K\times C\times P \tag{4}$$

Despite the *C* factor values derived from the remote sensing data (C_{FVC} from 2005 to 2007) and literature (C_{LIT} 2007), all of the abovementioned factors were kept constant. This ensures assessing the impact of the different *C* factors on soil loss. The spatial resolution of the calculation of *C* factor values and potential soil erosion in the Xiangxi catchment and all subunits is 45 m, as this is the resolution of the database.

3 RESULTS AND DISCUSSION

The crop and management factor *C* was calculated for the years 2005, 2006, and 2007 based on the fractional vegetation cover (FVC) as a function of the normalized differenced vegetation index (NDVI). Derived soil loss was modeled in order to provide information on the effect of the *C* factor values. Analyses were conducted on the macroscale for the Xiangxi catchment (3 200 km^2), on the mesoscale for the backwater area (560 km^2), and on the microscale (2.8 and 88 km^2) for the Xiangjiaba and Quyuan subcatchments.

3.1 NORMALIZED DIFFERENCED VEGETATION INDEX

The NDVIs for 2005 (-1 to 0.979), 2006 (-1 to 0.99), and 2007 (-1 to 0.976) indicate areas with almost no and very low vegetation cover (dark color) and high vegetation cover (light color) in the total Xiangxi catchment and the subunits considered (Figs. 1a, 1b, and 1c). Throughout the time period, slight changes in the NDVI values can be observed. High vegetation cover characterizes the northern, western, and eastern Xiangxi catchment. This is due to the largely forested headwater zone with a few scattered plots of agriculture and settlements, and the river network showing lower NDVI values. The backwater area and the subcatchments show more diverse pattern of NDVI values. Lower NDVI values characterize the agricultural land east of the Xiangxi River. NDVI values of nearly -1 are observed on the very narrow and steep sloping ridges in the Quyuan subcatchment that show no vegetation. The inundated Xiangxi River surface in the backwater area shows NDVI values of -1. Equally, dense clouds and haze occur as dark patches indicating low NDVI values. This is the case especially for 2005 (Fig. 1a). This effect was masked for computing the FVC.

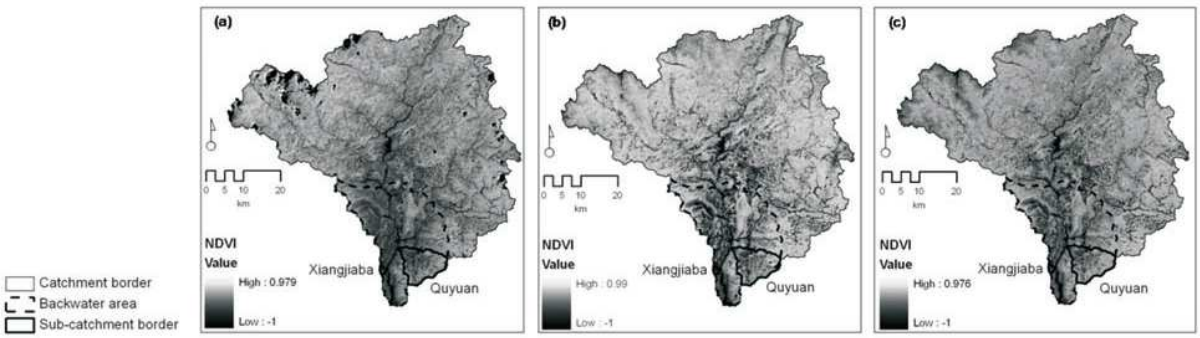

Figure 1 *Comparative multitemporal analysis on normalized differenced vegetation index (NDVI) based on Landsat-TM images in the Xiangxi catchment and the subunits for (a) September 2005, for (b) September 2006, and for (c) September 2007.*

3.2 FRACTIONAL VEGETATION COVER

The FVC ranges between 0 and 100% in the total Xiangxi catchment. Its spatial distribution in the Xiangxi catchment and all subunits considered quasi mirrors the findings of the NDVI (Figs. 1 and 2). High fractional vegetation cover of 90% to 100% is observed in the large headwater zone of the Xiangxi catchment and slightly decreases by 10% to 20% toward the areas adjacent to the river network. FVC of 70% to 80% largely characterizes the backwater area and the subcatchments Xiangjiaba and Quyuan. Extremely low FVC (<10%) to very low FVC (>10% to 20%) characterize the inundation area of the Xiangxi River in the backwater area and in the area of the larger settlements Gufu and Gaoyang alongside the river in the central catchment. Moderate FVC (>30% to 60%) is observed in close distance to the settlement areas and alongside the Xiangxi River in the backwater area. Throughout the Xiangxi catchment, the generally high FVC only changes slightly from 2005 to 2007, showing the highest mean FVC of 93.99% in 2005, decreasing to a mean FVC of 92.89% in 2006, and followed by small increase in 2007 with a mean FVC of 93.95% (Table 1). Changes in FVC between 2005 and 2007 are more distinct in the backwater area and the subcatchments, generally showing less mean FVC than in the total catchment (Table 1). For all subunits, the lowest mean FVC is observed for 2006 ranging between approximately 75% to almost 90%. Within the backwater area, the Xiangjiaba subcatchment shows distinct lower mean FVC (2005: 79.53%; 2006: 75.12%; and 2007: 83.27%) with higher variation compared to the Quyuan catchment (2005: 91.11%; 2006: 89.89%; and 2007: 93.17%), see Table 1.

3.3 C FACTOR ESTIMATES

In the Xiangxi catchment, the C_{FVC} values show similar spatial pattern from 2005 to 2007 (Figs. 3a, 3b, and 3c). C_{FVC} values were predominantly derived for areas adjacent to the river network in the headwater zone, for the larger settlement areas and their close surroundings, almost for the complete western backwater area, alongside the inundation area of the Xiangxi River, and the western Quyuan subcatchment. For areas with masked clouds and haze (Figs. 2a, 2b, and 2c), no C_{FVC} values were derived. Mean C_{FVC} values range from 0.02 to 0.05 for all scales and years and show hardly any spatial and temporal change (Table 2). However, variations are more pronounced in the Xiangxi catchment and in the backwater area. Regarding the minimum and maximum C_{FVC} values, a spatial and temporal change with increasing values from 2005 to 2007 is more obvious.

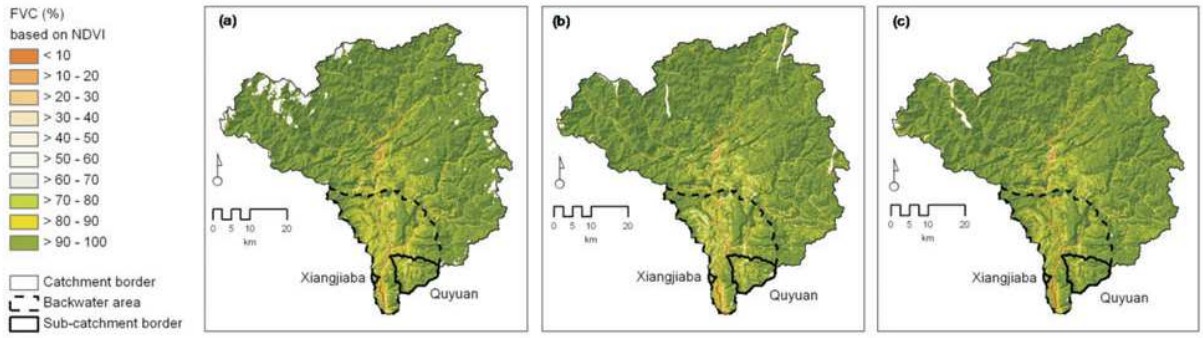

Figure 2 *Comparative multitemporal analysis on fractional vegetation cover (FVC) in percent (%) based on the NDVI from Landsat-TM images in the Xiangxi catchment and the subunits for (a) September 2005, for (b) September 2006, and for (c) September 2007. White patches in the northern and eastern headwater zones of the catchment refer to the masked clouds and haze.*

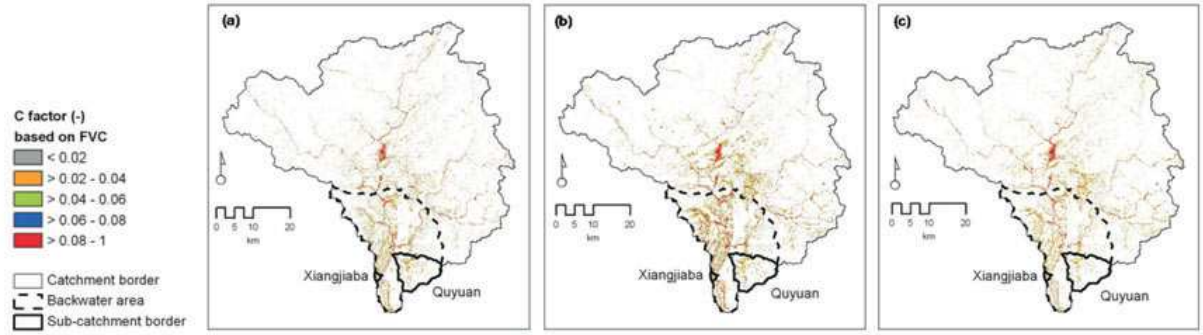

Figure 3 *Comparative multitemporal analysis on the crop and management factor (C factor) based on the fractional vegetation cover (FVC) in the Xiangxi catchment and the subunits for (a) the September 2005, for (b) September 2006, and for (c) September 2007. (-) in C factor (-) refers to the dimensionless C factor.*

Minimum (2005 and 2006: 0.001; 2007: 0.01) and maximum values (2005: 0.87; 2006: 0.93; and 2007: 0.98) in the Xiangxi catchment and in the backwater area are highly different. For the Quyuan and Xiangjiaba subcatchments, the ranges in values are distinctly less, except for the Quyuan subcatchment in 2007 (Table 2). The lowest ranges in values are observed for the Xiangjiaba subcatchment (2005: 0.001 - 0.13; 2006: 0.001 - 0.58, and 2007: 0.01 - 0.20). Compared to the mean C_{LIT} values in 2007 (based on the land use classification from 2007) taken from literature, the C_{FVC} values are very low (Table 2). Mean C_{LIT} values based on literature decrease from the Xiangxi catchment (0.32) to the backwater area (0.27). Within the backwater area, the Quyuan subcatchment shows a higher mean *C* factor of 0.29 compared to the Xiangjiaba subcatchment with a mean factor *C* of 0.21. Whereas the range of C_{LIT} starts with the lowest of 0.08 for residential land, and the broad majority of C_{FVC} values in the Xiangxi catchment are below this value of 0.08 (2005: 88.9%; 2006: 87.6%; and 2007: 85.5%). Slight agreements between the C_{FVC} values and C_{LIT} are observed only for *C* factor values of 0.08 in settlement areas (Gufu and Gaoyang). Taking the area (pixel count) into

account, *C* factor values based on the FVC were derived for distinct less area for all scales and years (e.g., for Xiangxi catchment in 2005: 230.7 km^2; in 2006: 296.8 km^2; and in 2007: 209.2 km^2), as compared with those from literature for an area coverage of 506.6 km^2 (Table 2).

Table 1 *Comparative multitemporal analysis on the fractional vegetation cover (FVC) in percent and on C factor derived from FVC (C_{FVC}) from 2005 to 2007.*

	2005	2005	2006	2006	2007	2007	2007
	FVC (%)	C_{FVC} (-)	FVC (%)	C_{FVC} (-)	FVC (%)	C_{FVC} (-)	C_{LIT}
Xiangxi catchment							
Minimum	0.00	0.001	0.00	0.001	0.00	0.01	0.08
Maximum	100.00	0.87	100.00	0.93	100.00	0.98	0.46
Mean	93.99	0.04	92.89	0.04	93.95	0.05	0.32
Standard deviation	12.71	0.07	13.55	0.06	12.44	0.07	0.17
N	——	113 929	——	146 564	——	103 287	250
Backwater Area							
Minimum	0.00	0.001	0.00	0.001	0.00	0.01	0.08
Maximum	100.00	0.87	100.00	0.93	100.00	0.98	0.46
Mean	86.49	0.03	85.19	0.04	88.55	0.05	0.27
Standard deviation	17.71	0.06	19.76	0.06	18.35	0.07	0.17
N	——	48 996	——	59 124	——	37 245	79
Quyuan sub-catchment							
Minimum	0.00	0.001	0.00	0.001	0.00	0.01	0.10
Maximum	100.00	0.59	100.00	0.66	100.00	0.98	0.46
Mean	91.11	0.03	89.89	0.03	93.17	0.04	0.29
Standard deviation	11.93	0.04	11.51	0.04	10.50	0.04	0.17
N	——	5 494	——	5 794	——	3 515	9 198
Xiangjiaba sub-catchment							
Minimum	0.00	0.001	0.00	0.001	0.00	0.01	0.10
Maximum	100.00	0.13	100.00	0.58	100.00	0.20	0.46
Mean	79.53	0.02	75.12	0.03	83.27	0.03	0.21
Standard deviation	11.61	0.02	13.25	0.03	12.62	0.02	0.14
N	——	582	——	764	——	370	921

Data are based from literature for the land use classification from 2007 (C_{LIT}) for the Xiangxi catchment and the subunits backwater area, Quyuan and Xiangjiaba subcatchments. The C factors from literature are 0.13 for orange orchards (SHI ET AL., 2004), 0.18 for paddy field (LIU and LUO, 2005), 0.46 for dry land (LIU and LUO, 2005), 0.1 for garden plots (LIU and LUO, 2005), 0.08 for residential area with homegardens (LIU and LUO, 2005), and 0.2 for fallow land, respectively, land with lower vegetation (ERENCIN, 2000). N is the count of pixels on the estimated C factor values having a pixel size of 45×45 m. (-) in C_{FVC} (-), and C_{LIT} (-) refers to the dimensionless C factor.

3.4 SOIL LOSS POTENTIAL

The spatial and temporal pattern of soil loss potential in the Xiangxi catchment clearly reflects the pattern on the C_{FVC} values (Figs. 3 and 4). Mean potential soil losses in the Xiangxi catchment range from 9.32 to 11.50 t ha^{-1} a^{-1}. They are slightly lower compared to mean potential soil losses in

the backwater area that range from 10.99 to 14.17 t ha^{-1} a^{-1} and show the same slight increase from 2005 to 2007 (Table 2). The subcatchment Xiangjiaba shows the highest mean potential soil loss in the catchment area and backwater area for each year with an increase from 2005 (11.66 t ha^{-1} a^{-1}) to 2006 (16.32 t ha^{-1} a^{-1}), and a decrease from 2006 to 2007 (14.62 t ha^{-1} a^{-1}). However, maximum potential soil losses in the Xiangjiaba subcatchment (from 66.70 to 109.60 t ha^{-1} a^{-1}) range below those in the other scales by a multiple (Table 2). Compared to the mean potential soil losses as well as the ranges of values, taking into account C_{LIT}, the soil losses based on C_{FVC} values are considerably lower. While mean potential soil loss in the Xiangxi catchment in 2007 is 2 662.10 t ha^{-1} a^{-1} based on C_{LIT}, and the mean potential soil loss based on C_{FVC} in 2007 is lower by the factor of 1.6 (Table 2). This difference in mean potential soil loss still increases in scale by a factor of 2.7 for the backwater area and by the factors of 5.9 and 8.7 for the Quyuan and Xiangjiaba subcatchments respectively

Table 2 *Annual average soil loss potential (t ha^{-1} a^{-1}) in the Xiangxi catchment and in the subunits for the years 2005, 2006, and 2007 (all for September).*

	Soil loss in 2005 based on C_{FVC} in 2005	Soil loss in 2006 based on C_{FVC} in 2006	Soil loss in 2007 based on C_{FVC} in 2007	Soil loss in 2007 based on C_{LIT} for land use classification 2007
Xiangxi catchment				
Minimum	0.00	0.00	0.00	0.00
Maximum	1,133.44	1,498.19	1,646.93	2,662.10
Mean	9.32	10.98	11.50	120.62
Standard deviation	21.90	26.02	28.82	170.37
Backwater area				
Minimum	0.00	0.00	0.00	0.00
Maximum	607.08	708.58	873.60	2,397.94
Mean	10.99	13.59	14.17	125.79
Standard deviation	23.46	24.48	28.31	174.55
Quyuan subcatchment				
Minimum	0.00	0.00	0.00	0.00
Maximum	385.73	180.32	285.60	1,689.85
Mean	10.38	9.10	11.05	157.75
Standard deviation	18.64	14.76	18.85	228.92
Xiangjiaba subcatchment				
Minimum	0.00	0.00	0.00	0.00
Maximum	66.70	99.27	109.60	957.09
Mean	11.66	16.32	14.62	129.96
Standard deviation	13.06	19.48	16.60	150.62

Modeled soil loss potential is based on C factor values calculated from FVC (CFVC). For the year 2007 potential soil loss was further modeled using C factor values from literature. These C factors are 0.13 for orange orchards (SHI ET AL., 2004), 0.18 for paddy field (LIU and LUO, 2005), 0.46 for dry land (LIU and LUO, 2005), 0.1 for garden plots (LIU and LUO, 2005), 0.08 for residential area with homegardens (LIU and LUO, 2005), and 0.2 for fallow land, respectively, land with lower vegetation (ERENCIN, 2000). Further, USLE factors are kept constant.

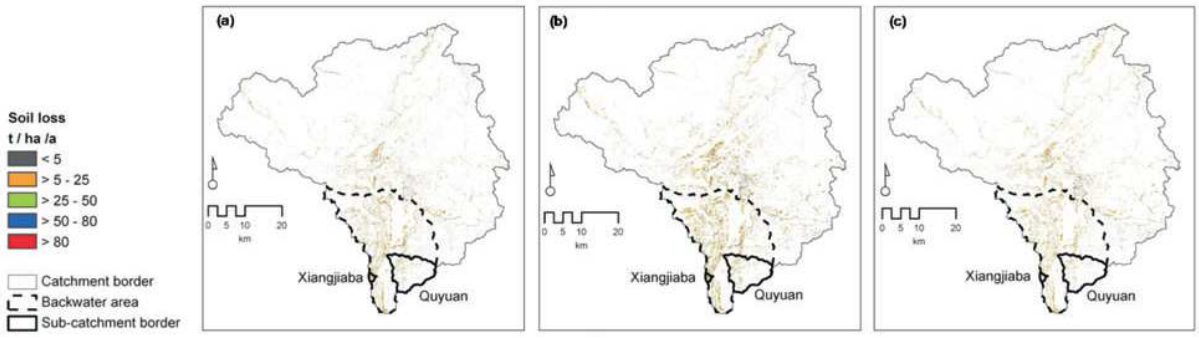

Figure 4 *Map on potential soil loss (t ha^{-1} a^{-1}) with varying C factor values from the multitemporal fractional vegetation cover analysis in the Xiangxi catchment and the subunits for (a) September 2005, for (b) September 2006, and for (c) September 2007. Soil loss is graded into erosion categories according to the Soil Erosion Rate Standard, Technological Standard of Soil and Water Conservation SD238-87, issued by Ministry of Water Resources of China (*XU ET AL.*, 2009).*

5 CONCLUSIONS

The *C* factor represents the vegetation cover and crop and management practices and thus is a major and sensitive factor in the USLE in order to predict the long-term annual average soil loss potential. Considering several subfactors, the calculation of *C* factor values from field investigations is very time consuming. An adequate alternative for larger research areas is the assignment of *C* factor values from literature, which correspond to land use classes, e.g., classified with Landsat-TM images. Further, the NDVI based on Landsat-TM images serves as an environmental covariate of vegetation. The calculation of the FVC from the NDVI provides information on the percentage of the vegetation cover on the large scale and enables the calculation of the *C* factor considering the soil loss ratio taking into account the specific conditions of subfactors (ZHOU ET AL., 2008).

Our results show that (1) the assignment of *C* factor values from literature (C_{LIT}) and (2) the derivation of *C* factor values from FVC based on NDVI (C_{FVC}) correspond to the land use in the Xiangxi catchment and are thus adequate methods to assess the *C* factor on a macroscale. Taking into account a multitemporal series of FVC from 2005, 2006, and 2007, we observe a comparably similar spatial and temporal pattern on the degree of vegetation cover (Figs. 2a, 2b, and 2c; Table 1). In general, very high (90% to 100%) FVC characterizes the headwater zone of the Xiangxi catchment. Scattered plots of farmland within the headwater zone and regions alongside the river network show lower FVC (60% to 80%). Considering the different study scales of the Xiangxi catchment, the backwater area, and the Xiangjiaba and Quyuan subcatchments, we observe a slight decrease of mean FVC (Table 1). We conclude that this decrease mainly results from the high land use dynamics due to the impoundment of the Xiangxi River and larger farmland plots in the backwater area. Paved roads and settlement area as well as the farmland area (dry land farming, orange orchards, and garden land)

are generally reflected lower in NDVI values (Fig. 1). As the FVC was calculated based on the scaled renormalized NDVI, the fraction of vegetation is accordingly lower.

Based on the FVC, the derived values of C_{FVC} distinctly reflect the spatial and temporal pattern of the vegetation cover (Figs. 2 and 3). Generally, high FVC values result in low *C* factor values (close to 0) and high *C* factor (close to 1) values result from low FVC values. The higher the *C* factor values, the less their effect from crop and management practices and the higher their contribution to a high soil loss potential. For large areas in the northern, western and eastern headwater zones of the Xiangxi catchment and scattered plots in the backwater area, no C_{FVC} values were derived (Figs. 3a, 3b, and 3c). In fact, these areas are corresponding to areas showing FVC of 80% and more (Figs. 2a, 2b, and 2c). Applying the regression function established by YANG and SHI (1994) in order to predict *C* factor values from FVC, an FVC of 78.3% equals a *C* factor of 0.

The USLE is a prediction and assessment tool on the potential soil loss on agriculturally used land. Different cropping and management systems have an effect on soil erosion (WISCHMEIER and SMITH, 1965). Therefore, an FVC of 78.3% appears to be an adequate threshold to limit the calculation of *C* factor values if it is assumed that areas with FVC higher than 78.3% represent forest land. Taking only farmland into account and comparing C_{FVC} to C_{LIT}, a similar spatial pattern can be observed. C_{LIT} mainly appears on the scattered plots of farmland and alongside the river network in the headwater zone of the Xiangxi catchment and the largely used agriculturally backwater area. However, C_{FVC} is highly underestimated in terms of pixel counts (Table 1). This is as the supervised land use classification based on Landsat-TM images still shows areas with vegetation cover of more than 78.3% as farmland. Compared to C_{LIT}, based on the land use classification of 2007 as a reference to C_{FVC} 2007, the values of C_{FVC} are distinctly underestimated as well (Table 1). Approximately 85% to 89% of the total C_{FVC} values are below the lowest value of 0.08 of C_{LIT}.

C_{FVC} of 0.002 and below are typical for dense and nondense woodland (LIU and LUO, 2005), and therefore, it is not considered in C_{LIT} because the USLE is only applied to agriculturally used land. The reason of the high variability of C_{FVC} and C_{LIT} values can be found in the temporal dimension. Whereas C_{LIT} values represent common seasonal crop rotation within one year, and C_{FVC} corresponds to the given vegetation cover of the date of survey. Thus, the values on C_{FVC} based on the Landsat-TM images exclusively refer to the month September when the harvest of most of the crops, such as maize, begins. Only slight correlations between C_{FVC} and C_{LIT} are observed for settlement areas that are expected to show only small annual variations of FVC.

Taking into account that the C_{LIT} values represent the annual crop cycle, the mean potential soil loss in the Xiangxi catchment of 120.62 t ha^{-1} a^{-1} (Table 2) shows reliable estimates (SCHÖNBRODT ET AL., 2010, s*ubmitted*). The C_{LIT} values were obtained for several studies within the Three Gorges Reservoir area and are considered to reflect the real situation in the Xiangxi catchment.

Potential soil loss considering C_{FVC} values (Xiangxi catchment: 11.50 to 120.62 t ha^{-1} a^{-1} for 2007) is assumed to be strongly correlated to the time specific vegetation cover based on the date of survey of the Landsat-TM scenes.

ACKNOWLEDGMENTS

This study was conducted within the framework of the Sino-German Yangtze Project funded by the Federal German Ministry of Education and Research (BMBF) (No. 03 G 0669), and coordinated by the German Jülich Research Centre (FZJ). The authors would like to thank both for their support. We are also thankful to Xiang Wei and his students from the Faculty of Engineering, China University of Geosciences (CUG) in Wuhan for their collaboration and excellent support.

REFERENCES CITED

BEHRENS, T., SCHMIDT, K., SCHOLTEN, T., 2008. An approach to remove uncertainties in nominal environmental covariates and soil class maps. in: Hartemink, A.E., McBratney, A., Mendoca-Santos, M.L. (Eds.), Digital Soil Mapping with Limited Data. Springer-Verlag, New York, pp. 213-224.

BOETTINGER, J.L., RAMSEY, R.D., BODILY, J.M., COLE, N.J., KIENAST-BROWN, S., NIELD, S.J., SAUNDERS, A.M., STURM, A.K., 2008. Landsat spectral data for digital soil mapping. in: Hartemink, A.E., McBratney, A., Mendoca-Santos, M.L. (Eds.), Digital Soil Mapping with Limited Data. Springer-Verlag, New York, pp. 193-202.

BRADY, N.C., WEIL, R.R., 2007. The nature and properties of soil. 14th Edition. Prentice Hall, New Jersey, pp. 980.

CAI, Q.G., WANG, H., CURTIN, D., ZHU, Y., 2005. Evaluation of the EUROSEM model with single event data on steeplands in the Three Gorges Reservoir Areas, China. *Catena* 59 (1), 19-33.

DE ASIS, A.M., OMASA, K., 2007. Estimation of vegetation parameter for modeling soil erosion using linear spectral mixture analysis of Landsat ETM data. ISPRS *Journal of Photogrammetry and Remote Sensing* 62 (4), 309-324.

DE JONG, S.M., 1994. Derivation of vegetative variables from a Landsat TM image for modelling soil erosion. *Earth Surface Processes and Landforms* 19 (2), 165-178.

EASTMAN, J.R., FULK, M., 1993. Long sequence time-series map evaluation using standardized principal components. *Photogrammetric Engineering and Remote Sensing* 59 (6). 991-996.

ERENCIN, Z., 2000. C-Factor mapping using remote sensing and GIS - a case study of LOM Sak/Lom Kao, Thailand: [Dissertation]. ITC, Holland.

HE, K.Q., LI, X.R., YAN, X.Q., GUO, D., 2008. The landslides in the Three Gorges Reservoir region, China and the effects of water storage and rain on their stability. *Environmental Geology* 55 (1), 55-63.

HUANG, Z.Q., ZHOU, W.C., ZHOU, J.M., ZHU, M., 2006. Land use of the Three Gorges Reservoir Area and the effect on its landscape pattern in the recent 50 years. *Wuhan University Journal of Natural Sciences* 11 (4), 910-914.

JENSEN, J.R., 2000. Remote sensing of the environment: an earth resource perspective. Prentice Hall, New Jersey, pp. 544.

LILLESAND, T.M., KIEFER, R., CHIPMAN, J.W., 2007. Remote sensing and image interpretation. 6th Edition. John Wiley and Sons, New York, pp. 768.

LIU, Y., LUO, Z., 2005. A study on estimation of the amount of soil erosion in small watershed based on GIS: a case study in the Three Gorge Area of China. *International Geoscience and Remote Sensing Symposium Proceedings* 3, 1859-1863.

MCDONALD, B., WEBBER, M., DUAN, Y.F., 2008. Involuntary resettlement as an opportunity for development: the case of urban resettlers of the Three Gorges Project, China. *Journal of Refugee Studies* 21 (1), 82-102.

MENG, Q.H., FU, B.J., YANG, L.Z., 2001. Effects of land use on soil erosion and nutrient loss in the Three Gorges Reservoir Area, China. *Soil Use and Management* 17 (4), 288-291.

NEUBERT, M., MEINEL, G., 2005. Atmosphärische und Topographische Korrektur von IKONOS-Daten mit ATCOR. in: Strobl, J., Blaschke, T., Griesebner, G. (Eds.), Angewandte Geoinformatik 2005. Beiträge zum 17, AGIT-Symposium, Salzburg, Heidelberg, Wichmann, pp. 503-512 (in German).

PIMENTEL, D., 2006. Soil erosion: a food and environmental threat. *Environment Development and Sustainability* 8 (1), 119-137.

RENARD, K.G., FOSTER, G.R., WEESIES, G.A., MCCOOL, D.K., YODER, D.C., 1997. Predicting soil erosion by water: a guide to conservation planning with the Revised Universal Soil Loss Equation (RUSLE). USDA, Agriculture Handbook, Washington, DC. 703, pp. 384.

RICHARDS, J.A., JIA, X., 2006. Remote sensing digital image analysis: an introduction. 4th Edition, Springer-Verlag, Berlin. pp. 439.

RICHTER, R., 2010. Atmospheric/Topographic Correction for Satellite Imagery (ATCOR 2/3 User Guide, Version 7.1, January 2008). 165. http://atcor.ch/pdf/atcor3_manual.pdf

ROUSE, J.W., HAAS, R. W., SCHELL, J.A., HARLAN, J.C., 1974. Monitoring the vernal advancement and retrogradation (greenwave effect) of natural vegetation. NASA/GSFCT Type III Final Report, Greenbelt, MD, USA.

SCHÖNBRODT, S., EHRET, D., SEEBER, C., BEHRENS, T., FREI, M., ROHN, J., KING, L., KAUFMANN, H., XIANG, W., SUBKLEW, G., SCHOLTEN, T., 2010. Geo-risks in the highly dynamic Three Gorges Reservoir ecosystem: interactions of soil erosion, mass movements, and land use. *Earth Surface Processes and Landforms* (Submitted).

SEEBER, C., HARTMANN, H., XIANG, W., KING, L., 2010. Land use change and causes in the Xiangxi Catchment, Three Gorges Area derived from multispectral data. *Journal of Earth Science* 21 (6), 846-855.

SHI, Z.H., CAI, C.F., DING, S.W., WANG, T.W., CHOW, T.L., 2004. Soil conservation planning at the small watershed level using RUSLE with GIS: a case study in the Three Gorges Area of China. *Catena* 55 (1), 33-48.

SHI, X.Z., YU, D.S., XU, S.X., WARNER, E.D., WANG, H.J., SUN, W.X., ZHAO, Y.C., GONG, Z.T., 2010. Cross-reference for relating genetic soil classification of China with WRB at different scales. *Geoderma* 155 (3-4), 344-350.

SUN, X.X., ZHANG, J.X., LIU, Z.J., 2008. Vegetation cover annual changes based on MODIS/TERRA NDVI in the Three Gorges Reservoir Area. *The International Archives of the Photogrammetry, Remote Sensing and Spatial Information Sciences* 37(Part B7), 1397-1400.

SURIYAPRASIT, M., SHRESTHA, D.P., 2008. Deriving land use and canopy cover factor from remote sensing and field data in inaccessible mountainous terrain for use in soil erosion modelling. *The International Archives of the Photogrammetry, Remote Sensing and Spatial Information Sciences* 37 (Part B7), 1747-1750.

TAN, Y., BRYAN, B., HUGO, G., 2005. Development, land-use change and rural resettlement capacity: a case study of the Three Gorges Project, China. *Australian Geographer* 36 (2), 201-220.

TARBOTON, D.G., 1997. A new method for the determination of flow directions and upslope areas in grid digital elevation models. *Water Resources Research* 33 (2), 309-319.

WANG, G., WENTE, S., GERTNER, G.Z., ANDERSEN, A., 2002. Improvement in mapping vegetation cover factor for the Universal Soil Loss Equation by geostatistical methods with Landsat Thematic Mapper Images. *International Journal of Remote Sensing* 23 (18), 3649-3667.

WISCHMEIER, W.H., SMITH, D.D., 1965. Predicting rainfall - erosion losses from cropland east of the Rocky Mountains - guide for selection of practices for soil and water conservation. USDA, Agriculture Handbook, Washington DC, pp. 282.

WISCHMEIER, W.H., SMITH, D.D., 1978. Predicting rainfall erosion losses: a guide to conservation planning. USDA, Agriculture Handbook, Washington DC, pp. 537.

XU, Y.Q., PENG, J., SHAO, X.M., 2009. Assessment of soil erosion using RUSLE and GIS: a case study of the Maotiao River Watershed, Guizhou Province, China. *Environmental Geology* 56 (8), 1643-1652.

YANG, Y.S., SHI, D.M., 1994. Study on soil erosion in the Three Gorges Area of the Changgjiang River. Southeast Univ. Press, Nanjing (in Chinese).

ZHOU, P., 2008. Landscape-scale soil erosion modeling and ecological restoration for a mountainous watershed in Sichuan, China: [Dissertation]. Department of Forest Ecology, University of Helsinki, Helsinki, Finland.

ZHOU, P., LUUKKANEN, O., TOKOLA, T., NIEMINEN, J., 2008. Effect of vegetation cover on soil erosion in a mountainous watershed. *Catena* 75 (3), 319-325.

MANUSCRIPT 3

Approximation and Spatial Regionalization of Rainfall Erosivity Based on Sparse Data in a Mountainous Catchment of the Yangtze River in Central China

Published in ENVIRONMENTAL SCIENCE AND POLLUTION RESEARCH, January 2013

DOI: 10.1007/S11356-012-1441-8

Sarah Schönbrodt-Stitt[1)]*, Anna Bosch[1)], Thorsten Behrens[1)], Heike Hartmann[2)], Xuezheng Shi[3)], Thomas Scholten[1)]

1) Institute of Geography, Department of Physical Geography and Soil Science, University of Tübingen, Tübingen, Germany

2) Slippery Rock University, College of Health, Environment and Science, Department of Geography, Geology and the Environment, Slippery Rock, PA, USA

3) Chinese Academy of Sciences, Institute of Soil Science, Department for Soil Resources and Remote Sensing Application, Nanjing, P. R. China

* Corresponding author. University of Tübingen, Department of Geosciences, Chair of Physical Geography and Soil Science, Rümelinstraße 19-23, D-72070, Tübingen, Germany, Tel. +49 (0)7071 29 74054, Fax. + 49 (0)7071 29 5391, E-mail. sarah.schoenbrodt-stitt@uni-tuebingen.de

ABSTRACT

In densely populated countries like China, clean water is one of the most challenging issues of prospective politics and environmental planning. Water pollution and eutrophication by excessive input of nitrogen and phosphorous from nonpoint sources is mostly linked to soil erosion from agricultural land. In order to prevent such water pollution by diffuse matter fluxes, knowledge about the extent of soil loss and the spatial distribution of hot spots of soil erosion is essential. In remote areas such as the mountainous regions of the upper and middle reaches of the Yangtze River, rainfall data are scarce. Since rainfall erosivity is one of the key factors in soil erosion modeling, e.g., expressed as *R* factor in the Revised Universal Soil Loss Equation model, a methodology is needed to spatially determine rainfall erosivity. Our study aims at the approximation and spatial regionalization of rainfall erosivity from sparse data in the large (3,200 km²) and strongly mountainous catchment of the Xiangxi River, a first order tributary to the Yangtze River close to the Three Gorges Dam. As data

on rainfall were only obtainable in daily records for one climate station in the central part of the catchment and five stations in its surrounding area, we approximated rainfall erosivity as *R* factors using regression analysis combined with elevation bands derived from a digital elevation model. The mean annual *R* factor (R_a) amounts for approximately 5,222 MJ mm ha^{-1} h^{-1} a^{-1}. With increasing altitudes, R_a rises up to maximum 7,547 MJ mm ha^{-1} h^{-1} a^{-1} at an altitude of 3,078 m a.s.l. At the outlet of the Xiangxi catchment erosivity is at minimum with approximate R_a=1,986 MJ mm ha^{-1} h^{-1} a^{-1}. The comparison of our results with *R* factors from high-resolution measurements at comparable study sites close to the Xiangxi catchment shows good consistence and allows us to calculate grid-based R_a as input for a spatially high-resolution and area-specific assessment of soil erosion risk.

KEYWORDS

Rainfall erosivity, *R* factor, Soil erosion modeling, Spatial regionalization, Elevation bands, Three Gorges ecosystem, Yangtze River

1 INTRODUCTION

Soil erosion is one of the most pressing global environmental problems of our times. In the 1990s, 105 million hectares or 16% of the total land area of Europe (without Russia) were affected by soil erosion (JONES ET AL., 2012). New calculations by the Joint Research Centre of the EU estimate the current area affected by soil erosion to be 1.3 million km² for the EU-27. Approximately 20% of the area exhibits severe soil loss of more than 10 t ha^{-1} a^{-1} (JONES ET AL., 2012). Globally, China belongs to those countries most affected by soil erosion (e.g., HAO ET AL., 2004; CAI ET AL., 2005). The area affected by soil erosion by water is estimated to almost 3.7×10^6 km², accounting for about 38% of China's territory (HAO ET AL., 2004).

In the scientific discourse, the loss of soil by erosion is recognized as a silent global crisis affecting soil fertility, water storage and availability, food production, and climate change (e.g., MONTGOMERY, 2007). It also threatens the stability of ecosystems and socioeconomic structures (PIMENTEL, 2006). Discharge of sediments and particle-bounded agrochemicals, followed by a contamination of adjacent water bodies, can affect food security and drinking water quality in many parts of the world. In densely populated and fast-developing countries like China, clean water is one of the most challenging issues of prospective politics and environmental planning (BERGMANN ET AL., 2012).

Approximately 560,000 km² of the land area in the Yangtze River catchment is affected by soil erosion by water (ZHOU, 2008). In particular, the reservoir area of the Three Gorges Dam (TGD)

belongs to one of the most severely eroded area in the Yangtze River catchment, which is due to the rapid growth of population, coupled with the widespread deforestation and expansion of agricultural land during the last century (LU and HIGGITT, 2000). The TGD at the midstream of the Yangtze River causes massive environmental changes in a region that exhibits the highest soil erosion rates in China (ZHOU, 2008). The average soil loss rate by erosion in the reservoir area of the TGD is estimated to 32.8 t ha^{-1} a^{-1} (WU ET AL., 2011) and 120.62 t $ha^{-1}a^{-1}$ in the Xiangxi catchment within the reservoir area (SCHÖNBRODT ET AL., 2010). According to the Soil Erosion Rate Standard, Technological Standard of Soil and Water Conservation SD238-87 (c.f. XU ET AL., 2009) almost 77% of the total soil loss occur in areas of high to extreme erosion grades (WU ET AL., 2011).

The rapidly changing and highly dynamic land use and land management practices along the TGD (SEEBER ET AL., 2010; SUBKLEW ET AL., 2010) might still intensify soil erosion and the contamination of water bodies in the medium to long term (MENG ET AL., 2001). This, in fact, demonstrates the urgent need for reducing soil erosion in order to maintain the ecological and socioeconomic sustainability as well as the functionality of the TGD (SHI ET AL., 2004). In order to minimize soil erosion, e.g., through well-adapted land management and conservation practices, information on the quality and quantity of soil loss and its spatial and temporal variability is needed. For large areas, predictive tools such as erosion models are commonly applied. Such models can provide a scientific base for decision making by assessing current erosion processes and predicting future trends of soil erosion (MORGAN ET AL., 2011).

Since the detachment of soil particles by raindrop impact and their transport down slope by overland flow are the two main driving processes of soil erosion (CHORLEY, 1978; GHAHRAMANI ET AL., 2011), a good knowledge of the relevant properties of rainfall at a certain place is one essential precondition for sound soil erosion modeling. To describe these properties of precipitation, the term "rainfall erosivity" is used (WISCHMEIER 1962; STOCKING and ELWELL, 1976; LAL, 1990; HUDSON, 1995). The main intrinsic factors controlling rainfall erosivity are (1) total amount of rainfall, (2) duration of rainfall, (3) kinetic energy of rainfall, and (4) intensity of rainfall as well as its spatial and temporal variability within one rainfall event (e.g., WISCHMEIER and SMITH, 1958; SALAKO, 1995; AUERSWALD, 1998; SEUFFERT, 1998; NEARING ET AL., 2005).

Many rainfall simulation experiments showed that, especially the intensity and kinetic energy of rainfall are even more relevant than the amount of rainfall (e.g., WISCHMEIER and SMITH, 1978; NEARING ET AL., 2005). In this context, WISCHMEIER and SMITH (1958, 1978) developed the "energy-time-intensity" (*EI* index). Both the rainfall energy and intensity determine the rainfall erosivity that is directly proportional to the soil loss provided that all other erosive factors are held constant (TOY and FOSTER, 1998). For instance, the raindrops' mass and terminal velocity control the kinetic energy of a

rainfall event and thus widely determine the detachment of soil particles (MORGAN and NEARING 2011; SCHOLTEN ET AL., 2011; GEIßLER ET AL., 2012).

Besides the parameters directly linked to a rainfall event, the terrain also indirectly controls rainfall erosivity by the feature elevation (BOLINNE ET AL., 1980; GOOVAERTS, 1999; MIKHAILOVA ET AL., 1997; WANG ET AL., 2002). The formation of rainfall is connected to condensation processes that depend on the elevation. Thus, the precipitation is characterized by a vertical profile of air masses in the different mountain ranges (elevation zones) and appears as vertically differentiated (MÖLG ET AL., 2009).

Recent studies also show that wind direction and wind speed influence erosivity of rainfall by wind-driven raindrops to a certain extent (CORNELIS ET AL., 2004; ERPUL ET AL., 2005; DE LIMA ET AL., 2009).

Following these findings, a simple physical description of rainfall erosivity is almost impossible. Instead, most soil erosion models use rainfall intensity, rainfall duration, and/or kinetic energy alone to describe the role of precipitation for soil erosion (e.g., MORGAN and NEARING, 2011). One of such models is the so-called (Revised) Universal Soil Loss Equation (R)USLE (WISCHMEIER and SMITH, 1965; RENARD ET AL., 1997). The RUSLE is a well-established and worldwide applied empirical equation that uses the rainfall erosivity factor *R*, calculated following Eq. 1 (BROWN and FOSTER, 1987; RENARD ET AL., 1997):

$$R_a = \frac{1}{n} \sum_{j=1}^{n} \sum_{k=1}^{m_j} (EI_{30})_k \qquad \text{(Eq. 1)}$$

where R_a is the average annual rainfall erosivity (MJ mm ha^{-1} h^{-1} a^{-1}), n is the number of years of records, m_j is the number of erosive storm events of a given year j, and EI_{30} is the rainfall erosivity index of a single storm event k. EI_{30} is the product of the total storm kinetic energy (E) and the maximum 30-min intensity (I_{30}) and is defined as:

$$EI_{30} = \left(\sum_{r=1}^{0} e_r v_r \right) I_{30}$$

where e_r is the unit rainfall energy (MJha^{-1}mm^{-1}), and v_r is the rainfall volume (mm) during a time period r. I_{30} is the maximum rainfall intensity during a period of 30 min in the event (mmh^{-1}). e_r is defined as:

$$e_r = 0.29\,[1 - 0.72exp(-0.05 i_r)]$$

where i_r is the rainfall intensity during the time interval (mm h^{-1}).

RENARD ET AL. (1997) further define the criteria for the identification of an erosive single storm event, e.g., a threshold value of >12.7 mm to separate erosive from nonerosive rainfall as suggested by WISCHMEIER and SMITH (1978).

Numerous studies from different regions worldwide found that the *R* factor correlates the strongest with the soil loss (e.g., RENARD and FREIMUND, 1994). Thus, it is the most commonly used index for rainfall erosivity (WISCHMEIER, 1959; STOCKING and ELWELL, 1976; WISCHMEIER and SMITH, 1978; LO ET AL., 1985; RENARD and FREIMUND, 1994; FERRO ET AL., 1999; DE SANTOS LOUREIRO and DE AZEVEDO COUTINHO, 2001; WANG ET AL., 2002; SHAMSHAD ET AL., 2008; DIODATO and BELLOCCHI, 2009).

According to the empirical nature of the RUSLE, the *R* factor is regionally variable and must be determined for each region separately. Its precise calculation, however, necessitates consistent long-term measurements of precipitation for a recommended period of more than 22 years with a high temporal resolution to assess single storm events (WISCHMEIER and SMITH, 1978). For many regions worldwide, including the Xiangxi catchment at the Yangtze River, rainfall data are not available in a sufficient and adequate spatial and temporal resolution (ARNOLDUS, 1977; RICHARDSON ET AL., 1983; BAGARELLO and D'ASARO, 1994; RENARD and FREIMUND, 1994; YU and ROSEWELL, 1998; MIKHAILOVA ET AL., 1997; DE SANTOS LOUREIRO and DE AZEVEDO COUTINHO, 2001; DA SILVA, 2004). To overcome these restrictions, many approaches have been developed to calculate erosivity indexes and the *R* factor for specific regions with sparse data (e.g., YU and ROSEWELL, 1998; DA SILVA, 2004; SHAMSHAD ET AL., 2008; KAVIAN ET AL., 2011; ALIPOUR ET AL., 2012).

Those alternative approaches can be very effective according to their correlation with the soil loss due to their regional or scale-dependent determination approach (RENARD ET AL., 1997). They further show that, for many regions worldwide, monthly and daily precipitation data already offer a useful and valid approximation of rainfall erosivity when used for the region of origin (STOCKING and ELWELL, 1976, ARNOLDUS, 1977; LO ET AL., 1985; RENARD and FREIMUND, 1994). The same is true for the strength of correlation between such indices and the *R* factor of the RUSLE.

Due to the development of the RUSLE as empirical model based on data in the moderate climate zone in the Middle West of the USA, an adequate representation of rainfall erosivities of other climatic regions by the *R* factor calculated in its original way (Eq. 1) is questionable. Therefore, alternative erosivity indices were developed. The most common ones are the *KE>25* index by HUDSON (1995) and the AI_{max} by LAL (1976). The *KE>25* index classifies tropical rainfall events with <25 mmh^{-1} as non-relevant for soil erosion, since the intensity is too low to induce erosion processes

like particle detachment and overland flow (HUDSON, 1995). The AI_{max} is based on a physical weighting function and was developed in order to overcome the restrictions of climate-geographical transferability of the empirical RUSLE EI_{30} index (SUKHANOVSKI ET AL., 2002).

In addition, several studies have aimed at the assessment of the rainfall erosivity using regression functions. To meet the fact of scarce data availability, they mostly incorporate the amount of rainfall in temporal variation. Most regressions in the studies are based on annual precipitation P_a (e.g., VAN DER KNIJFF ET AL., 1999), precipitation per month P_m (FU ET AL., 2005), precipitation per day P_d (YU and ROSEWELL, 1998; MEN ET AL., 2008), and on single rainfall events or precipitation per hour P_e (e.g., MANNAERTS and GABRIELS, 2000). WISCHMEIER (1962) and ATESHIAN (1974) also use the return period of high precipitation totals based on the fact that the rainfall erosivity is strongly linked to extreme rainfall events (DVWK, 1990).

All these studies suggest that the *R* factor can be calculated satisfactorily with daily rainfall data instead of the highly data-requiring EI_{30} index. Furthermore, most approaches account for a region-specific modification and adaption of the *R* factor for climatic conditions different from those the empirical *R* factor was developed for originally. The majority of regression functions enable an approximation of rainfall erosivity particularly for humid climate conditions in the subtropics and tropics (e.g., ROOSE, 1976; MEN ET AL., 2008; SHAMSHAD ET AL., 2008; YU and ROSEWELL, 1998).

In this study, we aim at finding the best approximation for rainfall erosivity for subtropical rainfall regimes, represented by the Xiangxi catchment in Central China. The algorithm should allow to (1) overcome limited data and (2) to calculate the *R* factor of the RUSLE.

An area-wide, spatially explicit determination of *R* factors requires extrapolation, in our case based on elevation bands. Thus, the algorithm should be applicable for the whole range of topographic settings in such a highly mountainous region like the Xiangxi catchment.

2 MATERIAL AND METHODS

2.1 STUDY SITE

Our study area is the Xiangxi catchment (3,209 km², Figure 1) largely covering the counties Zigui, Xingshan, and Shennongjia located in western Hubei Province, Central China (SCHÖNBRODT ET AL., 2010). After a passage of nearly 100 km, the Xiangxi River joins the Yangtze River almost 40 km westward of the Three Gorges Dam as a first class tributary at 62 m a.s.l. The largest distance in the west-east direction is approximately 72 km and from north to south is approximately 73 km.

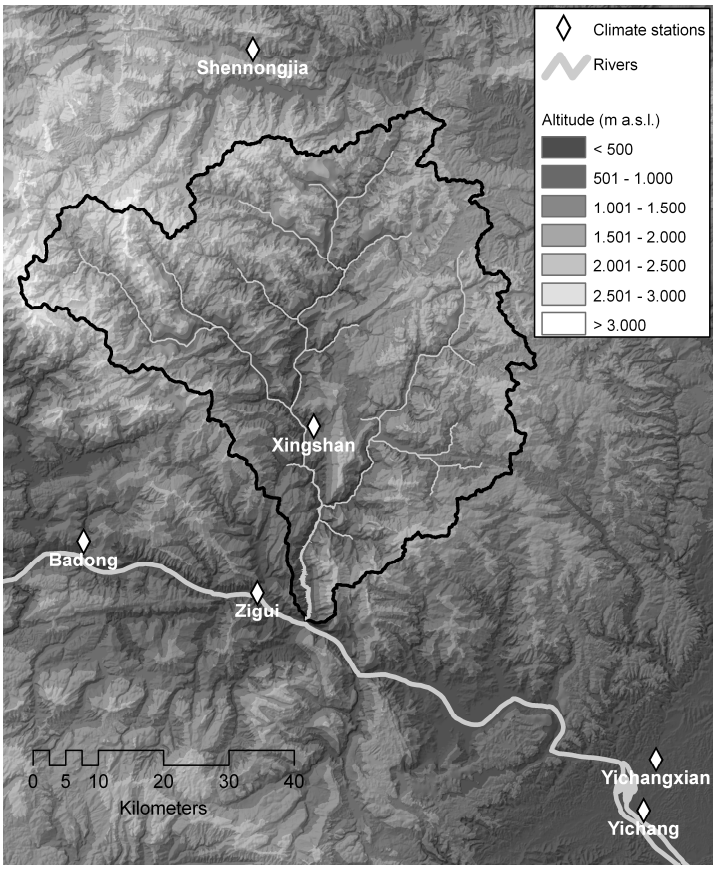

Figure 1 *Elevation range and location of climate stations in the Xiangxi catchment and its surrounding area. The DEM is derived from SRTM data (version 4, JARVIS ET AL., 2008).*

The Xiangxi catchment belongs to the humid subtropics of China and its climate is mainly characterized by prevailing winds from the north, and the influence of the southwest monsoon (HE ET AL., 2003). The mountainous terrain strongly impacts the climate in the Xiangxi catchment. The Qinling mountain range in the north of the catchment serves as climatic border between North and Central China that hinders the cold air masses from the north advancing to the south. As a consequence of the southwest monsoon and the barrier effect of the topography, the climate of the Xiangxi catchment typically exhibits hot humid summers and moderate dry winter seasons (HE ET AL., 2003). The study site shows a unimodal rainfall regime with one rainy season. Mean annual precipitation (MAP) at Xingshan climate station is 991 mm for the period 1971-2000 of which 78% falls between May and October (Figure 2). The mean annual temperature is 16.9 °C for the same period.

Seventy-three percent of the catchment area shows steep to extremely steep slopes with inclinations above 20° (mean slope angle, 39°; standard deviation, 22.8°). The mountainous relief of the Xiangxi catchment ranges from over 3,078 m a.s.l. (Mount Shennongjia) in the Shennongjia Forest

region to 62 m a.s.l. at the outlet (Figure 1). Mean elevation is 1,230 m a.s.l. The range of elevation causes a distinct vertical climate spectrum accounting for an orographic precipitation pattern (HE ET AL., 2003; WU ET AL., 2006). WU ET AL. (2006) differentiate five thermal zones according to the elevation in the Xiangxi catchment. These are from the outlet to the highest elevation: the Mid subtropics, the Northern subtropics, the Southern temperate, the Mid temperate, and the Northern temperate. Analogous to the thermal zones, WU ET AL. (2006) further define four elevation bands with (1) <500 m a.s.l., (2) 500-800 m a.s.l., (3) 800-1,200 m a.s.l., and (4) >1,200 m a.s.l., characterized by a strong correlation between precipitation, respectively temperature and elevation (WU ET AL., 2006). In the different zones, the annual precipitation increases progressively with the elevation from 1,000 mm at the outlet, to 1,200 mm at 500 m a.s.l., 1,600 mm at 800 m a.s.l., 2,000 mm at 1,200 m a.s.l., and 2,400 mm at elevations above 1,200 m a.s.l. (WU ET AL., 2006).

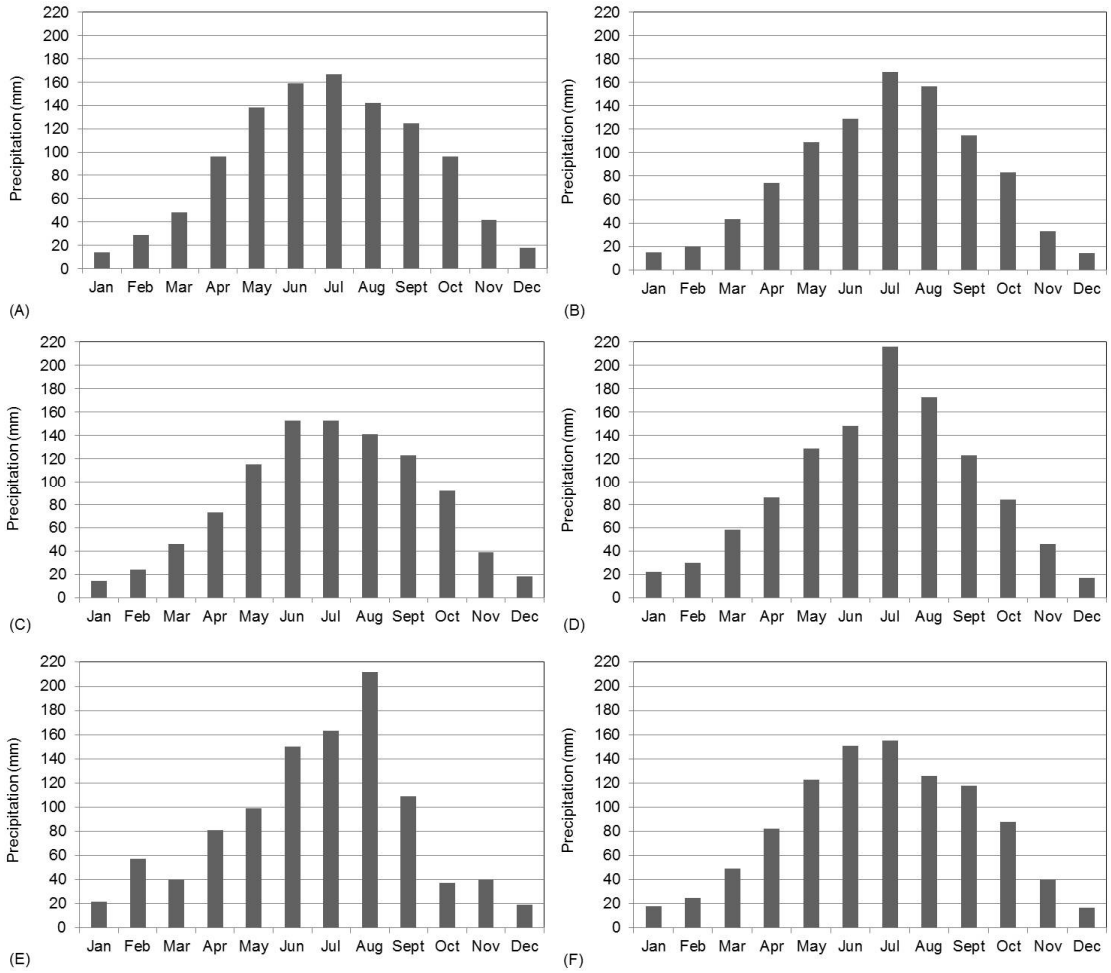

Figure 2 *Diagrams on mean monthly precipitation (mm) for (A) Badong station, (B) Shennongjia station, (C) Xingshan station, (D) Yichang station, (E) Yichangxian station, and (F) Zigui station. Except for Shennongjia (1975-2000) and Yichangxian stations (2003-2007) the data on precipitation refer to the WMO 30-years climate normal period from 1971 to 2000.*

2.2 GEODATABASE AND PROCESSING

For the derivation of rainfall erosivity from precipitation data and the regionalization of *R* factors in the Xiangxi catchment we used climate data from the National Meteorological Information Centre of China (NMIC) and a Digital Elevation Model (DEM). The DEM is generated from SRTM data in a spatial resolution of 90×90 m (version 4, JARVIS ET AL., 2008). We resampled it to 45×45 m in order to spatially fit other grids on ecosystem analyses in the Xiangxi catchment.

As daily precipitation data were only available for one station (Xingshan station) in the Xiangxi catchment, we decided to include precipitation data from five other available climate stations lying closest to the border of the Xiangxi catchment (Figure 1, Table 1). According to the NMIC, these stations are Badong, Shennongjia, Yichang, Yichangxian, and Zigui. Doing so enables us to enlarge the spatial data density. All stations belong to the low to medium mountain range between 134 and 950 m a.s.l. (Table 1). The periods of available data vary from nearly 30 to 50 years, except for Yichangxian station for which only 5 years of data were available. The precipitation data were preprocessed to meet homogeneity requirements. The homogeneity of the precipitation records was tested by calculating the von Neumann ratio, the cumulative deviations, the Bayesian procedures (BUISHAND, 1982), and by applying the standard normal homogeneity test (ALEXANDERSON, 1986). Inhomogenities were only identified for Zigui station with 1998 being the first year after a detected break. For the time period from 1998 to 2007 a homogeneity adjustment was conducted following the recommendations for the case of sudden shifts by AGUILAR ET AL. (2003). Mean annual precipitation (MAP), erosivity indices, and *R* factors for the stations Badong, Xingshan, Yichang, and Zigui refer to the climate normal period of 30 years from 1971 to 2000, recommended by the World Meteorological Organization (WMO) allowing comparison of observations and of climate trends. For Shennongjia and Yichangxian stations, statistics refer to the periods of available data from 1975 to 2000 and 2003 to 2007, respectively (Table 1).

Table 1 *Geographical position (UTM WGS 1984, Zone 49 N; X = Northing, Y = Easting), elevation, and length of daily rainfall records of the climate stations in the Xiangxi catchment and its surrounding area.*

Station	X	Y	Altitude (m a.s.l.)	Start date of record (day-month-year)	End date of record (day-month-year)	Length of daily record (year/month/day)	MAP (mm)
Badong	442491	3437891	295	01-07-1952	31-12-2007	45/06/00	1,074
Shennongjia	469423	3512773	950	01-01-1975	31-12-2007	32/11/29	961
Xingshan	477772	3455484	275	01-01-1958	31-12-2007	50/00/00	991
Yichang	528850	3396689	134	01-08-1951	31-12-2007	56/07/00	1,132
Yichangxian	530978	3396689	116	01-01-2003	31-12-2007	05/00/00	—
Zigui	469765	3429644	151	01-04-1959	31-12-2007	48/09/00	992

MAP mean annual precipitation

The worldwide application of the RUSLE brings along a diversity of units used for the assessment of soil loss and rainfall erosivity. To compare the results of different studies, we converted all units to the international standardized SI unit MJ mm ha^{-1} h^{-1} a^{-1} following FOSTER ET AL. (1981) and DETTLING (1989).

Due to the lack of a sufficient spatial and temporal data resolution for deriving *R* factors for the Xiangxi catchment, we made use of the findings from other studies (Table 4). In order to evaluate the power of the regressions applied in this study for the Xiangxi catchment, we compared our results with those reported by SHI ET AL. (2004), LIU and LUO (2005), WU ET AL. (2011), and SHI ET AL. (2012) for the reservoir area of the TGD.

Table 2 *Indices to approximate the erosivity of rainfall.*

Erosivity index	Region	Equation	Rainfall parameters	Author(s)
Fournier Index	West Africa	$F = \frac{P_{m_{max}}^{\ 2}}{MAP}$	F = Fournier index, P_{mmax}= mean prec. of the months with the highest total rainfall (mm), MAP = mean annual prec. (mm)	FOURNIER (1960)
AI_m Index	West Nigeria, Africa	$AI_m = \sum_{1}^{l} \frac{\sum_{1}^{k} a i_m}{100}$	a = amount of rainfall (cm), i_m = maximum intensity of a rainfall event (cm h^{-1}), k = 31, l = 12	LAL (1976)
Modified Fournier Index	Morocco, Africa	$F_{mod} = \frac{\sum_{i=1}^{12} P_m^{\ 2}}{MAP}$	F_{mod} = Modified Fournier Index, P_m = monthly prec. (mm), MAP = annual prec. (mm)	ARNOLDUS (1977)
Burst Factor	South Africa, Africa	$BF = \sum_{i=1}^{12} \frac{P_{d_{max;Mi}} P_{m;e>12.5}}{P_a}$	BF = Burst factor, P_a = annual prec. (mm), $P_{dmax;\,Mi}$ = maximum daily prec. in month i (mm), $P_{m;\,e>12.5}$ = monthly prec. from rainfall events ≥ 12.5 mm	SMITHEN and SCHULZE (1982)
Universal (Onchev's) Index		$UI = \frac{P_{e \geq 9.5;i \geq 0.18}}{\sqrt{D_{e;i \geq 0.18}}}$	UI = Universal index of one rainfall event, $P_{e \geq 9.5;\, i \geq 0.18}$ = amount of a rainfall event ≥ 9.5 mm and with an intensity i ≥ 0.18 mm min^{-1}, $D_{e;\, i \geq 0.18}$ = duration of the rainfall event with the intensity i ≥ 0.18 mm min^{-1}	ONCHEV (1985)

***Table 2** (continued)*

Erosivity index	Region	Equation	Rainfall parameters	Author(s)
KE>25 Index	Tropical Africa	$KE > 25 = E$	*KE* > *25* = KE > 25 index, *E* = kinetic energy of all rainfall events with an intensity of > 25 mm h^{-1}, the determination of *E* is analogous to EI_{30} by Wischmeier and Smith (1958)	HUDSON (1995)
A Index		$A = 10^{-2} \sum \Delta E\, b\, I_e{}^{\alpha}$ with: $\Delta E = 0.5 \rho \vartheta^2 \Delta k$ $\alpha = 0.9\,; b = 1 \;\; for\; I_e < 76\, mm\, h^{-1}$ $\alpha = 1\,; b = \frac{1}{1.22} \;\; for\; I_e \geq 76\, mm\, h^{-1}$	*A* = *A* index of one rainfall event, Δ*E* = kinetic energy of *n* raindrops with *ρ* = density of water (kg m^{-3}), *ϑ* = mean fall velocity of the raindrops (cm h^{-1}), Δ*h* = amount of precipitation within time step Δ*t* (mm), Δ*t* = time step (s), I_e = mean intensity of one rainfall event (m s^{-1})	SUKHANOVSKI ET AL. (2002)

MAP mean annual precipitation, prec. precipitation

2.4 SPATIAL REGIONALIZATION OF *R* FACTORS USING ELEVATION BANDS

For the regionalization of *R* factors, we considered the assumption of a causal relation between the amount of rainfall received and elevation (WU ET AL., 2006) as crucial. Since the strong influence of the elevation on precipitation is known, we further assumed that also the *R* factors strongly depend on the elevation based on the findings by WU ET AL. (2006).

We therefore calculated the increase of annual precipitation per 100 meters using Eq. 2:

$$\wedge P_a = \left(\frac{P_a 2 - P_a 1}{Elev2 - Elev1}\right) \times 100 \qquad \text{(Eq. 2)}$$

where ΔP_a is the increase of annual precipitation (mm) per 100 meters, P_a2 is the annual precipitation (mm) at the upper limit of the elevation band, P_a1 is the annual precipitation (mm) at the lower limit of the elevation band, and *Elev2* is the elevation (m a.s.l.) at the upper limit of the elevation band and *Elev1* is the elevation (m a.s.l.) at the lower limit of the elevation band.

Analogous to Eq. 2, the increase of mean annual *R* factors per 100 meters was calculated using Eq. 3:

$$\wedge R_a = \left(\frac{R_a 2 - R_a 1}{Elev2 - Elev1}\right) \times 100 \qquad \text{(Eq. 3)}$$

where ΔR_a is the increase of annual *R* factors (MJ mm ha^{-1} h^{-1} a^{-1}) per 100 meters, R_a2 is the mean annual *R* factor (MJ mm ha^{-1} h^{-1} a^{-1}) of the upper limit of the elevation band, R_a1 is the mean annual *R* factor (MJ mm ha^{-1} h^{-1} a^{-1}) of the lower limit of the elevation band, and *Elev2* is the elevation (m a.s.l.) at the upper limit of the elevation band and *Elev1* is the elevation (m a.s.l.) at the lower limit of the elevation band.

Table 3 *Regression functions to approximate the erosivity of rainfall based on the mean annual R factor R_a.*

Type of regression	Region	Equation	Rainfall parameters	Author(s)
Regression based on the return period of high precipitation sums	East Cost and Rocky Mountains, USA	$R_a = MAP\, P_{1/2}\, P_{24/2}\, k_1\, k_2$	R_a = mean annual *R* factor (100 foot tons inch $acre^{-1}h^{-1}$), MAP = mean annual prec. *(mm)*, $P^{1.2}$ = one-hour-prec. with two-years return period (mm), $P^{24.2}$ = 24-hour-prec. with two-years return period (mm) , k_1; k_2 = regional constants	WISCHMEIER (1962)
	USA	$R_a = P_{6/2}{}^{2.2}k$	R_a = mean annual *R* factor (foot ton inch $acre^{-1}h^{-1}a^{-1}$), $P_{6/2}$ = six-hour-prec. with two-years return period (mm), *k* = regional constant	ATESHIAN (1974)
Regression based on the mean annual precipitation MAP	West Africa	$R_a = (0.5 \pm 0.05)MAP$	R_a = mean annual *R* factor (100 foot tons inch $acre^{-1}h^{-1}a^{-1}$), MAP = mean annual prec. (mm)	ROOSE (1976)
	Belgium, Europe	$R_a = 159.56 + 0.27MAP$	R_a= mean annual *R* factor (tmcm$ha^{-1}h^{-1}10^{-2}$), MAP = mean annual prec. (mm)	BOLINNE ET AL. (1980)
Regression based on the mean annual precipitation MAP	Bavaria, Germany, Europe	$R_a = 0.083MAP - 1.77$	R_a = mean annual *R* factor (kJ mm m^{-2} h^{-1}), MAP = mean annual prec. (mm)	ROGLER and SCHWERTMANN (1981)
	Hawaii, USA	$EI_{30} = 3.48MAP + 38.46$	EI_{30} = mean annual EI_{30} index ($100Nh^{-1}$), MAP = mean annual prec. (cm)	LO ET AL. (1985)

***Table 3** (continued)*

Type of regression	Region	Equation	Rainfall parameters	Author(s)
	North Italy, Europe	$R_a = MAP_i$	R_a = mean annual R factor (MJ mm ha^{-1} h^{-1} a^{-1}), MAP$_i$ = mean prec. in year i (mm)	VAN DER KNIJFF (1999)
Regression based on precipitation per month P_m	Loess Plateau, China	$R_a = 8\,(3462 P_{m;\,d \geq 9}^{2670})$	R_a = mean annual R factor (MJ km^{-2} h^{-1} a^{-1}), P_{m9} = mean prec. per month for days with prec. with ≥ 9 mm (mm)	FU ET AL. (2005)
Regression based on precipitation per day P_d	New South Wales, Australia	$R_{mj} = \alpha[1 + \mu \cos(2\pi f j - \omega)] \sum_{k=1}^{n} P_{d>12.7}^{\beta}$ with: $f = \frac{1}{12}$ $\omega - \frac{\pi}{6}$ $\alpha = 0.369\,(1 + 0.098^{\frac{3.26\varphi}{MAP}})$ $\beta = 1.49$ $\mu = 0.29$	R_{mj} = R factor of the month j (MJ mm ha^{-1} h^{-1}), $P_{d>12.7}$ = daily prec. of days with ≥ 12.7 mm (mm), n = number of days with prec. with ≥ 12.7 mm, k = index of the number of days with prec. with ≥ 12.7 mm, α, β, μ = regional constants, MAP = mean annual precipitation (mm), φ = mean prec. during summer season (May-October) (mm)	YU and ROSEWELL (1998)
	Cape Verde	$EI_{30} = 0.0723 P_{d;\,d \geq 9}^{1.58}$	EI_{30} = EI_{30} Index of a rainfall event (kJ mm m^{-2} h^{-1}), $P_{d;\,d \geq 9}$ = daily prec. of days with ≥ 9 mm (mm)	MANNAERTS and GABRIELS (2000)
Regression based on precipitation per day P_d	Portugal, Europe	$EI_{30_{month}} = 7.05 rain_{10} - 88.92 days_{10}$	$EI_{30month}$ = EI_{30} Index of a month (MJ mm ha^{-1} h^{-1}), $rain_{10}$ = monthly prec. from days with ≥ 10 mm (mm), $days_{10}$ = number of days in one month with prec. with ≥ 10 mm	DE SANTOS LOUREIRO and DE AZEVEDO COUTINHO (2001)

***Table 3** (continued)*

Type of regression	Region	Equation	Rainfall parameters	Author(s)
	Malaysia	(i): $EI_{30} = 6.97 rain_{10} - 11.23 days_{10}$ (ii): $EI_{30} = (0.266 rain_{10}^{2.071})(days_{10}^{-1.367})$	EI_{30} = EI_{30} Index of one month (MJmmha^{-1}h^{-1}), $rain_{10}$ = monthly prec. from days with ≥ 10 mm (mm), $days_{10}$ = number of days in one month with prec. with ≥ 10 mm	SHAMSHAD ET AL. (2008)
Regressions based on single rainfall events or rainfall per hour	Rhodesia, Africa	$R_a = \left[\sum_{k=1}^{n} E_k i_k\right]$ with: $E_k = 29.8 - \frac{127.5}{I_k}$	R_a = R factor of one year (J mm m^{-2} h^{-1}), E_k = kinetic energy of a rainfall event (J m^{-2} mm^{-1}), I_k = rainfall intensity (mm h^{-1}), k = index of the number of rainfall events within one year, n = number of rainfall events within one year with > 12.5 mm (mm)	STOCKING and ELWELL (1976)
	West Amazonia	$R_{e/d} = 0.335 P_{e/d \geq 13}^{1.81}$	$R_{e/d}$ = R factor of a rainfall event or of a day respectively (MJ mm ha^{-1} h^{-1}), $P_{e/d \geq 13}$ = prec. of a rainfall event or of a day with ≥ 13 mm respectively (mm)	ELSENBEER ET AL. (1993)
	Sicily, Italy	$R_{e/d} = k_1 P_{e/d \geq 13}^{k_2}$ with: $k_1 = 0.332$ $k_2 = 1.548$	$R_{e/d}$ = R factor of a rainfall event or of a day respectively (MJ mm ha^{-1} h^{-1}), $P_{e/d \geq 13}$ = prec. of a rainfall event or of a day with ≥ 13 mm respectively (mm), k_1, k_2 = regional constants for Sicily	BAGARELLO and D'ASARO (1994)
Regressions based on single rainfall events or rainfall per hour	Cape Verde	$R_e = 0.06 P_{e<9}^{1.81} D_e^{-0.36}$	R_e = R factor of a rainfall event (kJ mm m^{-2} h^{-1}), $P_{e<9}$ = prec. of a rainfall event with < 9 mm (mm), D_e = duration of this rainfall event (h)	MANNAERTS and GABRIELS (2000)

Table 3 *(continued)*

Type of regression	Region	Equation	Rainfall parameters	Author(s)
	South Italy	$R_m = 0.01174 \left(\sqrt{P_m \cdot P_{d_{max;Mi}}^{0.52} \cdot P_{h;Mi}^{1.18}}\right)$	R_m = *R* factor of a month (MJ mm ha^{-1} h^{-1}), P_m = monthly prec. (mm), $P_{dmax;\,Mi}$ = maximum daily prec. in month *i* (mm), $P_{h;\,Mi}$ = maximum prec. per hour in month *i* (mm)	DIODATO and BELLOCCHI (2009)
Regressions based on the Fournier Index *F*	East Brazil	$R_m = 42.307F + 69.763$	R_m = *R* factor of a month (MJ mm ha^{-1} h^{-1} a^{-1}), *F* = Fournier Index	DA SILVA (2004)
	Malaysia	$R_m = 227F^{0.549}$	R_m = *R* factor of a month (MJ mm ha^{-1} h^{-1} a^{-1}), *F* = Fournier Index	SHAMSHAD ET AL. (2008)
Regressions based on the Modified Fournier Index F_{mod}	Morocco, Africa	$R_a = 0.264F_{mod}^{1.5}$	R_a = mean annual *R* factor (tm cm ha^{-1} h^{-1} a^{-1}), F_{mod} = Modified Fournier Index	ARNOLDUS (1977)
	Belgium, Europe	$R_a = -168.42 + 3.27F_{mod}$	R_a= mean annual *R* factor (tm cm ha^{-1} h^{-1}10^{-2}), F_{mod} = Modified Fournier Index	BOLINNE ET AL. (1980)
	Bavaria and Hesse, Germany	$R_a = 15.485 + 0.602F_{mod}$	R_a = mean annual *R* factor (kJ mm m^{-2} h^{-1}), F_{mod} = Modified Fournier Index	DVWK (1990)
	East China	$R_a = \alpha F_{mod}^{\beta}$ with: $\alpha = 10^{2.124-1.496\beta+0.00214P_{d_{max}}}$ $\beta = 0.8363 + \frac{18.144}{P_{d_{>12}}} + \frac{24.455}{MAP_{>12}}$	R_a = mean annual *R* factor (MJ mm h m^{-2} h^{-1} a^{-1}), F_{mod} = Modified Fournier Index, P_{dmax} = maximum daily prec. in an average year, $P_{d>12}$ = mean daily prec. with > 12 mm (mm), $MAP_{>12}$ = mean annual prec. from days with > 12 mm prec. (mm)	MEN ET AL. (2008)

prec. precipitation

The derivation of elevation bands was done using ArcGIS 10.0. Finally, *R* factors were assigned to each pixel in the DEM according to the increase of *R* factors within the elevation band in order to spatially regionalize the erosivity of rainfall in the Xiangxi catchment.

Table 4 *Mean annual R factors for different study areas in the humid subtropics in China.*

Autor(s)	Study site	MAP (mm)	Elevation m (a.s.l.)	Slope (°)	*R* factor (MJ mm ha^{-1} h^{-1} a^{-1})	Method
WU ET AL. (2011)*	Three Gorges Reservoir Area (size = 57,600 km²)	1,000 - 1,200	19 - 2,964	range: 0-85° average: 17.9°	range: 3,576 - 6,717, average: 4,745	cited in ZHANG and FU (2003)
SHI ET AL. (2004)	Wangjiaqiao watershed, Hubei Province (size = 16.7 km²)	1,016	184 - 1,180 cited in (SHI ET AL., 2012)	range: 2-58° average: 23° (cited in SHI ET AL., 2012)	average: 2,880	WISCHMEIER and SMITH (1978)
LIU and LUO (2005)	Taipingxi watershed, Hubei Province (size = 26.14 km²)	1,300	80-1,321	not mentioned	average: 4,969	WISCHMEIER and SMITH (1978)
SHI ET AL. (2012)	Wangjiaqiao watershed, Hubei Province (size = 16.7 km²)	1,016	184 - 1,180	range: 2-58° average: 23°	range: 3,187.9 - 8,029.9 average: 4,928	WISCHMEIER and SMITH (1978)

*MAP mean annual precipitation. F_{mod} Modified Fournier Index. *The study region by WU ET AL. (2011) does not cover Shennongjia County with the Mount Shennongjia (3,078 m a.s.l.) that is covered by the Xiangxi catchment.*

3 RESULTS AND DISCUSSION

3.1 MEAN ANNUAL PRECIPITATION AND EROSIVITY INDICES

With 1,132 mm Yichang station exhibits the highest MAP (Table 1). MAP at Badong, Xingshan, and Zigui are 1,074, 991, and 992 mm, respectively. Shennongjia shows the lowest MAP of all stations with 961 mm.

Only three of the erosivity indices developed for worldwide application are suitable for our study area because they can be calculated using daily precipitation data only. These are (1) the Burst factor, (2) the Fournier index (F), and (3) the modified Fournier index (F_{mod}). However, we only calculated F and F_{mod} (Tables 3 and 4). Due to the fact that SMITHEN and SCHULZE (1982) do not give an erosivity classification of the Burst factor and do not explain its quantitative relation to the EI_{30} index, the Burst factor cannot be sufficiently evaluated here.

Both F and F_{mod} can directly be used to approximate the R factor (Table 3).

In terms of our data availability, the regressions of DA SILVA (2004) and SHAMSHAD (2008) can be applied for calculating F. For the F_{mod}, we tested the regressions of ARNOLDUS (1977), BOLINNE ET AL. (1980), DVWK (1990), and MEN ET AL. (2008).

The erosivity indices F and F_{mod} are highest for Yichang (Table 5). F for all stations lies within class 2 of the classification of the Fournier index (ODURO-AFRIYE, 1996) indicating low erosivity risk except for Yichang station. Yichang station exceeds the values up to moderate erosivity risk (class 3), which is due to a higher MAP.

F_{mod} for all stations show higher index values ranging from 131.8 (Shennongjia station) to 166.7 (Yichang station). Compared to MAP, the F_{mod} also shows a consistent distribution (Table 5) with Yichang showing the highest and Shennongjia the lowest F_{mod}.

Both indices vary not only with MAP but with annual rainfall distribution as well (Table 1 and 5). F considers the precipitation of that month with the maximum precipitation and the MAP. Thus, Shennongjia shows distinct lower MAP (961 mm) than Badong station (1,074 mm) but a higher F of 28.7 compared to 26.9 for Badong because the maximum monthly rainfall during July is slightly higher than for Badong (Badong, 167 mm; Shennongjia, 169 mm; Figure 2).

The F_{mod} combines the precipitation totals of all months and MAP (Table 2). Typically, the F_{mod} shows higher correlation with MAP than F (RENARD ET AL., 1997). This is also true for the Xiangxi catchment where the F_{mod} stronger correlates with MAP (Figure 3).

Consequently, we decided for the F_{mod} to approximate the R factor using the regressions according to ARNOLDUS (1977), BOLINNE ET AL. (1980), DVWK (1990), and MEN ET AL. (2008).

3.2 *R* FACTORS

Along with the F_{mod} we focused on regressions (Table 3) based on (1) annual precipitation sums P_a (ROOSE, 1976; BOLINNE ET AL., 1980; ROGLER and SCHWERTMANN, 1981; LO ET AL., 1985; VAN DER KNIJFF ET AL., 1999) and regressions based on (2) daily precipitation P_d (ELSENBEER ET AL., 1993; BAGARELLO and D'ASARO, 1994; YU and ROSEWELL, 1998; MANNAERTS and GABRIELS, 2000; DE SANTOS LOUREIRO and DE AZEVEDO COUTINHO, 2001; SHAMSHAD ET AL., 2008; MEN ET AL., 2008).

Due to a lack of discussion of units, we did not use the equation to calculate the R factor proposed by FU ET AL. (2005). Regressions based on the return period of high precipitation totals (WISCHMEIER, 1962; ATESHIAN, 1974) and those requiring rainfall data per hour or per rainfall events (STOCKING and ELWELL, 1976; MANNAERTS and GABRIELS, 2000; DIODATO and BELLOCCHI, 2009)

were also excluded from further analysis due to lack of rainfall records with the necessary time resolution.

Table 5 *Mean erosivity indices for the approximation of the rainfall erosivity and mean annual R factors R_a (MJ mm ha^{-1} h^{-1} a^{-1}) for the Xiangxi catchment calculated from 1971 to 2000 based on erosivity indices and regression equations.*

Type of approximation/Author(s)	Climate station				
	Badong	Shennongjia	Xingshan	Yichang	Zigui
Erosivity indices					
Fournier Index (FOURNIER, 1960)	26.9	28.7	23.5	41.1	24.2
Modified Fournier Index (ARNOLDUS, 1977)	152.9	131.8	138.4	166.7	138.5
R factors based on regression equations using the mean annual precipitation MAP					
ROOSE (1976)	9,225.2	8,149.1	8,483.7	9,684.5	8,482.3
BOLINNE ET AL. (1980)	44.3	41.0	42.0	42.0	42.0
ROGLER and SCHWERTMANN (1981)	882.0	777.1	809.7	809.7	809.6
LO ET AL. (1985)	415,709.4	371,702.0	385,388.1	434,490.9	385,327.8
VAN DER KNIJFF (1999)	1,409.2	1,244.8	1,296.0	1,479.4	1,295.7
R factors based on regression equations using precipitation per day P_d					
ELSENBEER ET AL. (1993)	5,093.2	3,130.7	4,091.7	5,575.1	4,168.6
BAGARELLO and D'ASARO (1994)	1,853.0	1,231.6	1,546.9	2,001.4	1,562.3
YU and ROSEWELL (1998)	4,895.2	3,285.0	4,121.2	5,400.6	4,142.0
MANNAERTS and GABRIELS (2000)	4,784.9	3,345.5	4,009.0	5,276.4	4,079.4
DE SANTOS LOUREIRO and DE	2,977.5	1,972.9	2,505.2	3,179.7	2,520.6
SHAMSHAD ET AL. (2008)	5,417.9	4,266.3	4,908.6	5,791.3	4,838.4
R factors based on regression equations using the Modified Fournier Index F_{mod}					
ARNOLDUS (1977)	4,898.5	3,919.1	4,215.2	5,573.7	4,223.9
BOLINNE ET AL. (1980)	32.5	25.7	27.8	36.9	27.9
DVWK (1990)	1,075.7	948.5	988.0	1,158.5	989.1
MEN ET AL. (2008)	2,157.9	1,821.4	1,981.3	2,579.3	1,983.7

The resulting *R* factors of the tested regression equations vary strongly (Table 5). They range from lowest approximately 26 to highest 434,491 MJ mm ha^{-1} h^{-1} a^{-1}.

In order to evaluate the power of the regressions applied in this study for the Xiangxi catchment, we compared our results with those reported by SHI ET AL. (2004), LIU and LUO (2005), WU ET AL. (2011), and SHI ET AL. (2012). The *R* factors from these studies are based on high-resolution rainfall measurements using the method by WISCHMEIER and SMITH (1978). The study sites

are located close to our study site in the Three Gorges reservoir area, e.g., in Zigui county 50 km northwest of the TDG (Wangjiaqiao watershed) and in Yichang county 5 km northwest of the TGD (Taipingxi watershed). They exhibit a humid subtropical monsoon climate regime and mountainous topography. In terms of MAP and range of elevation these study sites are directly comparable to the Xiangxi catchment. Thus, based on this precondition of physio-geographic comparability, we decided to handle these study results as adequate evaluation data.

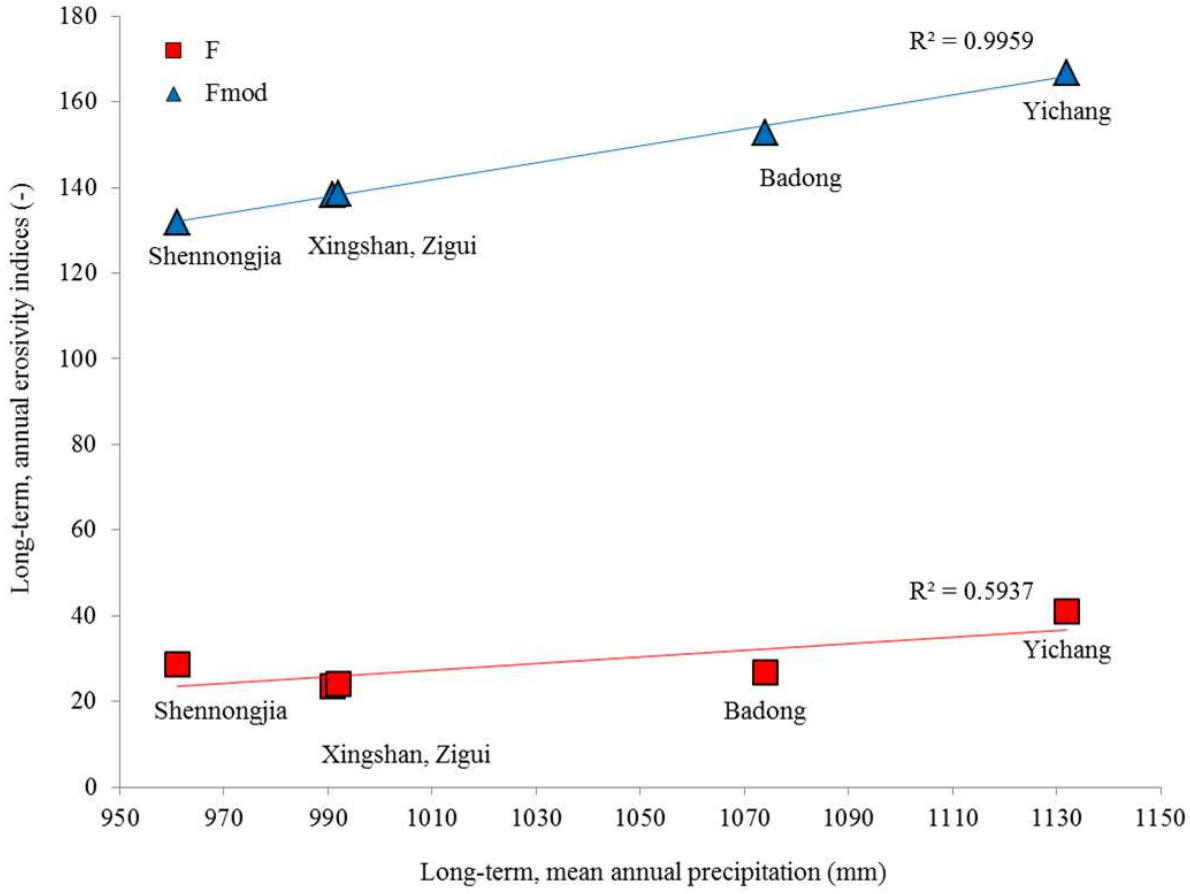

Figure 3 *Relation between long-term, mean annual precipitation and long-term, annual erosivity indices Fournier Index F and Modified Fournier Index* F_{mod}.

The MAP in the study sites from the evaluation data ranges from 1,016 to 1,300 mm and accounts for humid subtropical climate with monsoonal rains (LIU and LUO, 2005). With a total range of elevation from 19 to 2,964 m a.s.l. the evaluation data cover the low to high mountain range (Table 4) as we can observe it in the Xiangxi catchment. The topography in the evaluation study sites is characterized by a prevalence of steep sloping hills and mountains of average 18-23° (SHI ET AL., 2004, 2012; WU ET AL., 2011). Exhibiting these climatic and topographic settings, the evaluation sites

are directly comparable to the Xiangxi catchment in terms of precipitation characteristics, mountain range, and morphology (c.f. "Study site").

The results of our study show that the *R* factors calculated according to ROOSE (1976) are distinctly higher (8,149-9,225 MJ mm ha^{-1} h^{-1} a^{-1}) than the evaluation data sets of SHI ET AL. (2004, 2012), LIU and LUO (2005), and WU ET AL. (2011). This reflects the different climatic conditions in Roose's study region (tropical West Africa close to the equator with two rainy seasons) for which the regression function was developed. Thus, the relation between the *R* factor and the total annual precipitation is not valid for mountainous regions like the Three Gorges Project area and other transition areas with unimodal annual rainfall patterns (ROOSE, 1976).

Ranging from approximately 777-882 MJ mm ha^{-1} h^{-1} a^{-1}, the *R* factor values derived from the regression by ROGLER and SCHWERTMANN (1981) are distinctly lower than the evaluation data (Table 5). The regression proposed by ROGLER and SCHWERTMANN (1981) is based on mean annual rainfall data and was conducted from experiments in Bavaria in Germany. Due to distinct lower MAP in the moderate climate zone, this regression strongly underestimates the rainfall erosivity in the subtropical Xiangxi catchment. The same is true for the *R* factor values derived from the regression by the DVWK (1990) ranging approximately 949-1,159 MJ mm ha^{-1} h^{-1} a^{-1} that are lower compared to our "target" values of R_a.

Ranging from 1,231 and 1,245 MJ mm ha^{-1} h^{-1} a^{-1} for Shennongjia station to 2,001 and 1,479 MJ mm ha^{-1} h^{-1} a^{-11} for Yichang station, the *R* factor values derived from the regressions by BAGARELLO and D'ASARO (1994) and VAN DER KNIJFF ET AL. (1999) are also distinctly less than our evaluation data. These we due to semiarid to moderate climate regimes which are characterized by the effect of the Mediterranean Sea for Sicily (BAGARELLO and D'ASARO, 1994) and the effect of the Alps for North Italy (VAN DER KNIJFF ET AL., 1999). Both regression models incorporating MAP and single storm events (Table 3) do not account for the humid monsoonal rainfall regime in the Xiangxi catchment and provide an underestimation of the rainfall erosivity. Also the *R* factor values derived from the regression by DE SANTOS and DE AZEVEDO COUTINHO (2001) ranging from 1,973 MJ mm ha^{-1} h^{-1} a^{-1} for Shennongjia station to 3,180 MJ mm ha^{-1} h^{-1} a^{-1} for Yichang station are in their total range slightly less than our evaluation data. Here, the rainfall erosivity is based on a regression using the EI_{30} index derived for Portugal with a dry summer season and humid winter season, which is completely opposite to the precipitation pattern in the Xiangxi catchment with a rainfall maximum of 78% from May to October.

Compared to all other *R* factors calculated for the Xiangxi catchment, those based on the regressions by BOLINNE ET AL. (1980) and LO ET AL. (1985) can be interpreted as outliers (Table 5).

BOLINNE ET AL. (1980) incorporated MAP and the F_{mod} resulting in *R* factors ranging from approximately 41 to 44 MJ mm ha^{-1} h^{-1} a^{-1} and approximately 26 to 37 MJ mm ha^{-1} h^{-1} a^{-1}. Both regression functions are based on three stations in Belgium only. Due to the small data base and the different climatic conditions, the regression is not applicable to the Xiangxi catchment.

Those *R* factors calculated according to the regression by LO ET AL. (1985) developed for conditions in Hawaii show extreme high values ranging from approximately 371,702 to 434,491 MJ mm ha^{-1} h^{-1} a^{-1}. However, it must be considered that Hawaii exhibits extreme rainfall events in terms of amount and intensity and thus extremely high rainfall erosivity (LO ET AL., 1985).

Concluding, a transfer of the regression functions by ROOSE (1976), BOLINNE ET AL. (1980), ROGLER and SCHWERTMANN (1981), LO ET AL. (1985), DVWK (1990), BAGARELLO and D'ASARO (1994), VAN DER KNIJFF ET AL. (1999), and DE SANTOS and DE AZEVEDO COUTINHO (2001) to the conditions in the Xiangxi catchment is not recommended due to different climatic settings.

The results based on the regressions according to ARNOLDUS (1977), ELSENBEER ET AL. (1993), YU and ROSEWELL (1998), MANNAERTS and GABRIELS (2000), MEN ET AL. (2008), and SHAMSHAD ET AL. (2008) correspond with the results using the evaluation data (Tables 4 and 5).

However, due to the bimodal rainfall regime for Peninsular Malaysia (MAP of 2,500 mm) and Western Amazonia (MAP of 3,300 mm) showing tropical erosive events, for which the regression by SHAMSHAD ET AL. (2008) and ELSENBEER ET AL. (1993) were derived, we assume that this equation is not transferrable to the climatic settings in the Xiangxi catchment. The same can be concluded for the regressions by ARNOLDUS (1977) and MANNAERTS and GABRIELS (2000). The regressions were conducted for Morocco characterized by Saharan-continental to Mediterranean climate and for the Cape Verde with annual rainfalls ranging from 150 to 800 mm in an area with a maximum elevation of 1,000 mm. We assume that the orographic effect on precipitation that WU ET AL. (2006) described for the Xiangxi catchment and thus rainfall erosivity cannot be revealed adequately using both equations.

The regression derived by YU and ROSEWELL (1998) rely on data from New South Wales in South Australia exhibiting an arid to humid subtropical and oceanic climate. MEN ET AL. (2008) conducted the regression from data from the North China Plain (MAP of 350-818 mm) characterized by semi-arid conditions. The regressions are based on daily precipitation data and F_{mod}.

The resulting *R* factor values lie within the range of our evaluation data (Table 4). The regression by MEN ET AL. (2008) integrates F_{mod} accounting for the maximum daily precipitation of days with more than 12 mm and the average, annual summed precipitation from days with more than 12 mm precipitation. The threshold value of 12 mm is similar to the threshold value of 12.7 mm as suggested by WISCHMEIER and SMITH (1978) and was reported as a practical threshold for separating

erosive and nonerosive storms for the Yellow River basin in China (XIE ET AL., 2002). Thus, F_{mod} combines the precipitation totals of all single erosive storm events within 1 year and correlates with MAP (c.f. "Mean annual precipitation and erosivity indices"). The regression by YU and ROSEWELL (1998) also accounts for single erosive storm events using the threshold value of 12.7 mm precipitation (Table 3). However, the regression by YU and ROSEWELL (1998) considers regional relations derived from 79 stations in New South Wales, and the tropics. We assume that the regional constants accounting for the broad range of rainfall regimes in the study region of YU and ROSEWELL (1998) cannot be adequately transferred to the subtropical Xiangxi catchment.

Consequently, we decided to continue our analysis with the *R* factors according to MEN ET AL. (2008). This method fits best to our objectives regarding sparse data considering the precipitation characteristics in the Xiangxi catchment.

3.3 SPATIAL DISTRIBUTION OF *R* FACTORS

Given the causal relation between precipitation and elevation in the Xiangxi catchment as stated by WU ET AL. (2006) (c.f. "Study site"), we also assume an increase of R_a depending on the increase of precipitation with the elevation. Thus, we spatially regionalized the *R* factors based on elevation bands taking into account (1) R_a in each elevation band and (2) the increase of R_a within each elevation band.

Based on the linear, high correlation between MAP and R_a (Figure 4), mean annual *R* factors for each elevation band in the Xiangxi catchment could be derived according to the division method by WU ET AL. (2006) using Eq. 4:

$$R_a = 3.9723\text{MAP} - 1{,}986.8 \text{ (with } r^2 = 0.94) \quad \text{(Eq. 4)}$$

with R_a = mean annual *R* factor (MJ mm ha^{-1} h^{-1} a^{-1}) calculated according to MEN ET AL. (2008) for the according elevation band and MAP = mean annual precipitation (mm).

Analogous to the increase of P_a in the different elevation bands as stated by WU ET AL. (2006), R_a increases progressively from about 1,986 MJ mm ha^{-1} h^{-1} a^{-1} at the outlet to 7,547 MJ mm ha^{-1} h^{-1} a^{-1} at the highest elevation in the Xiangxi catchment (Table 6).

The increase in P_a per 100 m using Eq. 2 and the increase in R_a per 100 m using Eq. 3 are given in Table7. Below 500 m a.s.l. the increase in P_a is almost 46 mm per 100 m (Table 7). This accounts for an increase of R_a of approximately 181 MJ mm ha^{-1} h^{-1} a^{-1} per 100 m. With approximately 530 MJ mm ha^{-1} h^{-1} a^{-1} per 100 m the highest increase in R_a can be observed within the elevation band from 500 to 800 m a.s.l. (Table 7). This is due to the high increase of *Pa* from 1,200 to 1,600 mm in

the humid northern subtropics in the Xiangxi catchment with intensive convective precipitation (HE ET AL., 2003). The lowest increase in P_a of 21 mm per 100 m accounts for an increase of R_a of approximately 85 MJ mm ha^{-1} h^{-1} a^{-1} per 100 m for altitudes above 1,200 m a.s.l. in the mid- and northern temperate zone of the Xiangxi catchment (Table 7).

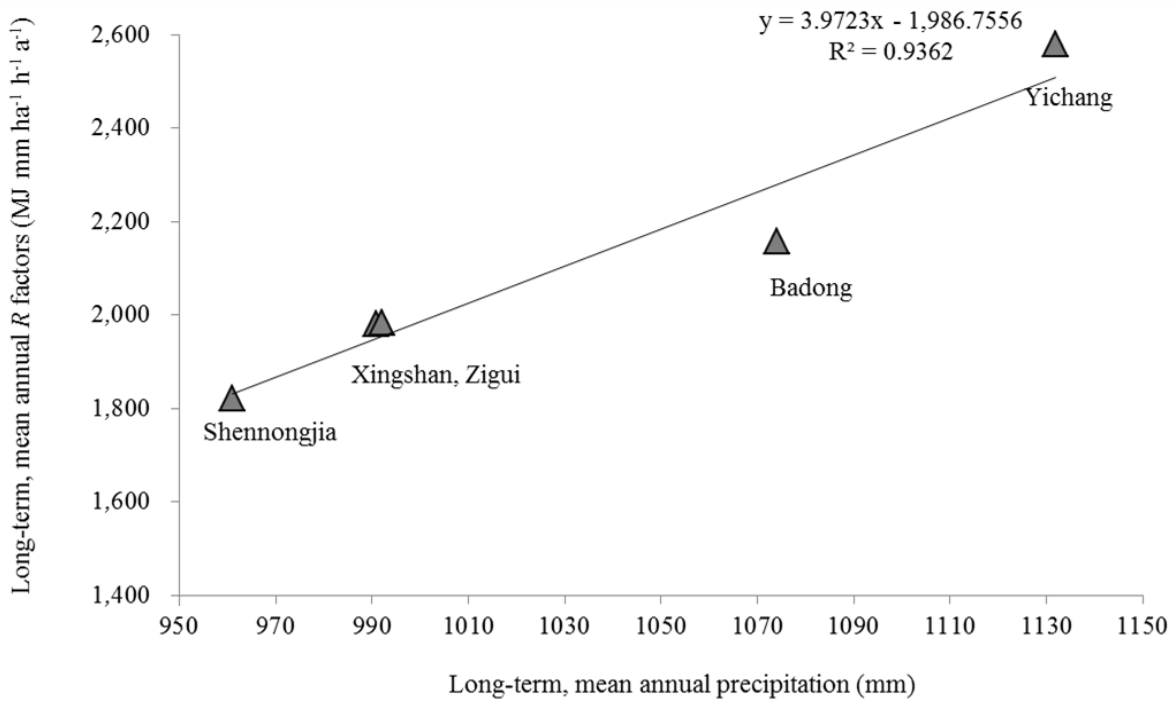

Figure 4 *Relation between long-term, mean annual precipitation and long-term, mean annual rainfall R factors derived according to MEN ET AL. (2008) in the Xiangxi catchment.*

Table 6 *Limits of the elevation bands and the annual precipitation at the limit of each elevation band according to WU ET AL. (2006) and mean annual R factors (R_a) calculated according to MEN ET AL. (2008).*

Elevation band (m a.s.l.)	Annual prec. (mm)	Mean R_a (MJ mm ha^{-1} h^{-1} a^{-1})
62	1000	1,985.5
500	1200	2,779.9
800	1600	4,368.9
1200	2000	5,957.8
3078	2400	7,546.7

prec. precipitation

Moreover, a close link between MAP and elevation is typical for climates with intensive convective precipitation (HE ET AL., 2003) such as in the Xiangxi catchment. Here, it can be assumed that precipitation is mainly erosive with high rainfall intensities. Comparable ranges of *R* factors from

elevation-based regionalization were given by GOOVAERTS (1999) for a study area in Portugal with a *R* factor range of 600 MJ mm ha^{-1} h^{-1} a^{-1} per 100 m increase in elevation (GOOVAERTS, 1999), which is comparable with our increase of R_a of approximately 530 MJ mm ha^{-1} h^{-1} a^{-1} per 100 m for the elevation band from 500 to 800 m a.s.l. in the Xiangxi catchment.

Table 7 *Increase of the annual precipitation and mean annual R factors (R_a) for the different elevation bands in the Xiangxi catchment calculated according to MEN ET AL. (2008).*

Elevation band (m a.s.l.)	Increase of annual prec. per 100 m (mm)	Increase of the mean R_a (MJ mm ha^{-1} h^{-1} a^{-1})
< 500	45.7	181.4
500-800	133.3	529.7
800-1200	100.0	397.2
> 1200	21.3	84.6

prec. precipitation

If we take into account the superimposed role of the climate regime for the characteristics of rainfall events with regard to rainfall erosivity, such as intensity, kinetic energy, and duration (BOLINNE ET AL., 1980; MIKHAILOVA ET AL., 1997; GOOVAERTS, 1999; WANG ET AL., 2002), we conclude that the spatial regionalization of *R* factors using the regression equations given by MEN ET AL. (2008) is adequate for the conditions in the Xiangxi catchment.

The results show that our elevation-dependent spatial regionalization of *R* factors is in good accordance with findings of other studies under comparable climate conditions and the evaluation data sets we used (SHI ET AL., 2004; LIU and LUO, 2005; WU ET AL., 2011; SHI ET AL., 2012).

We further conclude that, under the given situation of sparse data availability, our spatial regionalization offers optimal results. Due to the low spatial density of rainfall data from five available gauging stations for the Xiangxi catchment, we decided not to use common regionalization methods such as regression kriging as used by MEUSBERGER ET AL. (2012) for 71 gauging stations or inverses distance weighting and further geostatistical approaches using 121 gauging stations as reported by ALIPOUR ET AL. (2012). The number of our available gauging stations is too low and the spacing is too large. Thus, we expected that the small-scale variability of precipitation due to the orographic effect will not be captured adequately in the grid regionalization. According to WEILGUNI (2006), *R* factors from spatially sparse data can also be regionalized analogous to the regionalization of precipitation using a spatial explicit feature as long as this feature interacts with the *R* factor, which can be described by a mathematical function. Since the strongly mountainous topography of the Xiangxi catchment causes a vertically zoned climate, we used the elevation as an additional feature and,

therefore, elevation bands to regionalize the *R* factor based on the findings by WU ET AL. (2006). Considering this dependency, the division method by WU ET AL. (2006) serves as superior advantage in our research to regionalize the *R* factors based on sparse data.

Due to the fact, that data from only five climate stations were available, the precipitation pattern in the macroscale and strongly mountainous Xiangxi catchment cannot be adequately represented by the MAP (Table1). The MAP recorded by the stations on higher altitudes is expected to be higher than on lower altitudes as stated by WU ET AL. (2006). However, we observe a high correlation of MAP and R_a (Figure 4). Therefore, we consider the findings by WU ET AL. (2006) as a relevant and valuable basis for our *R* factor regionalization based elevation bands taking into account that not only rainfall but also rainfall erosivity increases with elevation. Already BIEGER ET AL. (2012) used the altitudinal pattern in the Xiangxi catchment as benefit and sufficiently adjusted the low annual precipitation and volume of discharge through a regionalization using elevation bands. Also GASSMAN ET AL. (2007) reported of the elevation being a useful additional proxy for eco-hydrological modelling using SWAT by simulating elevation bands to account for orographic precipitation.

For the Xiangxi catchment, the long-term (1971-2000) mean R_a amounts 5,222 MJ mm ha^{-1} h^{-1} a^{-1}, generally showing enormous rainfall erosivity. Figure 5 reveals the spatial distribution of the rainfall erosivity in the Xiangxi catchment. The rainfall erosivity pattern clearly reflects the altitudinal layers in the Xiangxi catchment due to the regionalization based on elevation bands. We observe a narrow strip of relatively low rainfall erosivity in the steep topography of the lower reaches of the Xiangxi River belonging to the Mid Subtropics below 500 m a.s.l. (WU ET AL., 2006). However, according to the global assessment of land vulnerability to water erosion by BATJES (1996), *R* factors >1,250 MJ mm ha^{-1} h^{-1} a^{-1} already account for high rainfall erosivity. This, in fact, would mean high to extreme rainfall erosivity to a hundred per cent for the Xiangxi catchment. Against the background of an expected increase of precipitation greatly across China during the second half of the twenty-first century, SUN ET AL. (2002) especially expect in the Yangtze River basin a significant boost of rainfall erosivity.

4 CONCLUSION

Rainfall erosivity crucially influences soil erosion. The results of various studies indicate the determining role of the climate regime to cover the characteristics of rainfall events that control rainfall erosivity.

For the assessment of rainfall erosivity in soil erosion models primarily the kinetic energy and the intensity of rainfall are considered, e.g., when calculating the rainfall erosivity factor *R* of the

RUSLE soil erosion model. Its determination requires at least hourly precipitation data. Data at such a high temporal resolution are scarce in most countries and regions of the world, like in our study area, the Xiangxi catchment in Central China. Several studies have aimed at alternative indices and functions in order to quantify rainfall erosivity using sparse data sets for different regions worldwide.

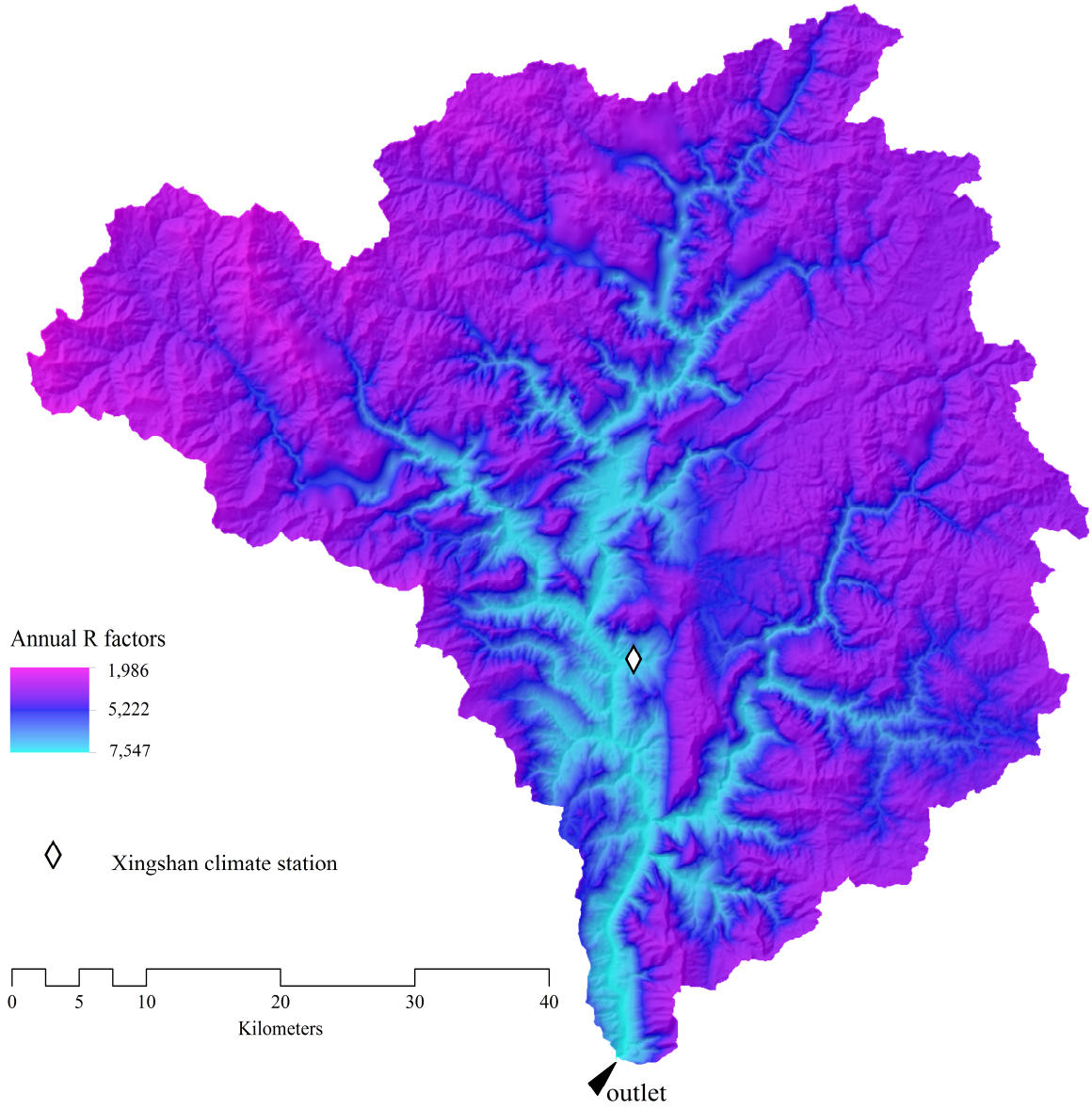

Figure 5 *Spatial distribution of R factors in the Xiangxi catchment based on mean annual R factors according to* MEN ET AL. *(2008). R factors are in SI unit (MJ mm ha^{-1} h^{-1} a^{-1}).*

To overcome the restriction of limited data, we tested a large number of approaches and equations, which can be run with daily data or even coarser temporal resolution. Furthermore, we accounted for the role of topography and climate (highly mountainous and subtropical monsoon in our

case) as covariables to spatially regionalize rainfall erosivity. The barrier effect of the Qinling mountain range, the monsoon climate, and the mountainous terrain of the Xiangxi catchment exhibits a vertically zoned climate, which allows for a regionalization of rainfall erosivity using elevation bands.

The results of various studies indicate the crucial role of the climate regime to cover the characteristics of rainfall events that control rainfall erosivity. We conclude that the regression function by MEN ET AL. (2008) performs best to calculate the *R* factor of the RUSLE soil erosion model according to our evaluation data. It can be run with limited data and is accounts for the whole range of elevation in such a highly mountainous region like the Xiangxi catchment. Thus, for us, the spatial regionalization of *R* factors using the equation by MEN ET AL. (2008) incorporating the Modified Fournier index is most adequate for the Xiangxi catchment considering that a larger number of gauging stations with less spacing would enhance the accuracy of regionalization. Our approach of approximation and spatial regionalization of *R* factors based on sparse data is within the same range of the R factors from other studies in the reservoir area of the TGD used for evaluation. It further fulfills our requirements to overcome limited data, both in space and time, and to address the mountainous topography in the Xiangxi catchment. The grid-based *R* factors allow for modeling a spatially high-resolution and area-specific soil erosion risk potential in the Xiangxi catchment.

6 ACKNOWLEDGEMENTS

This study was conducted within the framework of the Sino-German joint research project YANGTZE GEO. The funding by the German Federal Ministry for Education and Research (BMBF, grant no. 03G 0669) is highly acknowledged.

7 REFERENCES

AGUILAR, E., AUER, I., BRUNET, M., PETERSON, T.C., WIERINGA, J., 2003. WCDMP No. 53, WMD/TD No. 1186: Guidelines on climate metadata and homogenization. World Meteorological Organization, Geneva, Switzerland, pp. 51, available from http://www.wmo.ch/pages/prog /wcp/wcdmp/wcdmp_series/documents/WCDMP-53.pdf.

ALEXANDERSSON, H., 1986. A homogeneity test applied to precipitation data. *Journal of Climatology* 6, 661-675.

ALIPOUR, Z.T., MAHDIAN, M.H., PAZIRA, E., HAKIMKHANI, S., SAEEDI, M., 2012. The determination of the best rainfall erosivity index for Namak Lake Basin and evaluation of spatial variations. *Journal of Basic and Applied Scientific Research* 2, 484-494.

ARNOLDUS, H.M.J., 1977. Methodology used to determine the maximum potential average annual soil loss due to sheet and rill erosion in Morocco. *FAO Soils Bulletin* 34, 39-51.

ATESHIAN, K.H., 1974. Estimation of rainfall erosion index. *Journal of Irrigation and Drainage Engineering* (ASCE) IR-3, 293-307.

AUERSWALD, K., 1998. Bodenerosion durch Wasser, in: Richter, G. (Ed.), Bodenerosion; Analyse und Bilanz eines Umweltproblems. Wissenschaftliche Buchgesellschaft, Stuttgart, pp. 33-42 (in German).

BAGARELLO, V., D'ASARO, F., 1994. Estimating single storm erosion index. *Transactions of the American Society of Agricultural Engineers* 37, 785-791.

BATJES, N.H., 1996. Global assessment of land vulnerability to water erosion on a ½° by ½° grid. *Land Degradation and Development* 7, 353-365.

BERGMANN, A., BI, Y., CHEN, L., FLOEHR, T., HENKELMANN, B., HOLBACH, A., HOLLERT, H., HU, W., KRANZIOCH, I., KLUMPP, E., KÜPPERS, S., NORRA, S., OTTERMANNS, R., PFISTER, G., ROß-NICKOLL, M., SCHÄFFER, A., SCHLEICHER, N., SCHMIDT, B., SCHOLZ-STRAKE, B., SCHRAMM, K.W., SUBKLEW, G., TIEHM, A., TEMOKA, C., WANG, J., WESTRICH, B., WILKEN, R.D., WOLF, A., XIANG, X., YUAN, Y., 2012. The Yangtze-Hydro Project: a Chinese-German environmental program. *Environmental Science and Pollution Research* 19, 1341-1344.

BIEGER, K., HÖRMANN, G., FOHRER, N., 2012. Simulation of streamflow and sediment with the Soil Water Assessment Tool in a data scarce catchment in the Three Gorges Region, China. *Journal of Environmental Quality*, doi:10.2134/jeq2011.0383 (online).

BOLINNE, A., LAUANT, A., ROSSEAU, P., PAUWELS, J.M., GABRIELS, D., AELTERMANN, J., 1980. Provisional rain erosivity map of Belgium, in: DeBoodt, M., Gabriels, D. (Eds.), Assessment of Erosion. John Wiley and Sons, Chichester, pp. 111-120.

BROWN, L.C., FOSTER, G.R., 1987. Storm erosivity using idealized intensity distributions. *Transactions of the American Society of Agricultural Engineers* 30, 379-386.

BUISHAND, T.A., 1982. Some methods for testing the homogeneity of rainfall records. *Journal of Hydrology* 58, 11-27.

CAI, G.G., WANG, H., CURTIN, D., ZHU, Y., 2005. Evaluation of the EUROSEM model with single event data on Steeplands in the Three Gorges Reservoir Area, China. *Catena* 59, 19-33.

CHORLEY, R.J., 1978. The hillslope hydrological cycle. in: Kirkby, M.J. (Ed.), Hillslope hydrology. Wiley, Chichester, pp. 1-42.

CORNELIS, W.M., OLTENFREITER, G., GABRIELS, D., HARTMANN, R., 2004. Splash-saltation of sand due to wind-driven rain: vertical deposition flux and sediment transport rate. *Soil Science Society of America Journal* 68, 532-540.

DA SILVA, A.M., 2004. Rainfall erosivity map for Brazil. *Catena* 57, 251-259.

DE LIMA, J.L.M.P., TAVARES, P., SINGH, V.P., DE LIMA, M.I.P., 2009. Investigating the importance of rainstorm direction on overland flow and soil loss in a laboratory circular soil-flume. *Geoderma* 152, 9-15.

DETTLING, W., 1989. Eine mathematische Betrachtung des R-Faktors. *Zeitschrift für Geomorphologie* 33, 373-377 (in German).

DIODATO, N., BELLOCCHI, G., 2009. Assessing and modelling changes in rainfall erosivity at different climate scales. *Earth Surface Processes and Landforms* 34, 969-980.

DVWK, 1990. Grundlagen der Verdunstungsermittlung und Erosivität von Niederschlägen. Deutscher Verband für Wasserwirtschaft und Kulturbau (Eds.) Parey-Verlag, Hamburg (in German).

ELSENBEER, H., CASSEL, D.K., TINNER, W., 1993. A daily rainfall erosivity model for Western Amazonia. *Journal for Soil and Water Conservation* 48, 439-444.

ERPUL, G., GABRIELS, D., NORTON, L.D., 2005. Sand detachment by wind-driven raindrops. *Earth Surface Processes and Landforms* 30, 241-250.

FERRO, V., PORTO, P., YU, B., 1999. A comparative study of rainfall erosivity estimation for southern Italy and southeastern Australia. *Hydrological Sciences Journal* 44, 3-24.

FOSTER, G.R., MCCOOL, D.K., RENARD, K.G., MOLDENHAUER, W.C., 1981. Conversion of the universal soil loss equation to SI metric units. *Journal for Soil and Water Conservation* 36, 355-359.

FOURNIER, F., 1960. Climat et erosion; la relation entre l'erosion du sol par l'eau et les precipitations atmospheriques. Presses universitaires de Frances, Paris, pp. 201.

FU, B.J., ZHAO, W.W., CHEN, L.D., ZHANG, Q.J., LÜ, Y.H., GULINCK, H., POESEN, J., 2005: Assessment of soil erosion at large watershed scale using RUSLE and GIS: a case study in the Loess Plateau of China. *Land Degradation and Development* 16, 73-85.

GASMAN, P.W., REYES, M.R., GREEN, C.H., ARNOLD, J.G., 2007. The Soil and Water Assessment Tool: historical development, applications, and future research directions. *American Society of Agricultural and Biological Engineers* 50, 1211-1250.

GEIßLER, C., KÜHN, P., BÖHNKE, M., BRUELHEIDE, H., SHI, X., SCHOLTEN, T., 2012. Measuring splash erosion under vegetation using sand-filled splash cups. *Catena* 91, 85-93.

GHAHRAMANI, A., YOSHIHARU, I., MUDD, S.M., 2011. Field experiments constraining the probability distribution of particle travel distances during natural rainstorms on different slope gradients. *Earth Surface Processes and Landforms* 37, 473-485.

GOOVAERTS, P., 1999. Using elevation to aid the geostatistical mapping of rainfall erosivity. *Catena* 34, 227-242.

HAO, F., CHANG, Y., NING, D., 2004. Assessment of China's economic loss resulting from the degradation of agricultural land in the end of 20th century. *Journal of environmental Sciences* 16, 199-203.

HE, L., KING, L., JIANG, T., 2003. On the land use in the Three Gorges Reservoir area. *Journal of Geographical Sciences* 13, 416-422.

HUDSON, N., 1995. Soil conservation. 3rd edition, London, Batsford, pp. 210.

JARVIS, A., REUTER, H.I., NELSON, A., GUEVARA, E., 2008. Hole-filled seamless SRTM data V4, International Centre for Tropical Agriculture (CIAT), available from http://srtm.csi.cgiar.org.

JONES, A., PANAGOS, P., BARCELO, S., BOURAOUI, F., BOSCO, C., DEWITTE, O., GARDI, C., ERHARD, M., HERVÁS, J., HIEDERER, R., JEFFERY, S., LÜKEWILLE, A., MARMO, L., MONTANARELLA, L., OLAZÁBAL, C., PETERSEN, J.E., PENIZEK, V., STRASSBURGER, T., TÓTH, G., VAN DEN

EECKHAUT, M., VAN LIEDEKERKE, M., VERHEIJEN, F., VIESTOVA, E., YIGINI, Y., 2012. The state of soil in Europe - A contribution of the JRC to the EEA Environment State and Outlook Report - SOER 2010. Luxembourg: Publications Office of the European Union, 76 pp, doi: 10.2788/77361 (online).

KAVIAN, A., FATHOLLAH NEJAD, Y., HABIBNEJAD, M., SOLEIMANI, K., 2011. Modeling seasonal rainfall erosivity on a regional scale: a case study from Northeastern Iran. *International Journal of Environmental Research* 5, 939-950.

LAL, R., 1976. Soil erosion problems on an alfisol in western Nigeria and their control. Communications and Information Office, IITA Monograph no. 1, Ibadan, Nigeria, pp. 208, available from http://library.wur.nl/isric.

LAL, R., 1990. Soil erosion in the Tropics: principles and management. McGraw-Hill, New York, pp. 580.

LIU, Y., LUO, Z., 2005. A study on estimation of the amount of soil erosion in small watershed based on GIS: a case study in the Three Gorge Area of China. *Geoscience and Remote Sensing (IGARSS), IEEE International Geoscience and Remote Sensing Symposium* 3, 1859-1863.

LO, A., EL-SWAIFY, S.A., DANGLER, E.W., SHINSHIRL, L., 1985. Effectiveness of EI30 as an erosivity index in Hawaii, in: El-Swaify, S.A., Moldenhauer, W.C., Lo, A. (Eds.), Soil Erosion and Conservation. *Soil Conservertaion Society of America*, Ankeny, pp. 384-392.

LU, X., HIGGITT, D., 2000. Estimating erosion rates on sloping agricultural land in the Yangtze Three Gorges, China, from caesium-137 measurements. *Catena* 39, 33-51.

MANNAERTS, C.M., GABRIELS, D., 2000. Rainfall erosivity in Cape Verde. *Soil and Tillage Research* 55, 207-212.

MEN, M., YU, Z., XU, H., 2008. Study on the spatial pattern of rainfall erosivity based on geostatistics in Hebei Province, China. *Frontiers of Agriculture in China* 2, 281-289.

MENG, Q.H., FU, B.J., YANG, L.Z., 2001. Effects on land use on soil erosion and nutrient loss in the Three Gorges Reservoir Area, China. *Soil Use and Management* 17, 288-291.

MEUSBERGER, K., STEEL, A., PANAGOS, P., MONTANARELLA, L., ALEWELL, C., 2012. Spatial and temporal variability of rainfall erosivity factor for Switzerland. *Hydrology and Earth System Sciences* 16, 167-177.

MIKHAILOVA, E.A., BRYANT, R.B., SCHWAGER, S.J., SMITH, S.D., 1997. Predicting rainfall erosivity in Honduras. *Soil Science Society of America Journal* 61, 273-279.

MÖLG, T., CHIANG, J.C.H., GOHM, A., CULLEN, N.J., 2009. Temporal precipitation variability versus altitude on a tropical high mountain: observations and mesoscale atmospheric modelling. *Quaterly Journal of the Royal Meteorological Society* 135, 1439-1455.

MONTGOMERY, D.R., 2007. Dirt: The erosion of civilizations. University of California Press, Ltd., London, pp. 285.

MORGAN, R.P.C., NEARING, M.A. (Eds.), Handbook of erosion modelling. 1st edition 2011, Blackwell Publishing Ltd., pp. 416.

NEARING, M.A., JETTEN, V., BAFFAUT, C., CERDAN, O., COUTURIER, A., HERNANDEZ, M., LE BISSONNAIS, Y., NICHOLS, M.H., NUNES, J.P., RENSCHLER, C.S., SOUCHÈRE, V., VAN OOST, K., 2005. Modeling response of soil erosion and runoff to changes in precipitation and cover. *Catena* 61, 131-154.

ODURO-AFRIYIE, K., 1996. Rainfall erosivity map for Ghana. *Geoderma* 74, 161-166.

ONCHEV, N.G., 1985. Universal index for calculating rainfall erosivity. in: El-Swaify, S.A., Moldenhauer, W.C., Lo, A. (Eds.), Soil Erosion and Conservation. *Soil Conservation Society of America*, Ankeny, pp. 424-431.

PIMENTEL, D., 2006. Soil erosion: a food and environmental threat. *Environment, Development and Sustainability* 8, 119-137.

RENARD, K.G., FREIMUND, J.R., 1994. Using monthly precipitation data to estimate the R-factor in the revised USLE. *Journal of Hydrology* 157, 287-306.

RENARD, K.G., FOSTER, G.R., WEESIES, G.A., MCCOOL, D.K., YODER, D.C., 1997. Predicting soil erosion by water: a guide to conservation planning with the Revised Universal Soil Loss Equation (RUSLE). USDA Agriculture Handbook No.703, pp. 384.

RICHARDSON, C.W., FOSTER, G.R., WRIGHT, D.A., 1983. Estimation of erosion index from daily rainfall amount. *Transactions of the American Society of Agricultural Engineers* 26, 153-156.

ROGLER, H., SCHWERTMANN, U., 1981. Erosivität der Niederschläge und Isoerodentkarte Bayerns. *Zeitschrift für Kulturtechnik und Flurbereinigung* 22, 99-112 (in German).

ROOSE, E.J., 1976. Use of the universal soil loss equation to predict erosion in West Africa. *Soil Conservation Society of America*, Ankeny, Iowa, pp. 60-74.

SALAKO, F.K., 1995. Rainfall temporal variability and erosivity in subhumid and humid zones of southern Nigeria. *Land Degradation and Development* 17, 541-555.

DE SANTOS LOUREIRO, N., DE AZEVEDO COUTINHO, M., 2001. A new procedure to estimate the RUSLE EI30 index based on monthly rainfall data and applied to the Algarve region, Portugal. *Journal of Hydrology* 250, 12-18.

SCHOLTEN, T., GEIßLER, C., GOC, J., KÜHN, P., WIEGAND, C., 2011. A new splash cup to measure the kinetic energy of rainfall. *Journal of Plant Nutrition and Soil Science* 174, 596-601.

SCHÖNBRODT, S., SAUMER, P., BEHRENS, T., SEEBER, C., SCHOLTEN, T., 2010. Assessing the USLE crop and management factor C for soil erosion modeling in a large mountainous watershed in Central China. *Journal of Earth Science* 21, 835-845.

SEEBER, C., HARTMANN, H., XIANG, W., KING, L., 2010. Land use change and causes in the Xiangxi catchment, Three Gorges Area, derived from multispectral data. *Journal of Earth Science* 21, 846-855.

SEUFFERT, O., 1998. Zukunftsperspektiven der Bodenerosionsforschung, in: Richter, G. (Ed.), Bodenerosion; Analyse und Bilanz eines Umweltproblems. Wissenschaftliche Buchgesellschaft, Stuttgart, pp. 152-168 (in German).

SHAMSHAD, A., AZHARI, M.N., ISA, M.H., WAN HUSSIN, W.M.A., PARIDA, B.P., 2008. Development of an appropriate procedure for estimation of RUSLE EI30 index and preparation of erosivity maps for Pulau Penang in Peninsular Malaysia. *Catena* 72, 423-432.

SHI, Z.H., CAI, C.F., DING, S.W., WANG, T.W., CHOW, T.L., 2004. Soil conservation planning at the small watershed level using RUSLE with GIS. A case study in the Three Gorges Area of China. *Catena* 55, 33-48.

SHI, Z.H., AI, L., FANG, N.F., ZHU, H.D., 2012. Modeling the impacts of integrated small watershed management on soil erosion and sediment delivery: a case study in the Three Gorges Area, China. *Journal of Hydrology* 438-439, 156-167.

SMITHEN, A.A., SCHULZE, R.E., 1982. The spatial distribution in Southern Africa of rainfall erosivity for use in the universal soil loss equation. *Water SA* 8, 74-78.

STOCKING, M.A., ELWELL, H.A., 1976. Rainfall erosivity over Rhodesia. *Transactions of the Institute of British Geographers New Series 1*, 231-245.

SUBKLEW, G., ULRICH, J., FÜRST, L., HÖLTKEMEIER, A., 2010. Environmental impacts of the Yangtze Three Gorges Project - an overview of the Chinese-German research Cooperation. *Journal of Earth Science* 21, 817-823.

SUKHANOVSKI, Y.P., OLLESCH, G., KHAN, K.Y., MEIßNER, R., 2002. A new index for rainfall erosivity on a physical basis. *Journal of Plant Nutrition and Soil Science* 165, 51-57.

SUN, G., MCNULTY, S.G., MOORE, J., BUNCH, C., NI, J., 2002. Potential impacts of climate change on rainfall erosivity and water availability in China in the next 100 years. Proceedings of the 12th Intern. Soil. Conserv. Conference, Beijing, China, available from http://efetac4.sref.info.

TOY, T.J., FOSTER, G.R., 1998. Guidelines for the use of the Revised Universal Soil Loss Equation (RUSLE) version 1.06 on mined land, construction sites, reclaimed land. Office of Surface Mining, Reclamation, and Enforcement, pp.149, available from http://www.greenfix.com /Channel%20Web/pdfs/RUSLE%20Guidelines.pdf.

VAN DER KNIJFF, J.M., JONES, R.J.A., MONTANARELLA, L., 1999. Soil erosion risk management in Italy. European Comission, European Soil Bureau, pp. 52.

WANG, G., GERTNER, G., SINGH, V., SHINKAREVA, S., PARYSOW, P., ANDERSON, A., 2002. Spatial and temporal prediction and uncertainty of soil loss using revised universal soil loss equation: a case study in rainfall and runoff erosivity for soil loss. *Ecological Modelling* 153, 143-155.

WEILGUNI, V., 2006. Regionalisierung des Niederschlags. Wiener Mitteilungen Band 197, Methoden der hydrologischen Regionalisierung, pp. 71-92 (in German).

WISCHMEIER, W.H., SMITH, D.D., 1958. Rainfall energy and its relationship to soil loss. *Transactions American Geophysical Union* 39, 285-291.

WISCHMEIER, W.H., 1959. A rainfall erosion index for a universal soil-loss equation. *Soil Science Society of America Journal* 23, 246-249.

WISCHMEIER, W.H., 1962. Rainfall erosion potential. *Journal of Agricultural Engineering Research* 43, 212-225.

WISCHMEIER, W.H., SMITH, D.D., 1965. Predicting rainfall-erosion losses from cropland east of the Rocky Mountains - Guide for Selection of Practices for Soil and Water Conservation. Agriculture Handbook No. 282, USDA, Washington, DC, pp. 47, available from http://naldc.nal.usda.gov/download/CAT87208342/PDF.

WISCHMEIER, W.H., SMITH, D.D., 1978. Predicting rainfall erosion losses - a guide to conservation planning. Agriculture Handbook No. 537, USDA, Washington, DC, pp. 58, available from http://naldc.nal.usda.gov/download/CAT79706928/PDF.

WU, Y.J., KING, L., JIANG, T., 2006. Climatic vertical graduation and its use in the Xiangxi River catchment, in: Cai, Q., Fohrer, N. (Eds.), Sino-German Workshop on Environmental Impacts of Large-scale Hydraulic Engineer. Programme and Abstracts, March 2006, Xingshan, pp. 104-108.

WU, C., ZHOU, Z., XIAO, W., WANG, P., TENG, M., HUANG, Z., 2011. Estimation of soil erosion in the Three Gorges Reservoir Area of China using RUSLE, remote sensing and GIS. *Journal of Food, Agriculture and Environment* 9, 728-734.

XIE, Y., LIU, B., NEARING, M.A., 2002. Practical thresholds for separating erosive and non-erosive storms. *Transactions of the American Society of Agricultural Engineers* 45, 1843-1847.

XU, Y., PENG, J., SHAO, X., 2009. Assessment of soil erosion using RUSLE and GIS: a case study of the Maotiao River watershed, Guizhou Province, China. *Environmental Geology* 56, 1643-1652.

YU, B., ROSEWELL, C.J., 1998. RECS: A program to calculate the R-factor for the USLE/RUSLE using BOM/AWS Pluviograph data. ENS Working Paper No. 8/98, pp. 15.

ZHOU, P., 2008. Landscape-scale erosion modeling and ecological restoration for a mountainous watershed in Sichuan, China. Univ. Helsinki Tropic. Forest. Rep. 35, pp. 95.

MANUSCRIPT 4

Degradation of Cultivated Bench Terraces in the Three Gorges Area - Field Mapping and Data Mining

Published in ECOLOGICAL INDICATORS, Vol. 34, pp. 478-493, November 2013

DOI: 10.1016/j.ecolind.2013.06.010

Sarah Schönbrodt-Stitt[1)*], Thorsten Behrens[1)], Karsten Schmidt[1)], Xuezheng Shi[2)], Thomas Scholten[1)]

1) Institute of Geography, Department of Physical Geography and Soil Science, University of Tübingen, Tübingen, Germany

2) Chinese Academy of Sciences, Institute of Soil Science, Department for Soil Resources and Remote Sensing Application, Nanjing, P. R. China

* Corresponding author. University of Tübingen, Department of Geosciences, Chair of Physical Geography and Soil Science, Rümelinstraße 19-23, D-72070, Tübingen, Germany, Tel. +49 (0)7071 29 74054, Fax. + 49 (0)7071 29 5391, E-mail. sarah.schoenbrodt-stitt@uni-tuebingen.de

GRAPHICAL ABSTRACT

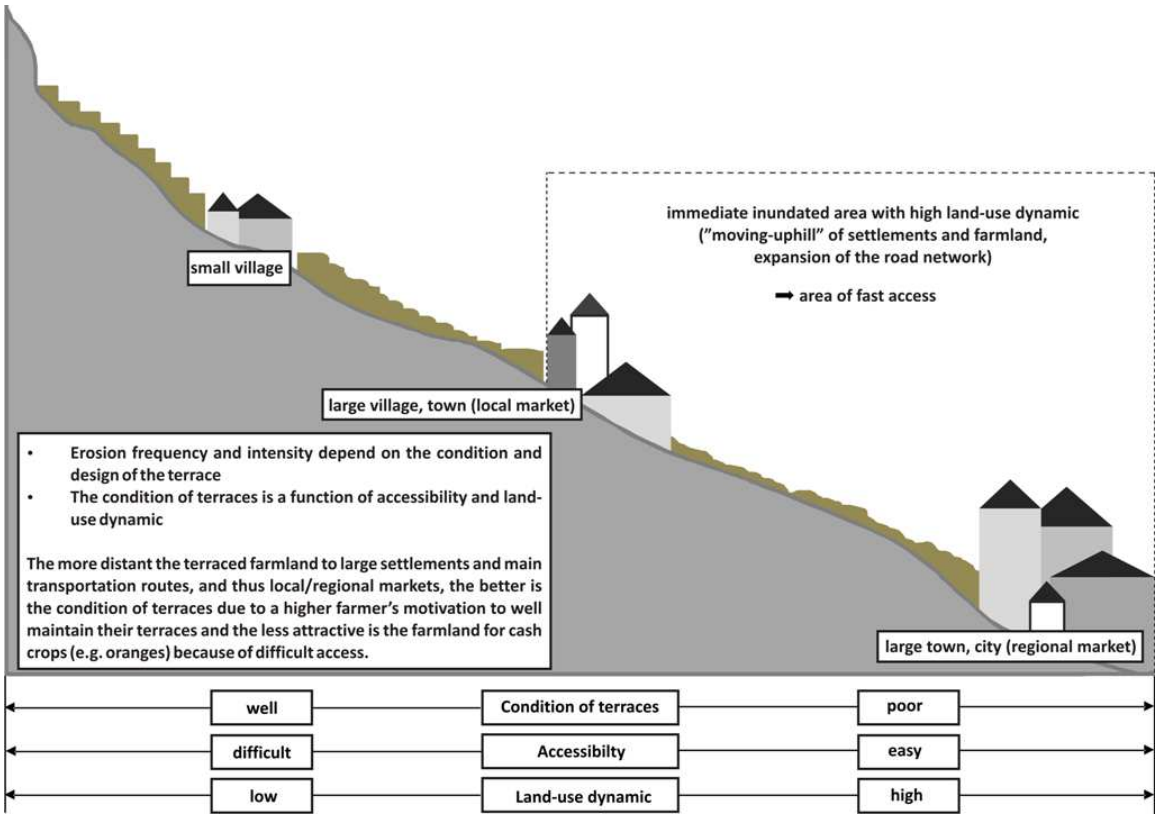

HIGHLIGHTS

(i) We assess the degradation of farming terraces in the Three Gorges ecosystem.

(ii) We combine field mapping and Random Forests successfully.

(iii) Indicators for anthropogenic effects and natural drivers were combined.

(iv) Terrace degradation distinctly ranges from well maintained to completely collapsed.

(v) Distances to roads, settlements, and rivers explain the varying terrace conditions

ABSTRACT

Due to resettlements, construction of new infrastructure, and new land reclamation the rapid agricultural changes in the Three Georges Area (TGA) in Central China are expected to force the degradation of the cultivated terraced landscape. Consequently, increased soil erosion can hamper a sustainable land management in the mountainous TGA. This paper presents the model framework *TerraCE* (Terrace Condition Erosion) for determining the causes for different terrace conditions and terrace degradation based on field surveys and spatial data mining. For a total of 987 bench terrace plots in the Xiangxi catchment we collected data on their state of maintenance and terrace design to account for terrace stability and thus capability of soil conservation. Assessing the driving factors of terrace degradation was done by embedding terrain-based predictors and distance-transforms of remote-sensing data as indicators of environmental and anthropogenic influences. Random forests classification and regression models were applied for data mining. Terrace degradation in the Xiangxi catchment is obvious. The sequence of degradation ranges from 'well maintained' (21%), 'fairly maintained' (44%), and 'partially collapsed' (23%) to 'completely collapsed' (11%) terraces. The cross-validation error of the supervised *TerraCE* model is below 8%, allowing for reasonable and valid interpretations of the causes of terrace degradation. Data mining reveals indicators for anthropogenic effects such as the distance to settlements or to roads as major drivers for the spatial distribution of terrace conditions. The effect of relief, which can be regarded as the major natural driver for terrace degradation by erosive action is tributary but altered and overlaid by land use dynamics associated with the Three Gorges Dam. An important indicator representing a combined effect of terrain and human activity is the distance to stream channels of different orders. Applying *TerraCE* we reveal mechanisms of terrace degradation in disturbed environments and present a framework for standardized mapping and analysis of terrace degradation under cultivation. The approach might also be used to develop guidelines for terrace planning in mountainous terraced landscapes of limited carrying capacity, with respect to socio-economic as well as environmental conditions.

KEYWORDS

Bench terraces, terrace degradation, terrace mapping, data mining, distance transforms, Three Georges Area

1 RESEARCH BACKGROUND

1.1 FARMING TERRACES AND TERRACE DEGRADATION

Worldwide, estimated 75 billion tons of soil are eroded each year (WACHS and THIBAULT, 2009). Especially in mountain areas, soil erosion is one of the most pressing environmental problems affecting soil fertility, water availability, and farmland productivity (POSTHUMUS and STROOSNIJDER, 2010; MONTGOMERY, 2007). Here, the erosive effect of extreme climate and terrain triggering soil erosion processes by water can be most effectively alleviated by farming terraces (e.g., HUDSON, 1981; INBAR and LLERENA, 2000; SHI ET AL., 2004). Consequently, terracing serves as key technology for soil and water conservation and for a suitable land management (SHRESTRA ET AL., 2004; CAO ET AL., 2007).

Due to the terracing, steep slopes are converted into an artificial sequence of relatively flat surfaces (MONTGOMERY, 2007). The erosive slope length and angle, and thus the runoff potential distinctly decrease resulting in a reduction of terrain-induced soil erosion and sediment yield (ARNAEZ ET AL., 2010; EL ATTA and AREF, 2010; SHI ET AL., 2012). Bench terraces (synonym for slope or stone terraces) are the major recommended type of terrace for steep sloping areas (HUDSON, 1981; SHI ET AL., 2012). In order to stabilize the vertical terrace riser, dry-stone walling along the contour lines is largely applied (HUDSON, 1981; BELLIN ET AL., 2009; SHI ET AL., 2012).

Under optimum conditions, these engineering structures form a ‘hydraulic equilibrium’ state between the geomorphic settings and anthropogenic use (BRANCUCCI and PALIAGA, 2006; CHEMIN and VAROTTO, 2008). From the Mediterranean, for instance, HAMMAD ET AL. (2004) report a decrease of average soil loss on bench terraces compared to non-terraced plots by factors up to 20. In the highly vulnerable Chinese Loess region, decreases of soil loss of average 49% were observed (LI and NGUYEN, 2008). Applying the WATEM/SEDEM erosion and sediment transportation model for a small watershed sloping in average with 23° in Central China, SHI ET AL. (2012) report a reduction of soil loss and sediment yield by approximately 17% and 32% for bench terraces combined with furrow-ridge tillage. Terraces are further likely to favor the interception of overland flow and to enhance the infiltration in the long-term (e.g., BELLIN ET AL., 2009; EL ATTA and AREF, 2010; SHI ET AL., 2012), to reduce the erosion-induced nutrient loss (DAMENE ET AL., 2012), to promote agricultural productivity (POSTHUMUS and STROOSNIJDER, 2010), and to expand available land for cultivation (ZHANG, 2008).

In contrast to the above benefits, numerous studies such as from Saudi Arabia (EL ATTA and AREF, 2010), the Andes in Peru (INBAR and LLERENA, 2000), from the Chinese Loess region (e.g., LI and LINDSTROM, 2001), from Italy (e.g., BAZZOFFI and GARDIN, 2011), from Greece (e.g., KOULOURI and GIOURGA, 2007), from Spain (e.g., BELLIN ET AL., 2009), Indonesia (VAN DIJK, 2002), Thailand (SANG-ARUN ET AL., 2006), and the Yemen Highlands (PIETSCH and MABIT, 2012) have proven that despite terracing, soil erosion can be a serious problem.

Particularly, inadequate terrace design and mismanagement strongly affect the stability of bench terraces and favor soil erosion (e.g., SANG-ARUN ET AL., 2006; KOULOURI and GIOURGA, 2007; LESSCHEN ET AL., 2008; BELLIN ET AL., 2009). Causes for this phenomenon are seen in a lack of local knowledge of adequate terracing (e.g., ESTEVE ET AL., 2004), in a lack of individual farmers' motivation and uncertainty regarding tenure (WILLIAMS, 1990; DEININGER and JIN, 2006), in a shortage of labor and investments (INBAR and LLERENA, 2000), a shift of production (BELLIN ET AL., 2009; BEVAN ET AL., 2012), and land shortage and fragmentation (CORBEELS ET AL., 2000). Mostly, these causes interact with each other and are discussed to result from an agricultural abandonment (e.g., KOULOURI and GIOURGA, 2007; LESSCHEN ET AL., 2008; EL ATTA and AREF, 2010) due to social, economic and/or political upheavals such as rural-urban migration (e.g., AW-HASSAN ET AL., 2000; INBAR and LLERENA, 2000; KOULOURI and GIOURGA, 2007).

According to INBAR and LLERENA (2000) who studied erosional processes on bench terraces in Peru, the supporting terrace wall mainly determines the terrace stability. Typically, walls of bench terraces left to degrade exhibit bulges and upsetting by erosive action followed by more intense wall disorders such as breaches that further lead to complete collapses (INBAR and LLERENA, 2000; LASANTA ET AL., 2001; BRANCUCCI and PALIAGA, 2006; LESSCHEN ET AL., 2008; BELLIN ET AL., 2009). The natural geomorphic system will progressively annul the former balanced terraced system (BRANCUCCI and PALIAGA, 2006; BAZZOFFI and GARDIN, 2011). This will increase the slope length and slope gradient, followed by an acceleration of runoff (e.g., EL ATTA and AREF, 2010; KOULOURI and GIOURGA, 2007). Consequently, the capability of a terrace to protect the soil against surface erosion by water is reduced, defined as terrace degradation by BAZZOFFI and GARDIN (2011).

By evaluating the potential of the terrace design to reduce soil erosion and applying flow traces, BELLIN ET AL. (2009) proved that terraces that were not longer maintained do not longer retain water and promote an increased contribution of runoff from cropland to the drainage network. Within 50 years, the portion of runoff was observed to increase from 9% to 31%. According to SIDLE ET AL. (2006) and BAZZOFFI and GARDIN (2011) poorly designed and maintained terraces represent significant sediment sources.

As an answer on the increasing interest on terraced landscapes, several studies within the European Cross Compliance Framework and the Interregional ALPTER project focused on varying

conditions of terraces and their degradation (e.g., COMOLLI, 2005; SCARAMELLINI and VAROTTO, 2008; BAZZOFFI and GARDIN, 2011). All studies have in common to especially account for the condition of the supporting walls of bench terraces and the terraced sloped instability, since the terrace' 'state of maintenance' (BELLIN ET AL., 2009) strongly controls the soil erosion. However, by now, no standard on the assessment and evaluation of terrace degradation and its effects exists. Whereas BELLIN ET AL. (2009) differentiate between intact or leaking terrace walls, COMOLLI (2005), BRANCUCCI and PALIAGA (2006), and BAZZOFFI and GARDIN (2011) apply a higher grade of differentiation for terraces in North Italy. By mapping different percentages of abandonment or degradation of terraces from 'conserved' to 'removed' (BAZZOFFI and GARDIN, 2011), respectively 'well maintained' to 'completely collapsed' (COMOLLI, 2005), they classified terraces in terms of their condition.

While much is known about terrace degradation due to agricultural abandonment, until now no attention was paid to terrace degradation in areas experiencing agricultural intensification and rapid ecosystem changes. Since the reservoir of the Three Gorges Area (TGA) in China currently belongs to the most dynamic large-scale anthropogenic influenced regions in the world (e.g., YANG ET AL., 2002; CUI ET AL., 2011), rapid land use changes in this widely terraced landscape (SHI ET AL., 2012) are expected to likewise impact terracing.

1.2 THE THREE GORGES AREA

Due to the river impoundment by the Three Gorges Dam (TGD), the TGA is largely characterized by resettlements, construction of new infrastructure, and new land reclamation for agricultural cultivation (CUI ET AL., 2011). Combined with the mountainous topography accounting for 90% of the TGA, abundant precipitation, highly erodible soils (CUI ET AL., 2011), and population pressure (ZHANG, 2008), the land use changes occur in a region exhibiting a low environmental carrying capacity (HEGGELUND, 2006; ZHANG, 2008) and the highest soil erosion rates in China (ZHOU, 2008). Estimations on annual soil loss based on empirical modeling, remote sensing, and radionuclides inventory account for an average soil loss from 32.8 to 45 t ha^{-1} and a total amount of annual soil loss of 1.891×10^8 t mainly caused by water (LU and HIGGITT, 2000; ZHANG, 2008; WU ET AL., 2011). According to the Chinese Soil Erosion Rate Standard almost 77% of the total soil loss occurs in areas of high to extreme erosion grades (WU ET AL., 2011).

Along with the soil erosion, manifold environmental and socio-economic threats occur such as reservoir siltation with threat to the long-term safe operation of the TGD (SHI ET AL., 2004; ZHANG, 2008) and deterioration of the aquatic systems (PONSETI and LÓPEZ-PUJOL, 2006). For instance, the farmland supply of suspended material is estimated to be 90% (CUI ET AL., 2011). Thus, discharge of sediment and associated contamination of adjacent waterbodies (e.g., LIU ET AL., 2003; CUI ET AL.,

2011), are expected to further boost the ecological degradation in this strongly manufactured landscape (ZHANG, 2008).

The reclamation of steep slopes, their destabilization due to artificial fluctuations of the reservoir's water level, and the increasing number of landslides (EHRET ET AL., 2010; CUI ET AL., 2011) still might accelerate the soil erosion potential. ZHANG (2008) concerns an already serious soil erosion problem causing a latent crisis of the agricultural environment which can likely been aggravated by the conflict potential between relocates from the resettlements and agricultural land.

This is especially true against the background of soil erosion being strongly related to cultivated slopes (LU and HIGGITT, 2000; CUI ET AL., 2011). Sloping farmland accounts for 74% of the total farmland in the TGA and for approximately 15% of the farmland with slopes above the critical threshold of 25° over which cultivation is prohibited according to the Water and Soil Conservation Law (ZHANG, 2008; CUI ET AL., 2011). According to CUI ET AL. (2011) average soil loss rates on sloping farmland range from almost 45 to 67 t ha^{-1} a^{-1} and are likely to annually exceed 10×10^3 t km^2 in some places. Thus, cultivation on slopes is the largest contributor to soil erosion and sediment delivery in the TGA (e.g., CUI ET AL., 2011; WU ET AL., 2011).

This demonstrates the urgent need for reducing soil erosion in order to maintain the sustainability of the TGA. In order to minimize soil erosion, e.g., through well-adapted land management and conservation practices, information on soil loss and its spatial and temporal variability is required. This of course, also includes the effect of terraces on soil erosion, especially, since bench terraces are widely applied in the TGA (e.g., SHEN ET AL., 2010; SHI ET AL., 2012).

Based on these considerations and restrictions, the objectives of the present study are as follows:

(i) to undertake an initial attempt to account for terrace degradation of solely cultivated terraces in the highly dynamic TGA and

(ii) to aim at the causes of the terrace degradation in order to emphasize the understanding of the processes triggering terrace degradation and thus, influencing the terraced landscape in the mountainous TGA.

Since there has been no terrace inventory and no further data available, we developed a framework that integrates field surveys and data mining. Within this framework remote sensing data serve as a fast and available supplier for the derivation of area-wide and spatial indicators on the assessment of terrace degradation on the landscape level.

2 *TERRACE* - MODELING AND ANALYZING TERRACE CONDITIONS

In order to invest the above study objectives we developed *TerraCE* (Terrace Condition Erosion) - a framework for modeling and analyzing terrace conditions. Due to sparse data availability and limited access to the mountainous terrain the framework consists of a two-step approach aiming at

(i) collecting data on terrace degradation by considering different conditions of terraces using field surveys and

(ii) explaining the terrace degradation by implementing environmental and anthropogenic indicators and using data mining techniques.

As we are interested in determining the relevant indicators affecting terrace degradation characterized by land use changes we made use of two assumptions:

(i) generally, bench terraces are the product of human activity driven by terrain settings (e.g., INBAR and LLERENA, 2000), and

(ii) the spatial distribution of the degree of degradation of bench terraces is driven by the distance to settlements and to the reservoir as well as their accessibility (e.g., by roads).

These assumptions enable us to develop environmental indicators as proxy-drivers for the effects of terrain and human impact on terrace degradation.

Since terracing is generally linked to specific terrain conditions, digital terrain analysis can provide indicators, which show effects on terrace condition. Based on the resolution of the available digital elevation model (DEM), terrain analysis does not aim at providing indicators describing the local terrace design such as terrace slope, wall height or width of the terrace risers. Instead terrain analysis in our study provides information on the background - or natural - landscape surface characteristics without terraces. This allows determining effects relevant for differentiating terrace conditions, since the general flow paths and velocities of surface water still follows the natural relief above the plot scale. For instance, if the contributing area increases, we assume that the water pressure by infiltration and interflow on the terrace unit, and thereby the risk of wall failures, increases too. Additionally, terrain can be used as a proxy for other environmental covariates such as climate or parent material (BEHRENS ET AL., 2010a, b). Typical examples are aspect and slope. Together they can be used as a proxy for solar insolation, and thus also indicate the distribution of various soil properties (e.g., BEAUDETTE and O'GEEN, 2009).

Since no precise information nor spatial data on the human activities in the TGA such as market prices, technological development, and structural changes - as described as main drivers of soil erosion by ESTEVE ET AL. (2004) - are available, we derived proxy indicators from remote sensing data. According to INBAR and LLERENA (2000) the distance from a village is an important component in the process of terrace degradation. Hence, we used spatial Euclidean distance transforms as

indicators on the human influence. The datasets used to derive the distance transforms were the road network and the settlements (c.f., Section 3.4.2). We further assumed the distance to the river network to be an indicator for anthropogenic influences on terrace conditions. Due to the river impoundment, the tributaries of the Yangtze River became navigable. Consequently, comparable to the road network, we applied distance transforms to different orders of the river network system as proxies on the accessibility of terraces and thus human activity.

By embedding environmental and anthropogenic indicators as well as terrace condition classes from field surveys into a spatial data mining framework, we aim at a better understanding of the causes of terrace degradation and the strength and direction of the driving factors. The general workflow of this study is presented in Figure 1.

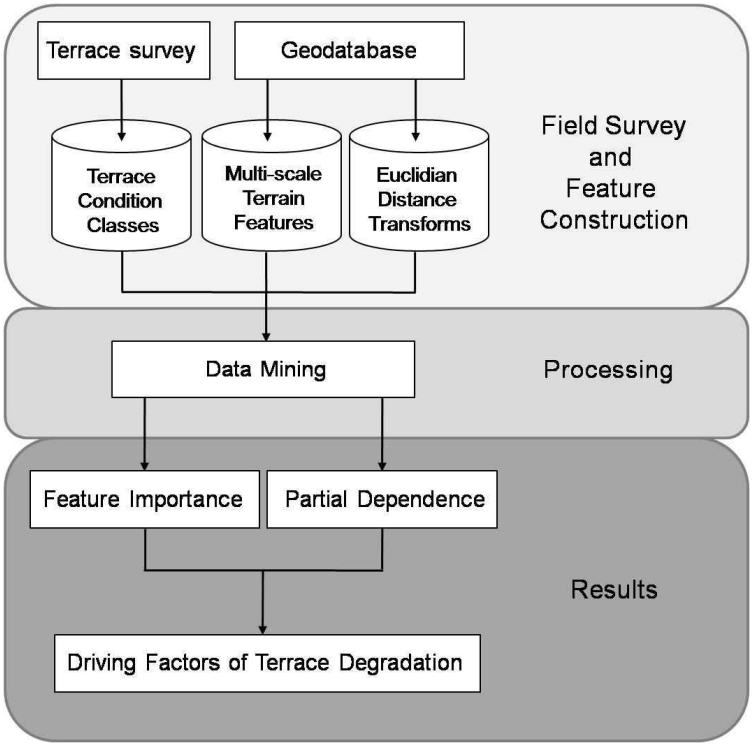

Figure 1 *Model framework of TerraCE.*

3 MATERIALS AND METHODS

3.1 STUDY AREA

The study area is the backwater area (560 km²) with the test sites Xiangjiaba (2.8 km²) and Quyuan (88 km²) and is located in the southern Xiangxi catchment (SCHÖNBRODT-STITT ET AL., 2013) largely covered by the counties Zigui and Xingshan (Figure 2). It serves exemplarily for the situation within the TGA within the BMBF funded Yangtze Geo project (SUBKLEW ET AL., 2010).

As a main tributary to the Yangtze River, the Xiangxi River became inundated. The impoundment stretches from the outlet approximately 35 km toward the central Xiangxi catchment close to the district town of Xingshan, Gaoyang (Figure 2). The study area belongs to the humid subtropics showing a distinct unimodal rainfall regime from May to October with 78% or rainfall during these months (SCHÖNBRODT-STITT ET AL., 2013). The mean annual precipitation at Xingshan station close to Gaoyang is 991 mm for the period from 1971 to 2000. Mean annual temperature is 16.9 °C for the same period (SCHÖNBRODT-STITT ET AL., 2013).

The morphology ranging from 62 m a.s.l. at the outlet to 1994 m a.s.l. in the south-east of the backwater area is closely linked to the lithology. Extremely steep slopes with a maximum slope angle of 78° and narrow valleys characterize the predominantly Triassic formation of the eastern bank of the Xiangxi River (EHRET ET AL., 2010). The western bank is characterized by a more intense weathering of the predominantly Jurassic formation (EHRET ET AL., 2010). It typically exhibits a slightly less steep sloping morphology (Figure 2). Mean slope inclination in the study area is 24° (standard deviation is 10°).

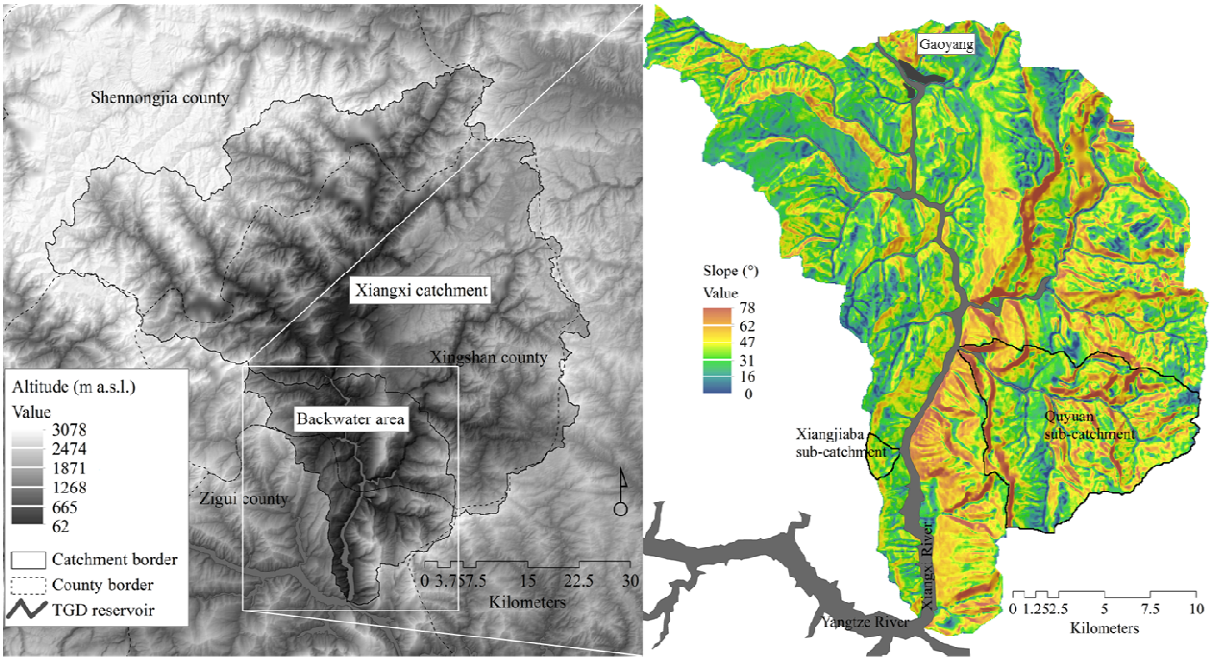

Figure 2 *Location of the study area and range of altitude and slope inclination. The DEM was derived from SRTM data (version 4, JARVIS ET AL., 2008).*

The land use is strongly linked to the terrain with the Xiangxi River acting as a kind of dividing line between mainly agricultural cultivation on the western riverside and mainly forests and shrubs with scattered plots of cultivation on the eastern riverside (SEEBER ET AL., 2010). Management cash crop farming mixed with lower productive subsistence farming located on higher altitudes strongly characterize the agricultural use in the west, both typically on terraced farmland with contour

cultivation (SEEBER ET AL., 2010). Typical crops in the backwater area are oranges as cash crop, rice, dry land crops (rape, wheat, soybean, and maize), and garden fruits (such as legumes, chili).

3.2 TERRACE SURVEY AND MAPPING

Since there has been no terrace inventory or further adequate data on terrace distribution and condition available for the TGA, we developed a field survey scheme.

In a first step, based on an initial survey and the findings achieved by COMOLLI (2005) and BAZZOFFI and GARDIN (2011) we hypothesized four classes of terrace condition and applied the terminology based on the classification of varying terrace conditions by COMOLLI (2005). The mapped terraces were classified into:

(i) well maintained,
(ii) fairly maintained,
(iii) partially collapsed, and
(iv) completely collapsed.

In a second step, a detailed terrace survey was conducted in selected areas for precise measurements and for categorizing terrace condition on site. The final step was a survey with major focus on dominant terrace condition but for larger areas to provide a bigger dataset for data mining.

The surveys were conducted in 2009 and 2010. Only terraces that were cultivated at the time of survey were mapped.

3.2.1 DETAILED TERRACE SURVEY

We mapped the terrace degradation by considering the four classes of terrace condition as described in the previous section. Moreover, we developed a standardized field mapping scheme for terrace design, terrace maintenance conditions, cultivation as well as erosion pattern. Terrace design we assessed by measuring the height of the terrace wall (cm), the width of the terrace riser (cm), the slope angle of the terrace riser (°) and the slope angle (°) of the terrain itself on which the terrace was located as these parameters are considered to determine the geometry of a terrace (HUDSON, 1981). To account for the state of maintenance of a terrace, we focused on structural wall disorders, the frequency of different types of wall disorders, and their intensities. These were bulges, upsetting, wall failures that occur on approximately the half of the terrace wall, and complete wall collapses. Identification and classification of wall disorders is based on the work of BRANCUCCI and PALIAGA (2006). A schematically draft of the surveyed wall disorders is given in Figure 3.

We considered the partially small-scale heterogeneity of the terrace design by dividing each terrace plot into three homogeneous segments and analyzed them separately. For further data analysis, the average value of the numerical data was calculated. Concerning the state of maintenance the dominant terrace condition was assigned to the whole plot.

The detailed terrace inventory was conducted within the test areas Xiangjiaba and Quyuan (c.f., Section 3.1, Figure 2). In order to avoid subjectivity and to assure that the whole range of terrace conditions is covered the terrace plots were randomly selected from agricultural land based on a land use classification dataset for the Xiangxi catchment (SEEBER ET AL., 2010). Initially, 308 points (88 points for Xiangjiaba and 220 points for Quyuan) were selected to provide enough samples for potential reduction due to restrictions in access and land use changes.

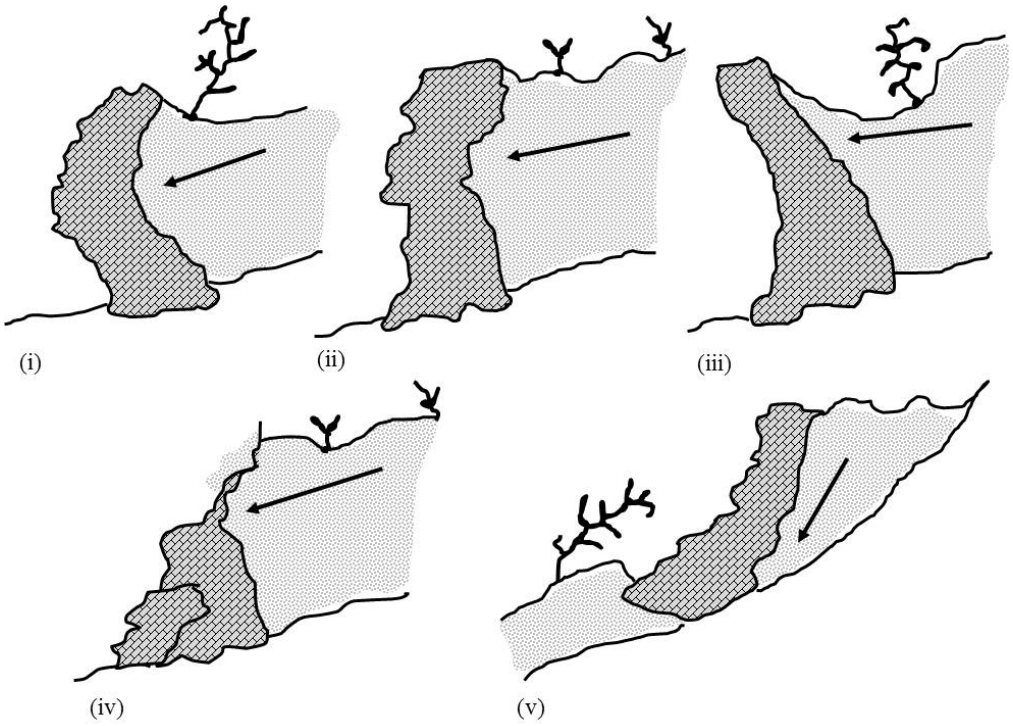

Figure 3 *Surveyed wall disorders (i and ii) bulges, (iii) upsetting, (iv), wall failures, and (v) complete wall collapses. (after BRANCUCCI and PALIAGA, 2006; modified).*

Since the land use classification dataset was based on a Landsat5-TM scene from 2007 the classification was not very precise and did not show current land use pattern in all cases. Hence, 29% of the randomly selected points had to be excluded from the survey. Additional 21% of the samples could not have been surveyed due to restricted access, e.g., extremely steep terrain, missing roads, and other logistic reasons. Finally, 158 points in the two small test areas were accessible bench terraces and mapped in detail.

3.2.2 REMOTE TERRACE INVENTORY

Due to the fact, that a detailed inventory on the terrace conditions is very time consuming, a 'quasi-remote' inventory exclusively on the terraces' dominant state of maintenance was conducted for a larger area. The advantages of this quasi-remote inventory lie in a faster survey process and thus, in generating a larger data set to be implemented into the data mining approach. For this survey no sampling points were previously selected. Instead, along a strip of approximately 35 km length from the outlet of the Xiangxi catchment to Gaoyang (Figure 2), each terrace plot referring to a homogenous land use was mapped based on a topographic map at a scale of 1:10,000. This strip is directly adjacent to the impounded Xiangxi River. Due to newly constructed roads this area is easy to access in a generally steep sloped and rugged terrain. The mapping was conducted from each opposite bank of the Xiangxi River in order to assess the complete range of terraces on the slopes on both riversides. The classification of the terrace plots into the given, predefined classes was done according to the detailed terrace survey.

Data from the terrace inventory refers to a spatial resolution of 45 m. This provides exact support of field data and computed data for modeling to avoid negative, random influences from finer scale on the final description of terrace conditions as well as the data mining process (c.f., Section 3.4).

3.3 GEODATABASE

Our basic data sources available for analysis, modeling, and interpretation were a digital elevation model (DEM) and remote sensing images. Three preprocessed Landsat5-TM images (atmospheric, radiometric, and geometric corrections using ATCOR for ERDAS IMAGINE®) each with 6 bands from 2005 (2005-09-09), 2006 (2006-09-12), and 2007 (2007-09-15) were also available as input for data mining analysis. They were used in order to assess a possible influence of the land cover on the terrace conditions possibly over time.

Due to the processing of the multiple datasets of various cell sizes we met the need of same cell sizes by re-sampling the SRTM-DEM (version 4, JARVIS ET AL., 2008) and Landsat data to a joint resolution of 45 m. Since the SRTM-DEM is our main data basis and the terrain parameters derived from the DEM exhibit the key indicators (e.g., elevation, slope, curvature, aspect; c.f., Section 3.4.1) in analyzing the terrace conditions, we decided for a finer resolution than in the original data. This was required due to the steep slopes resulting in very few pixels along a slope which produced artifacts on several terrain attributes such as flow accumulation. Furthermore, the loss of accuracy in analyzing the impact of terrain on the terrace conditions due to a re-sampling of the SRTM data to the same cell size of Landsat is not supportable. In contrast, by re-sampling the Landsat data to 45 m we do not

incorporate a higher false accuracy compared to a re-sampling of the SRTM data from 90 to 30 m. In this case, the loss of information is affordable.

An ortho-rectified panchromatic and geo-referenced SPOT5 image (2007-09-21) with a resolution of 5 m and Google Earth data were used as data basis for deriving anthropogenic indicators by digitizing (c.f., Section 3.4.2).

The different maps of terrace conditions produced by the detailed and the remote inventory were merged for data mining and analysis.

3.4 FEATURE CONSTRUCTION FOR DATA MINING

3.4.1 TERRAIN FEATURES AS ENVIRONMENTAL INDICATORS FOR TERRACE DEGRADATION

We derived local, regional, and combined geomorphometric terrain attributes as environmental indicators on the condition of terraces. The terrain attributes derived are: elevation, slope (TARBOTON, 1997), projected distance to the stream, aspect deviances (to 0°, to 45°, to 90°, and to 135°), relative profile curvature, relative richness, topographic roughness, local elevation (BEHRENS, 2003), mean, maximum and minimum curvature (SHARY ET AL., 2002), relative horizontal curvature (KLEEFISCH and KÖTHE, 1993), hemispherical dispersion (HODGSON and GAILE, 1999), and waxing and waning slopes (HUBER, 1994). To account for the influence of multiple scales, which proved to be important in digital soil mapping applications in several studies (e.g., BEHRENS ET AL., 2010a, b; SMITH ET AL., 2006; ZHU, 2008), all terrain attributes derived on the original resolution of 45 m were averaged on the basis of local moving window filters with sizes of 7 × 7 as well as 17 × 17 pixels. This allows capturing more general trends in terrain as additional indicators for terrace condition analysis (BEHRENS ET AL., 2010a).

3.4.2 DISTANCE TRANSFORMS AS ANTHROPOGENIC INDICATORS FOR TERRACE DEGRADATION

Spatial distance transforms provide information on distant objects. This will help to quantify relationships between objects according to Tobler's First Law of Geography where "everything is related to everything, but near things are more related than distant things" (TOBLER, 1970). Based on those grids of spatial distance transforms we can extract distances of certain locations and can assume different human impacts on terrace conditions from those locations of varying distances. However, careful processing and generation of the primary data used to apply the distance transforms on is required.

Based on the SPOT5 scene and GPS tracks, the road network in the Xiangxi catchment was digitized. The road network was classified into three classes: major roads, side roads, and paths. In

order to calculate Euclidian distance transforms, the road network classes were not treated separately but combined in (i) major roads, (ii) major roads and side roads, and (iii) major roads, side roads, and paths. This approach avoids artifacts which would stem from isolated segments and accounts for the fact of continuous changes in traffic density.

A total of 4420 settlements were digitized based on the SPOT5 scene and Google Earth images. They were further grouped according to their size in (i) settlements 0-6 ha, (ii) settlements 6-12 ha, (iii) settlements 12-18 ha, and (iv) major centers, and derived as binary layer inputs for the Euclidian distance transforms. Due to their proportionally very large area the two largest towns in the Xiangxi catchment (Gaoyang 79 ha; Gufu 109 ha) are contained within the group of major centers. We considered the settlements as local, regional, and central markets having high local and regional influence as economic trading areas.

The river network used for the Euclidian distance transforms is derived from the DEM using the D8 flow accumulation algorithm (TARBOTON, 1997) and was classified according to the stream ordering method proposed by STRAHLER (1957). Comparable to the road network a sequential grouping of orders was used to derive the transforms as following: (i) stream lines of 1st order, (ii) stream lines of 1st and 2nd order, (iii) stream lines of 1st to 3rd order, (iv) stream lines of 1st to 4th order, (v) stream lines of 1st to 5th order, (vi) stream lines of 1st to 6th order, and (vi) stream lines of 1st to 7th order.

Additionally, the Euclidean distance to the Xiangxi shoreline after the impoundment based on the SPOT5 scene was also used as a potential anthropogenic indicator on human influence on terrace condition.

3.5 DATA MINING ALGORITHM

In total 81 indicators were derived as spatial grid datasets for data mining analysis and modeling. The data of the surveyed areas was extracted for further processing. The basic data mining algorithm used in this study is random forests - an ensemble of randomized CART decision trees (BREIMAN ET AL., 1984; BREIMAN, 2001) which proved to be a powerful prediction and analysis technique in digital soil mapping (GRIMM ET AL., 2008; BEHRENS ET AL., 2010b). We used the 'Random Forest' package by LIAW and WIENER (2011) for the R Project for Statistical Computing (R DEVELOPMENT CORE TEAM, 2011). Since the terrace conditions mapped (c.f., Section 3.2) follow an ordinal scale, we applied both regression and classification analysis.

3.6 FEATURE IMPORTANCE AND PARTIAL DEPENDENCE ANALYSIS

Random forest provides measures of the importance of each feature - or indicator - in a model in terms of a ranking. The higher the value the more important the corresponding indicator. We used the mean increase in accuracy as the importance measure, which is calculated by comparing the difference in the influence on model accuracy between an indicator and a randomly permuted version of it at each split in a tree when it is selected (BREIMAN, 2001; GRIMM ET AL., 2008).

Since feature importance analysis provides a ranking and not a selection of the indicators, we tested different sizes of subsets to derive a minimum set of indicators required for building accurate models. Therefore, we also compared the importance ranking resulting from regression analysis as well as from supervised classification.

We analyzed the partial dependence between the indicator and terrace condition according to CUTLER ET AL. (2007) and LIAW and WIENER (2011) in order to describe the marginal effect of an indicator on the terrace condition, after accounting for the average effect of all other indicators. The function being plotted describes the effect on the target as a continuous function using Eq. (1):

$$f' = \frac{1}{n}\sum_{i=1}^{n} f(x, x_{iC}) \qquad \text{(Eq. 1)}$$

where x is the indicator for which partial dependence is sought, and x_{iC} are the other indicators in the data. The summand is the predicted regression function (LIAW and WIENER, 2011). Hence, partial dependence allows easy and direct interpretations of the effects of an indicator contributing to the model. Compared to correlation analysis provided by linear regression approaches, the partial dependence as provided by random forests allows for describing non-linear influences on the target variable. However, the partial dependency analysis only provides relative relations to the target variable. Partial dependence is provided as a plot.

4 RESULTS

4.1 TERRACE CONDITIONS IN THE BACKWATER AREA

In total, 987 bench terraces were mapped in the backwater area of the Xiangxi catchment (Table 1). They cover an area of 10.6 km² which accounts for 1.9% of the area of the study site. The mapped terraces are spatially distributed all-over the hillslopes adjacent to the impounded Xiangxi River (Figure 4) on almost the whole range of altitudes in the backwater area from lowest 137 to 1402 m a.s.l. (n = 987). In average, the mapped terraces are located on an altitude of 337 m a.s.l. The general slope gradient of the terraced hillslopes ranges from 0° to 40° with an average slope gradient of 23°. With approximately 97%, the distinct majority of the bench terraces were mapped as cultivated

(Table 1). Mainly the terraces were associated with oranges (77%), followed by cultivation with dry land crops such as rape, wheat, and maize (15%), and garden land typically cropped with vegetables and fruits (7%). According to their total frequency and percentage of occurrence shown in Table 1, the mapped terrace condition classes are 'fairly maintained' (44.3%), 'partially collapsed' (23.4%), 'well maintained' (21.0%), and 'completely collapsed' (11.3%).

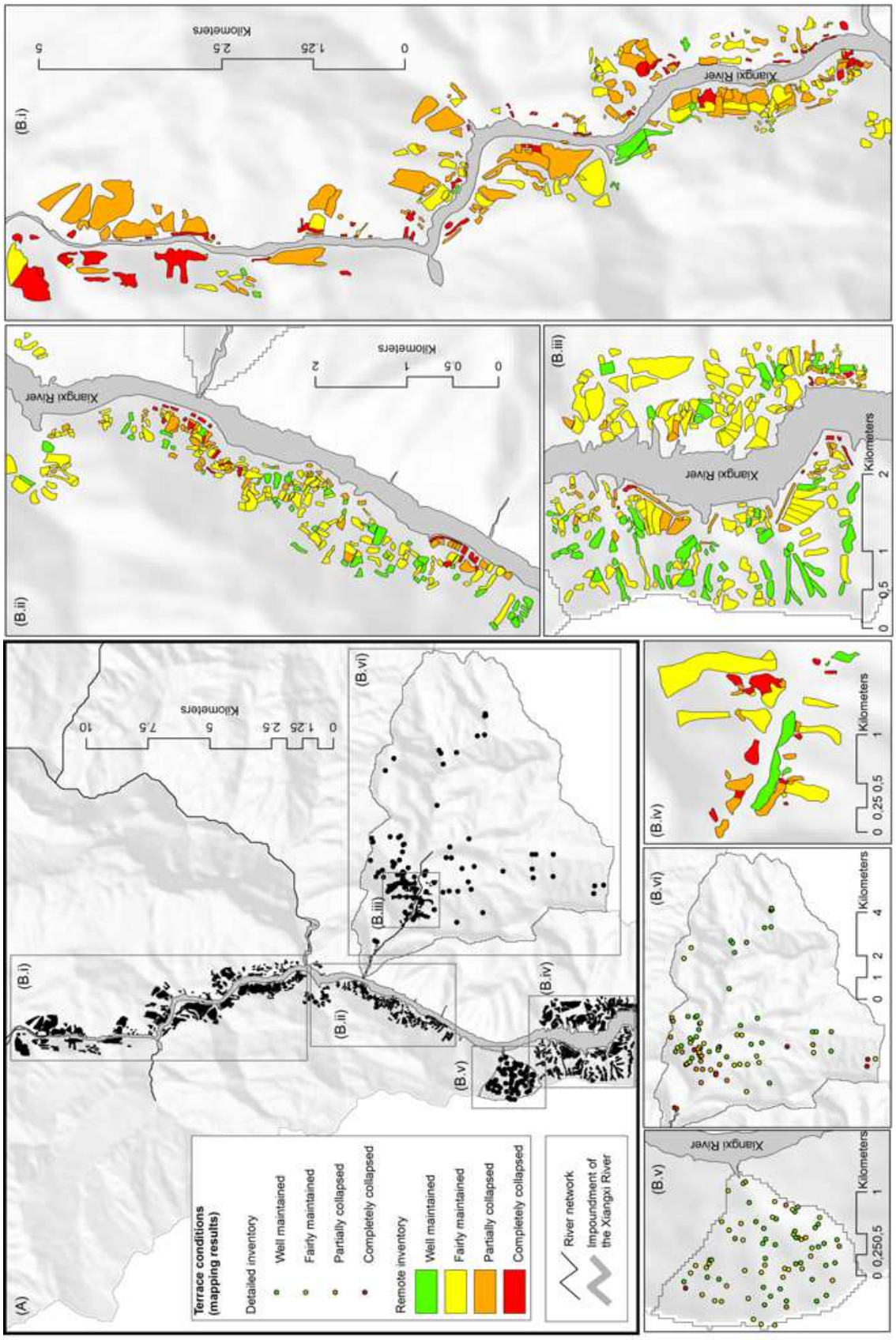

Figure 4 *Overview (A) and detailed views (B.i to B.vi) on the spatial distribution of the different types of terraces mapped including 'well maintained' terraces, 'fairly maintained' terraces, 'partially collapsed' terraces, and 'completely collapsed' terraces in the Xiangxi catchment.*

A subset of 158 terrace plots were analyzed in the detailed terrace survey (c.f., Section 3.2.1). Figure 5 schematically illustrates the results of this survey in terms of the averaged parameters of the terrace design for each terrace condition class. Whereas 'well maintained' terraces typically occur on hillslope sites inclining with 20° in average, the slope where 'completely collapsed' terraces were found increases to average 30° (Figure 5). DEM-based analyses also shows a slight increase in the average terrain slope (Table 1) between the classes with 0-36° for 'well maintained' to 5-40° for 'completely collapsed' terraces. Analogous to the increase in terrain slopes, there is also an increase in the average inclinations of the terrace risers. 'Well maintained' terraces typically exhibit level and mostly (75%) slightly outward sloping terrace risers inclining with in average 8°. For terraces classified as 'fairly maintained' as well as 'partially' and 'completely collapsed', not only the percentage of occurrence of outward sloping terrace risers but also its inclinations drastically increase up to 100%, respectively, 18° for 'completely collapsed' terraces (Figure 5).

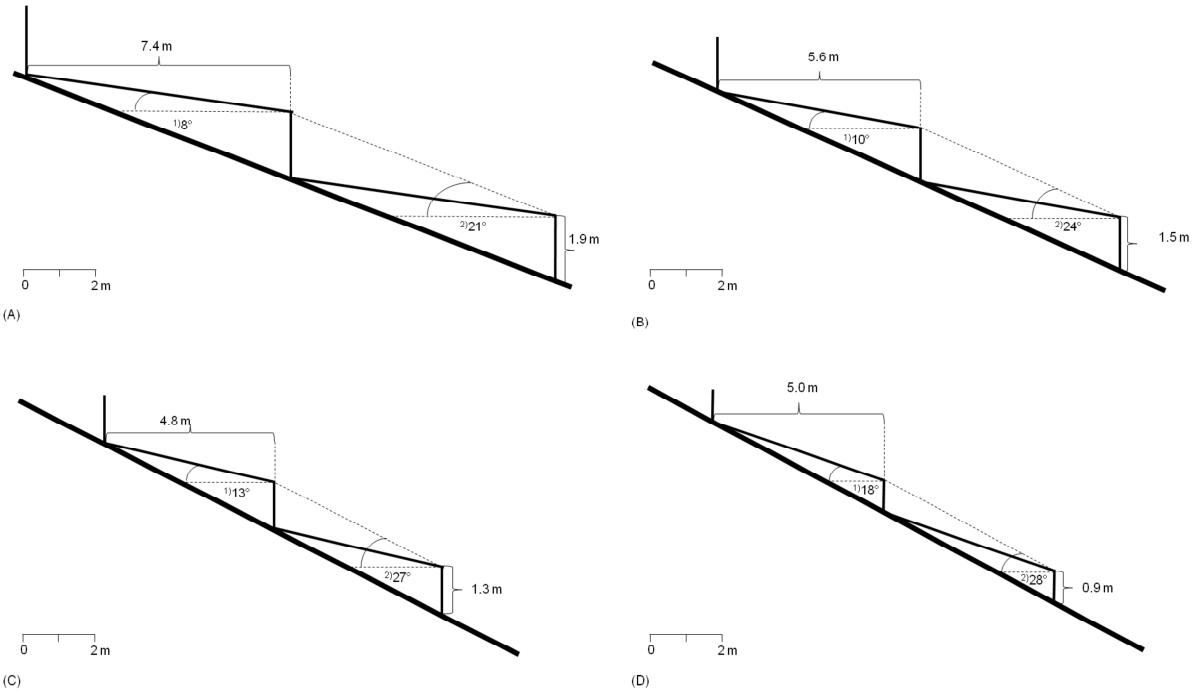

Figure 5 *Typical cross-section of the terrace design of 'well maintained' (A), 'fairly maintained' (B), 'partially collapsed' (C), and 'completely collapsed' terraces (D). Shown are the (1) average terrace slope (°), the (2) average terrain slope (°), the average height of the terrace wall (m), and the average width of the terrace riser (m).*

The average heights of the terrace walls even gradually decrease from highest 1.9 m for 'well maintained' terraces to lowest 0.9 m for 'completely collapsed' terraces (Figure 5). Thus, the average widths of terrace risers decrease from highest approximately 7.4 m again for 'well maintained' terraces to lowest 4.8 m for terraces classified as 'partially collapsed'.

The four surveyed classes of terrace condition do not only show clear evidence in terms of varying terrace design, but also their state of maintenance indicates a distinct sequence of degradation from well to collapsed. A relation to the background slope is obvious; jet might be problematic to derive from the DEM.

Table 1 *Characteristics of the surveyed terrace condition classes in the backwater area of the Xiangxi catchment given in total number and percentage. SD is standard deviation.*

Feature	Terrace condition class				Total
	Well maintained	Fairly maintained	Partially collapsed	Completely collapsed	
Total mapped terraces	207 (21%)	437 (44.3%)	231 (23.4%)	112 (11.3%)	987 (100%)
Remote terraces	139 (16.8%)	376 (45.4%)	209 (25.2%)	105 (12.7%)	829 (100%)
Detailed terraces	68 (43.0%)	61 (38.6%)	22 (13.9%)	7 (4.4%)	158 (100%)
Average size (ha)	0.8 (SD 1.2)	1.1 (SD 1.9)	1.4 (SD 2.9)	0.9 (SD 2.9)	1.08 (SD 3.8)
Terrain[a]					
Average altitude (m a.s.l.)	406 (SD 176)	348 (SD 157)	289 (SD 132)	260 (SD 174)	337 (SD 165)
Range of altitudes (m a.s.l.)	144-1108	137-1402	143-974	146-1382	137-1402
Average slope gradient (°)	22 (SD 7)	24 (SD 6)	24 (SD 6)	23 (SD 7)	23 (SD 7)
Range of slope gradient (°)	0-36	2-37	5-39	5-40	0-40
Land use					
Terraces mapped as cultivated	206 (99.5%)	432 (98.9%)	216 (93.5%)	99 (88.4%)	953 (96.6%)
Garden land	19 (30.2%)	16 (25.4%)	12 (19.0%)	16 (25.4%)	63 (6.6%)
Dry land	27 (19.0%)	59 (41.5%)	38 (26.8%)	18 (12.7%)	142 (14.9%)
Orange orchard	156 (21.2%)	356 (48.4%)	164 (22.3%)	59 (8.0%)	735 (77.1%)
Paddy	3 (100.0%)	0 (0%)	0 (0%)	0 (0%)	3 (0.3%)
Others (tea and chestnut)	1 (10.0%)	1 (10%)	2 (20%)	6 (60%)	10 (1.0%)

[a] *The parameter values on the terrain are based on DEM analyses.*

While terraces classified as 'well maintained' typically show an intact terrace structure in terms of supporting wall with in average only one bulge, respectively upsetting per terrace plot, the structure of 'fairly maintained' terraces already slightly deteriorates toward a less intact structure. For 'fairly maintained' terraces in average one bulge, respectively, one upsetting and in average four wall failures were detected. Frequent wall failures and wall collapses were mapped for terraces classified as 'partially collapsed' (Figure 6). Only at few points, these bench terraces exhibit a continuous structure of the supporting wall (Figure 7). For 'completely collapsed' terraces the structure is not longer existent (Figure 7). The number of wall failures such as breaches decrease in favor of serious collapses of the dry-stone walling (Figure 6A).

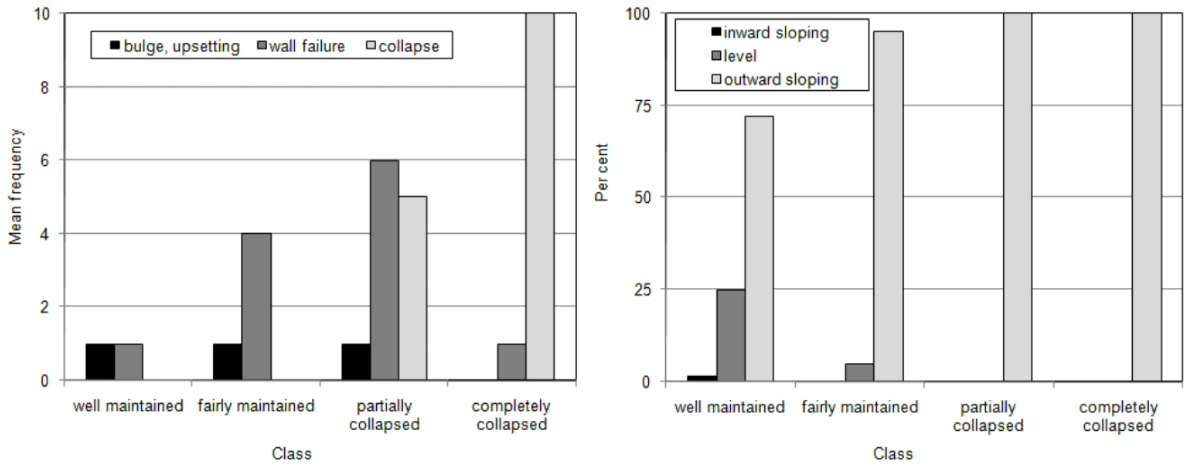

Figure 6 *Average frequency of wall disorders in each terrace condition class (A). Due to few observations of bulges and upsetting these wall disorders are grouped into one category. Percentage of different sloping terrace risers in each terrace condition class (B).*

4.2 MODELING ACCURACY AND INDICATOR IMPORTANCE

Initial modeling accuracy for the data mining approach based on a total of 81 features and using regression returns a root-mean-square-error of 0.325 indicating low differences between the predicted and the actually observed values, respectively terrace condition classes. The corresponding explained variance of the regression is R^2=79% and the OOB estimate of the error rate using classification is 8.3%. Both support the high modeling accuracy. However, the class 'completely collapsed' shows a comparable high error rate of 61% followed by the class 'well maintained' with an error rate of 17%. This might be a result of the lower spatial coverage (Table 1). Consequently, the classes 'fairly maintained' and 'partially collapsed' exhibit distinct lower class error rates (Table 2).

Table 2 *Model confusion matrix of the observed and predicted terrace condition classes and the class error including a total of 81 features. The numbers refer to pixels having a cell size of 45 m × 45 m.*

Observed terrace condition class	Predicted terrace condition class				Class error
	Well maint.	Fairly maint.	Partially collap.	Completely collap.	
Well maintained	599	105	13	0	0.165
Fairly maintained	36	2111	71	0	0.048
Partially collapsed	14	104	1437	2	0.077
Completely collapsed	7	13	10	19	0.612

maint. maintained, collap. collapsed

The generally high accuracy of the models, allows for subsequent analysis as well as interpretations. For both random forests approaches, the features were ranked according to their importance. The topmost 30 features were observed to be the same using classification and regression. Table 3 shows the ranking of those topmost 30 indicators according to their importance based on the

random forests classification model. It returned a mean decrease in accuracy ranging from highest 0.091 (ranking position 1) to lowest 0.016 (ranking position 30). Higher values of mean decrease in accuracy indicate features that have higher importance on the classification (CUTLER ET AL., 2007). The 10 topmost ranking positions are solely occupied with anthropogenic indicators (Table 3). The most important indicators are those directly related to the resettlements (distance to major centers) and to the Xiangxi River (distance of stream lines of 1st order) followed by distances to smaller settlements and to the road network. Below rank 10 mainly terrain attributes emerge as environmental indicators on the terrace degradation and its spatial distribution (Table 3).

Table 3 *The 30 out of 81 most important indicators in predicting the terrace condition classes. MDA is the mean decrease accuracy. Due to a higher differentiation of MDA, the numbers are given with four decimal places.*

Ranking position	MDA	Indicator
1	0.0910	Distance to major centers
2	0.0646	Distance of stream lines of 1st order
3	0.0602	Distance to settlements of 6-12 ha area size
4	0.0499	Distance to settlements of 12-18 ha area size
5	0.0386	Distance to major and side roads
6	0.0368	Distance of stream lines of 3rd order
7	0.0365	Distance to major and side roads, and paths
8	0.0365	Distance of stream lines of 2nd order
9	0.0360	Distance to major roads
10	0.0342	Distance to stream lines of 4th order
11	0.0312	Aspect deviance to 90° (17×17 pixel average)
12	0.0308	Aspect deviance to 90° (7×7 pixel average)
13	0.0288	Aspect deviance to 45° (7×7 pixel average)
14	0.0280	Aspect deviance to 45° (17×17 pixel average)
15	0.0249	Aspect deviance to 135° (17×17 pixel average)
16	0.0230	Mean curvature (17×17 pixel average)
17	0.0226	Distance to the Xiangxi River after impoundment
18	0.0225	Distance of settlements of a total of 4420
19	0.0222	Aspect deviance to 90°
20	0.0213	Distance to settlements of 0-6 ha area size
21	0.0207	Distance to stream lines of 6th order
22	0.0205	Distance to stream lines of 5th order
23	0.0192	Aspect deviance to 0° (17×17 pixel average)
24	0.0183	Aspect deviance to 45°
25	0.0177	Aspect deviance to 0° (7×7 pixel average)
26	0.0176	Topographic roughness (17×17 pixel average)
27	0.0176	Relative profile curvature (17×17 pixel average)
28	0.0174	Aspect deviance to 135° (7×7 pixel average)
29	0.0165	Relative richness (17×17 pixel average)
30	0.0160	Aspect deviance to 0°

While the ranking of the indicators gives us information on the explanatory strength and thus importance of an indicator on the terrace degradation, the partial dependence allows for an interpretation of the direction of influence. Figure 8 illustrates the partial dependence plots for the most important indicators of each category (anthropogenic and environmental indicators).

Figure 7 *Examples of the different terrace condition classes from the backwater area of the Xiangxi catchment; (A) 'well maintained' (A), 'fairly maintained' (B), 'partially collapsed' (C), and 'completely collapsed' (D). Photos by S. Schönbrodt-Stitt.*

The distance transforms of the major centers have the highest importance on the prediction of the terrace degradation (Table 3). In terms of the partial dependence, the worse terrace conditions were predicted in close distance to the major centers Gufu and Gaoyang (Figure 8). The distance to settlements of 6-12 ha size show a similar direction of influence, however the area surrounding the settlements that shows worst terrace conditions is smaller compared to the major settlements (about 7 km vs. 3.5 km).

For the distance to the Xiangxi River the worst conditions of terraces were also predicted close to the river. However, better conditions occur at much smaller distances compared to the settlements (i.e., < 1 km).

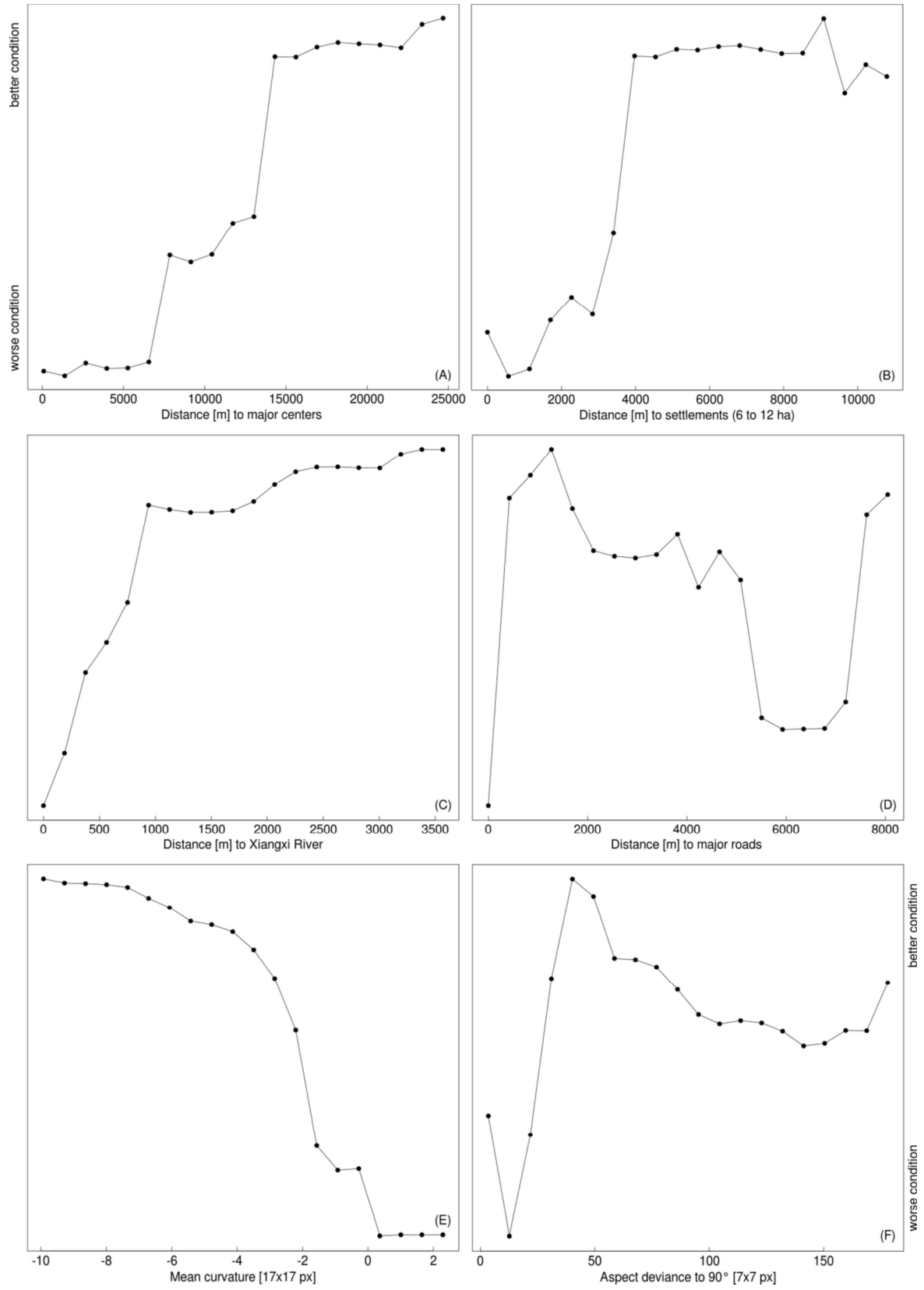

Figure 8 *Partial dependence plots for the distances (m) to major centers (A), to settlements of 6-12 ha area size (B), to the new Xiangxi River shoreline (C), to major roads (D), and of mean profile curvature (E) and aspect deviance to 90° (F).*

The distance to the major roads shows a very non-linear pattern (Figure 8D). The worst terrace conditions occur in distances below 500 m to the road network. The best terrace conditions occur around 1.5 km and around 8 km. The range between 5 km and 7 km is again characterized by worse terrace conditions.

Concerning the terrain attributes used as environmental indicators on the terrace conditions, negative mean curvatures at coarser scales, indicating smaller concave areas with limited access, show better conditions compared to flat or convex areas (Figure 8E). Aspect deviance to 90° indicates that the worst terrace conditions occur in the ENE-ESE sector (Figure 8F).

5 DISCUSSION

5.1 TERRACE DEGRADATION IN THE BACKWATER AREA

Contrary to the common knowledge, for instance as reported by HUDSON (1981), the heights of the supporting dry-stone walling of the surveyed bench terraces do not increase with higher slope angles of the terrain from ‘well maintained’ to ‘completely collapsed’ terraces (Figure 5). However, according to HUDSON (1981) a heightening of the walls is required as the slope angle is the most relevant limiting factor for the construction of bench terraces, particularly when slopes exceeds an angle of 25-30° (HUDSON, 1981). This is true for ‘partially’ and ‘completely collapsed’ terraces with average slope angles of the original terrain of 27-28° showing the lowest terrace walls with 1.3 and 0.9 m (Figure 5). Although there is no increase in the height of terrace walls, the decrease of the width of terrace risers from 7.4 for ‘well maintained’ terraces to 5.0 m for ‘partially’ and ‘completely collapsed’ terraces follows the findings achieved by HUDSON (1981) and BELLIN ET AL. (2009) according to which the width of terrace risers strongly depends on slope gradient. Typically, we would have expected the lowest average width of terrace riser for 'completely collapsed' terraces. Contrary to the above mentioned parameters of the terrace design, we assume the width of the terrace risers not adequately being represented by the low sample size of 'partially' and 'completely collapsed' terraces of $n = 22$, respectively, $n = 7$ from the detailed inventory of terraces (Table 1).

Generally, the shortening of the terrace risers combined with the increases of the terrain slope result in an increasing over-steepening of the terraces as all terrace condition classes exhibit outward sloping terrace risers (Figure 6B) to a hundred per cent. Even ‘well maintained’ terraces exhibit with 75% mostly outward sloping terrace risers, yet exhibit the lowest slope angle with 8°. As HUDSON (1981) described the terrace risers of bench terraces in steep sloping areas typically to be inward sloping or level and also SHI ET AL. (2004, 2012) report of level terraces as only soil conservation measure in the Wangjiiaqiao watershed close to our study area, we assume the surveyed bench terraces’ design to be not adequately adapted to the terrain in the study area. Though, bench terraces in

throughout the TGA are reported to exhibit a well-known technique with a long tradition (e.g., SHEN ET AL., 2010; SHI ET AL., 2012).

Additionally to the terrace design, the type and frequency of wall disorders provide us information on the state of maintenance of a terrace and consequently on its capability of soil conservation (BELLIN ET AL., 2009). Whereas 'well maintained' and 'fairly maintained' terraces typically show intact terrace structures (Figure 6), we observed a distinct worsening of the supporting walls and thus condition for 'partially collapsed' and 'completely collapsed' terraces. We consider the bulges and upsetting observed as only slight disturbances of the supporting walls that do not even occur on those terraces, to be "precursors" of a more complex destruction with numerous wall breaches and collapses. We therefore agree with INBAR and LLERENA (2000) who described the bulges and upsetting to develop prior to more serious wall failures and complete wall collapses due to increasing pressure on the terrace wall by saturated soil and their shearing effect and lack of constant maintenance.

Based on the term of terrace degradation as defined by BAZZOFFI and GARDIN (2011) and following the above findings, we consider the bench terraces in the backwater area of the Xiangxi catchment to clearly show a sequence of degradation terraces from 'well maintained' to 'completely collapsed' terrace conditions.

5.2 TERRACE DEGRADATION AND SOIL EROSION IN THE BACKWATER AREA

The increase in soil erosion fits the degradation of terraces and thus, their reduction of the capability to protect the soil against surface erosion (Table 4). Our results indicate that bench terraces cannot prevent soil erosion per se. Indicated by our results the frequency and magnitude of the mapped soil erosion is assumed to be related to the terrace condition classes (Table 4). This is in line with the findings by KOULOURI and GIOURGA (2007) who studied the evolution of soil and vegetation on terraced land following land abandonment in Lesvos Island, Greece, using experimental runoff plots. According to them, soil erosion on terrace land cannot be eliminated and strongly relates to the slope steepness, respectively steepness of the terrace riser. Furthermore, KOULOURI and GIOURGA (2007) outline the importance of the terraces' structure on the concentrated runoff and sediment removal. Thus, we conclude, that due to the intact structure and the comparably lowest slope of terrace risers of 'well maintained' terraces no rills could be observed, whereas the slight worsening of the terrace wall and higher steepness of terrace risers of 'fairly maintained' terraces already affect the removal of sediment (Table 4). The increasing average number of mapped rills from 2.3 for 'fairly maintained' terraces to 5.0 for 'partially' and 'completely collapsed' terraces (Table 4), we generally due to the increasing average number of wall failures and collapses and the terrace design exhibiting outward sloping terraced beds up to 18° located on extreme steep uphill sites up to 30° (Figures 5 and 6). Even

if the ‘completely collapsed’ terraces show a worse structure that might induce a higher concentrated runoff according to KOULOURI and GIOURGA (2007), there is no increase in the average frequency of rills compared to ‘partially collapsed’ terraces. With 3.6 even the standard deviation of the number of rills mapped on ‘partially collapsed’ terraces is higher than on ‘completely collapsed’ terraces (standard deviation of 1.4). We assume the worse terrace condition not to affect the frequency of rills, but rather their magnitude that we addressed with the spatial extent of the rill (Table 4). Thus, the worsening of condition of terraces classified as ‘completely collapsed’ compared to ‘partially collapsed’ terraces becomes obvious when looking at the average increases in depth and width of rills ranging from 2.8 to 3.0 cm, respectively from 3.1 to 3.5 cm, and the distinct increase in length of rills from 1.6 to 3.8 cm.

Table 4 *Average frequency and magnitude (depth, width, and length) of soil erosion rills per surveyed terrace plot (from the detailed terrace survey) and terrace condition class. SD is standard deviation.*

	Terrace condition class			
	Well maintained	Fairly maintained	Partially collapsed	Completely collapsed
Frequency	—	2.3 (SD 0.6)	5.0 (SD 3.6)	5.0 (SD 1.4)
Depth (cm)	—	2.7 (SD 0.6)	2.8 (SD 1.3)	3.0 (SD 0.0)
Width (cm)	—	3.0 (SD 0.0)	3.1 (SD 1.3)	3.5 (SD 0.7)
Length (m)	—	1.5 (SD 0.5)	1.6 (SD 0.9)	3.8 (SD 0.4)

We are aware that the above mentioned sample sizes of ‘partially’ and ‘completely collapsed’ terraces (Table 1) and the fact that there is no linear trend in the increase of the frequency of detected rills and their magnitude, only allow for a general conclusion of an increase of soil erosion following a worsening of the terrace conditions. We also suppose further factors to control the soil loss on bench terraces. According to GARDNER and GERRARD (2003) who monitored cultivated terrace plots in the Kathmandu valley in Nepal using erosion plots and measuring natural rainfall also rainfall duration and intensity have a high level of explanation for runoff up to approximately 80%. As for our study on a first inventory on terrace degradation in the TGA, monitoring was considered not practical and feasible, and for instance rainfall intensity and duration are expected to be distinctly less compared to the study site of GARDNER and GERRARD (2003) with mean annual rainfalls higher than 2000 mm, the effect of rainfall on the terrace degradation was not investigated.

Also the vegetation cover and its variability, e.g., cropping cycle are revealed to impact the runoff and soil losses on terraces (GARDNER and GERRARD, 2003). Our mapping results however show a relatively balanced distribution of the land uses (Table 1). The integration of three Landsat5-TM images for the assessment of the influence of the land cover within the data mining approach revealed no distinct effect on the terrace condition classes (Table 3). Only for paddy terraces under rice cropping, a distinct association with 'well maintained' terraces was observed based on the results

of the field mapping (Table 1). According to CHEN ET AL. (2012) paddy terraces constantly require high maintenance and mechanical cultivation in order to meet the major preconditions of intact walls and level terrace risers. Under flooded conditions the topsoil is also less susceptible to rainfall and thus, sediment removal than under dry land cultivation or fallow (CHEN ET AL., 2012). Thus, for the backwater area of the Xiangxi catchment with its periodically flooded rice fields and cultivation during summer season (SEEBER ET AL., 2010), we assume a generally higher effect of soil conservation of the paddy terraces with simultaneous high maintenance. In contrast, perennial tea and chestnuts seem to be closely linked to 'completely collapsed' terraces as they affect them up to 60% (Table 1). Each of this six surveyed plots is located in remote areas of the Quyuan test site. We expect the farmers of those plots to not constantly maintain these terraces as both crops are perennial and are expected to not require high labor input such as paddy rice.

5.3 CAUSES OF TERRACE DEGRADATION IN THE BACKWATER AREA

Our results clearly show that the causes of different terrace conditions, and thus terrace degradation in the TGA are multi-factorial (Table 3).

This general finding is in accordance with the results achieved by BEVAN ET AL. (2012) who studied the social and ecological context of terraces related to cycles of population growths on Antikythera Island, Greece. According to them, the influences on a terraced landscape and its modification, e.g., terrace degradation are discussed as highly complex resulting from multiple decisions and various human-environmental interactions that form a socio-ecological landscape (BEVAN and CONOLLY, 2011; BEVAN ET AL., 2012). We also generally agree with INBAR and LLERENA (2000) who stated terrace degradation to be a function of physical, economic, and socio-economic factors such as land use, distance from a village, etc. and transfer this statement to the TGA. As revealed by the data mining approach, foremostly anthropogenic indicators such as the distance to settlements and roads do explain the terrace degradation in the backwater area of the Xiangxi catchment (Table 3).

New about the knowledge on the process of terrace degradation in our study is that not agricultural abandonment explains the terrace degradation, for instance as observed by KOULOURI and GIOURGA (2007), LESSCHEN ET AL. (2008), and EL ATTA and AREF (2010) for bench terraces in the Mediterranean. As we surveyed cultivated bench terraces to almost a hundred per cent (Table 1) and SEEBER ET AL. (2010) could not detect abandoned farmland to a meaningful extent in the backwater area of the Xiangxi catchment, we prove terrace degradation as an effect of land cultivation, too. We assume this to be a direct consequence of complex cause-effect relationship of rapid land use changes (PONSETI and LÓPEZ-PUJOL, 2006), and massive dam-induced forced, rural and urban resettlements in

Zigui and Xingshan counties associated with the Xiangxi river impoundment by the TGD (HEMING ET AL., 2001; MCDONALD ET AL., 2008).

5.3.1 ANTHROPOGENIC EFFECTS ON TERRACE DEGRADATION

5.3.1.1 EFFECTS OF RESETTLEMENTS

According to their study on land use change in the Xiangxi catchment using satellite imagery, SEEBER ET AL. (2010) estimated the area lost to the river impoundment to be approximately 9 km². This land previously used for agriculture and settlement had to be compensated causing land use changes on approximately 26% of area of the steep sloping backwater area in close distance to the new Xiangxi reservoir (SEEBER ET AL., 2010). As the analysis of the partial dependence plots reveals (Figure 8) this is exactly the area of the worst terrace conditions of 'partially' and 'completely collapsed' terraces. Comparing the terraces of worse conditions close to larger settlements and the main road and river network to those of better conditions (well and fairly maintained) more distant to this dynamic areas (Figure 8), we suppose the forced resettlement (HEMING ET AL., 2001) to play an important role in the mismanagement of bench terraces leading to their degradation. Thus, we infer the resettled peasants to get confronted by challenges with farming steep sloping land after the impoundment. Farming those uphill-sites requires first of all time-consuming terracing generally necessitating high investments in material and labor (INBAR and LLERENA 2000; SHI ET AL., 2012).

According to HEMING ET AL. (2001) and PONSETI and LÓPEZ-PUJOL (2006) the loss of the traditional connection to the land after resettlement causes a lack of familiarity with the new farming environment and techniques. It can be made responsible for the mismanagement, even if the peasants were resettled to uphill-sites within close distance to their former home (PONSETI and LÓPEZ-PUJOL, 2006). For instance, 66% of the relocates in the TGA that were moved to steep infertile slopes at higher elevations were observed to refuse farming due to a reduced amount of land characterized by severe physical settings (HEMING ET AL., 2001). PONSETI and LÓPEZ-PUJOL (2006) explain this fact with the discrepancy between the long-time terracing experience of the 'uphill-peasants' and the lack of experience of the former 'downhill-peasants' that previously farmed the flat valley bottoms. This effect can be seen in the non-linear behavior of the partial dependence plot of the major roads (Figure 8D).

In the context of rural and urban resettlements in the TGA, also the aging of the rural population and governmental-driven settling of younger rural migrants in industrial jobs as stated by HEMING ET AL. (2001) and STEIL and DUAN (2002) are considered to hinder an adequate terrace construction and constant maintenance by repairing wall damages. A similar process was observed by INBAR and LLERENA (2000) for bench terraces in the Peruvian Andean Mountains where young

people are gravitating toward better job opportunities in the coastal cities causing an irreversible process of shortage of labor for long-term soil conservation.

5.3.1.2 EFFECTS OF CULTIVATION

Besides these resettlement-related effects, also the land reclamation for cultivation and the shift of agriculture, especially toward the cash crop production of oranges as detected by SEEBER ET AL. (2010), are expected to affect the terraced landscape in the study area. With the river impoundment, the implementation of orange orchard became highly recommended in the TGA as it is supposed to reduce soil and nutrient loss and favor a suitable use on uphill-sites exceeding slopes of 25°, and to boost the farmer's income after the TGD-associated resettlement (MENG ET AL., 2001; SHI ET AL., 2012). For instance, investigations by SHI ET AL. (2012) in Wangjiiaqiao watershed in Zigui county close to the Xiangxi catchment revealed an increase of orange orchards by the 2.8-fold accounting for approximately the same increase of orange orchards in the western backwater area of the Xiangxi catchment (SEEBER ET AL., 2010). In the Xiangxi catchment orange orchards distinctly predominate on terraces close to large settlements and main transportation routes such as trafficable main roads and rivers (SEEBER ET AL., 2010). This area also refers to the mid-tropic zone below an elevation of 500 m a.s.l. that is climatically suitable for citrus growth (WU ET AL., 2009). According to our findings from the partial dependence analysis, this area adjacent to the river banks of the Xiangxi refers to the location of terraces of higher degree of degradation (e.g., 'partially' and 'completely collapsed' terraces), too (Figure 8C).

As in Hubei province the area under orange cultivation increased by thousands of hectares with the support of governmental subsidies and investments (FOREIGN AGRICULTURAL SERVICE/USDA, 2007), we assume a cause-effect relationship between the governmental-driven implementation of orange orchards and the condition of terraces in our study area. As reported by several farmers during our survey the expenses for orange production (e.g., fertilizers, pesticides) often exceed their income, which we suppose to result from decreasing market prices, labor-intensive and costly harvesting, and a non-adequate governmental financial support. In this context, the lack of a cost and time-consuming maintenance of terraces would be a logical consequence of a simple cost-benefit-calculation. This is especially true against the background that for slope gradients above 10% (c.f., SHI ET AL., 2012) the spacing between the terraces decreases to such a point that their construction and maintenance is expensive and lack of investments limits their adoption. We support our assumption with observations done by SIDLE ET AL. (2006) for bench terraces in Thailand where farmers refused the maintenance terraces due to unavailable compensation of costs. A similar effect was observed by WILLIAMS (1990) for terrace hillside farming in Venezuela. Neither the knowledge nor the ability, but rather the farmers' motivation depending on economic-driven decisions is reported

to control the terrace development. According to WILLIAMS (1990), farmer's participation in terrace construction could be secured by support from external sources such as subsidy payment based on the cubic meter of dry-stone walling built.

5.3.1.3 EFFECTS OF ACCESSIBILITY

While the immediate reservoir area with high land-use dynamics is considered to present an area of fast access, the uphill-sites in higher altitudes distinctly show less accessibility. We suppose the newly constructed paved roads and navigable rivers after impoundment to exhibit important infrastructural connections and to favor the governmental-driven production of oranges as cash crop. We expect a fast accessible area with settlements acting as local and regional markets to be more attractive for the cash crop production (i.e., in terms of processing, marketing, and transport) than difficult to access farmland and small settlements and markets without any trading potential. For instance, focusing on high production and quality, the increase in orange cultivated area is associated with the construction of industry for post-harvest treatments and infrastructural connection (FOREIGN AGRICULTURAL SERVICE/USDA, 2007).

In contrast, the bench terraces more distant to the reservoir are considered to be primarily cultivated by experienced farmers for subsistence cultivation. Those terraces are difficult to access and the high terrain energy requires higher labor in cultivating. Furthermore, big cars cannot drive along unpaved and narrow side roads and paths, transportation by ship is impossible and larger settlements do not develop. Thus, we assume the steep sloping uphill-sites to be utterly not attractive for large-scale orange production and to be in some parts better protected as revealed by the partial dependence to curvature (Figure 8F).

A more difficult access to larger settlements via side roads and paths in a region of higher altitudes would further imply that uphill-peasants depend more on their farming products and thus properly maintained terraces. Available capital and efforts for maintaining terraces seem to be better invested.

However, considering the range of altitudes for the different terraces condition classes (Table 1) there is no clear trend in the distribution of worse terrace conditions ('partially' and 'completely collapsed' terraces) in this 'citrus belt' along the river banks of the Xiangxi (WU ET AL., 2009). Also the average altitudinal locations ranging from 406 m a.s.l. for 'well maintained' terraces to 260 m a.s.l. for 'completely collapsed' terraces and the relatively balanced distribution of land use within the terrace condition classes (Table 1) enable for only a rough conclusion on the dependency between the accessibility of terraces and orange plantations and its effect on terrace degradation. Due to a lack of discussion in literature, our assumption on the role of orange production on terrace degradation cannot be conclusively settled here.

However, due to the complexity of interactions in terraced landscapes (BEVAN ET AL., 2012) we consider an interpretation of the influences and their strength to be not sufficient when addressing an individual indicator, but rather consider their combination. Even if the distance transforms of the major centers exhibit by far the highest impact on terraces degradation (MDA = 0.091) compared to the further top 10 ranking anthropogenic indicators (MDA 0.065-0.034). This is especially true for the backwater area of the Xiangxi catchment where the road and infrastructure construction, the resettlements, and land reclamation for agricultural uses as well as shifts in agriculture associated to the TGD are closely related to each other (SEEBER ET AL., 2010).

5.3.2 TERRAIN EFFECT ON THE TERRACE DEGRADATION

Besides these anthropogenic effects, also the geomorphic settings affect the terrace conditions, albeit with less importance of the environmental indicators referring to the terrain (MDA 0.031-0.016). For instance, as derived by the partial dependence plot, terraces of worse condition are potentially located on slopes inclining between ENE and ESE (Figure 8F). This is supposed to be a typical proxy effect since slopes exposing northeast and southeast in the Xiangxi catchment mostly occur on Jurassic strata and to a slightly less extent on Silurian and Triassic strata (EHRET ET AL., 2010). Terraces of better condition mostly occur on south, north, and west exposing slopes referring to Precambrian to Cambrian and Devonian to Permian strata (EHRET ET AL., 2010). Here, two facts can serve as possible explanation for the different terrace conditions. On the one hand, the resistance to weathering on the Jurassic and Silurian strata, and the top formations of the Triassic is distinctly less compared to the weathering on the stable parent material such as sandstones and limestones of the other strata (EHRET ET AL., 2010). On the other hand, the Jurassic claystones, the Silurian marls, and the clayey formations of the middle and upper Triassic are prone to water saturation and exhibit deep seated and translational landslides (EHRET ET AL., 2010). This is in line with BAZZOFFI and GARDIN (2011) according to which dry-stone walling terraces built on compact and permeable bedrock are less vulnerable to the destruction by mass movements than terraces built on incoherent materials exhibiting higher risk of landsliding. In the case of our study area this would imply that water storage, high soil erosion susceptibility, and the occurrence of landslides induce the process of terrace destruction, and thus have an impact on terrace degradation. In turn, destroyed terraces are supposed do not offer enough control to combat soil erosion (Table 1) as damage spots of the ruined terraces' structure exhibit weak points vulnerable to concentrated runoff and sediment removal (KOULOURI and GIOURGA, 2007).

Besides the consideration of the aspect serving as a proxy for lithology, it can also refer to the solar radiation (EVANS and WINTERHALDER, 2000) as the exposure to the sun is described as a key component in the agricultural productivity of terraces. In this case, the aspect would not purely represent the terrain, but rather indicate farmer's decisions on the effort to maintain terraces of higher

or lower productivity related to the solar exposure. Under this consideration, the aspect serves as anthropogenic indicator.

We also considered the aspect to have a higher impact on the terrace conditions in the mountainous study site than the terrain slope as the feature importance does not rank the slope angle among those indicators of high importance (Table 3). This is contrary to the findings by HUDSON (1981) according to which the terrain slope is one of the main determinants of the terrace design. However, in terms of the terrace condition we assume the terrain slope to be strongly altered by the above proxy effects of the aspect

5.4 APPLICABILITY AND CONSTRAINTS OF THE MODEL FRAMEWORK

Our model framework *TerraCE* enables for the identification and spatial analysis of different terrace conditions and their causes under cultivation. It considers the sparse data availability and limited access to terrain and thus, improves our knowledge on terrace degradation by conducting the first inventory of bench terraces in the TGA and throughout China.

According to our results, the classification of terrace conditions by combining their design and state of maintenance proved as sufficient as we assessed the whole range of wall disorders. However, due to the fact, that such an inventory on bench terraced was conducted the first time in the TGA and was not based on any previous qualitative and quantitative information; our approach is certainly capable of improvements in terms of higher differentiation of terrace conditions. Moreover, direct measurements of soil loss and runoff would help to gain precise information on the effect of the terrace degradation on the soil erosion. An increase in sample sizes (Table 1), especially of those classes that are yet underrepresented, would improve the statistical analysis and its explanatory power on the spatial distribution of terrace conditions. As we do not have any information on the time the terraces were constructed, we are currently not able to assign a specific terrace condition to the age of a terrace in order to consider its influence on terrace degradation independent from the maintenance. Here, the monitoring of bench terraces over a longer period would eventually improve the understanding of the process of terrace degradation.

Further limitations of this approach unequivocally lie in the low spatial coverage of the mapping area. Especially, the hinterland of the backwater area could not have been covered (Figure 4). Our mapping approach was constrained by the limited access to the highly mountainous terrain and the time-consuming detailed survey on bench terraces. The absence of remote sensing data in a satisfactory high spatial resolution exhibits another limiting factor regarding a clear identification of the condition of bench terraces and their area-wide inventory in the study area. In this context, we consider our approach using field mapping as best affordable method. The 'quasi-remote' inventory on

the terrace conditions proved as a fast survey scheme covering a large area compared to the detailed inventory and gained a large training data set.

Applying random forests classification and regression models by embedding environmental and anthropogenic indicators mainly based on remote sensing data performed strongly (Table 2) and proved as valid approach in modeling terrace conditions. Strength and direction of the effect of the forced rapid agricultural changes and massive resettlement on terrace degradation can be clearly derived using indicator importance and partial dependence analyses.

Indeed, *TerraCE* does not serve as universal model in terms of describing global generalities for terrace degradation. It rather improves the understanding of the phenomenon of terrace degradation under forced resettlement in the TGA (HEMING ET AL., 2001) since we consider it to be a driving factor for land use dynamics affecting the terrace conditions. The relation between the terraces' state of maintenance and the cost and profit is valid for a free-market economy, however, in the TGA also the motivation to maintain terraces and the familiarity with the farming system strongly affect the 'treatment of terraces' in a region that accounts for a 'socio-ecological landscape' characterized by various human-environmental interactions as described by BEVAN ET AL. (2012). Foremost, by applying *TerraCE* we aim at a locally adapted model in order to assess the terrace conditions and their driving factors as well as to explain their effect on the terrace degradation. In this context, we discuss the costs and benefits of the mostly new installed cash crop oranges as being one reason for the lack of motivation of the farmers to maintain their terraces.

The modeling accuracy of *TerraCE* is high; however we assume that its significance on the effect on the terrace degradation can be still enlarged by incorporating more indicators affecting the development of terraces such as land tenure, ownership, cropping cycle and many more. Here, our model framework offers an open structure. *TerraCE* is readily transferable to other regions when the requirements on the data are fulfilled.

6 CONCLUSIONS AND OUTLOOK

Terrace degradation under cultivation in the backwater area of the Xiangxi catchment is obvious. The sequence of terrace degradation ranges from 'well maintained', 'fairly maintained', and 'partially collapsed' to 'completely collapsed' terraces. These different terrace conditions serve as indicators on the process of terrace degradation and are spatially distributed systematically.

For the first time, it was proven that spatial data mining tools in combination with specifically derived descriptive data on the effect of human activity and terrain can be used to derive the strength and direction of the effect of the rapid agricultural changes mainly due to forced resettlements on terrace degradation.

The effect of relief, which can be regarded as the major natural driver for terrace degradation by erosive action is tributary but altered and overlaid by land use dynamics associated with the Three Gorges Dam. Thus, foremost, anthropogenic indicators such as the distance transforms to settlements and roads affect the spatial distribution of terrace conditions and thus, terrace degradation. With increasing distances to main settlements and transportation routes (main roads and navigable rivers) and thus local and regional markets, the terraces exhibit better condition. We conclude this to be an effect of a higher farmer's motivation to constantly maintain terraces. The closer the terraces to new settlements, to the new Xiangxi River shoreline, and to the new major roads, the worse is their condition. The newly developed larger settlements and roads for a better infrastructural connection serve as preferential routes for claiming new agricultural land and existing terraced farmland for cash crop production as observed by SEEBER ET AL. (2010) for the Xiangxi catchment. Hence, a fast access to terraced farmland via main transportation routes is supposed to be a one reason for the terrace degradation whereas remote terraces in higher elevations and more distant to the new infrastructure are less attractive farmland for cash crops because of the difficult access. We conclude that the tempo of the land use dynamics hardly considers available capital for the restoration of terraces. Thus the motivation of maintaining is assumed to be driven by economic decisions. Moreover, a lack of familiarity with the new farming system hinders an adequate terracing by former downhill peasant previously farming the now impounded valley bottoms.

Under the above consideration we mainly assume the equilibrium state (BRANCUCCI and PALIAGA, 2006) of the terraces in our study area to be disturbed by the land use changes associated to the TGD. This should be urgently addressed by politics since the cultivated bench terraces have to be adapted to this new situation in order to keep their effectiveness in terms of soil conservation.

The results can help to improve the terrace planning in the mountainous TGA and its future development. Especially against the background of a limited environmental carrying capacity in the TGA the results emphasize the relevance of balanced human-environmental interactions for a sustainable land management. Furthermore, the consideration of terraces is an essential precondition in soil erosion risk evaluation. Thus, the incorporation of the local-specific variability of soil erosion due to terrace degradation is an important next step in soil erosion modeling incorporating the *TerraCE* approach. Here, precise and spatial information on the characteristics of terrace degradation would help to avoid over- or underestimations of the soil erosion risk potential. Moreover, we intend to extend the modeling approach toward areas beyond the backwater area directly affected as we expect the hinterland to be reclaimed in the future.

ACKNOWLEDGEMENTS

We thankfully acknowledge funding from the German Ministry of Education and Research (BMBF, grant no. 03 G 0669) for the German-Sino research collaboration YANGTZE. We thank Dr. Günter Subklew from the Research Centre Jülich for coordinating and Dr. Xiang Wei and the China University of Geosciences (Wuhan) for collaborating. Special thanks also go the Stephan Imbery, Julia Bär, and Moritz Koch for supporting in the field as well as Edgar A. Stitt for proofreading.

REFERENCES

ARNAEZ, J., LASANTA, T., ERREAN, M.P., ORTIGOSA, L., 2010. Land abandonment, landscape evolution, and soil erosion in a Spanish Mediterranean mountain region: the case of Camero Viejo. *Land Degradation and Development* 22 (6), 537-550.

AW-HASSAN, A., ALSANABANI, M., BAMATRAF, A.R., 2000. Impact of land tenure and other socioeconomic factors on mountain terrace maintenance in Yemen. CAPRi Working Paper No. 3, CGIAR System-wide Program on Property Rights and Collective Action, International Development Research Center (IDRC), Ottawa, Canada, pp. 42, http://www.capri.cgiar.org/pdf/CAPRIWP03.pdf (08/16/2013).

BAZZOFFI, P., GARDIN, L., 2011. Effectiveness of the GAEC standard of cross compliance retain terraces on soil erosion control. *Italian Journal of Agronomy*, doi: 10.4081/ija.2011.6.s1.e6.

BEAUDETTE, D.E., O'GEEN, A.T., 2009. Quantifying the aspect effect: an application of solar radiation modeling for soil survey. *Soil Science Society of America Journal* 73, 1345-1352.

BEHRENS, T., 2003. Digitael Reliefanalyse als Basis von Boden-Landschafts-Modellen - Am Beispiel der Modellierung periglaziärer Lagen im Ostharz. Boden und Landschaft 42, Universität Giessen, Giessen, pp. 189 (in German).

BEHRENS, T., ZHU, A.X., SCHMIDT, K., SCHOLTEN, T., 2010a. Multi-scale digital terrain analysis and feature selection in digital soil mapping. *Geoderma* 155, 175-185.

BEHRENS, T., SCHMIDT, K., ZHU, A.X., SCHOLTEN, T., 2010b. The ConMap approach for terrain-based digital soil mapping. *European Journal of Soil Science* 61, 133-143.

BELLIN, N., VAN WESEMAEL, B., MEERKERK, A., VANACKER, V., BARBERA, G.G., 2009. Abandonment of soil and water conservation structures in Mediterranean ecosystems - a case study from east Spain. *Catena* 76, 114-121.

BEVAN, A., CONOLLY, J., 2011. Terraced fields and Mediterranean landscape structure: an analytical case study from Antikythera, Greece. *Ecological Modelling* 222, 1303-1314.

BEVAN, A., CONOLLY, J., COLLEDGE, S., FREDERICK, C., PALMER, C., SIDDALL, R., STELLATOU, A., 2012. The long-term ecology of agricultural terraces and enclosed fields from Antikythera. *Human Ecology* 41 (2), 255-272.

BRANCUCCI, G., PALIAGA, G., 2006. The hazard assessment in a terraced landscape: preliminary result of the liguria (Italy) case study in the Interreg III Alpter Project. in: Nadim, N., Pöttler, R., Einstein, H., Klapperich, H., Kramer, S. (Eds.), Geohazards. ECI Symposium Series, Volume P07 (2006), pp.10, http://dc.engconfintl.org/geohazards/16 (01/15/2009).

BREIMAN, L., FRIEDMAN, J.H., OLSHEN, R.A., STONE, C.J., 1984. Classification and regression trees. Wadsworth International Group: Belmont, California, pp. 43-49.

BREIMAN, L., 2001. Random forests. Machine Learning 45, 5-32.

CAO, S., CHEN, L., FENG, Q., LIU, Z., 2007. Soft-riser bench terrace design for the hilly loess region of Shaanxi Province, China. *Landscape and Urban Planning* 80, 184-191.

CHEMIN, A., VAROTTO, M., 2008. Veneto. The "masiere" of the Brenta Valley. in: Scaramellini, G., Varotto, M. (Eds.), Terraced landscapes of the Alps - Atlas, pp. 97-101, ALPTER Project, Marsilio, Venice, Italy, http://www.alpter.net/ALPTER-Project-final-publications.html (04/11/2011).

CHEN, S.K., LIU, C.W., CHEN, Y.R., 2012. Assessing soil erosion in a terraced paddy field using experimental measurements and universal soil loss equation. *Catena* 95, 131-141.

COMOLLI, R., 2005. Soils and man-made terraces in Sondrio Region: pilot area of Pianazzola. ALPTER Terraced Landscapes of the Alpine Arc, Meeting Internazionale, 3-4 Novembre 2005, Sondrio SO, Italy. http://www.alpter.net/Documents-from-research-activities.html (01/15/2009).

CORBEELS, M., SHIFERAW, A., HAILE, M., 2000. Farmers' knowledge of soil fertility and local management strategies in Tigray, Ethopia. Managing Africa's Soil No. 1, pp. 24. IIED, London. http://pubs.iied.org/pdfs/7421IIED.pdf (11/01/2011).

CUI, P., GE, Y., LIN, Y., 2011. Soil erosion and sediment control effects in the Three Gorges reservoir Region, China. *Journal of Resources and Ecology* 2 (4), 289-297.

CUTLER, D.R., EDWARDS, T.C. JR., BEARD, K.H., CUTLER, A., HESS, K.T., GIBSON, J., LAWLER, J.J., 2007. Random forests for classification in ecology. *Ecology* 88, 2783-2792.

DAMENE, S., TAMENE, L., VLEK, P.L.G., 2012. Performance of farmland terraces in maintaining soil fertility: a case of Lake Maybar watershed in Wello, Northern Highlands of Ethiopia. *Journal of Life Sciences* 6, 125-1261.

DEININGER, K., JIN, S., 2006. Tenure security and land-related investments: evidence from Ethiopia. *European Economic Review* 50, 1245-1277.

EHRET, D., ROHN, J., DUMPERTH, C., ECKSTEIN, S., ERNSTBERGER, S., OTTE, K., RUDOLPH, R., WIEDENMANN, J., WEI, X., BI, R., 2010. Frequency ration analysis of mass movements in the Xiangxi Catchment, Three Gorges Reservoir Area, China. *Journal of Earth Science* 21, 824-834.

EL ATTA, H.A., AREF, I., 2010. Effect of terracing on rainwater harvesting and growth of Juniperus Procera Hchst. ex Endlicher. *International Journal of Environmental Science and Technology* 7, 59-66.

ESTEVE, J.F., IMESON, A., JARMAN, R., BARBERIS, R., RYDELL, B., CASTILLO SÁNCHEZ, V., VANDEKERCKHOVE, L., 2004. Pressures and drivers causing soil erosion. in: Van-Camp, L., Bujarrabal, B., Gentile, A.R., Jones, R.J.A., Montanarella, L., Olazabal, C., Selvaradjou, S.K. (Eds.), Reports of the Technical Working Groups Established Under the Thematic Strategy for Soil Protection. Volume II Erosion. EUR 21319 EN/2, Office for Official Publications of the European Communities, Luxembourg. http://ec.europa.eu/environment/soil/pdf/vol2.pdf (01/27/2013).

EVANS, T.P., WINTERHALDER, B., 2000. Modified solar insolation as an agronomic factor in terraced environments. *Land Degradation and Development* 11, 273-287.

FOREIGN AGRICULTURAL SERVICE/USDA, 2007. Situation and outlook for citrus, Citrus - Special Feature Article. Office of Global Analysis http://www.fas.usda.gov/2007/whatsnewfeb07.asp (10/24/2011).

GARDNER, R.A.M., GERRARD, A.J., 2003. Runoff and soil erosion on cultivated rainfed terraces in the Middle Hills of Nepal. *Applied Geography* 23, 23-45.

GRIMM, R., BEHRENS, T., MÄRKER, M., ELSENBEER, A., 2008. Soil organic carbon concentrations and stocks on Barro Colorado Island - digital soil mapping using random forests analysis. *Geoderma* 146, 102-113.

HAMMAD, A.A., HAUGEN, L.E., BØRRESEN, T., 2004. Effects of stonewalled terracing techniques on soil water conservation and wheat production under Mediterranean conditions. *Environmental Management* 34, 701-710.

HEGGELUND, G., 2006. Resettlement programmes and environmental capacity in the Three Gorges Dam project. *Development and Change* 37, 179-199.

HEMING, L., WALEY, P., REES, P., 2001. Reservoir resettlement in China: past experience and the Three Gorges Dam. *The Geographical Journal* 167, 195-212.

HODGSON, M.E., GAILE, G., 1999. A cartographic modeling approach for surface orientation-related applications. *Photogrammetric Engineering & Remote Sensing* 65, 85-95.

HUBER, M., 1994. The digital geo-ecological map - concepts, GIS-methods and case studies. *Physiogeographica* 20, Basel, pp. 144.

HUDSON, N., 1981. Soil conservation. Cornell University Press, London, pp. 324.

INBAR, M., LLERENA, C.A., 2000. Erosion processes in high mountain agricultural terraces in Peru. *Mountain Research and Development* 20, 72-79.

JARVIS, A., REUTER, H.I., NELSON, A., GUEVARA, E., 2008. Hole-filled seamless SRTM data V4, International Centre for Tropical Agriculture (CIAT), available from http://srtm.csi.cgiar.org.

KLEEFISCH, B., KÖTHE, R., 1993. Wege zur rechnergestützten bodenkundlichen Interpretation digitaler Reliefdaten. Geologisches Jahrbuch Reihe F Band F 27, 59-122, Schweizerbart Science Publishers (in German).

KOULOURI, M., GIOURGA, C., 2007. Land abandonment and slope gradient as key factors of soil erosion in Mediterranean terraced lands. *Catena* 69, 274-278.

LASANTA, T., ARNÁEZ, J., OSERÍN, M., ORTIGOSA, L.M., 2001. Marginal lands and erosion in terraced fields in the Mediterranean mountains - a case study in the Camero Viejo (Northwestern Iberian System, Spain). *Mountain Research and Development* 21, 69-76.

LESSCHEN, J.P., CAMMERRAT, L.H., NIEMANN, T., 2008. Erosion and terrace failure due to agricultural abandonment in a semi-arid environment. *Earth Surface Processes and Landforms* 33, 1574-1584.

LI, Y., LINDSTROM, M.J., 2001. Evaluating soil quality - soil redistribution relationship on terraces and steep hillslope. *Soil Science Society of America Journal* 65, 1500-1508.

LI, Y., NGUYEN, M.L., 2008. Effectiveness of soil conservation measures in reducing soil erosion and improving soil quality in China, assessed by using fallout radionuclides, in: Zdruli, P., Costantini, E. (Eds.),''Moving ahead from assessments to action: could we win the struggle with land degradation?'' 5th Int. Conference on Land Degradation, Valenzano Bari, Italy 18-22 September 2008. Book of abstracts. ISBN 2-85352-399-3, II, 287-290.

LIAW, A., WIENER, A., 2011. Package 'randomForest'. http://cran.r-project.org/web/packages/randomForest/randomForest.pdf (08/12/2011).

LIU, S.M., ZHANG, J., CHEN, H.T., WU, Y., XIONG, H., ZHANG, Z.F., 2003. Nutrients in the Changjiang and its tributaries. *Biogeochemistry* 62, 1-18.

LU, X., X., HIGGITT, D.L., 2000. estimating erosion rates on sloping agricultural land in the Yangtze Three GOrges, China, from caesium-137 measurements. *Catena* 39, 33-51.

MCDONALD, B., WEBBER, M., DUAN, Y., 2008. Involuntary resettlemet as an opportunity for development: the case of urban resettlers of the Three Gorges Project, China. *Journal of Refugee Studies*, doi: 10.1093/jrs/fem052

MENG, Q.H., FU, B.J., YANG, L.Z., 2001. Effects of land use on soil erosion and nutrient loss in the Three Gorges Reservoir Area, China. *Soil Use and Management* 17, 288-291.

MONTGOMERY, D.R., 2007. Dirt: The erosion of civilizations. University of California Press, Ltd., London, pp. 285.

PIETSCH, D., MABIT, L., 2012. Terrace soils in the Yemen highlands: using physical, chemical and radiometric data to assess their suitability for agriculture and their vulnerability to degradation. *Geoderma* 185-186, 48-60.

PONSETI, M., LÓPEZ-PUJOL, J., 2006. The Three Gorges Dam project in China: history and consequences. ORIENTATS-2006, *Revista HMiC* Nr. IV, 151-188.

POSTHUMUS, H., STROOSNIJDER, L., 2010. To terrace or not: the short-term impacts of bench terraces on soil properties and crop response in the Peruvian Andes. *Environment, Development and Sustainability* 12, 263-276, doi: 10.1007/s10668-009-993-4

R DEVELOPMENT CORE TEAM, 2011. R: A language and environment for statistical computing. R Foundation for Statistical Computing, Vienna, Austria. ISBN 3-900051-07-0, http://www.R-project.org/

SANG-ARUN, J., MIHARA, M., HORAGUCHI, Y., YAMAJI, E., 2006. Soil erosion and participatory remediation strategy for bench terraces in northern Thailand. *Catena* 65, 258-264.

SCARAMELLINI, G., VAROTTO, M. (Eds.), 2008. Terraced landscapes of the Alps - Atlas. ALPTER Project, Marsilio, Venice, Italy, pp. 125, http://www.alpter.net/ALPTER-Project-final-publications.html (04/11/2011).

SCHÖNBRODT-STITT, S., BOSCH, A., BEHRENS, T., HARTMANN, H., SHI, X., SCHOLTEN, T., 2013. Approximation and spatial regionalization of rainfall erosivity based on sparse data in a mountainous catchment of the Yangtze River in Central China. ENVIRONMENTAL SCIENCE AND POLLUTION RESEARCH, doi: 10.1007/s11356-012-1441-8

SEEBER, C., HARTMANN, H., WI, X., KING, L., 2010. Land use change and causes in the Xiangxi catchment, Three Gorges Area derived from multispectral data. *Journal of Earth Science* 21, 846-855.

SHARY, P.A., SHARAYA, L.S., MITUSOV, A.V., 2002. Fundamental quantitative methods of land surface analysis. *Geoderma* 107, 1-35.

SHEN, Z., GONG, Y., LI, Y., LIU, R., 2010. Analysis and modeling of soil conservation measures in the Three Gorges reservoir Area in China. *Catena* 81, 104-112.

SHI, Z.H., CAI, C.F., DING, S.W., WANG, T.W., CHOW, T.L., 2004. Soil conservation planning at the small watershed level using RUSLE with GIS. A case study in the Three Gorges Area of China. *Catena* 55, 33-48.

SHI, Z.H., AI, L., FANG, N.F., ZHU, H.D., 2012. Modeling the impacts of integrated small watershed management on soil erosion and sediment delivery: a case study in the Three Gorges Area, China. *Journal of Hydrology* 438-439, 156-167.

SHRESTRA, D.P., ZINCK, J.A., VAN RANST, E., 2004. Modeling land degradation in the Nepalese Himalaya. *Catena* 57, 135-156.

SIDLE, R.C., ZIEGLER, A.D., NEGISHI, J.N., RAHIM NIK, A., SIW, R., TURKELBOOM, F., 2006. Erosion processes in steep terrain - truths, myths, and uncertainties related to forest management in Southeast Asia. *Forest Ecology and Management* 224, 199-225.

SMITH, M.P., ZHU, A.X., BURT, J.E., STILES, C., 2006. The effects of DEM resolution and neighborhood size on digital soil survey. *Geoderma* 137, 58-69.

STEIL, S., DUAN, Y., 2002. Policies and practice in the Three Gorges resettlement: a field account. *Forced Migration Review* 12, 10-13.

STRAHLER, A.N., 1957. Quantitative analysis of watershed geomorphology. *Transactions American Geophysical Union* 38, 913-920.

SUBKLEW, G., ULRICH, J., FÜRST, L., HÖLTKEMEIER, A., 2010. Environmental impacts of the Yangtze Three Gorges Project - an overview of the Chinese-German research cooperation. *Journal of Earth Science* 21, 817-823.

TARBOTON, D.G., 1997. A new method for the determination of flow directions and upslope areas in grid digital elevation models. *Water Resources Research* 33, 309-319.

TOBLER, W.R., 1970. A computer movie simulating urban growth in the Detroit region. *Economic Geography* 46, 234-240.

VAN DIJK, A.I.J.M., 2002. Water and sediment dynamics in bench-terraced agricultural steeplands in West Java, Indonesia. Amsterdam, pp. 378.

WACHS, T., THIBAULT, M, (Eds.) 2009. Benefits of sustainable land management. WOCAT (World Overview of Conservation Approaches and Technologies), Berne, Switzerland, pp. 16. http://www.unccd.int/Lists/SiteDocumentLibrary/Publications/CSD_Benefits_of_Sustainable_Land_Management.pdf (12/03/2012).

WILLIAMS, L.S., 1990. Agricultural terrace evolution in Latin America. Ohio University. http://sites.maxwell.syr.edu/clag/yearbook1990/williams.pdf (02/27/2013).

WU, D.M., YU, Y.C., XIA, L.Z., YIN, S.X., YANG, L.Z., 2011. Soil fertility indices of citrus orchards land along topographic gradients in the Three Gorges Area of China. *Pedosphere* 21, 782-792.

WU, Y., LIAO, W., KING, L., YUAN, X., 2009. Analysis and utilization of the climatic resources in Xiangxi River basin. International Conference on Environmental Science and Information

Application Technology, ESIAT 2009, Wuhan, China, 3 Volumes, 217-220, doi: 10.1109/ESIAT.2009.177

YANG, S.L., ZHAO, Q.Y., BELKIN, I.M., 2002. Temporal variation in the sediment load of the Yangtze River and the influences of human activities. *Journal of Hydrology* 263, 56-71.

ZHANG, B., 2008. Impact on mountainous agricultural development in the Three Gorges Reservoir Area forced by migrants of the Three Gorges Project. *Chinese Journal of Population, Resources and Environment* 6, 83-89.

ZHOU, P., 2008. Landscape-scale erosion modeling and ecological restoration for a mountainous watershed in Sichuan, China. Academic dissertation, Tropical Forestry Reports 35, University of Helsinki Viikki Tropical Resources Institute VITRI, Helsinki, Finland, pp. 95 https://www.doria.fi/ bitstream/handle/10024/37384/landscap.pdf?sequence=1 (05/29/2013).

ZHU, A.X., 2008. Spatial scale and neighborhood size in spatial data processing for modeling the natural environment. in: Mount, N.J., Harvey, G.L., Aplin, P., Priestnall, G. (Eds.), Representing, Modeling and Visualizing the Natural Environment: Innovations in GIS 13, pp. 147-165, InCRC Press, Florida.

ACKNOWLEDGEMENTS - OR WORDS OF THANKS AND APPRECIATION -

This dissertation thesis was undertaken with the manifold support and patience of many people. I would like to gratefully and sincerely thank each of them!

My first debt of gratitude goes to my supervisor Prof. Dr. Thomas Scholten. During the past five years he patiently provided the vision, encouragement and all-time advice that I needed to proceed in the field and at the desk. I thank him for providing me the possibility to become a PhD student within the Yangtze Project and a member of the work group of Soil Science and Geomorphology at the Department of Geosciences at the Eberhard Karls University Tübingen. Thank you very much.

I am also very grateful to Prof. Dr. Gerhard Gerold from the Department of Landscape Ecology at the Institute of Geography at the Georg August University Göttingen for kindly agreeing to serve as the second reviewer of this dissertation.

Moreover, I wish to sincerely express my gratitude to Dr. Thorsten Behrens and Dr. Karsten Schmidt for their friendly guidance, patience, and always helpful suggestions throughout the last years. I highly appreciate the time they always took in order to push me, to navigate me through the 'endless vastness' of data mining, and to support me at the right time. I really learnt a lot from them and acknowledge their honesty and the enjoyable collaboration.

I thankfully appreciate funding from the German Federal Ministry of Education and Research (BMBF, grant no. 03 G 0669) for the German-Chinese joint research collaboration YANGTZE GEO and thus, for financially supporting my research. My warmest thanks I would further like to express to Dr. Günter Subklew from the German Jülich Research Centre for the coordinative support of the whole project, his professional advice, and for sharing his substantial know-how.

I highly acknowledge Prof. Dr. Xiang Wei from the Department of Geotechnical Engineering and Engineering Geology at the China University of Geosciences in Wuhan for his support in organizing administrative affairs and for his numerous and helpful explanations concerning the geology, the landscape in the Three Gorges Area, and the Chinese cuisine.

I would like to extent my warmest thanks to the students of the Department of Geotechnical Engineering and Engineering Geological at the China University of Geosciences (Wuhan) Renneng Bi, Jiwei Jiang, Xiaojuan Dong, Zhihong Lin, Qijia Li, and also to the many Chinese student that have not been named here but who have also taken part in the field campaigns for their always flexible, original, and above all superb support in organizing. I particularly thank for their companionship and translations during the field campaigns. It was always fun with you guys!

I also warmly acknowledge the fruitful work, the enthusiasm for their work as well as excellent support and enjoyable assistance in the field with the diploma students Patrick Saumer,

Stephan Imbery, and Anna Bosch, and the student research assistants Julia Bär and Moritz Koch. I wish you every success in the future and in continuing your scientific work.

Dr. Peter Kühn and Sabine Flaiz as well as the student research assistants from the Laboratory of Soil Science - I would like to thank you all for your high quality laboratory work over the last years.

Dear Edgar A. Stitt, I deeply appreciate our short conversations in the car from home to the main station and back, your always motivating and helpful words of understanding and support, and your interest in my work. Besides your friendship, I highly acknowledge your proofreading of the present thesis and the manuscripts.

Words of deepest thanks and appreciation go to my family for sharing their love to the nature with me, their financial support during my internships abroad, for their organizational talent, and their always honest and lovely words during up-and-downs. In the end it's all good.

Words of endless thanks and appreciation go to my husband Steven and to my lovely daughter Ronja for their longing when I was in China and 'somewhere else'. I deeply thank for their mental and amusing distraction and consent when I was much into my thoughts. You always encouraged and understood me in dealing with all the challenges I have faced. Together with you I have my best field trips!

CURRICULUM VITAE

Dipl.-Geogr. Sarah Schönbrodt-Stitt

Eberhard Karls University Tübingen ▪ Department of Geosciences ▪ Chair of Physical Geography and Soil Science

Rümelinstraße 19-23 ▪ D-72070 Tübingen ▪ Phone + 49 (0) 7071 29-74054 ▪ Fax + 49 (0) 7071 29-5391 ▪ E-Mail sarah.schoenbrodt-stitt@uni-tuebingen.de

Date of birth September 14th, 1981 ▪ *Place of birth* Eberswalde ▪ *Nationality* German ▪ *Familiy* married, two children

EDUCATION

2012 – Present	Coordinator of the joint research project YANGTZE GEO, funded by the Federal Ministry for Education and Research
2008 – Present	PhD student at the Eberhard Karls University Tübingen
2001 – 2007	Studies of Geography with focus on Physical Geography and Landscape Ecology, and Geology, Bioclimatology, and Environment- and Resources Economy at the Georg August University Göttingen and Ernst Moritz Arndt University Greifswald
	Topic of diploma thesis (06/2007) "Inventarisierung und bodenkundliche Charakterisierung von *Bas-fonds* im Einzugsgebiet des Oberen Ouémé in Benin, Westafrika"

SCIENTIFIC WORK EXPERIENCE

02/2008 – 06/2008	Graduate assistant of Prof. Dr. Gerhard Gerold, Department of Landscape Ecology, Institute of Geography at the Georg August University Göttingen
10/2007 – 02/2008	Graduate assistant with Prof. Dr. Bernd Diekkrüger in the BMBF-funded research project IMPETUS, Hydrology Working Group, Department of Geography at the Rheinische Friedrich Wilhelms University Bonn
07/2007 – 08/2007	Student assistant in the coordination office of SFB 552 – STORMA (Stability on Rainforest Margins in Indonesia) at the Georg August University Göttingen
04/2006 – 07/2004	Student assistant with Prof. Dr. Bernd Diekkrüger in the BMBF-funded research project IMPETUS, Hydrology Working Group, Department of Geography at the Rheinische Friedrich Wilhelms University Bonn
11/2004 – 12/2004	Student assistant with Prof. Dr. Beate Michalzik, Department of Landscape Ecology, Institute of Geography at the Georg August University Göttingen

INTERNSHIPS

09/2005 – 11/2005	Internship with the Desert Research Foundation of Namibia (DRFN; Dr. Mary Seely and Dr. Patrik Klintenberg) and Directorate of Rural Water Supply

	Oshakati, Namibia; partially funded by the German Academic Exchange Service (DAAD); aspects of water management, water scarcity, and water supply
04/2005 – 06/2005	Internship in the oasis of Tozeur, South Tunisia, with the Centre de Recherche phoenicicole de Dégache (Research Centre for Date Palms in Dégache), and the Regional Office for Rural Development Tozeur, Tunisia; aspects of soil salinization and water management
08/2004 – 10/2004	Leibniz Centre for Agricultural Landscape Research (ZALF), Department of Landscape Information Systems; Dr. W. Hierold, Müncheberg, Germany; aspects of glaciology in North Germany, land use and land use systems in North Germany

LECTURES

Summer semester 2010	Advanced seminar 'Bodenerosion' with focus on soil erosion together with Prof. Dr. Thomas Scholten and Dr. Christian Geißler, University of Tübingen
Summer semester 2009	Advanced seminar 'Bodenerosion' with focus on soil erosion together with Prof. Dr. Thomas Scholten and Dr. Christian Geißler, University of Tübingen

MEMBERSHIPS

Baobab Benin e.V.	Association for the sustainable development of Benin in West Africa and cultural exchange between Germany and Benin
DGB	Deutsche Bodenkundliche Gesellschaft; German Soil Science Society
GfUE	Förderverein Geographie für Umwelt und Entwicklung e.V.; Association for the Advancement of Geography for the Environment and Development

FIELD EXPERIENCE

2008 – 2012	Several weeks of fieldwork in the Xiangxi-Catchment, Central China with the project YANGTZE GEO within the framework of the FONA program (BMBF-funded grant No. 03 G 0669A and 03 G 0827A)
2006	Eleven weeks of fieldwork in the Upper Ouémé Catchment (Haute Vallée de l'Ouémé), North Benin, with the IMPETUS project (BMBF-funded, grant no. 01 LW 0301A and funded by the MSWF Northrhine-Westfalia (grant no. 223-21200200)
2005	Thirteen weeks of fieldwork in Oshana Region, N-Namibia, together with the Desert Research Foundation of Namibia (DRFN) and the Rural Water Supply Namibia; partly DAAD-funded)
2005	Nine weeks of fieldwork in Tozeur, South Tunisia, together with the Research Centre for Date Palms in Dégache and the Regional Office for Rural Development Tozeur, Tunisia; self-funded
2001 – 2006	Several short fieldtrips in Germany and to Austria, Sweden, and Tunisia

SCIENTIFIC PUBLICATIONS, BOOKS, AND CONFERENCE CONTRIBUTIONS

SCIENTIFIC PAPERS (PEER REVIEWED) AND BOOKS

(Alphabetical order)

GIERTZ, S., STEUP, G., **SCHÖNBRODT, S.**, 2012. Use and constraints on the use of inland valley ecosystems in Central Benin: results from an inland valley survey. *Erdkunde* 66, 239-253, DOI: 10.3112/erdkunde.2012.03.04

GIERTZ, S., **SCHÖNBRODT, S.**, 2008. Geomorphology of Benin. in: Judex, M., Thamm, H.P. (Eds.), IMPETUS Atlas Benin. Research Results 2000 - 2007. Department of Geography, University of Bonn, Germany. pp. 63-64.

GIERTZ, S., STEUP, G., SINTONDJI, L., GBAGUIDI, F., **SCHÖNBRODT, S.**, 2008. Survey of Inland Valleys in the Upper Ouémé Catchment. in: Judex, M., Thamm, H.P. (Eds.), IMPETUS Atlas Benin. Research Results 2000 - 2007. Department of Geography, University of Bonn, Germany, pp. 99-100.

SCHOLTEN, T., **SCHÖNBRODT-STITT, S.**, SUBKLEW, G., 2012. Das Verbundprojekt YANGTZE-GEO. in: Scholten, T., Schönbrodt-Stitt, S. (Hrsg.), Umweltforschung im Drei-Schluchten-Ökosystem in China - Ergebnisse der Forschungsarbeiten zur Risikoabschätzung von Bodenerosion, Hangrutschungen, diffusen Stoffeinträgen und Landnutzungswandel. Tübinger Geographische Studien 151, 11-18. ISBN 978-3-88121-089-8.

SCHÖNBRODT-STITT, S., BEHRENS, T., SCHMIDT, K., SHI, X.Z., SCHOLTEN, T., 2013. Degradation of cultivated bench terraces in the Three Gorges Reservoir Area - field mapping and data mining. *Ecological Indicators* 34, 478-493, DOI: 10.1016/j.ecolind.2013.06.010

SCHÖNBRODT-STITT, S., BOSCH, A., BEHRENS, T., HARTMANN, H., SHI, X., SCHOLTEN, T., 2013. Approximation and spatial regionalization of rainfall erosivity based on sparse data in a mountainous catchment at the Yangtze River in Central China. *Environmental Science and Pollution Research*, DOI: 10.1007/s11356-012-1441-8

SCHÖNBRODT-STITT, S., SCHOLTEN, T., 2012. Das Einzugsgebiet des Xiangxi. in: Scholten, T., Schönbrodt-Stitt, S. (Hrsg.), Umweltforschung im Drei-Schluchten-Ökosystem in China - Ergebnisse der Forschungsarbeiten zur Risikoabschätzung von Bodenerosion, Hangrutschungen, diffusen Stoffeinträgen und Landnutzungswandel. Tübinger Geographische Studien 151, 19-26. ISBN 978-3-88121-089-8.

SCHÖNBRODT-STITT, S., BEHRENS, T., SHI, X., SCHOLTEN, T., 2012. GIS-basierte Erfassung und Analyse der Bodenerosion durch Wasser im Drei-Schluchten-Ökosystem. in: Scholten, T., Schönbrodt-Stitt, S. (Hrsg.), Umweltforschung im Drei-Schluchten-Ökosystem in China - Ergebnisse der Forschungsarbeiten zur Risikoabschätzung von Bodenerosion, Hangrutschungen, diffusen Stoffeinträgen und Landnutzungswandel. Tübinger Geographische Studien 151, 27-83. ISBN 978-3-88121-089-8.

SCHÖNBRODT-STITT, S., BEHRENS, T., BIEGER, K., EHRET, D., FREI, M., XIA, Y., HÖRMANN, G., SEEBER, C., SCHLEIER, M., BI, R., WIEGAND, M., SCHMALZ, B., FOHRER, N., CAI, Q., KAUFMANN, H., KING, L., ROHN, J., SUBKLEW, G., XIANG, W., SHI, X., SCHOLTEN, T., 2012. Umweltforschung im Drei-Schluchten-Ökosystem in China - Eine Synthese. in: Scholten, T., Schönbrodt-Stitt, S. (Hrsg.), Umweltforschung im Drei-Schluchten-Ökosystem in China -

Ergebnisse der Forschungsarbeiten zur Risikoabschätzung von Bodenerosion, Hangrutschungen, diffusen Stoffeinträgen und Landnutzungswandel. Tübinger Geographische Studien 151, 283-291. ISBN 978-3-88121-089-8.

SCHÖNBRODT, S., SAUMER, P., BEHRENS, T., SEEBER, C., SCHOLTEN, T., 2010. Assessing the USLE crop and management factor C for soil erosion modeling in a large mountainous watershed in Central China. *Journal of Earth Science* 21, 835-845.

STREHMEL, A., **SCHÖNBRODT-STITT, S.**, FOHRER, N., SCHOLTEN, T. ET AL., Mega construction site Three Gorges reservoir - a rapid changing landscape. *in preparation*.

SUBKLEW, G., XIANG, W., **SCHÖNBRODT-STITT, S.**, SCHOLTEN, T., 2012. Der Drei-Schluchten-Staudamm am Yangtze und seine ökologischen Implikationen - Eine Einführung. in: Scholten, T., Schönbrodt-Stitt, S. (Hrsg.), Umweltforschung im Drei-Schluchten-Ökosystem in China - Ergebnisse der Forschungsarbeiten zur Risikoabschätzung von Bodenerosion, Hangrutschungen, diffusen Stoffeinträgen und Landnutzungswandel. Tübinger Geographische Studien 151, 1-10. ISBN 978-3-88121-089-8.

CONFERENCE CONTRIBUTIONS, ABSTRACTS, AND OTHER PUBLICATIONS

(Alphabetical order)

GIERTZ, S., STEUP, G., STADLER, C., **SCHÖNBRODT, S.**, DIEKKRÜGER, B., GOLDBACH, H., 2006. Analysis and Evaluation of the Agro-potential of Inland-Valleys in the Upper Ouémé catchment (Benin, West Africa). Tropentag 2006, Conference on International Agricultural Research for Development, 11-13 October 2006, Bonn, Germany.

MAZAMBANI, C., **SCHÖNBRODT, S.**, KLINTENBERG, P., 2006. Water Supply: a Gift from God or does it come with a cost? World Water Week 2006, 20-26 August 2006, Stockholm International Water Institute, Stockholm, Sweden, pp. 150-151.

SCHOLTEN, T., BEHRENS, T., FOHRER, N., KAUFMANN, H., KING, L., ROHN, J., **SCHÖNBRODT, S.**, SUBKLEW, G., XIANG, W., 2010. The Yangtze Project: Studying Land Use Change, Soil Erosion, Mass Movements and Diffuse Matter Fluxes in a Highly Dynamic Ecosystem. EcoChange Conference, 08-14 September 2010, Kiel, Germany, Book of Abstracts p. 48.

SCHOLTEN, T., BEHRENS, T., KAUFMANN, H., KING, L., ROHN, J., **SCHÖNBRODT, S.**, SUBKLEW, G., XIANG, W., 2009. Three-Gorges-Dam: Studying the ecological impacts in a highly dynamic Ecosystem. EGU General Assembly 2009, Geophysical Research Abstracts 11, EGU2009-0, 19-24 April 2009, Vienna, Austria.

SCHÖNBRODT-STITT, S., STREHMEL, A., FOHRER, N., SCHOLTEN, T., 2013. Mega construction site Three Gorges reservoir - a rapidly changing environment. Abstract submission (05/30/2013) to Anthropocene, Special Issue: 'Landscapes in the Anthropocene'.

SCHÖNBRODT-STITT, S., STUMPF, F., SCHMIDT, K., SCHOLTEN, T., 2013. Tübinger Forscher koordinieren geowissenschaftliche Forschungen am Yangtze. Forum der Geoökologie (VGöD) 24(1), 23-24.

SCHÖNBRODT-STITT, S., SCHOLTEN, T., 2013. The Three Gorges Dam at the Yangtze River and its ecological implications. Meeting of Matariki Network of Universities 2013 "Disaster Preparedness, Response and Resilience", 28-30th April 2013, University of Durham, UK.

SCHÖNBRODT-STITT, S., STUMPF, F., SCHMIDT, K., BEHRENS, T., SCHOLTEN, T., 2013. Bodenerosionsmodellierung in einem kleinen Gebirgseinzugsgebiet im Reservoir des Drei-Schluchten-Staudamms. Workshop der Deutschen Bodenkundlichen Gesellschaft "Möglichkeiten modellgestützter Bodenerosionsermittlung - Anwendung des Modells Erosion 3D", 13.-15. März 2013, Berlin-Spandau.

SCHÖNBRODT-STITT, S., STUMPF, F., SCHMIDT, K., ALTHAUS, P., RENNENG BI, BIEGER, K., BUZZO, G., DUMPERTH, C., FOHRER, N., ROHN, J., STREHMEL, A., UDELHOVEN, T., XIANG, W. ZIMMERMANN, K., SCHOLTEN, T., 2013. Studying and understanding the environmental impacts of the Three Gorges Dam in China. EGU General Assembly 2013, Geophysical Research Abstracts 15, EGU2013-6013, 07-12 April 2013, Vienna, Austria.

SCHÖNBRODT-STITT, S., STUMPF, F., SCHMIDT, K., BEHRENS, T., XIANG, W., SCHOLTEN, T., 2013. Ökologische Implikationen des Drei-Schluchten-Staudamms in China. Deutscher Geographentag 2013, Passau.

SCHÖNBRODT-STITT, S., SCHMIDT, K., STUMPF, F., ALTHAUS, P., BI, R., BIEGER, K., DUMPERTH, C., FOHRER, N., ROHN, J., STREHMEL, A., SUBKLEW, G., UDELHOVEN, T., XIANG WEI, ZIMMERMANN, K., SCHOLTEN, T., 2012. YANGTZE GEO: The Three Gorges Dam - Environmental research at the Yangtze River. IALE-D Jahrestagung 2012, 24-26 October 2012, Eberswalde, Germany.

SCHÖNBRODT-STITT, S., SCHMIDT, K, BEHRENS, T., SCHOLTEN, T., 2012. Terrace - Analysis and prediction of the condition of farming terraces in the area of the Three Gorges Dam. Digital Soil Mapping Workshop, 06-07 September 2012, Tübingen, Germany.

SCHÖNBRODT-STITT, S., SCHMIDT, K., BEHRENS, T., SCHOLTEN, T., 2012. Does agricultural intensification cause terrace degradation? Eurosoil2012, Abstract n. 2236 (ID internet n. 19531), Eurosoil 2012, 02-07 July 2012, Bari, Italy.

SCHÖNBRODT, S., BEHRENS, T., BIEGER, K., EHRET, D., FREI, M., HÖRMANN, G., SEEBER, C., SCHLEIER, M., SCHMALZ, B., FOHRER, N., KAUFMANN, H., KING, L., ROHN, J., SUBKLEW, G., XIANG, W., SCHOLTEN, T., 2012. The German-Chinese research collaboration YANGTZE-GEO: Assessing the geo-risks in the Three Gorges Reservoir area. EGU General Assembly 2012, Geophysical Research Abstracts 14, EGU2012-9329, 22-27 April 2012, Vienna, Austria.

SCHÖNBRODT, S., BEHRENS, T., BIEGER, K., EHRET, D., FREI, M., HÖRMANN, G., SEEBER, C., SCHLEIER, M., SCHMALZ, B., FOHRER, N., KAUFMANN, H., KING, L., ROHN, J., SUBKLEW, G., XIANG, W., SCHOLTEN, T., 2011. Ecosystem changes due to river impoundment by the Three Gorges Dam in Central China. Workshop Processes in the Yangtze River System - Experiences and Perspectives. 28-29 November 2011, Aachen. in: Küppers, S., Subklew, G., Wilken, R.D. (Eds.), Processes in the Yangtze River System – Experiences and Perspectives. Energie und Umwelt Band 123, 38.

SCHÖNBRODT, S., SCHMIDT, K., BEHRENS, T., SCHOLTEN, T., 2011. The Impact of the Three Gorges Project on Man-made Terraces (China). Workshop Processes in the Yangtze River System - Experiences and Perspectives. 28-29 November 2011, Aachen. in: Küppers, S, Subklew, G, Wilken R.D. (Eds.). Processes in the Yangtze River System - Experiences and Perspectives. Energie und Umwelt Band 123, 38.

SCHÖNBRODT, S., BEHRENS, T., SCHMIDT, K., SCHOLTEN, T., 2011. Modellierung von Terrassen als Erosionsschutz im Gebiet des Drei-Schluchten-Staudamms (China). DBG Jahrestagung 2011, 03-09 September, Berlin, Potsdam, Germany.

SCHÖNBRODT, S., BEHRENS, T., SCHOLTEN, T., 2010. Soil properties and soil erodibility in the Xiangxi catchment. EcoChange Conference, 08-14 September 2010, Kiel, Germany, Book of Abstracts pp. 49-50.

SCHÖNBRODT, S., BEHRENS, T., IMBERY, S., SCHOLTEN, T., 2010. Soil Erosion Modeling in Terraced Landscapes - examples from the Three-Gorges-Area, China. IUSS 19th World Congress of Soil Science 2010, 01-06 August 2010, Brisbane, Australia.

SCHÖNBRODT, S., BEHRENS, T., SCHOLTEN, T., 2010. Three Gorges Reservoir Area: soil erosion under natural condition vs. soil erosion under current land use. EGU General Assembly 2010, Geophysical Research Abstracts 12, EGU2010-13154, 02-07 May 2010, Vienna, Austria.

SCHÖNBRODT, S., BEHRENS, T., IMBERY, S., SCHOLTEN, T., 2010. Modeling the erosion risk potential induced by terraces and their condition in a highly dynamic watershed close to the Three-Gorges-Dam. 6th Alexander von Humboldt International Conference "Climate Change, Natural Hazards, and Societies" 2010, 14-19 March 2010, Mérida, Mexico.

SCHÖNBRODT, S., BEHRENS, T., IMBERY, S., SCHOLTEN, T., 2009. A conceptual Terrace-Condition-Erosion model to assess soil erosion on farming terraces induced by their condition. 13. Workshop zur Großskaligen Hydrologischen Modellierung: Hydrologische Modellierung zur Bewertung von Ökosystemdienstleistungen und Landschaftsfunktionen, 25-27 November 2009, Dresden, Germany.

SCHÖNBRODT, S., BEHRENS, T., IMBERY, S., SCHOLTEN, T., 2009. GIS-based analysis and assessment of soil erosion by water in the Three-Gorges-Ecosystem, P. R. China. 10 Years Sino-German Yangtze Research Cooperation, Workshop IV: Environmental Impacts of the Yangtze Three Gorges Project: Land Use Change, Soil Erosion and Mass Movements, Deutschland und China - Gemeinsam in Bewegung, 24-30 October 2009, Wuhan, China.

SCHÖNBRODT, S., BEHRENS, T., IMBERY, S., SCHOLTEN, T., 2009. GIS-based assessment and analysis of soil erosion by water in the Three-Gorges Ecosystem - A new approach to model soil erosion on farming terraces by their condition. DBG Jahrestagung 2009, 05-13 September 2009, Bonn, Germany.

SCHÖNBRODT, S., BEHRENS, T., SCHOLTEN, T., 2009. GIS-based assessment and analysis of soil erosion by water in the Three-Gorges ecosystem. EGU General Assembly 2009, Geophysical Research Abstracts 11, EGU2009-10715, 19-24 April 2009, Vienna, Austria.

STUMPF, F., **SCHÖNBRODT-STITT, S.**, SCHMIDT, K., BEHRENS, T., SCHOLTEN, T., 2013. Erosion modeling in Central China: soil data acquisition by conditioned Latin Hypercube sampling and incorporation of legacy data. EGU General Assembly 2013, Geophysical Research Abstracts 15, EGU2013-4233-1, 07-12 April 2013, Vienna, Austria.

STUMPF, F., **SCHÖNBRODT-STITT, S.**, SCHMIDT, K., BEHRENS, T., SCHOLTEN, T., 2013. Erosion modeling in Central China: soil data acquisition by conditioned Latin Hypercube sampling and incorporation of legacy data. Digital Soil Mapping Workshop, 11-12 April 2013, Tübingen, Germany.

STUMPF, F., **SCHÖNBRODT-STITT, S.**, SCHMIDT, K., BEHRENS, T., SCHOLTEN, T., 2013. Erosions-modellierung in Zentralchina: Conditioned Latin Hypercube Sampling als Grundlage für eine

Bodenlandschaftsmodellierung. Jahrestagung der Deutschen Bodenkundlichen Gesellschaft 2013, Kommission V / Thema 7 (Digital Soil Mapping), 07.-12. September 2013, Rostock

SUBKLEW, G., **SCHÖNBRODT-STITT, S.**, SCHOLTEN, T., XIANG, W., WILKEN, R.D., 2013. Das "Yangtze-Projekt" - zehn Jahre erfolgreiche deutsch-chinesische Zusammenarbeit. Business Guide Deutschland China, 6th edition, 162-163, Wegweiser® Media & Conferences.

DECLARATION BY THE CANDIDATE

I hereby declare that this dissertation is the product of my own work and effort and that it has not been submitted anywhere for any award. I further declare that all the sources I have used or quoted have been indicated and acknowledged as complete references.

ERKLÄRUNG

Hiermit erkläre ich, dass ich die vorliegende Dissertation, abgesehen von der Beratung durch meine Betreuer, selbstständig verfasst habe und keine weiteren Quellen und Hilfsmittel als die hier angegebenen verwendet habe. Diese Arbeit hat weder ganz noch in Teilen bereits an anderer Stelle einer Prüfungskommission zur Erlangung des Doktorgrades vorgelegen. Ich erkläre, dass die vorliegende Arbeit gemäß der Grundsätze zur Sicherung guter wissenschaftlicher Praxis der Deutschen Forschungsgemeinschaft erstellt wurde.

Signature:

Date and place: